University of Venda
Creating Future Leaders

UNIVERSITY OF VENDA

School of Environmental Sciences

Department of Ecology and Resource Management

Synthesis, characterization and performance evaluation of iron(III) oxide coated bentonite clay – silica rich reddish black Mukondeni clay soils composites for the defluoridation of groundwater

Tholiso Ngulube

Student No: 11601328

UNIVERSITY OF VENDA
LIBRARY

Supervisor : Prof Wilson Mugera Gitari

Co- supervisor : Prof Hlanganani Tutu

A research dissertation submitted to the Department of Ecology & Resource Management, University of Venda, in fulfillment of requirement of Masters of Environmental Sciences

April 2016

© University of Venda

University of Venda
Creating Future Leaders

DEDICATION

This research is dedicated to my mom, **Beria Witness** who encouraged me to make something out of myself. As a young girl, she told me constantly and consistently that I could do or be anything I wanted. She worked so hard and consequently never had that chance to become educated, but she gave me that chance.

© University of Venda

University of Venda
Creating Future Leaders

DECLARATION

I declare that this is my own work and it contains no material which has been accepted for the award of any other degree or diploma in any university or other tertiary institutions. To the best of my knowledge I also believe that it contains no material previously published by another person except where due reference has been made.

Tholiso Ngulube November 2015

Signature .....

© University of Venda

University of Venda
Creating Future Leaders

ABSTRACT

Clay materials have been proposed as adsorbent mediums to remove fluoride from groundwater. This study investigated the removal of fluoride from aqueous solutions by newly synthesised iron(III) oxide coated bentonite clay, locally available silica rich reddish black Mukondeni clay soils and their ceramic composite. Raw bentonite clay was first activated by NaOH to remove geological fluoride in bentonite clay and thereafter coated with iron(III) oxides whereas silica rich reddish black Mukondeni clay soils were used raw. Physicochemical and mineralogical characterisation was done by X-Ray Fluorescence (XRF), X – Ray Diffraction (XRD), Scanning Electron Microscopy (SEM), Scanning Electron Microscopy - Energy Dispersive Spectroscopy (SEM-EDS), Fourier Transform Infrared (FTIR), Transmission Electron Microscopy (TEM) and Brunauer Emmet Teller (BET). Cation Exchange Capacity (CEC) and Point of Zero Charge (PZC) were determined using standard methods. Results showed that both clay soils are alumina silicate materials and quartz was the major mineral phase in the clays. BET showed that iron(III) oxide coated bentonite clay has a surface area of 132.3018 m^2/g whereas silica rich reddish black Mukondeni clay soils have a surface area of 43.2077 m^2/g. A batch fluoride sorption scheme was applied to evaluate their fluoride adsorption capacities and the system variables investigated included, initial sorbate concentration, agitation time, adsorbent dose, co-existing ions, pH and temperature. A maximum fluoride removal capacity of 1.596 mg/g was recorded for iron (III) oxide coated bentonite clay, which was higher compared to 0.08 mg/g of the silica rich reddish black Mukondeni clay soils and even much higher compared to that of the composite ceramic pellets (0.03 mg/g). It was also observed that the iron(III) oxide coated bentonite clay worked effectively over a wide range of pH (2 – 12) but the maximum fluoride removal was at pH 2. Between the pH range of 6 and 9 the fluoride removal capacity was above 70% and the material exhibited minimal metal leaching. On the contrary silica rich reddish black Mukondeni clay soils worked effectively only at pH 2 but exhibited minimal metal leaching across all tested pHs. The experimental data fitted well to the Freundlich isotherm for both clay soils which showed that adsorption took place on a multilayer surface. The adsorption kinetics fitted the pseudo second order model indicating chemisorption and the rate kinetics were regulated by external and internal diffusion for both clay soils. The high adsorption capacity of iron(III) oxide-coated bentonite clay indicated the potential use of this adsorbent for fluoride removal from aqueous medium whereas the low adsorption capacity of the silica rich reddish black Mukondeni clay soils and the composite ceramic pellets can be

© University of Venda

University of Venda
Creating Future Leaders

enhanced by metal modification which has been shown to increase the adsorption of different clay soils.

Keywords: Adsorption isotherms, kinetics, thermodynamics, mechanisms, bentonite clay, Mukondeni clay soils, composite ceramic pellets and fluoride.

UNIVERSITY OF VENDA
LIBRARY

© University of Venda

University of Venda
Creating Future Leaders

ACKNOWLEDGEMENTS

First and foremost my eternal gratitude goes to my creator for giving me the gift of life to make this research a possibility.

Numerous people assisted me to complete this thesis. I would like to express my gratitude for their assistance, inspiration and encouragement. To begin with, let me thank my supervisor, **Prof Mugera Gitari** for his attentive and challenging guidance. He has been a strong and respectful supervisor. His care for technicality, scientific precision, his investigative and skeptical mind pushed me to ambitious research work. He showed faith in my ability to carry out scientific work especially when I was hesitant and getting weary through my work. Together with my co supervisor **Prof Hlanganani Tutu**, I am grateful to them for their academic guidance. It is because of them that this research is a success; its compilation would not have been possible without their valuable suggestions and comments.

My Research Group Members, (ERWPCG) have highly contributed to this dissertation by always being active in discussing my project ideas and approaches. They shared their scientific knowledge providing opportunities to work together and a space where I could develop as a scientist. In particular, I am grateful to **Anthony Izuagie** who has provided me with insights and high level knowledge in analytical chemistry. I enjoyed collaborating with him because he treated me as a peer and was open to innovation. Exceptional mention goes to **Tshimangadzo Ratshivhadelo** for her tireless assistance in laboratory work not forgetting, my academic mentor, **Vhahangwele Masindi** who helped me with analysis when things were tough. I am indebted to him because he stood by me when I needed him most.

A special thank you goes to the Director of Research and Innovation, University of Venda, National Research Foundation and Water Research Commission. Thank you for the financial support from the beginning through to the end of my research. I never struggled with funds to run the project.

Finally, I thank my family for believing in my capabilities. They have been patient, proud and happy to sail with me in this boat. My mum, **Beria,** for your unconditional love and understanding, I will always remain indebted to you. My brother and sister, **Khathutshelo** and **Sithokozile** for serving as a pillar of support, you guys are the best.

© University of Venda

University of Venda
Creating Future Leaders

ACADEMIC OUTPUTS

Conference proceedings

Ngulube, T., Gitari, W.M. and Hlanganani, T., 2015. Synthesis, characterisation and performance of iron(III) oxide coated bentonite clay in the removal of fluoride from drinking water. 1st UNIVEN – WSU International Research Conference. East London. 2nd to 4th Sept 2015. Research and innovation for sustainable development and the transformation of society.

Ngulube, T., Gitari, W.M. and Hlanganani T., 2015. Defluoridation of groundwater using mixed Mukondeni clay soils: 4th YWP-ZA Biennial & 1st Africa YWP Conference. CSIR, Pretoria. 16 to 18 November 2015.

Manuscripts being prepared for submission to international peer reviewed journals

Ngulube, T., Gitari, W.M. and Hlanganani, T., 2015. Synthesis, characterization and performance of iron(III) oxide coated bentonite clay in groundwater defluoridation. *Fluorine Chemistry*.

Ngulube, T., Gitari W.M. and Hlanganani T., 2015. Evaluation of the fluoride adsorption capacity of silica rich reddish black Mukondeni clay soils. *South African Journal of Science*.

Published journal articles related to this work

Vhahangwele, M., Wilson, G. and Tholiso, N., 2015. Kinetics and equilibrium studies for removal of fluoride from underground water using cryptocrystalline magnesite. *Journal of Water Reuse and Desalination*, 5(3), pp. 282 – 292.

Masindi, V., Gitari, W.M. and Ngulube, T., 2014. Defluoridation of drinking water using Al^{3+} -modified bentonite clay: Optimization of fluoride adsorption conditions. *Toxicological & Environmental Chemistry,* http://dx.doi.org/10.1080/02772248.2014.977289

Manuscript submitted to international peer reviewed journals

Masindi, V., Gitari, W.M and Ngulube, T. Synthesis of cryptocrystalline magnesite/bentonite clay composite for the removal of fluoride from aqueous solution. *Journal of Chemical Engineering.* September 30. 2015.

© University of Venda

University of Venda
Creating Future Leaders

ACRONYMS AND ABBREVIATIONS

AAS	: Atomic adsorption Spectroscopy
BET	: Brunauer-Emmett-Teller method
CEC	: Cation Exchange Capacity
DWA	: Department of Water Affairs
DWAF	: Department of Water Affairs and Forestry
DWS	: Department of Water and Sanitation
EC	: Electrical conductivity
FTIR	: Fourier Transform Infrared
pH	: Potential Hydrogen
pH*i*	: Initial pH
PZC	: Point of Zero Charge
TDS	: Total Dissolved Solids
XRD	: X-ray Diffraction
XRF	: X-ray Fluorescence
WHO	: World Health Organisation
WRC	: Water Research Commission

NOTE : Please refer to the periodic table of elements for the elements

© University of Venda

University of Venda
Creating Future Leaders

TABLE OF CONTENTS

DEDICATION ii
DECLARATION iii
ABSTRACT iv
ACKNOWLEDGEMENTS vi
ACADEMIC OUTPUTS vii
LIST OF FIGURES xvi
INTRODUCTION 1
1.1 Background information 1
1.2 Problem statement 3
1.4 Research objectives 4
1.4.1 General objective 4
1.4.2 Specific objectives 4
1.5 Research questions 5
1.6 Hypothesis 5
1.7 Assumption 5
1.8 References 6
CHAPTER 2 9
REVIEW OF LITERATURE 9
2.0 Introduction 9
2.1 Fluoride 9
2.1.1 Chemistry and environmental occurrence 9
2.1.2 Fluoride chemistry in water 10
2.2 Fluoride and human health 10
2.2.1 The fluoride problem in South Africa 11
2.3 Sustainable water defluoridation technologies 13
2.3.1 The concept of appropriate technology 13
(a) Water defluoridation research in fluoride endemic areas in Africa. 14
(i) Nalgonda technique for domestic defluoridation 15
2.3.1 The techniques 16
2.3.1.1 Membrane filtration processes 16
(i) Reverse osmosis 16
(ii) Electro dialysis 17
2.3.1.2 Precipitation processes 17

UNIVERSITY OF VENDA
LIBRARY

© University of Venda

University of Venda
Creating Future Leaders

(a) Precipitation of fluoride 17
(i) Lime 17
(b) Coprecipitation of fluoride 18
(ii) Alum 18
2.3.3 Adsorption process 18
2.3.3.1 Bone and bone charcoal 20
2.3.3.2 Activated alumina (AA) 21
2.3.3.3 Clays soils 22
(i) Mechanisms of adsorption onto clay soils 23
(ii) Kaolin clay 24
(iii) Other clays 24
(iv) Shortcomings of raw clay filter mediums 26
2.3.4 Merits of the adsorption process 27
2.4 Adsorption using bentonite clay 28
2.4.1 Bentonite clay 28
2.4.2 Mineralogy and physicochemical properties 28
2.4.3 Chemical modification of bentonite 29
2.4.3.1 Metal oxide coatings 30
2.4.3.2 Alkali activation 31
2.4.4 Application of bentonite clay in water defluoridation 32
2.5 Mukondeni clay soils 33
2.5.1 Mineralogy of Mukondeni clay soil 34
2.5.2 Mukondeni clays soils and water defluoridation 35
2.6. Composite adsorbents and defluoridation. 36
2.7 References 37
CHAPTER THREE 46
METHODOLOGY 46
3.0 Introduction 46
3.1 Sampling 46
3.2 Preparation of adsorbent materials 47
3.2.1 Preparation of the silica rich reddish black Mukondeni clay soils 47
3.2.2 Synthesis of the iron(III) oxide coated bentonite clay 48
3.2.2.1 Activating bentonite clay with NaOH 48
3.2.2.2 Coating NaOH-activated bentonite clay with Fe_2O_3 48

© University of Venda

University of Venda
Creating Future Leaders

3.2.3 Clay composite fabrication method 48
3.2.3.1 Optimisation of fabrication parameters 49
(i) Optimisation of particle size 49
(ii) Optimisation of furnace temperature 49
(iii) Optimisation of firing time 49
(iv) Optimisation of clay ratios 50
3.2.3.1 Fabrication of silica rich reddish black Mukondeni soils - iron(III) oxide coated bentonite clay ceramic composite pellets. 50
3.3 Physicochemical and mineralogical characterization 50
3.3.1 Determination of Cation Exchange Capacity (CEC) 51
3.3.1.1 Calculation of CEC per 1 g 51
3.3.2 Determination of Point of Zero Charge (PZC) 51
3.3.3 Determination of mineralogy by X-ray diffraction (XRD) 52
3.3.4 Determination of elemental composition by X-ray fluorescence (XRF) 52
3.3.5 Determination of morphology by Scanning Electron Microscopy (SEM) 52
3.3.6 Determination of surface area by Brunauer–Emmett–Teller (BET) 52
3.3.7 Determination of functional groups by Fourier Transform Infrared (FTIR) 53
3.3.8 Transmission Electron Microscopy (TEM) 53
3.4 Preparation of fluoride solution 53
3.5 Determination of pH, EC, TDS and F^- 54
3.6. Batch adsorption experiments 54
3.6.1 Batch adsorption experiments using silica rich reddish black Mukondeni clay soils 54
3.6.1.1 Adsorption of fluoride as a function of contact time 54
3.6.1.2 Adsorption of fluoride as a function of adsorbent dosage 54
3.6.1.3 Adsorption of fluoride as a function of adsorbate concentration 55
3.6.1.4 Adsorption of fluoride as a function of temperature 55
3.6.1.5 Adsorption of fluoride as a function of competing ions 55
3.6.1.6 Adsorption of fluoride as a function of pH 56
3.6.1.7 Application of the optimized conditions for F^- adsorption using borehole water 56
3.6.2 Batch adsorption experiments using iron(III) oxide coated bentonite clay 56
3.6.2.1 Adsorption of fluoride as a function of contact time 56
3.6.2.2 Adsorption of fluoride as a function of adsorbent dosage 56
3.6.2.3 Adsorption of fluoride as a function of adsorbate concentration 57
3.6.2.4 Adsorption of fluoride as a function of temperature 57

© University of Venda

University of Venda
Creating Future Leaders

3.6.2.5 Adsorption of fluoride as a function of competing ions 57
3.6.2.6 Adsorption of fluoride as a function of pH 58
3.6.2 Application of the optimised conditions for F^- adsorption using Siloam borehole water. 58
3.7 Chemical stability testing 58
3.8 Regeneration studies 58
3.10 Calculation of % F^- removal and Adsorption Capacity 59
3.11 Adsorption Isotherms 59
3.11.1 The Langmuir Isotherm 60
3.11.2 The Freundlich isotherm 60
3.11.3 The Dubinin–Radushkevich isotherm 61
3.12 Thermodynamics 61
3.13 Adsorption kinetics 62
3.13.1 The pseudo first-order equation 62
3.13.2 Pseudo second order kinetics 63
3.14 Diffusion-based models 63
3.14.1 The intraparticle diffusion model 63
3.14.2 External diffusion 64
3.15 Statistical analysis 64
3.16 References 65
CHAPTER FOUR 66
DEFLUORIDATION OF GROUNDWATER USING SILICA RICH REDDISH BLACK MUKONDENI CLAY SOILS 66
ABSTRACT 66
4.1. Materials and methods 67
4.2 Results and discussions 68
4.2.1 Physicochemical and mineralogical characterisation of silica rich reddish black Mukondeni clay soils. 68
4.2.1.1 Cation Exchange Capacity (CEC) 68
4.2.1.2 Point of zero charge (PZC) of silica rich reddish black Mukondeni clay soils. 68
4.2.1.3 X - Ray Diffraction (XRD) analysis 69
4.2.1.4 X – Ray Fluorescence (XRF) Analysis 70
4.2.1.5 Scanning Electron Microscopy (SEM) analysis 71
4.2.1.6 Brunauer–Emmett–Teller (BET) analysis 72
4.2.1.7 Fourier Transform Infrared (FTIR) analysis 74
4.3 Batch adsorption experiments 76

© University of Venda

University of Venda
Creating Future Leaders

4.3.1 Effect of contact time on fluoride removal capacity 76
4.3.2 Effect of adsorbent dosage on fluoride removal capacity. 77
4.3.3 Effect of fluoride ion concentration on fluoride removal capacity 78
4. 3.4 Effect of temperature on fluoride removal capacity 79
4.3.5 Effect of competing ions on fluoride removal capacity 81
4.3.6 Effect of pH on fluoride removal capacity 82
4.4 Treatment of field water from Siloam borehole at optimized pH conditions and field pH conditions. 83
4.5 Chemical stability of the adsorbent 86
4.6 Adsorption Isotherms 87
4.6.1 Langmuir Isotherm 87
4.6.2 Freundlich Isotherm 89
4.6.3 Dubinin–Radushkevich isotherm model 90
4.7 Thermodynamic parameters 91
4.8 Adsorption kinetics 91
4.8.1 The pseudo first-order and pseudo second order models 91
4.9. Diffusion based models 93
4.10 Proposed adsorption mechanism of fluoride onto using silica rich Mukondeni clay soils 94
4.11 Performance comparison of silica rich reddish black Mukondeni clay soils with other clay adsorbents 95
4.12 Concluding remarks and future perspectives 96
4.13 References 98
CHAPTER FIVE 101
SYTHESIS OF IRON(III) OXIDE COATED BENTONITE CLAY AND ITS PERFORMANCE IN THE DEFLUORIDATION OF GROUNDWATER 101
ABSTRACT 101
5.0 Introduction 103
5.1 Materials and methods 103
5.2 Results and discussions 104
5.2.1 Activating bentonite clay with NaOH: Optimisation of reaction conditions 104
5.2.1.1 Release of fluoride from bentonite clay as a function of contact time 104
5.2.1.2 Release of fluoride as a function of NaOH concentration 105
5.2.1.3 Release of fluoride as a function of dosage 106
5.3 Coating NaOH-activated bentonite clay with iron(III) oxides: Optimisation of reaction conditions. 107

© University of Venda

University of Venda
Creating Future Leaders

5.4 Characterisation of the adsorbents 108
5.4.1 Cation Exchange Capacity (CEC) 108
5.4.2 Point of Zero Charge (PZC) analysis 109
5.4.3 X – Ray Diffraction (XRD) analysis 111
5.4.4 X- Ray Fluorescence (XRF) analysis 112
5.4.5 Scanning Electron Microscopy analysis 113
5.4.6 Brunauer–Emmett–Teller (BET) analysis 116
5.4.7 Fourier Transform Infrared (FTIR) analysis. 118
5.5 Batch adsorption experiments 119
5.5.1 Effect of contact time on fluoride removal capacity 119
5.5.2 Effect of dosage on fluoride removal capacity 120
5.5.3 Effect of concentration on fluoride removal capacity 121
5.5.4 Effect of temperature on fluoride removal. 122
5.5.5 Effect of competing ions on fluoride removal capacity 123
5.5.6 Effect of pH on fluoride removal capacity 124
5.6 Treatment of raw fluoride water from Siloam, Limpopo province, South Africa borehole at pH optimized conditions 126
5.7 Chemical stability of the adsorbent 128
5.8 Comparison of the percentage removal capacities of the raw bentonite clay and iron (III) oxide coated bentonite clay. 130
5.9 Adsorption Isotherms 130
5.9.1 Langmuir Isotherm 131
5.9.2 Freundlich Isotherm 132
5.9.3 Dubinin–Radushkevich isotherm model 133
5.10 Thermodynamics 134
5.11 Adsorption kinetics 135
5.12 Reuse and regeneration of iron(III) oxide coated bentonite clay 139
5.13 Proposed mechanism of fluoride adsorption onto iron(III) oxide coated bentonite clay 140
5.14 Comparing the adsorption capacity of iron(III) oxide coated bentonite clay with other clay adsorbents 141
5.15 Conclusions and Recommendations 142
5.16 References 144
FABRICATION OF IRON(III) OXIDE COATED BENTONITE CLAY - SILICA RICH REDDISH BLACK MUKONDENI CLAY SOILS CERAMIC COMPOSITE PELLETS AND THEIR PERFORMANCE IN GROUNDWATER DEFLUORIDATION 148

© University of Venda

University of Venda
Creating Future Leaders

ABSTRACT 148
6.0 Introduction 149
6.1 Materials and methods 149
6.2 Results and discussions 149
6.2.1 Optimisation of particle size 149
6.2.2 Optimisation of furnace temperature 149
6.2.2.1 X-ray Diffraction analysis 150
6.2.2.2 Scanning Electron Microscopy (SEM) – SEM coupled with Energy Dispersive Spectroscopy analysis 153
6.2.2.3 Brunauer Emmett Teller (BET) analysis 155
6.2.2.4 Fluoride adsorption experiments 156
6.2.3 Optimization of firing time 157
6.2.3.1 SEM – EDS analysis 157
6.2.3.2 Transmission Electron Microscopy (TEM) analysis 160
6.2.3.3 X Ray Diffraction (XRD) analysis 162
6.2.3.4 X-ray Fluorescence (XRF) analysis 163
6.2.3.5 Branuer Emmett Teller (BET) analysis 164
6.2.3.6 FTIR analysis 165
6.2.3.7 Fluoride adsorption experiments 166
6.2.4 Optimization of clay ratios 167
6.3 Conclusions 169
6.4 References 170
CHAPTER SEVEN 171
CONCLUSIONS AND RECOMMENDATIONS 171
APPENDICES 173

© University of Venda

University of Venda
Creating Future Leaders

LIST OF FIGURES

CHAPTER 2

Figure 2.1: Bone char domestic defluoridator (Wondimagegn, 2008)

Figure 2.2: The Nalgonda defluoridation as adopted for domestic use in Tanzania (Dahi, 2000)

Figure 2.3: Activated alumina-based domestic defluoridation filter (Daw, 2004)

Figure 2.4: Stratified column of brick chips used in household defluoridation (Padmasiri, 1998).

Figure 2.5: Crushed brick fluoride filter combined with experimental sand filter

Figure 2.6: Structure of bentonite (Clelyi and Doehler, 2010)

Figure 2.7: Clay pots made from Mukondeni clay soils

CHAPTER 3

Figure 3.1: Study area

CHAPTER 4

Figure 4.1: Point of zero charge of silica rich reddish black Mukondeni clay soils

Figure 4.2: XRD diffractogram of silica rich reddish black Mukondeni clay soils

Figure 4.3: SEM images of silica rich reddish black Mukondeni clay soils before (a) and after (b) defluoridation

Figure 4.4: Plot of BJH Adsorption dV / dlog (w) and Pore Volume against pore diameter for silica rich reddish black Mukondeni clay soils

Figure 4.5: FTIR spectra of silica rich reddish black Mukondeni clay soils before and after defluoridation

Figure 4.6: Percentage removal and adsorption capacity of silica rich reddish black Mukondeni clay soils as a function of contact time (1, 2 and 3 g, 10 mg/L F^- , 25ºC room temperature, 100 mL, 250 rpm, pH*i* = 6.423)

UNIVERSITY OF VENDA
LIBRARY

© University of Venda

University of Venda
Creating Future Leaders

Figure 4.7: Percentage removal and adsorption capacity of silica rich reddish black Mukondeni clay soils as a function of dosage (60 min contact time, 10 mg/L F^-, 25°C room temperature, 250 rpm, pH*i* = 5.937)

Figure 4.8: Percentage removal and adsorption capacity of silica rich reddish black Mukondeni clay soils as a function of initial fluoride concentration (60 min contact time, 1.5 g dosage, 25°C room temperature, 100 mL, 250 rpm, pH*i* = 6.111).

Figure 4.9: Percentage removal and adsorption capacity of silica rich reddish black Mukondeni clay soils as a function of temperature (60 min contact time, 1.5 g dosage, 100 mL, 250 rpm, pH*i* = 6.111).

Figure 4.10: Percentage removal of fluoride by silica rich reddish black Mukondeni clay soils as a function of competing ions (60 min contact time, 9 mg/L, 1.5 g dosage, 25°C room temperature, 100 mL, 250 rpm, pH*i* = 6.587).

Figure 4.11: Percentage removal of fluoride by silica rich reddish black Mukondeni clay soils as a function of pH (60 min contact time, 1.5 g dosage, 9 mg/L F^-, 25°C room temperature, 100 mL , 250 rpm)

Figure 4.12: Langmuir adsorption isotherm for fluoride adsorption onto variegated silica rich reddish black Mukondeni clay soils (1.5 g adsorbent dosage, 60 min of equilibration time, concentration was varied from 1 – 15 mg/L, pHi = 6,111)

Figure 4.13. Freundlich adsorption isotherm for fluoride adsorption onto silica rich reddish black Mukondeni clay soils (1.5 g adsorbent, 60 min of equilibration time, concentration was varied from 1 – 15 mg/ L, pH*i* = 6,111)

Figure 4.14: The Dubinin–Radushkevich adsorption isotherm for fluoride adsorption onto silica rich reddish black Mukondeni clay soils (1.5 g of adsorbent, 60 min of equilibration time, concentration was varied from 1 – 15 mg/ L, pHi = 6,111)

Figure 4.15 (a) and (b): Adsorption kinetics for fluoride sorption onto silica rich reddish black Mukondeni clay soils (1 g dosage, 10 mg/L adsorbate concentration, 25°C room temperature, and 250 rpm, pH*i* = 6.423).

Figure 4.16: Data fit onto the Weber Morris intraparticle diffusion model (1 g dosage, 10 mg/L adsorbate concentration, 25°C room temperature, and 250 rpm, pH= 6.423).

© University of Venda

University of Venda
Creating Future Leaders

CHAPTER 5

Figure 5.1: Release of fluoride from raw bentonite clay with time (0.1 M NaOH, 1 g/50 mL S/L ratio, 250 rpm, 25°C room temperature)

Figure 5.2: Release of fluoride from raw bentonite clay with varied NaOH concentrations (60 min contact time, 1 g/50 mL S/L ratio, 250 rpm, 25°C room temperature)

Figure 5.3: Release of fluoride from bentonite clay with varied dosages (60 min contact time, 0.01 M NaOH, 1 g/50 mL S/L ratio, 250 rpm, 25°C room temperature)

Figure 5.4: pHpzc of raw bentonite clay (a) and iron(iii) oxide coated bentonite clay (b)

Figure 5.5: XRD diffractogram of raw bentonite and iron(III) oxide coated bentonite clay

Figure 5.6: Morphology of raw bentonite (a) and iron(III) oxide coated bentonite clay (b) at different magnifications

Figure 5.7: EDS analysis of the adsorbents: Raw bentonite (a) and iron(III) oxide coated bentonite clay (b).

Figure 5.8: Plot of pore volume against diameter for raw (a) and (b) iron(III) oxide coated bentonite clay

Figure 5.9: The FTIR spectra of raw and iron(III) coated bentonite clay

Figure 5.10: Removal of fluoride by iron(III) oxide coated bentonite clay as a function of contact time (0.5, 1 and 2 g , 10 mg/L F^- , 25°C room temperature, 100 mL solution, 250 rpm, pH*i* = 6.653)

Figure 5.11: Removal of fluoride by iron(III) oxide coated bentonite clay as a function of dosage (30 min contact time, 5, 10, 20 mg/L F^- , 25°C room temperature, 250 rpm pH*i* = 7.434)

Figure 5.12: Removal of fluoride by iron(III) oxide coated bentonite clay as a function of concentration (30 min contact time, 2 and 3 g, 25°C room temperature, 100 mL solution, 250 rpm pH*i* = 6.263)

Figure 5.13: Percentage removal of fluoride by iron(III) oxide coated clay as a function of temperature. (30 min contact time, 25°C room temperature, 3 g/100 mL S/L ratio, 250 rpm).

Figure 5.14: Percentage removal of fluoride by iron(III) oxide coated bentonite clay as a function of co-existing ions (30 min contact time, 20 mg/L F^- , 25°C room temperature, 3 g/100 mL S/L ratio, 250 rpm pHi = 6.474)

© University of Venda

University of Venda
Creating Future Leaders

Figure 5.15: Percentage removal of fluoride by iron(III) oxide coated bentonite clay as a function of pH (30 min contact time, 5 mg/L F^-, 25°C room temperature, 3 g/100 mL S/L ratio, 250 rpm)

Figure 5.16: Langmuir adsorption isotherm (3 g adsorbent, 30 min of equilibration time, concentration was varied from 5 – 80 mg/ L pH*i* = 6.263)

Figure 5.17. Freundlich adsorption isotherm (3 g adsorbent, 30 min of equilibration time, concentration was varied from 5 – 80 mg/L pH*i* = 6.263)

Figure 5.18. The Dubinin–Radushkevich adsorption isotherm (3 g of adsorbent, 30 min of equilibration time, concentration was varied from 5 – 80 mg/ L pH*i* = 6.263)

Figure 5.19: Plot of equilibrium constants against 1/T

Figure 5.20 (a) and (b): Adsorption kinetics for fluoride sorption onto iron (III) oxide coated bentonite clay as a function of contact time (0.5, 1 and 2 g , 10 mg/L F- , 25°C room temperature, 100 mL fluoride solution, 250 rpm pH*i* = 6.653)

Figure 5.21: Data fit into (a) Intraparticle diffusion model and (b) External diffusion model (0.5, 1 and 2 g , 10 mg/L F^-, 25°C room temperature, 100 mL fluoride solution, 250 rpm pH*i* = 6.653)

Figure 5.22: Regeneration studies using 0.01 M NaOH (10 mg/L F^-, 100 mL solution, 2 g adsorbent dosage)

CHAPTER 6

Figure 6.1: Iron oxide (III) coated bentonite –silica rich reddish black Mukondeni clay soil composite pellets before (a) and after calcination (b,c,d)

Figure 6.2: XRD diffractogram of iron(III) oxide coated bentonite – silica rich reddish black Mukondeni clay soil composite pellets at 100, 600, 700, 800 and 900°C

Figure 6.3: SEM micrographs of iron(III) oxide coated bentonite – silica rich reddish black Mukondeni clay soil composite pellets at different calcination temperatures ((a) - 100, (b) - 600 and (c) - 800°C)

Figure 6.4: EDS spectrum of iron(III) oxide coated bentonite – silica rich reddish black Mukondeni clay soil composite pellets at different calcination temperatures ((a) - 100, (b) - 600 and (c) - 800°C)

© University of Venda

University of Venda
Creating Future Leaders

Figure 6.5: Morphology of iron(III) oxide coated bentonite – silica rich reddish black Mukondeni clay soil composite pellets at two magnifications and different firing times ((a) – 1 h, (b) – 2 h and (b) - 3 h)

Figure 6.6: SEM - EDS of iron(III) oxide coated bentonite – silica rich reddish black Mukondeni clay soil composite pellets at different firing times ((a) – 1 h, (b) – 2 h and (b) - 3 h)

Figure. 6.7: TEM images of iron(III) oxide coated bentonite – silica rich reddish black Mukondeni clay soil composite pellets at two magnifications and different firing times ((a) – 1 h, (b) – 2 h and (b) - 3 h)

Figure 6.8: The FTIR spectra of iron(III) oxide coated – silica rich reddish black Mukondeni clay soil composite pellets at different firing times ((a) – 1 h, (b) – 2 h and (b) - 3 h).

© University of Venda

University of Venda
Creating Future Leaders

LIST OF TABLES

CHAPTER 2

Table 2.1: The drinking water standards for fluoride specified by various authorities

Table 2.2: Different clay soils and their adsorption capacities in water defluoridation

CHAPTER 4

Table 4.1: Cation Exchange Capacity of variegated reddish black Mukondeni clay soils at pH 5.4 and 7.4

Table 4.2: Elemental composition of silica rich reddish black Mukondeni clay soils

Table 4.3: Surface area, pore volume and pore size of silica rich reddish black Mukondeni clay soils

Table 4.4: Adsorption of fluoride onto silica rich reddish black Mukondeni clay soils under field pH and optimized pH conditions.

Table 4.5: Concentration of metals before and after treatment with silica rich reddish black Mukondeni clay soils

Table 4.6: Leaching of metals into solution after defluoridation at pH 2, 6 and 12

Table 4.7: Adsorption isotherm parameters

Table 4.8: Activation energy values of removal of fluoride by silica rich Mukondeni clay soils

Table 4.9: Pseudo-second-order kinetic parameters for different adsorbent dosages for fluoride removal silica rich reddish black Mukondeni clay soils

Table 4.10: Comparison of different adsorption capacities of different clay adsorbents for fluoride

CHAPTER 5

Table 5.1: Surface areas of iron(III) oxide coated bentonite clay using various NaOH concentrations

Table 5.2: Cation Exchange Capacity of raw bentonite and iron(III) oxide coated bentonite clay

Table 5.3: Elemental composition of raw and iron(III) oxide coated bentonite clay

© University of Venda

University of Venda
Creating Future Leaders

Table 5.4: Surface area, pore volume and pore sizes of raw and iron(III) oxide coated bentonite clay

Table 5.5: Percentage fluoride removal and adsorption capacity by iron(III) oxide coated bentonite clay at various temperatures

Table 5.6: Adsorption of fluoride onto by iron(III) oxide coated bentonite clay under field and optimized conditions.

Table 5.7: Concentration of metals before and after treatment with iron(III) oxide coated bentonite clay

Table 5.8: Concentration of metals in solution after defluoridation at pH 2, 6 and 12

Table 5.9: Comparison of the percentage removal capacities of raw bentonite clay and iron(III) oxide coated bentonite clay.

Table 5.10: Langmuir, Freundlich and Dubinin-Radushkevich isotherm parameters for the sorption of fluoride onto iron(III) oxide coated bentonite clay

Table 5.11: Thermodynamic parameters

Table 5.12: Pseudo-second-order kinetic parameters for different adsorbent dosages for fluoride removal by iron(III) oxide coated bentonite clay

Table 5.13: Kinetic parameters of the fluoride adsorption onto iron(III) oxide coated bentonite clay

Table 5.14: Comparison of different adsorption capacities of different clay adsorbents for fluoride

CHAPTER 6

Table 6.1: Percentage weight of minerals in iron(III) oxide coated bentonite –silica rich reddish black Mukondeni clay soil composite pellets at different calcination temperatures

Table 6.2: Surface area, pore volume and pore sizes for iron(III) oxide coated bentonite – silica rich reddish black Mukondeni clay soil composite pellets at different temperatures

Table 6.3: Adsorption performance of iron(III) oxide coated bentonite – silica rich reddish black Mukondeni clay soil composite pellets at different temperatures.

Table 6.4: Mineralogical composition iron(III) oxide coated silica rich reddish black Mukondeni clay soil composite pellets at different times

Table 6.5: Elemental composition of iron(III) oxide coated – silica rich reddish black Mukondeni clay soil composite pellets at different firing times

© University of Venda

University of Venda
Creating Future Leaders

Table 6.6: Surface area, pore volume and pore sizes for iron(III) oxide coated bentonite – silica rich reddish black Mukondeni clay soil composite pellets at different temperatures

Table 6.7: Adsorption performance of iron(III) oxide coated bentonite – silica rich reddish black Mukondeni clay soil composite pellets at different firing times.

Table 6.8: Adsorption performance of iron(III) oxide coated bentonite silica rich reddish black Mukondeni clay soil composite pellets at different clay ratios.

© University of Venda

University of Venda
Creating Future Leaders

CHAPTER ONE

INTRODUCTION

1.1 Background information

The rural drinking water supply programme in South Africa was estimated to have 3.7 million boreholes that are dependent on groundwater by early 2004 (Water Research Commission, 2008). This obviously led to a decrease in water borne disease incidences. However, it has led to the emergence of a number of other problems including, pathogenic contamination of drinking water sources as a result of poor borehole construction set ups and unsanitary conditions and the excessive presence of chemical constituents like fluoride and arsenic, which have posed major environmental issues and a health problem. Different studies have shown that the occurrence of dental fluorosis in the majority of cases in South Africa are related to the fluoride content of groundwater used for drinking purposes (McCaffrey, 1993; WRC, 2001; Odiyo and Makungo, 2012).

Fluoride in drinking water may be beneficial or detrimental depending on its concentration and the total amount ingested. Fluoride is beneficial especially to young children below eight years of age when present within permissible limits of 1.0 – 1.5 mg/L for calcification of the dental enamel (Tomar, et al., 2014). Excess fluorides on the other hand cause dental fluorosis and/or skeletal fluorosis (Tomar, et al. 2014). South African standards for drinking water recommend an acceptable fluoride concentration of 1.5 mg/L (Department of Water Affairs and Forestry, 1996). The same guiding value of 1.5 mg/L for fluoride in drinking water has also been set by the World Health Organisation (WHO, 2011). Therefore, mitigation of fluorosis is a very significant area of research and needs continued attention until a reliable defluoridation technology is developed.

Technologies applied for the removal of excess fluoride from groundwater can be divided into two main categories, namely precipitation and adsorption. Precipitation processes involve the addition of chemicals and formation of fluoride precipitates. Among these are precipitations with calcium and aluminium salts (Feenstra, et al., 2007). In the adsorption method, raw water is passed through a bed containing the defluoridating material. The material retains fluoride either by physical, chemical or ion exchange mechanisms. The adsorbent gets saturated after a period of operation and requires regeneration. Precipitation

© University of Venda

methods however have many limitations which include, daily addition of chemicals, large volumes of sludge production and not being effective with water sources having high total dissolved solids and hardness (Ramdani, et al., 2010). The adsorption process is extensively used and gives satisfactory results (Cai, et al., 2015; Wang, et al., 2015; Wang, et al., 2013). For this reason adsorption seems to be a more attractive method for defluoridation in terms of cost, simplicity of design and operation. Moreover, the adsorbent can be easily regenerated and reused (Nur, et al., 2014; Shan and Guo, 2013; Teutli-Sequeira, et al., 2013).

Various naturally occurring materials that are available and abundant have been explored as adsorbents for the removal of fluoride from water (Paudyal, et al., 2013, Tomar, et al., 2014, Cai, et al., 2015). A great interest has grown towards naturally occurring adsorbents, preferably the development of an adsorbent demonstrating both a high adsorption capacity and low cost for removing inorganic contaminants from contaminated waters. Although a wide variety of adsorbents have been used for defluoridation, naturally available clays have been the adsorbents of choice in most developed countries (Mlilo, et al., 2010; Srinivasan, 2011; Atasoy and Ahin, 2013). It is extremely important to choose a technique that is cheap, requires only minor workloads and at the same time it should not be too complicated for uneducated people. Obviously it should not impart any adverse taste to the treated water and the maintenance and repair should be easy and affordable. Using clay minerals and soils for defluoridation fits well with all the above mentioned factors.

Bentonite clay is one of these low cost adsorbents which can be used for defluoridation. It belongs to the class of the aluminosilicate clays, which comprises of layers of aluminosilicate sheets. Bentonite clay typically contains SiO_2, Al_2O_3 and oxides of Mg, Ca and K which might contribute towards the fluoride adsorption. Srimurali, et al. (1998) reported that, low cost bentonite clay for fluoride removal from drinking water, showed a maximum of 46 % fluoride removal at an initial fluoride concentration of 5 mg/L and a pH of 2.8. Gitari, et al. (2013) modified bentonite clay with Fe^{3+} and the study showed that modification of the bentonite with Fe^{3+} increased the surface area and micropore area of the bentonite clay. Fe^{3+} bentonite was observed to be a suitable adsorbent for fluoride from aqueous solution as compared to raw bentonite.

In the Limpopo province of South Africa, Mukondeni clay soils have been used for pottery making and ceramic water filters for a very long time but their physicochemical

© University of Venda

University of Venda
Creating Future Leaders

characteristics had never been evaluated to determine how suitable they are for water treatment applications. Mukondeni clay soils have recently been getting more attention in water treatment applications (Denga, 2013; Abebe, et al., 2014). Thus, it becomes significant that the basic characteristics of these soils are evaluated and their scientific application in the treatment of water be assessed. Moreover these clay soils are locally and readily available, hence a breakthrough in their ability to remove contaminants from drinking water will come as an advantage to the local community most of whom are poor and cannot afford expensive water treatment methods.

This study seeks to determine the possibility of developing a low cost composite adsorbent from the locally available bentonite clay and Mukondeni clay soils which can effectively remove fluoride from water without altering the water quality beyond recommended DWS quality standards. Treatment by large scale and advanced defluoridation technologies has the disadvantage of being expensive in both plant construction and operation and maintenance costs (Vinati, 2015). It is such problems that force scientists to search for simple, available and economically affordable defluoridation techniques to protect rural communities from fluoride related problems. The main aim of this study is to develop a cheap adsorbent material which is cost effective and available to the general public at household level.

1.2 Problem statement

Human fluorosis in various regions of South African rural areas has been reported to occur as a result of consuming groundwater that has been contaminated by fluoride (Ncube and Schutte, 2005; WRC, 2008; Odiyo and Makungo, 2012). Acceptable amounts of fluoride in drinking water have a beneficial effect on the rate of occurrence of dental fluorosis, particularly among children however, excess intake of fluoride leads to various forms of fluoride related health problems (Kumar, et al., 2011). Such health problems related to the consumption of water with excessive fluoride are a general environmental concern especially in rural areas where boreholes still remain a major source of drinking water.

© University of Venda

1.3 Significance of study

Since fluorosis is one of the frequently occurring endemic disease, it follows that providing communities with adequately partially defluoridated water will reduce the prevalence and severity of fluorosis in affected areas. Many investigations have been done on how to remove the excess fluoride in drinking water. However, low cost defluoridation techniques that can be used by rural communities are hardly available. Therefore, the viable option is to look for locally available and cost-effective fluoride adsorbents. Therefore it is of utmost importance that naturally occurring clays be assessed for their potential in water defluoridation hence this study seeks to investigate the fluoride removal efficiency of iron(III) oxide coated bentonite clay and silica rich reddish black Mukondeni clay soils.

1.4 Research objectives

1.4.1 General objective

To fabricate an iron(III) oxide coated bentonite clay – silica rich reddish black Mukondeni clay soils ceramic composite adsorbent for the defluoridation of groundwater.

1.4.2 Specific objectives

- To evaluate the physicochemical and mineralogical properties of bentonite and Mukondeni clay soils.
- To evaluate the feasibility of activating bentonite clay with NaOH and coating its surfaces with iron(III) oxides.
- To evaluate the optimum conditions for removing fluoride from borehole water by iron(III) oxide coated bentonite clay and silica rich reddish black Mukondeni clay soils using batch experiments.
- To determine the adsorption mechanisms, kinetics and thermodynamics of the fluoride onto the iron(III) oxide coated bentonite clay and silica rich reddish black Mukondeni clay soils.

© University of Venda

University of Venda
Creating Future Leaders

1.5 Research questions

- What are the physicochemical and mineralogical properties of bentonite and Mukondeni clay soils?
- How feasible is it to activate bentonite clay with NaOH and to coat its surfaces with iron(III) oxides?
- Which conditions are optimum for removing fluoride from borehole water by iron(III) oxide coated bentonite clay and silica rich reddish black Mukondeni clay soils using batch experiments?
- What are the adsorption mechanisms, kinetics and thermodynamics of the fluoride onto the iron(III) oxide coated bentonite clay and silica rich reddish black Mukondeni clay soils?

1.6 Hypothesis

Iron(III) oxide coated bentonite clay – silica rich reddish black Mukondeni clay soils ceramic composite can remove excess fluoride from groundwater.

1.7 Assumption

It is assumed that the borehole water in Siloam, Nzhelele will be the representative of high fluoride borehole water across South Africa.

UNIVERSITY OF VENDA
LIBRARY

© University of Venda

University of Venda
Creating Future Leaders

1.8 References

Abebe, L.S., Smith, J.A., Narkiewicz, S., Oyanedel-Craver, V., Conaway, M., Singo, A., Samie, A., Mojapelo, P., Brant, J. and Dillingham, R., 2014. Ceramic water filters impregnated with silver nanoparticles as a point-of-use water-treatment intervention for HIV-positive individuals in Limpopo Province, South Africa: A pilot study of technological performance and human health benefits. *Journal of Water and Health,* 12(2), pp. 288-300.

Atasoy, A.D. and Ahin, O. M., 2013. Adsorption of fluoride on the raw and modified cement clay. *Clean.* doi:10.1002/clen.201300074.

Denga, M.E., 2013. Evaluation of the fluoride adsorption capacity of locally available clay in Vhembe district. A thesis submitted to the Department of Ecology and Resource Management, School of Environmental Sciences. University of Venda.

DWAF. 1996. South African Water Quality Guidelines. Volume 1: Domestic Water Use Second Edition.

Cai, H., Chen, G., Peng, C., Zhang, Z., Dong, Y., Shang, G., Zhu, X., Gab, C. and Wan. X., 2015. Removal of fluoride from drinking water using tea waste loaded withAl/Fe oxides: A novel, safe and efficient bio sorbent. *Applied Surface Science,* 328, pp. 34 – 44.

Feenstra, L., Vasak, L. and Griffioen J., 2007. Fluoride in groundwater: Overview and evaluation of removal methods. International groundwater resources assessment centre. Report nr. SP 2007-1.

Gitari, W.M., Ngulube, T., Masindi, V. and Gumbo J.R., 2013. Defluoridation of groundwater using Fe^{3+} modified bentonite clay: optimization of adsorption conditions, *Desalination and Water Treatment*, DOI: 10.1080/19443994.2013.855669.

Kumar, E., Bhavnagar, A., Kumarc, U. and Sillanpaad, M., 2011. Defluoridation from aqueous solutions by nano-alumina: Characterization and sorption studies. *Journal of Hazardous Materials*, 186, pp. 1042 – 1049.

McCaffrey, L.P. and Willis, J.P., 1993. Distribution of fluoride-rich groundwater in the eastern parts of Bophuthatswana, relationship to bedrock and soils and constraints on drinking water supplies: a preliminary report. Africa Needs Ground Water. An International Ground Water Convention, 1, pp. 1- 8.

UNIVERSITY OF VENDA
LIBRARY

© University of Venda

Mlilo, T.B., Brunson, L.R. and Sabatini, D.A., 2010. Arsenic and fluoride removal using simple materials. *J. Environ. Eng,* 136 (4), pp. 391–398.

Ncube, E. J. and Schutte, C.F., 2005. The occurrence of fluoride in South African groundwater: A water quality and health problem. *Water SA*. 31(1), pp. 35 – 40.

Nur, T., Loganathan, P., Nguyen, T.C., Vigneswaran, S., Singh, G and Kandasamy, J., 2014. Batch and column adsorption and desorption of fluoride using hydrous ferric oxide: solution chemistry and modeling, *Chemical Engineering Journal,* 247, pp. 93 –102.

Odiyo, J.O and Makungo, R., 2012. Fluoride concentrations in groundwater and impact on human health in Siloam Village, Limpopo Province, South Africa. *Water SA,* 38 (5), pp. 731 –736.

Paudyal, H., Pangeni B., Inoue, K., Kawakita, H., Ohto, K., Ghimire, K.N., Harada, H. and Alam, S., 2013. Adsorptive removal of trace concentration of fluoride ion from water by using dried orange juice residue. *Chemical Engineering Journal*, 223, pp. 844 – 853.

Ramdani, A., Taleb, S., Benghalem, A. and Ghaffour, N., 2010. Removal of excess fluoride ions from Saharan brackish water by adsorption on natural materials. *Desalination,* 250, pp. 408 – 413.

Shan, Y. and Guo, H., 2013. Fluoride adsorption on modified natural siderite: optimization and performance. *Chem. Eng. J*, 223, pp. 183 – 191.

Srimurali, M., Pragathi, A. and Karthikeyan, J., 1998. A study on removal of fluorides from drinking water by adsorption onto low-cost materials. *Environmental Pollution*, 99(2), 285 - 289.

Srinivasan, R., 2011. Advances in Application of Natural Clay and Its Composites in Removal of Biological, Organic, and Inorganic Contaminants from Drinking Water. *Advances in Materials Science and Engineering.* pp. 1 - 17.

Teutli-Sequeira, A., Martinez-Miranda,V., Solache-Rios, M and Linares- Hernandez, I., 2013. Aluminum and lanthanum effects in natural materials on the adsorption of fluoride ions, *J. Fluorine Chem*. 148, pp. 6 – 13.

© University of Venda

University of Venda
Creating Future Leaders

Tomar, V., Prasad, S., Kumar, D., 2014. Adsorptive removal of fluoride from aqueous media using citrus limonum (lemon) leaf. *Microchem. J.* 112, pp. 97 – 103.

Wang, J., Kang, D., Yu, X., Ge, M. and Chen, Y., 2015. Synthesis and characterization of Mg–Fe–La trimetal composite as an adsorbent for fluoride removal. *Chemical Engineering Journal*, 264, pp. 506 – 513.

Wang, J., Xu, W., Chen, L., Jia, Y., Lei Wang, L., Huang, X and Liu, J., 2013. Excellent fluoride removal performance by CeO2–ZrO2 nanocages in water environment. *Chemical Engineering Journal*, 231, pp. 198 – 205.

Vinati, A.B., Mahanty, B and Behera S.K., 2015. Clay and clay minerals for fluoride removal from water: A state-of-the-art review. *Applied Clay Science*, 114, pp. 340 – 348.

World Health Organization. 2011. Guidelines for drinking-water quality - 4th ed. ISBN 978 92 4 154815 1.

WRC. 2001. Distribution of Fluoride-Rich Groundwater in the Eastern and Mogwase Regions of the Northern and North-West Province. WRC Report No. 526/1/01 1.1 - 9.85 Pretoria. South Africa.

WRC. 2008. Knowledge for Growth on Development: Knowledge Review 2007/08. Water Research Commission, Pretoria.

© University of Venda

University of Venda
Creating Future Leaders

CHAPTER 2

REVIEW OF LITERATURE

2.0 Introduction

This chapter seeks to explore literature on the removal of fluoride from groundwater. An overview of previous studies on bentonite, clay soils and other adsorbents used to remove fluoride in aqueous solutions will be given. The literature review will also give a brief summary of processes for fluoride removal from groundwater and point of use systems for defluoridation of groundwater/appropriate technologies for defluoridation.

UNIVERSITY OF VENDA
LIBRARY

2.1 Fluoride

2.1.1 Chemistry and environmental occurrence

Fluoride is an ion of the chemical element fluorine which belongs to the halogen group. Fluorine is the most highly reactive element of the halogen family. According to Choudhary and Kar (1996), it has been estimated that fluorine is the seventeenth most abundant element constituting about 0.065 % of the earth's crust. Fluorine does not exist as a free element. It exists in water mainly as fluoride associated with monovalent cations such as NaF and KF that are water soluble, while those forms with divalent cations such as CaF_2 and PbF_2 are generally insoluble in water.

Naturally, fluoride is present in rocks and minerals. It occurs especially in most igneous rocks. Fluoride most abundantly occurs in nature as fluorite (CaF_2) and crinoline, a fluoride of aluminium and sodium (Na_3AlF_3) (Rowhani, 1986). It is also common in fluorspar and fluorapatite, a calcium fluorophosphate mineral. Other minerals include various micas, amphiboles, tourmalite, topaz, fluocerite and apophyllite (Ncube, 2002). Due to the weathering of such rocks, fluoride contaminates the ground water. Apart from natural sources, fluoride contamination is due to the effluents coming from various industries like the fertilizer industry, glass industry and semiconductor industry (Yakub and Soboyejo 2013).

© University of Venda

University of Venda
Creating Future Leaders

2.1.2 Fluoride chemistry in water

Shrikant and Nitin (2012) observed that, the fluoride content of surface and ground water is a function of many factors such as availability and solubility of the parent fluoride minerals with which this water comes in contact with, rock porosity, velocity of flowing water, temperature of the interactions between the rocks and the water, pH of the water and concentration of the calcium ions present in the water. When a fluoride compound is dissolved in water, the element fluorine will be present mainly as fluoride ions. However, depending on the ionic concentrations and pH of the solutions the fluoride is also present in solution as HF_2 and undissociated HF (Killedar and Bhargava, 1998).

2.2 Fluoride and human health

Fluoride is an ion of environmental concern and is regulated in the water supply. The presence of fluoride in drinking water has both beneficial and detrimental impacts on human health depending on its concentration (Ayoob and Gupta, 2006; Maiti, et al., 2011). In domestic water supply as well as in the industrial supply used in the food and beverage industries, fluoride concentrations should not exceed the required levels. High levels of fluoride in drinking water may cause dental and skeletal fluorosis. In various African countries, such as Kenya, Tanzania and certain parts of South African provinces (North West, Northern Cape and Limpopo) there are very high levels of fluoride in groundwater (as high as 30 mg/L) causing numerous cases of dental fluorosis in affected inhabitants, who source drinking water from untreated groundwater (Coetzee, et al., 2006).

At levels below 1 mg/L, it may result in problems like dental caries. World Health Organization (WHO) recommends it in the range of 0.5 – 1.5 mg/L (WHO, 2011). The South African permissible limit is also 1.5 mg/L (DWA, 2011). However, some countries, for example Tanzania, allow consumption of drinking water with the concentration of up to 8 mg/L of fluoride in areas with no alternative water sources (Kaseva, 2006). Thus the requirement of fluoride content varies among countries and depends on the geography and the age of people involved.

The drinking water standards for fluoride specified by various authorities are given in Table 2.1.

© University of Venda

University of Venda
Creating Future Leaders

Table 2.1: The drinking water standards for fluoride specified by various authorities

Authority	Permissible limit of fluoride concentration (mg/L)
World Health Organization, (2011)	0.5 - 1.5
United States Public Health, (2010)	0.7 – 1.2
Department of Water Affairs, (2011)	0.0 – 0.1

2.2.1 The fluoride problem in South Africa

The problems of fluoridation, fluorides and fluorosis in South Africa have been talked about since 1935. Some research studies include the following: Maughan-Brown (1935); Staz (1938) and Abrahams (1946) reported the presence of fluorosis amongst children in high fluoride areas. The most comprehensive work was undertaken by Ockerse (1941) and Ockerse and Meyer (1941) where they delineated areas of endemic fluorosis, the levels of fluoride in the different areas in South Africa and observed the occurrence of dental caries in these areas.

(Ockerse, 1941) recorded that in the endemic areas only 28 per cent, of the children showing mottled enamel had any dental caries, whereas in those same areas 69 per cent, of the children not showing mottling had one or more carious teeth. Considerable space is given to an account of the skeletal changes found in chronic fluorine poisoning. Several people showing such changes were seen in Gauteng, Limpopo, Northwest and Mpumalanga provinces, by then, the Transvaal Province had areas with about 9 to 11 mg/L of fluorine in the drinking water.

In the Northern Cape Province, Ockerse (1941) found a much higher prevalence of dental caries in Upington compared to Kenhardt and Pofadder areas. Fluorosis prevalence also varied according to the fluoride content of the drinking water. He concluded that, fluorosis is prevalent in certain areas in and around Kenhardt and Pofadder, fluorosis is so severe that it is a predisposing cause of dental caries.

In the Pilanesberg area (North West Province) Ockerse and Meyer (1941) found fluoride in the drinking water varied between 0.33-35 mg/L. They also found that climatic conditions influence fluoride levels i.e. lower after heavy rain. This could also explain why at higher

© University of Venda

levels of fluoride 10.45 mg/L only moderate and not as expected severe fluorosis was observed (lower fluoride levels during early calcification).

According to (WHO, 2004), North West, Limpopo, and Northern Cape have been identified as provinces displaying high levels of fluoride in groundwater, often as high as 30 mg/L. Ncube and Schutte (2005) assessed groundwater fluoride data from the Department of Water Affairs and Forestry's Water Management System database for the period 1996 – 2000, in order to establish the distribution of fluoride ion concentrations in groundwater and the impact of dietary fluoride on dental health in South Africa. The results indicated that the problem of high fluoride ion concentrations is prevalent in Limpopo, Northern Cape, North-West and KwaZulu-Natal Provinces, where large populations still live in rural areas and mostly use groundwater for drinking purposes. These results also corroborates with those of WHO (2002).

Another study was done in Limpopo province by Odiyo and Makungo (2012). They sampled ground water from three different sites in Siloam village i.e. the community borehole (GW1), an artesian spring (GW2) and private borehole (GW3) for the periods August–November 2006 and January–May 2007. They found the mean fluoride concentrations for GW1, GW2 and GW3 to be 5.1, 5.6 and 1.7 mg/L respectively. The fluoride concentrations in all the sampling points were higher than the DWAF (1996) and WHO (2011) guidelines for domestic use of 1 mg/L and 1.5 mg/L, respectively.

A WRC-funded study published in 2008 also investigated the health and nutritional status of sections of the Northern Cape population in relation to fluoride concentrations in drinking water (WRC, 2008). The findings showed the presence of fluorosis in different parts of the province varied from mild to severe, with Kamassies, Liliefontein and the peri-urban areas around Kimberly having particularly high frequencies of mild fluorosis. The mild fluorosis prevalent in these areas and, to a lesser extent in Kimberly itself, was inspite of low levels of fluoride (about 0.34 mg/L). The explanation for the greater than expected occurrence of mild fluorosis could lie in the uptake of supplementary fluoride through toothpastes and milk. The Northern Cape study indicated that fluoride levels of around 0. 3 mg/L generally have beneficial effect on permanent teeth, but have little effect on the primary teeth of young children (Moola, 2008).

The concentration of fluoride in the drinking water is therefore considered of substantial significance from a public health point of view and thus in response to the ever growing need

© University of Venda

to meet the legal requirements of fluoride levels, many methods of defluoridation have been developed.

2.3 Sustainable water defluoridation technologies

According to Nemade, et al. (2002), numerous commercial methods have been described employing various materials for the fluoride removal since 1930. For practical and financial reasons, however, high-technology water treatment is unavailable in many rural areas. Priority, therefore, should be given to the development of simple devices for defluoridation of drinking water at a preferentially home based level (Nemade, et al. 2002). A number of methods have been proposed for the defluoridation of water. Defluoridation devices should meet a number of the following requirements: modest investment, low maintenance cost, simple design, operationable by villagers, is able to reduce the fluoride content to permissible limits and improve the water quality in general. No single method seems to meet with all the requirements, but some techniques are more widely used than others.

2.3.1 The concept of appropriate technology

"Appropriate" means that besides being scientifically sound the technology should be acceptable to those who apply it and to those for whom it is used. This implies that technology should be compatible with the local culture. It must be capable of being adapted and further developed if necessary. In addition, it should preferably be easily understood and applied by community health workers and in some instances even by individuals in the community. Although different forms of technology are appropriate at different stages of development, their simplicity is always desirable. The most productive approach for ensuring that appropriate technology is available is to start with the problem and then to seek, or if necessary develop, a technology which is relevant to local conditions and resources (WHO, 1978).

An in-depth analysis of defluoridation research reveals that very few proven sustainable solutions have been developed so far. The adsorption/ion exchange processes are still the most widely used for fluoride removal techniques practiced in endemic areas of the developing countries (Nemade, et al., 2002; Thole, 2012; Vinati, et al., 2015). The Nalgonda technique and adsorption by bone char or a combination of both have been used in many

© University of Venda

countries like India and Tanzania at both domestic and community levels (Dahi, et al., 1996). Of late a major shift has occurred in the perception of people in India towards community based water supply treatment systems, with many preferring domestic defluoridation units (DDUs), especially using activated alumina. However, these DDUs are not available to the people in the fluoride endemic rural areas. Other techniques like reverse osmosis, electro coagulation, electrodialysis and nano filtration assure good quality water but are of high technology and high cost options for most of the fluoride endemic areas (Gosh, 2005).

Appropriate technologies (Nalgonda technique, Dahi, et al., 1996; adsorption using bone char Mjengera and Mkongo, 2003) have been applied in many parts of the world where endemic fluorosis is a problem. These countries include India, Thailand, Kenya, Tanzania and Ethiopia. High fluoride levels occur in ground waters in some parts of Africa however the East African countries have higher levels compared to the Southern African countries. In Tanzania for example, fluoride concentrations in ground water of up to 40 mg/L have been reported hence in such countries the use of appropriate technologies is most popular (Thole, 2012).

(a) Water defluoridation research in fluoride endemic areas in Africa.

The removal of fluoride from water has been researched on employing a number of materials among which are bauxite, gypsum, magnesite and their composite filters (Thole, et al. 2011a; Thole, et al. 2011b; Thole, et al. 2012). Calcium chloride ($CaCl_2$) and Sodium dihydrogen phosphate (NaH_2PO_4) as co-precipitation reagents in contact precipitation (Dahi, 1996; Dahi, 1997) cow bone char in batch and fixed bed (Mjengera and Mkongo, 2003; Bregnhoj, et al. 1997) activated carbon and activated carbon loaded separately with alumina, magnesia and calcium (Bablia, 1996).

The technology best demonstrated in Tanzania is the use of bone char at household level in a fixed bed. The bone char has high sorption capacity initially; however the media gets saturated with fluoride with time. The general practice around Arusha (Tanzania) is to replace the media when the effluent has a fluoride concentration of 2 mg/L, the maximum permissible limit as per International Reference Centre (IRC) in Hague, Netherland. The common set up shows that defluoridation of water with initial fluoride of 10 mg/L can treat up to about 1300 L of water with fluoride less than 2 mg/L. The mass of bone char used in

© University of Venda

such an investigation is 4 kg. Based on use of 20 L per family per day of the treated water, the 4 kg of bone char can be employed to treat water for sixty five days family use. This approximates to 20 to 25 kg of bone char in a year for a family (Dahi, 1996).

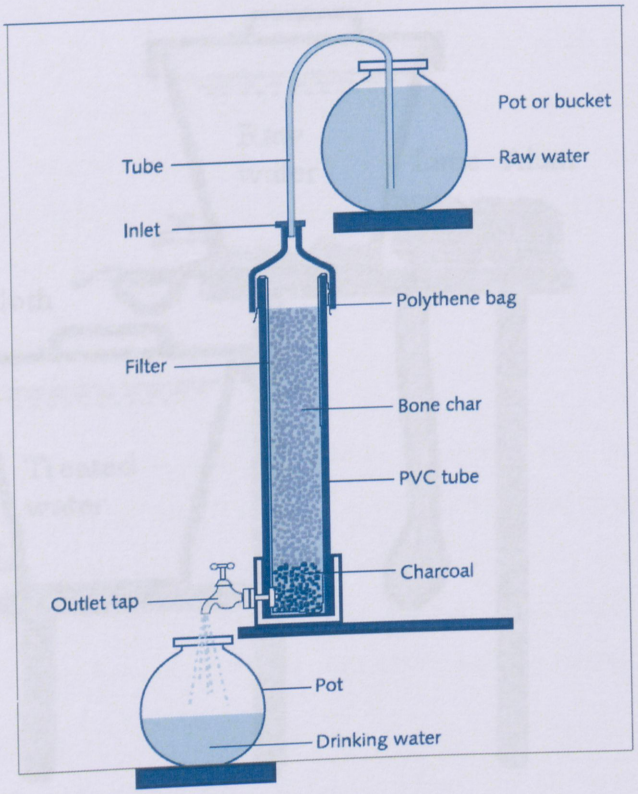


Figure 2.1: Bone char domestic defluoridator (Wondimagegn, 2008)

UNIVERSITY OF VENDA
LIBRARY

(i) Nalgonda technique for domestic defluoridation

The Nalgonda Technique has been introduced in African villages and studied at pilot scale in Kenya, Senegal and Tanzania (Dahi, 1996). Any container of 20 -50 L capacity is suitable for this purpose. A tap, fitted 3-5 cm above the bottom of the container is useful to withdraw treated water. Adequate amounts of lime water and bleaching powder are added to raw water and mixed well. Alum solution is added to it and stirred for 10 min. The contents are allowed to settle for 1 h and the clear water is withdrawn either through the tap or decanted slowly, without disturbing the sediment and filtered (Dahi, et al., 1996). The settled sludge may be discarded away from the source of water or preferably collected and sent for recycling. With domestic treatment, there is no capital investment and the cost of the treatment is only that of

© University of Venda

University of Venda
Creating Future Leaders

the chemicals. Of late, stainless steel defluoridation filters, which function on the Nalgonda technique, are developed to be used at domestic level (Hiremath, 2006; Mariappan and Vasudevan, 2011).

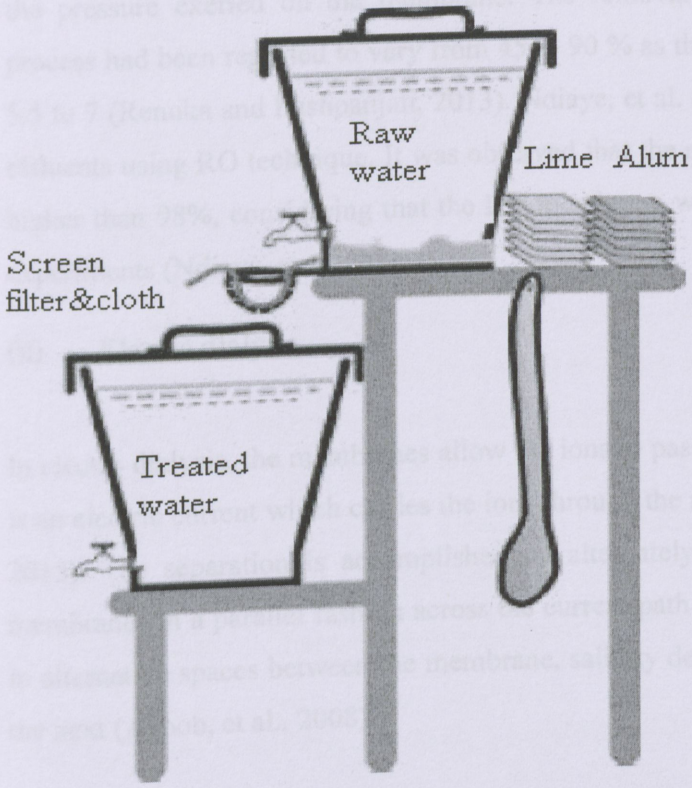


Figure 2.2: The Nalgonda defluoridation as adopted for domestic use in Tanzania (Dahi, 2000)

2.3.1 The techniques

Defluoridation methods using organic or inorganic substances in many laboratories and field studies nowadays are summarized as follows:

2.3.1.1 Membrane filtration processes

Reverse osmosis and electro dialysis are two membrane filtration processes which are widely used for the removal of fluoride in water (Ayoob, et al., 2008).

(i) Reverse osmosis

© University of Venda

University of Venda
Creating Future Leaders

Renuka and Pushpanjali (2013) reported that, in reverse osmosis, the hydraulic pressure is exerted on one side of the semi permeable membrane which forces the water across the membrane leaving the salts behind. The relative size of the pollutants left behind depends on the pressure exerted on the membrane. The removal of fluoride in the reverse osmosis process had been reported to vary from 45 to 90 % as the pH of the water can be raised from 5.5 to 7 (Renuka and Pushpanjali, 2013). Ndiaye, et al. (2005) studied fluoride removal from effluents using RO technique. It was observed that the rejection of fluoride ion was typically higher than 98%, considering that the RO membrane was fully regenerated after each set of experiments (Ndiaye, et al., 2005).

(ii) Electro dialysis

In electro dialysis, the membranes allow the ions to pass but not the water. The driving force is an electric current which carries the ions through the membranes (Renuka and Pushpanjali, 2013). The separation is accomplished by alternately placing cation and anion selective membranes in a parallel fashion across the current path to form an electro dialysis cell. Thus in alternative spaces between the membrane, salinity decreases in one space and increases in the next (Ayoob, et al., 2008).

UNIVERSITY OF VENDA
LIBRARY

2.3.1.2 Precipitation processes

According to Feenstra, et al. (2007), precipitation processes involve the addition of chemicals and formation of fluoride precipitates. Among these are precipitations with calcium and aluminium salts. Chemicals must be added daily in batches and precipitation techniques produce a certain amount of sludge every day. Defluoridation by precipitation can be grouped into two types which are: precipitation of fluoride by a suitable reagent through a chemical reagent and co precipitation of fluoride, which involves its simultaneous precipitation with a macro–component from the same solution through the formation of mixed crystals by adsorption or occlusion or mechanical entrapment.

(a) Precipitation of fluoride

(i) Lime

Addition of lime ($Ca(OH)_2$) or other calcium salts ($CaSO_4$ and $CaCl_2$) can be used to precipitate fluoride as insoluble CaF_2 and is the cheapest and most commonly used

© University of Venda

precipitation technique for defluoridation but principally used for high fluoride containing waste waters (Huang and Liu, 1999; Hu, et al., 2003).

The precipitation reaction using lime is as follows:

$$Ca(OH)_2 + 2F^- \rightarrow CaF_2 + 2OH^- \quad \ldots\ldots\ldots\

An ion exchange mechanism whereby F^- is exchanged with OH groups in the mineral structure is generally assumed to be the rate determining step in the adsorption process. This ion exchange process can be presented by the following equilibria:

$$MOH_2 + F^- \leftrightarrow MF + H_2O \quad \ldots\ldots\ldots\

temperature affects several factors which are important in the adsorption process. According to Robert (1988), for complete miscible systems, selective adsorption generally decreases with rise in temperature. It is the expected effect for an exothermic process. The physicochemical nature of the adsorbent can have profound effects on both rate and capacity for adsorption. Whereas solubility, molecular sizes, and charge (ionic species) are considered in the case of adsorbate (Benefield, 1982).

The criteria for the selection of suitable adsorbents includes adsorption capacity, cost of the medium, ease of operation, potential for reuse and possibility of regeneration. A wide range of materials have been assessed for fluoride uptake, these include: cryptocrystalline magnesite (Vhahangwele, et al., 2015), Al^{3+}-modified bentonite clay (Masindi, et al., 2014), Fe^{3+}-modified bentonite clay (Gitari, et al., 2013), tea waste (Cai, et al., 2015), Mg–Fe–La trimetal composite (Wang, et al., 2015) and dried orange juice residue (Paudyal, 2013). The mechanism of fluoride uptake and applications of some of the most frequently encountered adsorbents are reviewed in section 2.3.3.1.

2.3.3.1 Bone and bone charcoal

Smith and Smith (1937) were the first to identify the potential in fluoride removal of bone. They reported that degreased, caustic and acid bone material could effectively reduce fluoride concentration from 3.5 to 0.2 mg/L. The suggested removal capacity was of ion exchange in which the carbonate radical of the apatite ($Ca_9(PO_4)_6.CaCO_3$) comprising bone was replaced by fluoride to form an insoluble fluorapatite.

$$Ca_9\,(PO)_{4_6}.CaCO_3 + 2F^- = Ca_9\,(PO)_{4_6}.CaF_2 + CO_3^{2-} \quad \ldots\ldots\ldots\ldots\ldots\ldots\ldots\ldots\ldots\ldots\ldots\ldots\ldots\ldots (2.6)$$

According to Ayoob, et al. (2008), the high cost factor of bone, became an inhibiting factor for its wider use. It was later recognized that bone char produced by carbonizing bone at temperatures of 1100-1600°C had superior fluoride scavenging potential to unprocessed bone. Thereafter bone char replaced bone as a defluoridating agent (Sorg, 1978). The adsorption mechanism of the fluoride ion onto bone char is suggested to be ion exchange. The phosphate ion in the bone char is exchanged for fluoride ion.

Fan, et al. (2003) explained the uptake of fluoride on hydroxyapatite as:

© University of Venda

$$Ca_{10}\,(PO)_{46}(OH)_2 + nF^- = Ca_{10}\,(PO)_{46}.(OH)_{2-n}F_n + nOH^- \ldots\ldots\ldots\ldots\ldots\ldots\ldots\ldots\ldots (2.7)$$

At the application level, the success of this technique hinges mainly on the quality of bone charcoal. The bone charring process is crucial as any failure may result in a product of low defluoridating capacity, affecting the quality of water treated. Poor bone charcoal may render water with bad taste and smell and would be unaesthetically unpleasant to consumers. The consumers may dislike the process once they are exposed to such smell or taste (Ayoob, et al., 2008).

2.3.3.2 Activated alumina (AA)

The crystal structure of alumina contains cation lattice discontinuities giving rise to localized areas of positive charges (Srimurali and Karthikeyan, 2008). This makes alumina to attract various anionic species. Alumina has a high preference for fluoride compared to other anionic species, and hence is an attractive adsorbent.

In practice, alumina (Al_2O_3) is first treated with HCl to make it acidic.

$$Al_2O_3.H_2O + HCl \rightarrow Al_2O_3.HCl + H_2O \ldots\ldots\ldots\ldots\ldots\ldots\ldots\ldots\ldots\ldots\ldots\ldots\ldots\ldots\ldots\ldots\ldots (2.8)$$

When contacted with fluoride ions, this acidic form of alumina displaces the chloride ions and gets attached with the alumina.

$$Al_2O_3.HCl + NaF \rightarrow Al_2O_3.HF + NaCl \ldots\ldots\ldots\ldots\ldots\ldots\ldots\ldots\ldots\ldots\ldots\ldots\ldots\ldots\ldots\ldots\ldots (2.9)$$

To regenerate the adsorbent a dilute solution of sodium hydroxide is mixed with the adsorbent to get a basic alumina.

$$Al_2O_3.HF + 2NaOH \rightarrow Al_2O_3.NaOH + NaF + H_2O \ldots\ldots\ldots\ldots\ldots\ldots\ldots\ldots\ldots\ldots\ldots\ldots (2.10)$$

Further treatment with acid regenerates the acidic alumina.

© University of Venda

$$Al_2O_3.NaOH + 2HCl \rightarrow Al_2O_3.HCl + NaCl + H_2O \ldots\ldots\ldots\ldots\ldots\ldots\ldots\ldots\ldots\ldots\ldots\ldots\ldots\ldots (2.11)$$

AA has been used for defluoridation of drinking water in industrialized countries. However, recently this technology is gaining a wide attention in developing countries like India to be used as a filter media in household units (Figure. 2.3). Venkobachar, et al. (1997) reported that around 500 to 1500 L of safe water could be produced with 3 kg of activated alumina when the raw water fluoride is between 11 and 4 mg/L at natural water pH of 7.8 - 8.2.

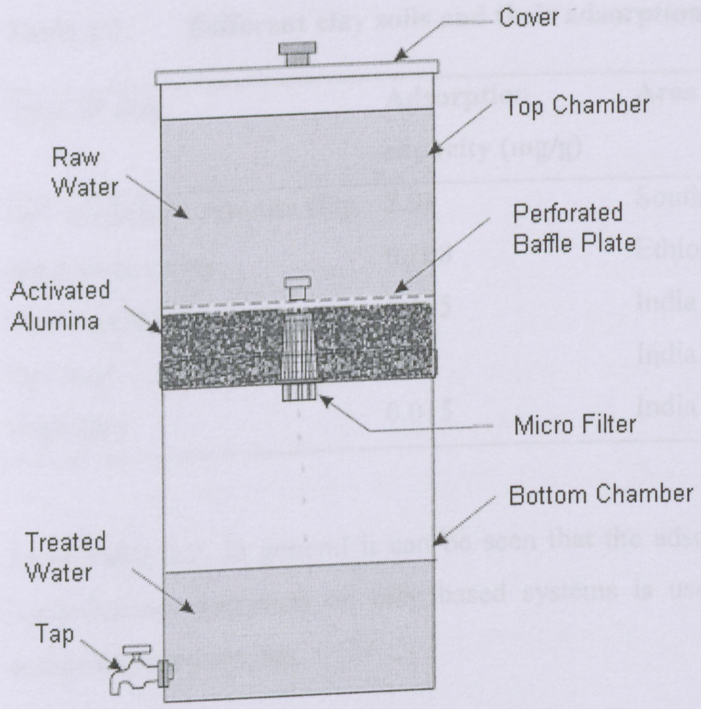


Figure 2.3: Activated alumina-based domestic defluoridation filter (Daw, 2004)

A disadvantage of this process is that the regeneration steps result in an aqueous solution containing fluoride. On the other hand, if the spent alumina is discarded, the cost of the defluoridation increases. Apart from that, spent alumina may leach out fluoride ions when it comes in contact with alkali.

2.3.3.3 Clays soils

The potential of soil based systems for defluoridation is under investigation in many fluoride endemic regions of the world, especially developing countries. The first comprehensive study of fluoride onto minerals and soils was published by Bower and Hatcher (1967). They

© University of Venda

observed that excess fluoride in water could be removed to different degrees by adsorption onto a variety of mineral and soil types. Thereafter, fluoride adsorption onto clay soils, both in natural and modified activated forms has been studied extensively (Agarwal, et al., 2002, Bhatnagar, et al., 2011 Daifullah, et al., 2003; Gitari, et al., 2013; Jiang and Zeng, 2003 ; Sujana and Anand, 2011; Tomar and Kumar, 2013).

Table 2.2 shows some of the clays that were applied in different countries for the removal of fluoride in water.

Table 2.2 Different clay soils and their adsorption capacities in water defluoridation

Type of clay	Adsorption capacity (mg/g)	Area of study	References
Fe^{3+} modified bentonite clay	2.91	South Africa	Gitari et al. (2013)
Bambawoha clay	0.168	Ethiopia	Hassen (2007)
Montmorillonite clay	1.485	India	Karthkeyan (2005)
Red mud	0.01	India	Rakshit (2004)
Fired clay	0.015	India	Rakshit (2004)

From Table 2.2, in general it can be seen that the adsorption capacity of the clays is low. Nevertheless adsorption on clay based systems is used in many parts of the world for defluoridation purposes.

(i) Mechanisms of adsorption onto clay soils

The fluoride adsorption process on clay mineral surfaces is based on the surface chemistry of the sorbent, the solution chemistry of fluoride, and a surface complex mechanism. An ion exchange mechanism where F^- is exchanged with OH^- groups in surface layer hydrated metal oxides such as aluminium or iron oxides, is generally assumed to be the determining step in the adsorption process. For a hydrated aluminium oxide surface these are:

$$AlOH_2^+ + F^- = AlF + H_2O \quad \ldots\ldots\ldots\

The surfaces of clays always contain ionizable functional groups which constitute the active sites on the surface, OH in this case, which can undergo proton transfer depending on the pH. This process is one determinant of surface charge. Since F^- is negatively charged, the more positive the surface of the adsorbent the more favorable it would be for fluoride adsorption.

(ii) Kaolin clay

The potential of kaolin clay for fluoride adsorption was studied by some researchers (Bower and Hatcher, 1967; Perrott, 1976; Semmens and Meggy, 1996; Kau, 1997). The factors found to influence fluoride sorption include solution pH, clay surface area, structure, aluminum content and the presence of certain exchangeable cations capable of forming fluoride precipitates (Hiemstra and Van - Riemsdijk, 2000). Although ion exchange reaction is regarded as the predominant form of fluoride sorption, fluoride may also be immobilized through the formation of complexes or precipitates with exchangeable cations such as magnesium, iron and calcium or be attracted to the clay electrostatically, in which case fluoride may be retained in the electric double layer (Kau, 1997). It was clearly demonstrated that disruption of the kaolin crystal structure occurred due to fluoride uptake and F/OH exchange occurred primarily with $Al(OH)_3$ rather than with OH^- from the crystal lattice of clay minerals. The reaction between kaolin and fluoride increases the pH of the solution through the release of hydroxide ions as represented in Equation 2.14.

$$n(kaolin-OH)_{(s)} + nFn_{(aq)} \leftrightarrow n(kaolin-F)_{(s)} + nOHn^-{}_{(aq)} \ldots\ldots\ldots\ldots\ldots\ldots\ldots (2.14)$$

(iii) Other clays

A study was done to investigate the adsorption characteristics of South African clay types and to correlate this with mineral composition and structure and adsorption mechanisms (Coetzee, 2006). This study assessed the fluoride adsorption characteristics of clay soils (kaolinite, bauxite, goethite, bentonite, and palygorskite) collected from different areas, where a high fluoride concentration in groundwater is a problem. Bauxitic clays were found to have the best overall potential as fluoride adsorbents. Simple chemical activation using 1% Na_2CO_3 solutions and dilute HCl could enhance adsorption capacity of certain clay types (Coetzee, 2006).

© University of Venda

University of Venda
Creating Future Leaders

Several researchers have studied the removal of F^- using fired clays (Bårdsen and Bjorvatn, 1995; Moges, et al., 1996; Hauge, et al. 1994). Hauge, et al. (1994) studied the defluoridation of drinking water using pottery. The study investigated the effect of firing clays on F^- adsorption. The results showed that clays fired at temperature up to 600°C gave higher F^- adsorption (Hauge, 1994). Moges, et al. (1996) studied the defluoridation of water using fired clay chips in Ethiopia. Their findings indicated that F^- adsorption is affected by factors such as initial concentration, mass of adsorbent and the pH of the solution (Moges, et al., 1996).

Natural clays present a major advantage due to their abundance in nature (locally availability). Since these clay minerals are widely available in many rural areas they can be used as an alternative defluoridating material. These clay soils can be packed in columns and used as adsorbents to remove fluoride from water. The use of clay powder in columns is possible, but troublesome mainly because of difficulties in packing the columns and controlling the flow. Domestic clay column filters are normally packed using clay chips found as waste from the manufacture of brick, pottery or tile as shown in Figure 2.4. The filter is based on up-flow in order to allow for settling of suspended solids within the filter bed.

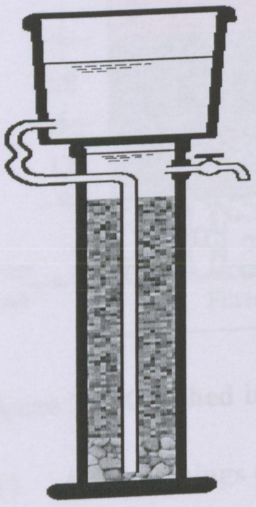


Figure 2.4: Stratified column of brick chips used in household defluoridation (Padmasiri, 1998).

UNIVERSITY OF VENDA
LIBRARY

© University of Venda

Some column filters using clays also incorporate other materials to aid the filtration processes. Agonafir and Ambelu (2007) conducted a study to determine the treatment duration of a crushed brick fluoride filter media made with sand filter and the fluoride adsorption capacity of the crushed bricks material per unit weight. They reported that crushed bricks fluoride removal filter media with experimental sand filter containing charcoal (Figure 2.5) has a very good effect in the fluoride removal from water. During the filter run, the residual fluoride concentration below the safe recommended limit (<1.5 mg/L) was observed until about 300 L of raw water that had fluoride concentrations of 8 mg /L was treated. The crushed bricks material showed high fluoride adsorption capacity (91.76 %) per unit weight (Agonafir and Ambelu, 2007).

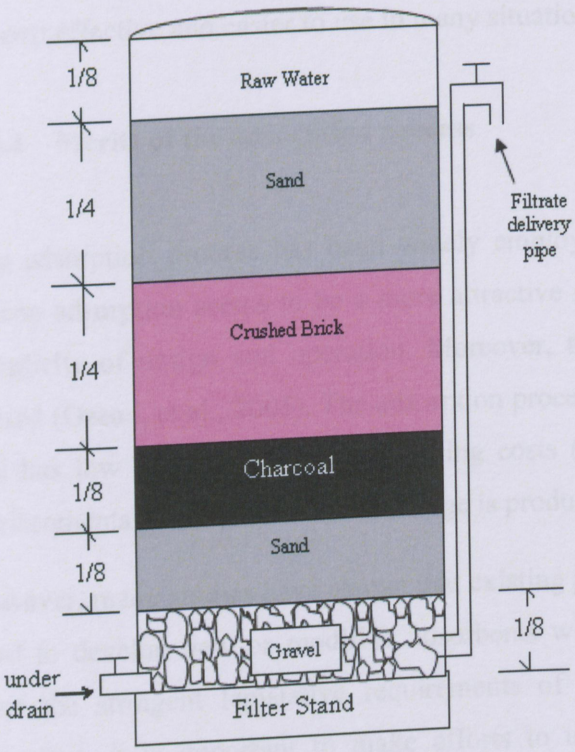


Figure 2.5: Crushed brick fluoride filter combined with experimental sand filter

(iv) Shortcomings of raw clay filter mediums

It has been observed that the exhaustion time of the filter unit is one disadvantage that the clay filter mediums have. This might be due to complete saturation of anion-exchange sites indicating the complete exhaustion of the filter media. Agonafir and Ambelu, (2007) reports that, as the filtration process proceeded, about 300 L of 8 mg/L fluoride water was

© University of Venda

defluoridated and the concentration observed to increase beyond the permissible upper limit (1.5 mg/L). This is a limitation because the media can only filter as much water during a certain period. Thus, the 300 L should be considered as the maximum volume water to defluoridate to the safe fluoride limits.

Studies recommend that only the water used for drinking and cooking purposes (usually less than 5 L per person per day) needs to be defluoridated. The entire water demand is often ten times higher and to defluoridate all these would be too expensive as well as producing a large amount of toxic sludge (Swiss Centre for Development Co-operation in technology and management, 2003). Another study conducted by Abaire (2009) in Ethiopia revealed that clay has low capacity as compared to bone char and therefore, the lifetime of the adsorption bed is very short. Nonetheless, clay minerals are widely available and adsorption by clay may be cost effective and easier to use in many situations.

2.3.4 Merits of the adsorption process

The adsorption process has been widely employed and gave satisfactory results. For this reason adsorption seems to be a more attractive method for defluoridation in terms of cost, simplicity of design and operation. Moreover, the adsorbent can be easily recovered and reused (Ozean, et al., 2005). The adsorption process may generate little or no toxic pollutants and has low initial capital and operating costs (Crini, 2006). Adsorption is safe from the environmental point of view as no sludge is produced (Unuabonah, et al., 2008).

However, many studies have shown that existing processes are limited in scope and there is a need to develop new or modified adsorbents with improved fluoride uptake properties to meet the stringent legislative requirements of 1.5 mg/L of fluoride in drinking water. Therefore, it is important to make efforts to understand various possible approaches to improve the fluoride uptake properties of potential materials including clay minerals and soils.

© University of Venda

University of Venda
Creating Future Leaders

2.4 Adsorption using bentonite clay

Natural clays are acquiring prominence due to their local availability, abundance and the capability to undergo modification to enhance the surface area, adsorption capacity and range of applicability (Monvisade and Simpson, 2009). Among those natural clays, bentonite has proven to be a promising adsorbent for fluoride removal.

2.4.1 Bentonite clay

Various definitions of bentonite have been given in literature, but generally all agree that bentonite is a rock term used to designate a naturally occurring, very fine grained material largely composed of the clay mineral, montmorillonite. Accordingly, a description and discussion of montmorillonite is applicable to bentonite as well. In addition to montmorillonite, bentonite may also contain feldspar, biotite, kaolinite, illite, cristobalite, pyroxene, zircon, and crystalline quartz (Parkes, 1982). By extension, the term bentonite is applied commercially to any plastic, colloidal, and swelling clay regardless of its geological origin. Such clays are ordinarily composed largely of minerals of the montmorillonite group (Adamis and Williams, 2005).

2.4.2 Mineralogy and physicochemical properties

Bentonite is a geological term for soil materials with a high content of a swelling mineral, which usually is montmorillonite. The remaining part of the bentonite may vary substantially in mineralogy within, and especially between different quarries, and depends basically on the geochemical conditions during the formation of the bentonite. Typical accessory minerals present in bentonites are other clay minerals, quartz, feldspars, gypsum, calcite, pyrite and various iron oxides/hydroxides. Amorphous and organic compounds may be present in significant amounts (Grim, 1968).

The montmorillonite mineral belongs to the smectite mineral group, in which all members have an articulated layer structure and swelling properties. Common for the smectite group is that the thickness of an individual mineral layer is around 1 nm and the extension of the other two directions may be up to several hundred nanometers. Each layer is composed of a central sheet of octahedrally coordinated cations, which on both sides are linked through shared

© University of Venda

oxygens to sheets of tetrahedrally coordinated cations. Minerals of this type are often referred to as 2:1 layer structures (Kutlić, et al., 2012).

The molecular formula for montmorillonite is usually given as $(M^{+}x \cdot nH_2O)$ $(Al_{2y}Mg_x)$ Si_4O_{10} $(OH)_2$, where $M^{+} = Na^{+}$, K^{+}, Mg^{2+} or Ca^{2+} (Brindley and Brown, 1980). The basic structure of bentonite is made up of two silica tetrahedral sheets with an intermediate aluminium octahedral sheet (Vimonses, et al., 2009) as can be seen in Figure 2.6.

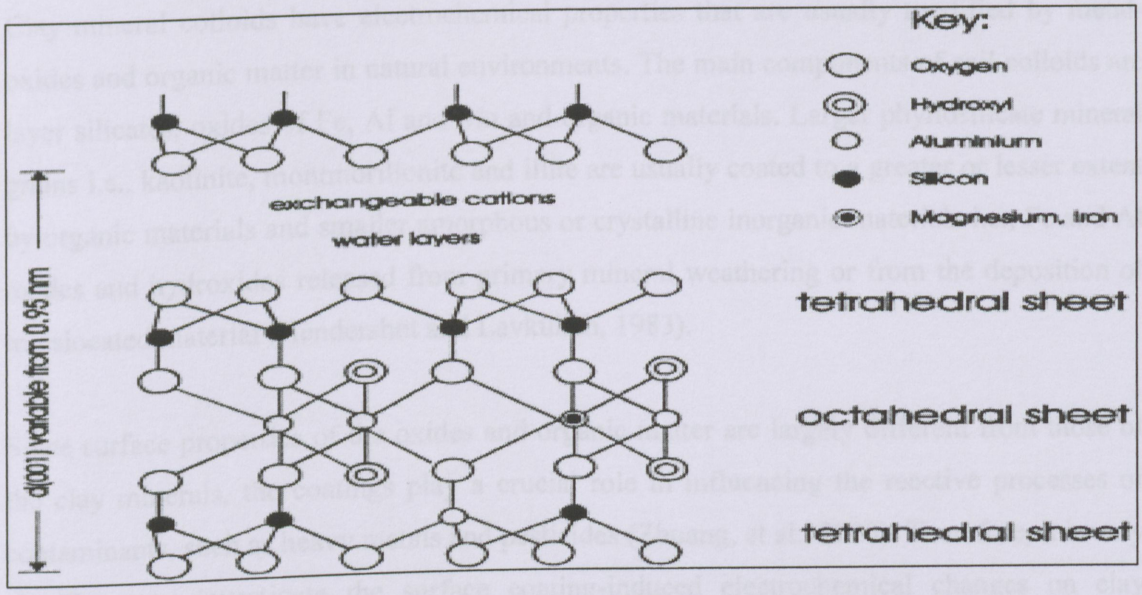


Figure 2.6: Structure of bentonite (Clelyi and Doehler, 2010)

As shown in Figure 2.6, bentonite clay is characterized by a 2:1 structure, meaning that the octahedral sheet of aluminium is sandwiched between two tetrahedral sheets of silicon (Alloways, 1997). However, elements can replace each other through isomorphous substitutions based on the charge valence and density (Sparks, 1997). For instance, aluminium can be replaced for silicon and magnesium can be replaced for aluminium (Langmuir, 1997). This type of clay has high swelling properties and surface area which enables it to retain water by adsorbing water molecules on its matrices through weak Van der Waal forces (Brady and Weils, 2004).

2.4.3 Chemical modification of bentonite

There has been great interest in developing modified clay based adsorbents for the removal of aqueous contaminants (Vinati, et al., 2015). Research has especially grown in developing an adsorbent having a high adsorption capacity and low cost. Basically the modification

© University of Venda

reactions are accomplished by replacing the interlayer cations (e.g. Na^+, K^+ and Ca^{2+}) with specific chemical species to alter the surface and/or structural characteristics of the host clays. There are different modification procedures which include the following:

2.4.3.1 Metal oxide coatings

Clay mineral colloids have electrochemical properties that are usually modified by metal-oxides and organic matter in natural environments. The main components of soil colloids are layer silicates, oxides of Fe, Al and Mn and organic materials. Larger phyllosilicate mineral grains i.e., kaolinite, montmorillonite and illite are usually coated to a greater or lesser extent by organic materials and smaller amorphous or crystalline inorganic materials i.e., Fe and Al oxides and hydroxides released from primary mineral weathering or from the deposition of translocated material (Hendershot and Lavkulich, 1983).

Since surface properties of the oxides and organic matter are largely different from those of the clay minerals, the coatings play a crucial role in influencing the reactive processes of contaminants, such as heavy metals and pesticides (Zhuang, et al., 2000). Therefore, it is very significant to investigate the surface coating-induced electrochemical changes on clay minerals. Many studies have been conducted in the relevant aspects (Chao, et al., 1964; Gallez, et al., 1976; Hendershot and Lavkulich, 1983; Sakurai, et al., 1990). Gallez, et al. (1976) found that, in mixed colloidal systems the amorphous Fe or Al oxide colloids tend to accumulate on the negatively charged surfaces of kaolinite modifying its charge properties. Hendershot and Lavkulich (1983) also found that even small quantities of iron oxides (approximately 4 %) could shift point of zero salt effect (PZSE) from less than 3 to 6.8 in a Fe-coated kaolinite system. Vinati, et al. (2015) observed that, the increased fluoride removal capacities of metal oxide modified clays is due to changes in the surface property of the clay during their modification where surfactant cations can attract and electrostatically hold fluoride anion, which replaces bromide ions associated with the surfactant head groups in an anion exchange process.

© University of Venda

2.4.3.2 Alkali activation

Clays invariably contain exchangeable cations and anions held to the surface. The prominent cations and anions found on clay surfaces are Ca^{2+}, Mg^{2+}, H^{+}, K^{+}, Na^{+}, SO_4^{2-}, Cl^{-}, PO_4^{3-} and NO_3^{-}. Most clays also contain fluoride. Concentrations of 2 to 4 g-F/kg have been reported (Day, 1963). These ions can be exchanged with other ions relatively easily without affecting the clay mineral structure (Tohidi and Ramez, 1997). Studies carried out on bentonite activation have shown that the process involves an ion-exchange reaction as follows:

$$Ca - bentonite + NaOH \therefore Na_2CO_3 \rightarrow Na - bentonite + Ca(OH)_2 \therefore CaCO_3 \ldots (2.15)$$

The chemical and mineralogical structures of bentonites can be activated by reaction with an alkali. Many studies performed on the alkaline reaction of bentonite have been directed to the montmorillonite alteration. Alkali activation is a method to enrich bentonite with sodium cations. Sodium-activated bentonite should therefore be considered as a not chemically modified substance, namely 'a substance whose chemical structure remains unchanged, even if it has undergone a chemical process or treatment, or a physical mineralogical transformation, for instance to remove impurities" (Kutlić, et al., 2012).

A study done by Gitari, et al., (2013) showed that raw bentonite leached some fluoride into water when used as an adsorbent for defluoridation. This shows that bentonite clay contains elements of fluoride in its structure hence the need to be activated to remove the geological fluoride ions before it can be used for defluoridation purposes. Alkaline treatment will lead to its physical, mineralogical transformation resulting in a fluoride free bentonite which can later on be used for defluoridation purposes.

Activation does not alter the crystal structure of the separate smectite layers. It changes only the stacking of the successive layers, which, in any case, is not a constant structural parameter and is largely dependent on many factors, such as the water content of smectite. Therefore, sodium exchange induced by activation, should not be considered a structural change of

© University of Venda

smectite and hence the bentonite. This is because Na^+ and Ca^+ are not part of the "structure" of bentonite as they are loosely bound in between the smectite platelets, modifying the surface electrical charge of them. Given the above, treatment of bentonite by sodium activation results in no change in its chemical structure and, therefore, sodium activated should be considered as identical to natural one.

2.4.4 Application of bentonite clay in water defluoridation

The successful application of bentonite in the removal of excess fluoride in drinking water has been proved by many studies (Bhatnagar, 2011; Gitari, et al., 2013; Karthikeyan, et al. 2005; Kamble, et al., 2009: Thakre, et al., 2010 and Tor, 2006). Karthikeyan, et al., (2005) conducted a study on fluoride removal using montmorillonite clay and results showed that the Langmuir maximum sorption capacity for fluoride was 1.485 – 1.910 mg/g at different temperatures. Thakre, et al. (2010) also did a study for defluoridation of drinking water by incorporating magnesium onto bentonite clay. They found out that magnesium modified bentonite has a maximum fluoride removal capacity of 2.26 mg/g at an initial fluoride concentration of 5 mg/L which was much better than unmodified bentonite clay. From the experimental results it was concluded that chemical modification enhances the fluoride removal efficiency of bentonite.

Gitari, et al. (2013) found nearly complete fluoride removal from an aqueous phase system using Fe^{3+}-modified bentonite at an adsorption capacity of 2.91 mg/g. In another study, fluoride removal by Al^{3+} modified bentonite was about 5.7 mg/g at room temperature (Vhahangwele, et al., 2014). A study done by Kamble et al. (2009) using chemically modified bentonite showed that alkali treatment of the adsorbent can regenerate it to be used again. The alkali treated adsorbent showed a high fluoride removal efficiency indicating that used adsorbent can be regenerated by the alkali treatment. This substantiates the mechanism of fluoride uptake through the replacement of hydroxyl group/anions from the oxide sites of bentonite-based adsorbents.

© University of Venda

University of Venda
Creating Future Leaders

2.5 Mukondeni clay soils

In South Africa, Mukondeni clay soils have been used to make clay pots and ceramic water filters but their physiochemical characteristics had never been studied to determine how suitable they are for these purposes. Mukondeni clay soils have recently been getting more attention in water treatment applications (Abebe, et al., 2014; Denga, 2013; Kallman, 2011). Thus, it becomes significant that the basic characteristics of these soils are evaluated and their scientific application in the treatment of water be assessed. Moreover these clay soils are locally and readily available, hence a breakthrough in their ability to remove contaminants from drinking water will come as an advantage to the local community most of whom are poor and cannot afford expensive water treatment methods.

A cooperative society called Mukondeni Pottery Cooperative which designs filters from the locally available clay has been established in the Mukondeni village. In addition to these filters, clay pots are also being made. The clay soils are treated before they can be shaped into different pots. They are shaped to produce traditional pots, dishes, decorated ornaments and flower pots. Clay pots are used for transportation and storage of drinking water. According to Bjorvatn and Bårdsen (1995), inexpensive, locally made ceramics may improve the quality of the water. They have always been used to keep water cool but studies are showing that the clay pots may reduce the fluoride content of the water (Hauge, et al. 1994; Bjorvatn and Bårdsen, 1995). Figure 2.7 shows the clay pots made from Mukondeni clay soils.



Figure 2.7: Clay pots made from Mukondeni clay soils

© University of Venda

Various researchers have assessed the fluoride binding effect of simple pottery (Ndegwa, 1980; Moges, 1990; Hauge, et al. 1994). Ndegwa (1980) reported a fluoride binding capacity in clayware of 80 mg-F/kg, while Zewge and Moges (1990) found out that pot chips were able to bind as much as 560 mg-F/kg. Hendrickson and Vik (1984), however, concluded that fluoride uptake in clayware is slow and of limited capacity. Hauge, et al. (1994) assessed the effect of firing temperature on the fluoride binding capacity of clay. They concluded that firing temperatures between 500 and 700°C produced clayware with optimal fluoride binding properties, while the fluoride binding processes were greatly reduced by firing above 800 degrees. A certain increase in the fluoride content could sometimes be seen when water was exposed to high-fired ceramics (Hauge, et al., 1994).

2.5.1 Mineralogy of Mukondeni clay soil

According to Dacosta, et al. (2013), the use of raw clay for pottery has a long history in the community of Mukondeni. However, its use in ceramic water filters requires that physical, geochemical and geotechnical properties of these materials be established to define the clay suitability for these purposes. Their study sought to identify the different types of clays in the area and to carry out the mineralogical, geochemical and geotechnical evaluation of the clay for making ceramic water filters in the newly established factory at Mukondeni Village. They found out that Mukondeni clay soils fall under three types which are gritty reddish, smooth greenish and black clays.

The three types of clay soils of Mukondeni fall into the smectite group with high swelling and shrinking potential. Silica (SiO_2) was found to be the highest component of the Mukondeni clay soils. According to Johari, et al. (2011), silica in clay soil exists as free form silica and as compound silica such as in kaolinite ($Al_2Si_2O_5(OH)_4$). In all types of clays, smectite is generally sticky with high plasticity and strength in both dry and wet state. As a result, it is the most preferred material used in the making of ceramic pots (Vitelli, 1999).

The most important property of clay soils that determines their uses for ceramic purposes is their plasticity property. This property allows the ceramist to create different shapes that have the ability of maintaining their forms before being fired (Dies, 2003). This property of clay soils can be influenced largely by their chemical composition and the nature of aggregate they contain. Some chlorite species can improve the plasticity of clay while others turn to

reduce the soil plasticity. Comparatively, soil containing greater than 95% kaolinate clay remains nonplastic (Guggenheim and Martin, 1995).

Although the type of clay found in Mukondeni is generally smectite, the potters prefer mixing the black and red when preparing the material for making ceramic pots. This might be influenced by the fact that the red clay is grittier and less sticky than the smooth black clay. High smectite content in black (55.08%) and green (55.69%) clays indicates that these materials are highly plastic and sticky than red clay with smectite content of 37.7%. The indications that red clay is more porous than the black and green clays were given by the gritty feeling they possess (Dacosta, et al., 2013).

2.5.2 Mukondeni clays soils and water defluoridation

In light of the above, it becomes important to evaluate Mukondeni clay's capacity in removing excessive fluoride in drinking water. As mentioned in section 2.5 that many types of clay have shown a potential of defluoridation water, Mukondeni clay soils can also be used as an adsorbent. Denga (2013) did a study using Mukondeni clay soil to defluoridate borehole water. Her study showed that Mukondeni clay soil is able to reduce fluoride concentrations from 8.87 mg/L to 5.10 mg/L. Although fluoride is not removed to within permissible limits, Mukondeni clay soil has a potential to be applied in the defluoridation processes if it can be modified to increase its adsorption capacity.

Bjorvatn and Bårdsen, (1995) used red soil (lateric clay), calcined at 570°C for three hours to defluoridate water. Fluoride containing water, at concentrations from 5.50 and 7.75 mg/L to 12, 30 and 130 mg/F^-/L were exposed to calcined laterite and later analysed for fluoride by the use of a fluoride selective electrode. Rapid reduction of the fluoride concentration to 0.48 mg/L in the water was observed.

Since calcination has proved to increase the adsorption capacities of clays, Mukondeni clay soils can also be thermally treated to enhance their efficiencies. Few scientific studies have been carried out on these soils hence the need to evaluate their defluoridation capacities. According to Dacosta, et al. (2013) the elevated plastic index characterising both the black and green clays indicates that they can crack easily during the burning of the pottery products. The reduced smectite concentration and plastic index values in red clay make it less

© University of Venda

plastic, less sticky with poor molding property. In view of this, it is recommended that in making ceramic pots and water filters, the red clay should be mixed with the other two clays (i.e., black and green). This will improve the molding property of red clay while reducing the stickiness of both green and/or black clay comprising of high percentage of smectite.

2.6. Composite adsorbents and defluoridation.

Studies have shown that making composite adsorbents can improve the adsorption capacities by synergesis of properties. Integration of an adsorbent with other materials through methods such as grafting, impregnation, chelation and crosslinking has better adsorption properties than the individual components effects (Chang and Juang, 2004). The synergy of adsorbent materials as composites have been tailored for gas, metals, pharmaceutical wastes, dyes and pesticide remediation. Composite adsorbents can be prepared with the sole aim of enhancing their selectivity, regeneration, surface area, mechanical strength and surface chemistry amongst others (Awual, et al., 2013; Auta and Hameed, 2013).

Mukondeni clay soils showed poor adsorption capacities in fluoride removal in water (Denga, 2013). On the other hand, bentonite clay has proved to be a good adsorbent in defluoridating water but has a weakness in raising the pH to above permissible limits (Gitari, et al., 2013) Realizing the weaknesses of these two clays, it becomes important to make a composite adsorbent of these two clays to improve their adsorption capacities.

© University of Venda

University of Venda
Creating Future Leaders

2.7 References

Abaire, B., Zewge, F. and Endalew, M., 2009. Water, sanitation and hygiene: sustainable development and multisectoral approaches. Operational experiences on small scale community defluoridation systems. 34th WEDC International Conference, Addis Ababa, Ethiopia.

Abrahams, L.C., 1946. The masticatory apparatus of Calvinia and Namaqualand in the North Western Cape of the Union of South Africa. Journal of the Dental Association of South Africa, 1, pp. 4-9.

Adamis, Z. and Williams, R.B., 2005. Environmental Health Criteria 231: Bentonite, Kaolin and Selected clay minerals. Geneva: World Health Organization.

Agarwal, M., Rai, K., Shrivastav, R. and Dass, S., 2002. A study on fluoride sorption by montmorillonite and kaolinite. *Water Air Soil Pollut,* 141(1–4), pp. 247–261.

Agonafir, A. and Ambelu, A., 2007. Treatment duration and adsorption capacity of crushed bricks in the removal of fluoride from drinking water. *Ethiopia J Health Sci.* 17(2).

Alloways, B.J., 1995. *Heavy metals in soils*. 2nd edition. London: Blackie academic and professional.

Awual, M. R., Ismael, M., Yaita, T., El-Safty, H., Shiwaku, S.A., Okamoto, Y. and Suzuki, S., 2013. Trace copper(II) ions detection and removal from water using novel ligand modified composite adsorbent, *Chem. Eng. J,* 222, pp. 67–76.

Auta, M. and Hameed, B.H., 2013. Coalesced chitosan activated carbon composite for batch and fixed-bed adsorption of cationic and anionic dyes, *Colloids Surface B, Biointerf,* 105, pp. 199–206.

Ayoob, S., Gupta, A., Venugopal, K. and Bhat, T., 2008. A Conceptual Overview on Sustainable Technologies for the Defluoridation of Drinking Water Critical Reviews in Environmental Science and Technology, 38(6), pp. 401- 470.

Bablia, K., 1996. Studies of water defluoridation using activated carbons and activated carbons loaded separately with Magnesia, Alumina and Calcium. MSc Thesis. Univesrity of Dar es Salaam, Tanzania.

Benefield, D., Larry, D., Judkins, Joseph, F. and Barron, L., 1982. Process chemistry for water and wastewater treatment, prentice hall, Englewood cliffs, New Jersey.

© University of Venda

University of Venda
Creating Future Leaders

Bjorvatn, K. and Bardsen, A. 1995. Use of activated clay for defluoridation of water. In: Proceedings of the First International Workshop on Fluorosis and Defluoridation of Water, Dahi, E., and Bregnhoj, H., Eds., International Society for Fluoride Research, Auckland, pp. 40 – 45.

Bhatnagar, A., Kumar, E. and Sillanpääb, M., 2011. Fluoride removal from water by adsorption-A review, *Chem. Eng. J,* 10, pp. 5 - 28.

Bradley, G. and Weils, D.H., 2004. *Elements of nature*. 5th ed. Blackies and sons: USA.

Bregnhøj, H., 1997. Critical sustainability parameters in the defluoridation of drinking water. 2nd International Workshop on Fluorosis and Defluoridation of Water. Copenhagen, Denmark. *Int. Soc. Fluoride Res.* pp. 191 – 197.

Bregnhøj, H., Dahi, E. and Jensen, M., 1997. Modeling defluoridation of water in bone char columns. In: Proceedings of the First International Workshop on Fluorosis and Defluoridation of Water 18–22 October 1995, Tanzania, The International Society for Fluoride Research, Auckland.

Bower, C.A. and Hatcher, J.T., 1967. Adsorption of fluoride by soils and minerals. *Soil Sci*, 103, pp. 151–154.

Cai, H., Chea, G., Peng, C., Zhang, Z., Dong,Y., Shang, G., Zhu, X., Gao, H., Xiao-chun and Wan, X., 2015. Removal of fluoride from drinking water using tea waste loaded with Al/Fe oxides: A novel, safe and efficient biosorbent. *Applied Surface Science*, 328, pp. 34 – 44.

Chang, M.Y and Juang, R.S., 2004. Adsorption of tannic acid, humic acid, and dyes from water using the composite of chitosan and activated clay, *J. Colloid Interf. Sci,* 278, pp. 18–25.

Chao, T.T., Harward, M.E., Fang, S.C., 1964. Iron or aluminum coatings in relation to sulfate adsorption characteristics of soils. *Soil Sci. Soc. Am. Proc,* 28, pp. 632–635.

Choudhary, N and Laur R., 1996. Fluoride emission during primary aluminum smelting. *Jour. Of India Association of environmental Management,* 23, pp. 86 - 93.

Coetzee, P.P., Coetzee, L., Puka, R. and Mubenga, S., 2006. Characterisation of selected South African clays for defluoridation of natural waters.

Crini, G., 2006. Non – conventional low cost adsorbents for dye removal: A review. *Bioresour Techn,* l97, pp. 1061 – 1085.

Dacosta, F. A., Muzerengi, C., Mhlongo, S.E and Mukwevho, G.F., 2013. Characterization of clays for making ceramic pots and water filters at Mukondeni village, Limpopo province, South Africa. *ARPN Journal of Engineering and Applied Sciences*, 8 (11), pp. 927 – 932.

© University of Venda

University of Venda
Creating Future Leaders

Dahi, E., 2000. The State of Art of Small Community Defluoridation of Drinking Water. 3rd International Workshop on Fluorosis Prevention and Defluoridation of Water, Chiang Mai, Thailand, pp. 137–167.

Dahi, E., Mtalo, F., Njau, B. and Henrik, H., 1996. Defluoridation using the Nalgonda Technique in Tanzania 22nd WEDC Conference. Reaching the unreached: challenges for the 21st century New Delhi, India.

Daifullah, A.A.M., Yakout, S.M. and Elreefy, S.A., 2007. Adsorption of fluoride in aqueous solutions using KMnO4-modified activated carbon derived from steam pyrolysis of rice straw. *Journal of Hazardous Materials*, 147, pp. 633–643.

Daw, R.K., 2004. Experiences with domestic defluoridation in India, Proceedings of the 30th WEDC International Conference on People-Centred Approaches to Water and Environmental Sanitation, Vientiane, Lao PDR, pp. 467 – 473.

Denga, M.E., 2013. Evaluation of the fluoride adsorption capacity of locally available clay in Vhembe district. A thesis submitted to the department of Ecology and Resource Management, School of Environmental Sciences. University of Venda.

Dies, R.W., 2003. Development of Ceramic Water filters for Nepal. M.Sc Thesis. Department of Civil and Environmental Engineering. Massachusetts Institute of Technology.

DWAF. 1996. *South African Water Quality Guidelines for Domestic Use* .1st edition.

Fan, X., Parker, D.J. and Smith, M.D., 2003. Adsorption kinetics of fluoride on low cost materials. *Water Res.* 37, pp. 4929 – 4937.

Feenstra, L., Vasak, L and Griffioen J., 2007. Fluoride in groundwater: Overview and evaluation of removal methods. International groundwater resources assessment centre. Report nr. SP 2007-1.

Gallez, A., Jua, A.S.R. and Herbillon, A.J., 1976. Surface and charge characteristics of selected soils in the tropics. *Soil Sci. Soc. Am. J,* 40, pp. 601– 608.

Gitari, W.M., Ngulube, T., Masindi, V. and Gumbo J.R., 2013. Defluoridation of groundwater using Fe^{3+}modified bentonite clay: optimization of adsorption conditions, *Desalination and Water Treatment*, DOI: 10.1080/19443994.2013.855669.

Gosh. U.C., 2005. Development of Defluoridation Media for Contaminated Groundwater and its Lab to Field Application 2005. Ministry of Water Resources and Central ground water Board (New Delhi) Project. Project No.: 23/43/2005-R&D/823.

Grim, R.E., 1968. *Clay mineralogy*, 2nd. Ed New York; McGraw-Hill.

© University of Venda

Guggenheim, S. and Martin, R.T., 1995. Definition of Clay and Clay Mineral: Joint Report of the AIPEA Nomenclature and CMS Nomenclature Committees. *Clays and Clay Minerals*, 43(2) pp. 255-256.

Hassen, A., 2007. Selection of clay adsorbents and determination of the optimum condition for defluoridation of ground water in rift valley region. A thesis submitted to the school of Graduate Studies of Addis Ababa University in Partial fulfillment of the requirements of the Degree of Masters of Science in Chemical Engineering (Process Engineering Stream).

Hauge, S., Österberg, R., Bjorvatn, K and Selvig K., 1994.Defluoridation of drinking water with pottery: effect of firing temperature. *Scand. J. Dent. Res,* 102, pp. 329 – 333.

Hendershot, W.H. and Lavkulich, L.M., 1983. Effect of sesquioxide coatings on surface charge of standard mineral and soil samples. *Soil Sci. Soc. Am. J*, 47, 1251–1260.

Hendrickson, K. and Vik, E, A., 1984. Adsorption in water treatment. Fluoride removal. Norwegian Institute for Water Research (NIVA), Report No. FP-83828, Oslo Norway.

Hiremath, S.S., 2006. *Textbook of Preventive and Community Dentistry*. Bengalore: Elsevier India.

Hiemstra, T. and VanRiemsdijk, W.H., 2000. Fluoride adsorption on Geoethite in relation to different types of surface sites. *J. Colloid Interface Sci,* 225, 94 – 104.

Huang, C. J. and Liu, J. C., 1999. Precipitate flotation of fluoride-containing wastewater from a semiconductor manufacturer. *Water Research. 33*(16), pp. 3403-3412.

Hu, C. Y., Lo, S. L., Kuan, W. H. and Lee, Y. D., 2008. Treatment of high fluoride-content wastewater by continuous electrocoagulation-flotation system with bipolar aluminum electrodes. *Separation and Purification Technology.* 60(1), pp. 1-5.

Jiang J, and Zeng J., 2003. Comparison of modified montmorillonite adsorbents. Part II: The effects of the type of raw clays and modification conditions on the adsorption performance. *Chemosphere*, 53, pp. 53 – 62.

Jimmy, L., Humphrey, G. E. and Keller, I.I., 1997. Separation process technology.

Johari I., Said S., Jaya R.P., Bakar B.H.A. and Ahmad Z.A., 2010. Chemical and Physical Properties of Fired- Clay Brick at Different Type of Rice Husk Ash. International Conference on Environmental Science and Engineering IPCBEE, IACSIT Press, Singapore. 8, pp. 171-174.

Kalibatonga, P.D., 2004. Adsorption of heavy metals from solution by South African industrial clay. A thesis submitted at Tshwane University of Technology.

© University of Venda

Kamble, S.P., Dixit P., Rayalu, S.S. and Labhsetwar, N.K., 2009. Defluoridation of drinking water using chemically modified bentonite clay. *Desalination,* 249, pp. 687 – 693.

Karthiken, G., Pius, A. and Alagumuthu, G., 2005. Fluoride adsorption studies of montmorillonite clay. *Indian Journal of Chemical Technology*, 12, pp. 263 – 272.

Kaseva, M. E., 2006. Optimization of regenerated bone char for fluoride removal. *Journal of Water and Health,* (4)1, pp. 139 – 147.

Kau, P.M.H., Smith, D.W. and Binning, P., 1997. Fluoride detention by kaolin clay. *J. Contamin. Hydrol*, 28, pp. 267–288.

Killedar, D.J. and Bhargava, D.S., 1998. An overview of Defluoridation methods (part-1). *Jour of Institution of public Health Engineers*, 1(1), pp. 6 – 13.

Kutlić, A., Bedeković, G. and Sobota, I., 2012. Bentonite processing. *Rud.-geol.-naft*. 24. pp. 61 – 65.

Langmuir, D., 1997. *Aqueous environmental geochemistry*. Prentice-Hall, Inc. Upper Saddle River: New Jersey.

Maiti, A., Basu, J.K. and De, S., 2011. Chemical treated laterite as promising fluoride adsorbent for aqueous system and kinetic modelling. *Desalination,* 265, pp. 28–36.

Mariappan, P. and Vasudevan, T., 2011. Domestic defluoridation techniques and sector approach for fluorosis mitigation. Pages 1-11 (Accessed on 2014 Mar. 4th). Available from: URL: www.twadboard.gov.in.

Masindi, V., Gitari, W.M. and Ngulube, T., 2014. Defluoridation of drinking water using Al^{3+} -modified bentonite clay: optimization of fluoride adsorption conditions. *Toxicol. Environ. Chem.* 96 (9), pp. 1294–1309.

Maughan-Brown, H., 1935. Our Land. Is our population satisfactory? The results of inspection of school ages. *South African Medical Journal,* 9, pp. 822.

Mjengera, H. and Mkongo, G., 2003. Appropriate defluoridation technology for use in fluoritic areas in Tanzania. *Physics and Chemistry of the Earth*, 28, pp. 1097–1104.

Moges, G., Zewge, F and Socher, M., 1996. Preliminary investigations on the defluoridation of water using fired clay chips, *J. African Earth Sciences,* 22 (4), pp. 479 - 482.

Monvisade, P. and Siriphanon, M., 2009. Chitosan intercalated montmorillonite: Preparation. Characterization and cationic dye adsorption. *App clay Sci,* 42, pp. 427 – 431.

© University of Venda

University of Venda
Creating Future Leaders

Moola, M.H., 2008. Fluoride in Drinking Water and its Effects on Human Health and Nutrition in Selected Towns of the Northern Cape Province, South Africa WRC Report No 1094/1/08 ISBN 978-1-77005-778-4.

Ncube, E.J., 2002. The distribution of fluoride in South Africa and the impact thereof on dental health. A dissertation submitted to the University of Pretoria.

Ncube, E. J. and Schutte, C.F., 2005. The occurrence of fluoride in South African groundwater: A water quality and health problem .*Water SA*. 31(1), pp. 35 – 40.

Ndegwa, W.M., 1980. Investigations leading to defluoridation of waters in Kenya. Thesis,University of Nairobi, Kenya.

Ndiaye, P.I., Moulin, P., Dominguez, L., Millet, J.C., Charbit, F., 2005. Removal of fluoride from electronic industrial effluent by RO membrane separation. *Desalination*, 173, pp. 25–32.

Nemade, P.D., Rao, A.V. and Alappat, B. J., 2002. Removal of fluorides from water using low cost adsorbents. *Water-science-and-technology*, *water-supply*, pp. 311- 317.

Ockerse, T., 1941. Endemic fluorosis in the Kenhardt and Gordonia districts, South Africa. *Journal of the American Dental Association,* 28, pp. 936 - 941.

Ockerse, T. and Meyer, H.P., 1941. Endemic fluorosis in the Pilansberg area and the occurrence of fluorine in the Saltpan, Pretoria district. *South African Dental Journal*, 15, pp. 62.

Odiyo, J.O. and Makungo. R., 2012. Fluoride concentrations in groundwater and impact on human health in Siloam Village, Limpopo Province, South Africa. *Water SA*, 38(5), pp. 731 – 736.

Oremusová, J. 2007. Manual for laboratory practice in physical chemistry for students of pharmacy, Department of Physical Chemistry, Faculty of Pharmacy, Comenius University, Bratislava, in Slovak.

Ozean, A.S., Erden, B. and Ozean, A., 2005. Adsorption of acid blue 193 from aqueous solutions onto BTMA activated bentonite. Colloid and surfaces. *A. Physicochem. Eng. Aspects*, 266, pp. 73 – 81.

Padmasiri, J.P., 1998. Low cost defluoridation of drinking water by means of brick chips. Proceedings of the 2nd International Workshop on Fluorosis and Defluoridation of Water. Nazareth, 19–22 November 1997. The International Society for Fluoride Research, Auckland.

Parker, S.P., 1988. *McGraw-Hill encyclopedia of the geological sciences*. 2nd ed. New York, McGraw-Hill, pp. 32 – 33; 69 –72; 400 – 401.

© University of Venda

University of Venda
Creating Future Leaders

Parkes, W.R., 1982. *Occupational lung disorders*. London, Butterworths, pp. 310 –318.

Paudyal, H., Pangeni, B., Inoue, K., Kawakita, H., Ohto, K., Ghimire, K.N., Harada, H., Alam, S., 2013. Adsorptive removal of trace concentration of fluoride ion from water by using dried orange juice residue. *Chemical Engineering Journal*, 223, pp. 844–853.

Perrott, K.W., Smith, B.F.L. and Inkson, R.H.E., 1976. The reaction of fluoride with soils and soil minerals. *J. Soil Sci*, 27, pp. 348.

Rakshit, P.K., 2004. Studies on the estimation of fluoride and defluoridation of drinking water. A project report submitted to the department of Chemical Engineering, Indian Institute of Science. India.

Renuka, P and Pushpanjali, K., 2013. Review on Defluoridation Techniques of Water. *The International Journal of Engineering and Science*, 2(3) pp. 86 – 94.

Robert E. T., 1988. Mass Transfer Operations, 3rd Ed.

Rowhani, S., 1986. Incidence of microbial, fluoride and nitrate pollution in groundwater. Seminar on technology transfer in water supply and sanitation in developing areas – Bophutatswana, Mamatho, 1 – 17.

Sakurai, K., Teshima, A., Kyuma, K., 1990. Changes in zero point of charge (ZPC), specific surface area (SSA), and cation exchange capacity (CEC) of kaolinite and montmorillonite, and strongly weathered soils caused by Fe and Al coatings. *Soil Sci. Plant Nutri,* 36 (1), pp. 73–81.

Semmens, B. and Meggy, A.B., 1996. The reaction of kaolin with fluorides. *J. Appl. Chem,* 16, pp. 122.

Shrikant, S. P. and Nitin, W. I., 2012. Studies on defluoridation- a critical review. *Journal of Engineering Research and Studies*, 3(I), pp. 111-119.

Smith, H.R. and Smith, L.C., 1937. Bone Contact Removes Fluorine. *Water Works Engineering*, 90, pp. 600-608.

Sorg, T.J., 1978. Treatment technology to meet the interim primary drinking water regulations for inorganics. *J. Am. Water Work Assoc*, 70, 105 –112.

Srimurali, M. and Karthikeyan, J., 2008. Activated alumina: defluoridation of water and household application – a study. Twelfth International Water Technology Conference, IWTC12. Alexandria, Egypt.

Sujana, M.G., Anand, S., 2011. Fluoride removal studies from contaminated ground water by using bauxite. *Desalination*, 267, pp. 222–227.

© University of Venda

University of Venda
Creating Future Leaders

Staz J., 1938. Dental caries in South Africa. *South African Journal of Medical Science,* 3, pp. 2 – 25.

Swiss Centre for Development Co-operation in technology and management (SKAT). 2003 Household water treatment 1 (Technical brief No. 58) Waterlines. January 2003; 21(3).

Thakre, D., Rayalua, S., Kawadea, R., Meshramb, S., Subrtc, J. and Labhsetwara, N., 2010. Magnesium incorporated bentonite clay for defluoridation of drinking water. *Journal of Hazardous Materials*, 180, pp. 122 –130.

Thole, B., 2011. Defluoridation kinetics of 200°C calcined bauxite, gypsum, and magnesite and breakthrough characteristics of their composite filter. *Journal of Fluorine Chemistry.* 132, pp. 529–535.

Thole, B., Mtalo, F.W. and Masamba, W.R.L., 2011. Water Defluoridation with 150 – 300°C Calcined Bauxite-Gypsum-Magnesite Composite (B-G-Mc) filters. *Water Resources Management VI, Wit Transactions on Ecology and Environment*, 145, pp. 383 – 393.

Thole, B., Mtalo, F.W. and Masamba, W.R.L., 2012. Effect of particle size on loading capacity and water quality in water defluoridation with 200°C calcined bauxite, gypsum, magnesite and their composite filter. *African Journal of Pure and Applied Chemistry*, 6 (2), pp. 26-34.

Tomar, V., Prasad, S. and Kumar, D., 2014. Adsorptive removal of fluoride from aqueous media using citrus limonum (lemon) leaf. *Microchem. J.* 112, pp. 97–103.

Tomar, V. and Kumar, D., 2013. A critical study on efficiency of different materials for fluoride removal from aqueous media. *Chem. Cent. J.* 7, pp. 51.

Unuabonah, E. I., Adeboual, K.O. and Dawodu, A.A., 2008. Equilibrium kinetic and sorber design studies on the adsorption of Aniline blue dye by sodium tetra borate – modified Kaolinite clay adsorbent. *J. Hazard Mater*, 157, pp. 397 – 409.

Vaiss, V.S., Berg, R.A., Ferreira, A.R., Borges, Jr I. and Leita˜o A.A. J., 2009. Phys. Chem. A, 113, pp. 6494 – 6499.

Venkobachar, C., Iyengar, L. and Mudgal, A., 1997. Household defluoridation of drinking water using activated alumina technology. Proceedings of the 2nd international workshop on fluorosis and defluoridation of water, Addis Ababa, Ethiopia, November 19-22, 1997. Dunedin, New Zealand, International Society for Fluoride Research.

Vinati A, Mahanty, B and Behera, S.K, 2015. Clay and clay minerals for fluoride removal from water: *A state-of-the-art review Applied Clay Science*, 114, pp. 340–348.

© University of Venda

University of Venda
Creating Future Leaders

Vitelli, K. D., 1999. Looking up at Early Ceramics in Greece. In: Skibo J.M and Feinman G.M (Editor). Pottery and People A Dynamic Interaction. University of Utah Press, Salt Lake City, USA. pp. 184-198.

Vhahangwele, M., Wilson, M.G. and Tholiso, N., 2015. Kinetics and equilibrium studies for removal of fluoride from underground water using cryptocrystalline magnesite. *Journal of Water Reuse and Desalination*, (5) 3, pp. 282 – 292.

Wang, J., Kang, D., Yu, X., Ge, M. and Chen, Y., 2015. Synthesis and characterization of Mg–Fe–La trimetal composite as an adsorbent for fluoride removal. *Chemical Engineering Journal*, 264, pp. 506–513.

World Health Organization. 2011. Guidelines for drinking-water quality - 4th ed. ISBN 978 92 4 154815 1.

World Health Organisation. 2004. Guidelines for drinking-water quality. 3rd Ed World Health Organization, Geneva, pp. 375–378, 301–303.

World Health Organization. 2002. Environmental Health Criteria 227. Fluoride. Geneva: World Health Organization.

Wondimagegn, A.A., 2008. Development of household defluoridation unit based on aluminium oxide hydroxide. A thesis a thesis submitted to the school of graduate studies of Addis Ababa University in partial fulfillment of the requirement for the degree of Masters of Science in Environmental Sciences.

Yakub, J. and Du, W.O., 2012. Mechanical properties, modelling and design of porous clay ceramics, *Mater. Sci. Eng. A,* 558, pp. 21–29.

Zewge, F. and Moges, G., 1990. Investigation of brick and pot chips as defluoridating media. Water supply and Sewerage Authority, Southern Regional Office, Awassa, and Department of Chemistry, Addis Ababa University, Addis Ababa, Ethiopia.

Zhuang, J., Yu, G.R., Liu, X.Y., 2000. Characteristics of lead sorption on clay minerals in relation to metal oxide. *Pedosphere,* 10 (1), pp. 11–20.

UNIVERSITY OF VENDA
LIBRARY

© University of Venda

University of Venda
Creating Future Leaders

CHAPTER THREE

METHODOLOGY

3.0 Introduction

This chapter will present all the materials and methods used for various experimental procedures, data collection, analysis and interpretation of data in this study.

3.1 Sampling

The bentonite clay was collected from Cape Bentonite, a mining company in Cape Town, South Africa and silica rich reddish black Mukondeni clay soils were collected from Mukondeni village, Limpopo province South Africa. The water for the defluoridation experiments was collected from a community borehole in Siloam village, Limpopo Province, South Africa.

3.1.1 Study area

Siloam Village is a rural community located in the Nzhelele Catchment of Limpopo Province, South Africa. The study area is located at latitude 22° 36' 05.48''S and longitude 30°10' 23.01''E as shown in Figure 3.1.

© University of Venda

University of Venda
Creating Future Leaders

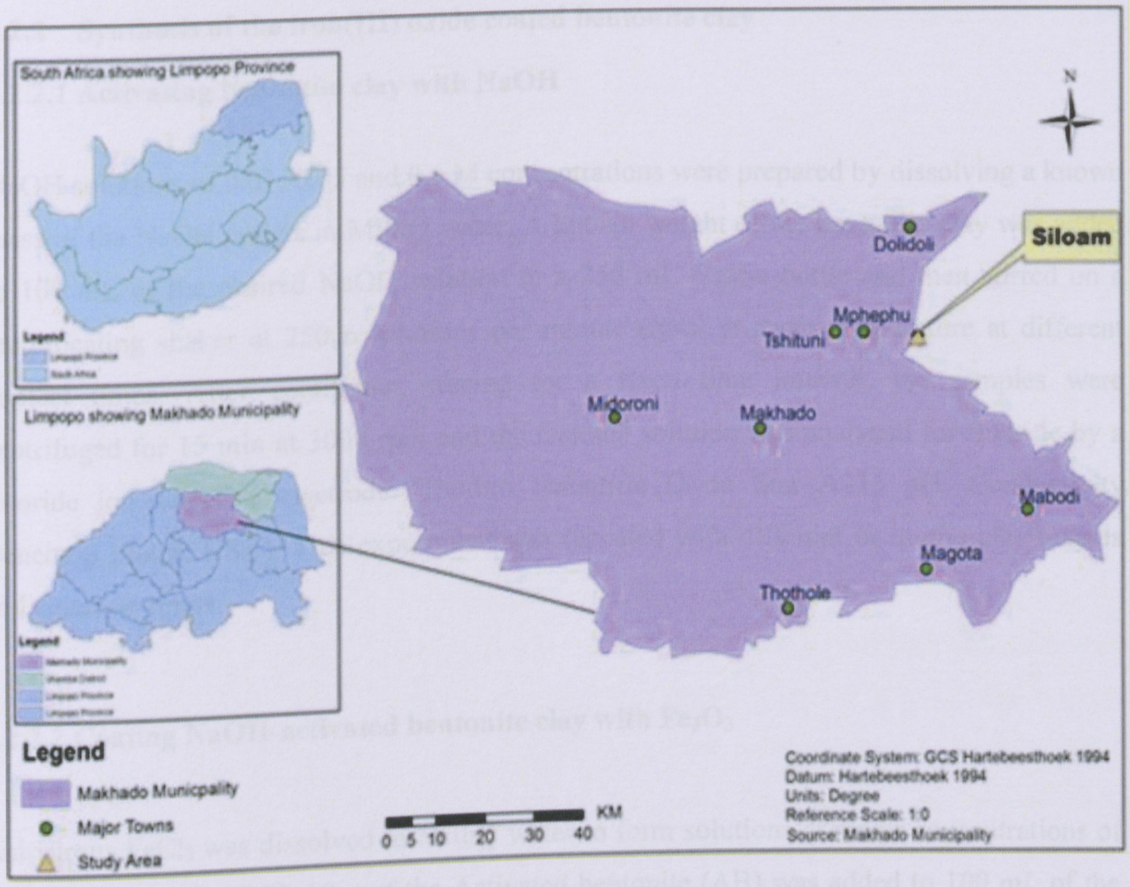


Figure 3.1 Study area

3.2 Preparation of adsorbent materials

3.2.1 Preparation of the silica rich reddish black Mukondeni clay soils

The silica rich reddish black Mukondeni clay soils were washed by rinsing with MilliQ water. 200 g of clay soil was washed by 1 L of MilliQ water. The rinsing was done by stirring the mixture for 5 min and then rinsing again with MilliQ water. After that, the mixture was agitated in a reciprocating shaker for 30 min. The samples were then centrifuged for 15 min at 3000 rpm. The supernatant which carried colloidal clay particles was filtered through a 0.45 µm pore cellulose nitrate membranes and the residual clay particles collected. The residual clay was left to dry in the oven for 12 h at 105°C. After drying the samples were milled into fine powder and passed through a 250 µm sieve.

© University of Venda

3.2.2 Synthesis of the iron(III) oxide coated bentonite clay

3.2.2.1 Activating bentonite clay with NaOH

NaOH solutions of 0.01, 0.05 and 0.1 M concentrations were prepared by dissolving a known mass of the NaOH pellets in MilliQ water. A known weight of the bentonite clay was added to 100 mL of the desired NaOH solution in a 250 mL plastic bottle and then stirred on a reciprocating shaker at 250 revolutions per minute (rpm) at room temperature at different contact times. After continuous stirring for a fixed time interval, the samples were centrifuged for 15 min at 3000 rpm and the residual solution was analyzed for fluoride by a fluoride ion selective electrode (Thermo Scientific Orion Star A215 pH/ Conductivity Benchtop Meter, USA). This experiment was repeated with different bentonite clay masses and agitation times.

3.2.2.2 Coating NaOH-activated bentonite clay with Fe_2O_3

Anhydrous $FeCl_3$ was dissolved in MilliQ water to form solutions at molar concentrations of 0.1 M, 0.3 M and 0.5 M. 10 g of the Activated bentonite (AB) was added to 100 mL of the solutions of different concentrations. The pH of the mixture was adjusted with 10 M NaOH solution until the final pH reached 6.5 and the solution was then shaken at 250 rpm on a reciprocating shaker. The mixture formed precipitates which were reddish brown in colour. The precipitates were then centrifuged and washed with distilled water until the pH of the filtrate was between 6 and 7. The residue was collected and dried in an oven at 105°C for 12 h. Afterwards, the sample was milled into fine powder by a Retsch RS 200 miller. It was then later on analysed for surface area using the Brunauer Emmett Teller method of analysis using a Micromeritics TriStar II 3020 Version 2.00. The same procedure was repeated with varying shaking times of 1 h, 3 h and 6 h for each different concentration of $FeCl_3$. Parameters optimised were $FeCl_3$ concentration and agitation time.

3.2.3 Clay composite fabrication method

The clay samples were milled into a fine powder using a Retsch RS 200 miller. For the clay to be moulded, 10 mL of MilliQ water was added to 40 g of clay. The resulting mixtures were then moulded into pellets, using a cylindrical plastic mold (a plastic lid in this case was used in the lab because of the absence of an extruder) with internal dimensions of approximately

© University of Venda

10 and 5 mm diameter and depth, respectively. The pellets were then allowed to cool at room temperature for 12 h before sintering in a furnace.

3.2.3.1 Optimisation of fabrication parameters

To determine which parameters are effective for the fabrication of ceramic pellets and the effect of these parameters on fluoride adsorption, four parameters were evaluated and are discussed in the preceding sections:

(i) Optimisation of particle size

Clay particle size was the first parameter to be optimised since it would determine the appropriate size of clay particles which will not crack upon heating. Three particle sizes were used and these were obtained by using different sized sieves to obtain 125, 250 and 500 µm grains of clay. Pellets were fabricated using the procedure presented in 3.2.3 and thereafter dried in the oven at 105°C for 12 h. The pellets were then allowed to cool at room temperature for 12 h thereafter heated in the furnace at 600°C for an hour.

(ii) Optimisation of furnace temperature

Pellets were fabricated using the procedure presented in 3.2.3 and thereafter dried in the oven at 105°C for 12 h. The pellets were then allowed to cool at room temperature for 12 h after which they were heated in the furnace for an hour. The sintering temperatures were 600, 700, 800 and 900°C. These pellets were then crushed into fine powder and used for defluoridation experiments.

(iii) Optimisation of firing time

Pellets were fabricated using the procedure presented in 3.2.3 and after that dried in the oven at 105°C for 12 h. The pellets were then allowed to cool at room temperature for 12 h after which they were heated in the furnace at 600°C. The firing times were 1 h, 2 h and 3h. These pellets were then crushed into fine powder and used for defluoridation experiments.

© University of Venda

University of Venda
Creating Future Leaders

(iv) Optimisation of clay ratios

Pellets were fabricated using the procedure presented in 3.2.3. The clay ratios were varied as follows iron(III) oxide coated bentonite (FeB): silica rich reddish black Mukondeni clay soil (SRRBM) (1:1, 1:2, 2:1, 3:1, 4:1, 5:1 and 6:1). i.e. ([10 g (FeB): 10 g (SRRBM)], [10 g (FeB): 20 g (SRRBM)], [20 g (FeB): 10 g (SRRBM)], [30 g (FeB): 10 g (SRRBM)], [40 g (FeB): 10 g (SRRBM)] [50 g (FeB): 10 g (SRRBM)] [60 g (FeB): 10 g (SRRBM)]). After drying in the oven at 105°C for 12 h, the pellets were then allowed to cool at room temperature for 12 h after which they were heated in the furnace at 600°C for 1 h. These pellets were then crushed into fine powder and used for defluoridation experiments.

3.2.3.1 Fabrication of silica rich reddish black Mukondeni soils - iron(III) oxide coated bentonite clay ceramic composite pellets.

To determine the optimum conditions for fabricating the ceramic pellets that would effectively remove fluoride from water, a defluoridation experiment was carried out at each stage of optimisation to determine which conditions gave the highest fluoride removal. The defluoridation experiments were carried out as follows:

A known weight (2 g) of the adsorbent was added to 100 mL of 10 mg/L fluoride solution in a 250 mL plastic bottle and then agitated on a reciprocating shaker at 250 rpm at room temperature. After continuous stirring for 60 min, the samples were filtered using a 0.45 µm pore cellulose nitrate membranes and the samples were analysed for F^-, pH, Temp and EC using a Thermo Scientific Orion Versa Star Advanced Electrochemistry meter. Thereafter the final ceramic pellets were fabricated using the procedure described in 3.2.3 using the following optimised conditions: (i) particle size = 250 µm, (ii) furnace temperature = (600°C), (iii) firing time = 1 h and (iv) clay ratio = 5:1.

3.3 Physicochemical and mineralogical characterization

Several techniques were used to characterize the adsorbents. These included Cation Exchange Capacity (CEC), Point of Zero Charge (PZC), X-ray diffraction (XRD), X-ray fluorescence (XRF), Scanning Electron Microscopy (SEM), Scanning Electron Microscopy coupled with

© University of Venda

Energy Dispersive Spectroscopy (SEM –EDS), Transmission Electron Microscopy (TEM), Brunauer–Emmett–Teller (BET) and Fourier Transform Infrared (FTIR)

3.3.1 Determination of Cation Exchange Capacity (CEC)

CEC was determined using the ammonium acetate method at pH 5.4 and pH 7.4 according to Chapman (1962)'s method. 0.5 g of the clay adsorbents was extracted using 25 mL aliquots of 1 M ammonium acetate. The samples were shaken for 15 min using a reciprocating shaker. After shaking, the samples were centrifuged at 30 000 rpm for 15 min. After centrifuging, the supernatant was decanted in a 250 mL bottle. The cumulative extract was brought to 100 mL and then filtered through 0.45 µm pore cellulose nitrate membranes. The filtrate was acidified by adding three drops of nitric acid and stored in the refrigerator until analysis by the Atomic Absorption Spectrometry (AAS). The samples were analysed for the availability of K^+, Na^+, Mg^{2+} and $Ca.^{2+}$

3.3.1.1 Calculation of CEC per 1 g

Atomic weight Na = 23

Equivalent weight = Atomic weight / number of valences

$Na^+ = 23/1$

By getting equivalent weight, the elements are now in equal terms

CEc is reported in meg/100 g, therefore the equivalent weights are multiplied by 10 to be converted to meq/100 g

$Na^+ = 23 * 10$

CEC = Concentration of ions in mg/L / meq/100 g

3.3.2 Determination of Point of Zero Charge (PZC)

To determine the point of zero charge (pH_{PZC}) of the clay adsorbents, 40 mL of 0.1 M KCl was measured into 100 mL bottles. The initial pH of the solution was adjusted to pHs 2, 4, 6, 8, 10 and 12 by adding 0.1 M HCl and 0.1 M NaOH solutions. The total volume of the solution in each bottle was topped to 50 mL by adding KCl. Afterwards, 0.5 g of the clay was added to the solutions and the mixtures were then equilibrated for 24 h using a Daihan Labtech thermostatic waterbath shaker. After shaking, the final pH values of the solutions

© University of Venda

were measured. The difference between the initial and the final pH was plotted against the initial pH. The point of intersection of the resulting curve with the co-ordinate that gives the distance along the horizontal axis at which $\Delta pH = 0$, was taken as the point of zero charge. The same procedure was repeated using 0.01 M and 0.001 M KCl.

3.3.3 Determination of mineralogy by X-ray diffraction (XRD)

The clay samples were milled in a tungsten carbide vessel and prepared according to the standardised PAnalytical backloading system, which provides nearly random distribution of the particles. The samples were analysed using a PANalytical X'Pert Pro powder diffractometer in θ–θ configuration with an X'Celerator detector and variable divergence and receiving slits with Fe filtered Co-Kα radiation (λ=1.789Å). The phases were identified using X'Pert Highscore plus software. The relative phase amounts (weight %) were estimated using the Rietveld method (Autoquan Program).

3.3.4 Determination of elemental composition by X-ray fluorescence (XRF)

The powdered clay samples were milled in a tungsten-carbide milling pot to achieve particle sizes < 75 micron. The samples were dried at 100°C and roasted at 1000°C to determine Loss On Ignition (LOI). 1 g sample was mixed with 6 g Lithiumtetraborate flux and fused at 1050°C to make a stable fused glass bead. The Thermo Fisher ARL Perform'X Sequential XRF with OXSAS software was used for analysis.

3.3.5 Determination of morphology by Scanning Electron Microscopy (SEM)

The morphology of the clay adsorbents was examined using a Hitachi X- 650 Scanning Electron Micro-analyser equipped with a CDU-lead detector at 25 kV. Powdered samples were mounted on aluminum pegs and coated with a thin film of gold to make them conductive.

3.3.6 Determination of surface area by Brunauer–Emmett–Teller (BET)

© University of Venda

The surface area and pore size distribution of the clay adsorbents was determined using the BET method of analysis using a Micromeritics TriStar II 3020 Version 2.00. Nitrogen adsorption isotherms were obtained at liquid nitrogen temperature. Before the determination of the adsorption isotherm, 5.2187 g of the sample was degassed at 180°C for 48 h. The degassing process was meant to remove adsorbed gases and moisture. The clay was then placed in a N_2 stream and the mass change of the solid due to gas adsorbed was measured relative to the change in partial pressure of N_2.

3.3.7 Determination of functional groups by Fourier Transform Infrared (FTIR)

To determine the functional groups in the clay adsorbents, 0.5 g sample of the clay was analyzed by Fourier-transform infrared spectroscopy (FTIR) flow-through continuous reactor. The infrared spectra in transmission mode were recorded in the 4000 – 400 cm^{-1} frequency region using a Bruker Alpha spectrometer. The measurements of the adsorption bands integrated intensity were made using OPUS software supplied by the Bruker instrument.

3.3.8 Transmission Electron Microscopy (TEM)

Electron transparent thin slices of dust particles were prepared for TEM analysis of clay minerals then sliced with a microtomem to obtain ultrathin (70 nm) cross sections of the embedded specimen. These sections were mounted on 400-mesh copper grids and analyzed with a JEM – 2100 Electron Microscope operating at 200 kV.

3.4 Preparation of fluoride solution

1000 mg/L fluoride solution was prepared by dissolving 2.2 g of NaF in MilliQ water. 100 mg/L dilution was made by extracting 100 mL of the solution from 1000 mg/L and transferring it to a 1000 mL volumetric flask. The volumetric flask was topped to 1000 mL using MilliQ water.

© University of Venda

3.5 Determination of pH, EC, TDS and F^-

Fluoride concentrations were measured by a fluoride ion selective electrode (Thermo Scientific Orion Star A215 pH/ Conductivity Benchtop Meter, USA) coupled to an 8157BNUMD Orion ROSS Ultra Triode pH/ATC electrode). A similar ion meter coupled with a pH, EC and TDS electrodes was used for measuring pH, EC and TDS of the treated samples. Before fluoride determination, a total ionic strength adjusting buffer (TISAB III) was added to the solutions in a ratio of 10:1 in order to maintain ionic strength and pH, and eliminate the interference effect of F^- ion complexing with metal cations.

3.6. Batch adsorption experiments

3.6.1 Batch adsorption experiments using silica rich reddish black Mukondeni clay soils

3.6.1.1 Adsorption of fluoride as a function of contact time

To evaluate the effect of contact time on the fluoride removal capacity of silica rich reddish black Mukondeni clay soils, 100 mL of 10 mg/L F^- solution was pipetted into 21, 250 mL bottles and 1 g, 2 g and 3 g of silica rich reddish black Mukondeni clay soils were added to each separate bottle. The mixture was agitated for 1, 5, 10, 15, 30, 60, and 180 min at 250 rpm using the Stuart reciprocating shaker. The experiments were carried out in triplicate at room temperature (25°C) and the mean values reported. After equilibration, the mixtures were centrifuged for 10 min at 3000 rpm. The samples were analysed for F^-, pH, Temp and EC using a Thermo Scientific Orion Versa Star Advanced Electrochemistry meter.

3.6.1.2 Adsorption of fluoride as a function of adsorbent dosage

To evaluate the effect of adsorbent dosage on the fluoride removal capacity of silica rich reddish black Mukondeni clay soils, 33 samples of 100 mL of 5, 10 and 15 mg/L F^- solution were pipetted into 33, 250 mL bottles and 0.1 g, 0.3 g, 0.5 g, 0.7 g, 0.9 g, 1 g, 1.2 g, 1.5 g, 1.7 g, 1.9 g and 2 g of silica rich reddish black Mukondeni clay soils were added to each bottle. The mixtures were then agitated for 60 min at 250 rpm using the Stuart reciprocating shaker. The experiments were carried out in triplicate at room temperature (25°C) and the mean values reported. After equilibration, the mixtures were centrifuged for 10 min at 3000 rpm.

© University of Venda

The samples were analysed for F^-, pH, Temp and EC using a Thermo Scientific Orion Versa Star Advanced Electrochemistry meter.

3.6.1.3 Adsorption of fluoride as a function of adsorbate concentration

To evaluate the effect of initial fluoride concentration on the fluoride removal capacity of silica rich reddish black Mukondeni clay soils 21 samples of 100 mL with 2, 5, 7, 9, 11, 13 and 15 mg/L F^- solution was pipetted into 21, 250 mL bottles and 1 g and 2 g of silica rich reddish black Mukondeni clay soils were added to each bottle separately. The mixtures were then agitated for 60 min at 250 rpm using the Stuart reciprocating shaker. The experiments were carried out in triplicate at room temperature (25°C) and the mean values reported. After equilibration, the mixtures were centrifuged for 10 min at 3000 rpm. The samples were analysed for F^-, pH, Temp and EC using a Thermo Scientific Orion Versa Star Advanced Electrochemistry meter.

3.6.1.4 Adsorption of fluoride as a function of temperature

To evaluate the effect of temperature on the fluoride removal capacity of silica rich reddish black Mukondeni clay soils the procedure written in 3.6.1.3 was repeated at different temperatures of 298 K, 308 K and 318 K. The shaking process was done using a.Daihan Labtech thermostatic water bath shaker.

3.6.1.5 Adsorption of fluoride as a function of competing ions

To evaluate the effect of competing ions on the fluoride removal capacity of silica rich reddish black Mukondeni clay soils, fluoride, sulphate, carbonate, nitrate and phosphate ions were used. To each 250 mL bottle, 10 mg/L of fluoride and 10 mg/L of each competing ion was added. To one 250 ml bottle, no competing ion was added, this was used as a control. 1.5 g of adsorbent dosage was added to each bottle. The mixtures were then agitated for 60 min at 250 rpm using the Stuart reciprocating shaker. The experiments were carried out in triplicate at room temperature (25°C) and the mean values reported. After equilibration, the mixtures were centrifuged for 10 min at 3000 rpm. The samples were analysed for F^-, pH, Temp and EC using a Thermo Scientific Orion Versa Star Advanced Electrochemistry meter.

© University of Venda

3.6.1.6 Adsorption of fluoride as a function of pH

To evaluate the effect of pH on the fluoride removal capacity of silica rich reddish black Mukondeni clay soils, 100 mL with 9 mg/L of F^- solution was pipetted into 6, 250 mL bottles. The pH of the solution was adjusted to 2, 4, 6, 8, 10 and 12 using 0.1 M of HCl and 0.1 M NaOH. 1.5 g of adsorbent dosage was added to each bottle. The mixtures were then agitated for 60 min at 250 rpm using the Stuart reciprocating shaker. The experiments were carried out in triplicate at room temperature (25°C) and the mean values reported. After equilibration, the mixtures were centrifuged for 10 min at 3000 rpm. The samples were analysed for F^-, pH, Temp and EC using a Thermo Scientific Orion Versa Star Advanced Electrochemistry meter.

3.6.1.7 Application of the optimized conditions for F^- adsorption using borehole water

The optimized conditions of 60 min of contact time, 1.5 g of adsorbent dosage, 298 K temperature and a pH of 2 established in the optimisation stages were applied for tht defluoridation of Siloam borehole water.

3.6.2 Batch adsorption experiments using iron(III) oxide coated bentonite clay

3.6.2.1 Adsorption of fluoride as a function of contact time

To evaluate the effect of contact time on the fluoride removal capacity of iron(III) oxide coated bentonite clay, 100 mL of 10 mg/L F^- solution was pipetted into 30, 250 mL bottles and 0.5, 1 and 2 g of iron(III) oxide coated bentonite clay was added. The mixtures were agitated for 1, 5, 10, 15, 30, 60, 180, 240, 300 and 360 min at 250 rpm using the Stuart reciprocating shaker. The experiments were carried out in triplicate at room temperature (25°C) and the mean values reported. After equilibration, the mixtures were centrifuged for 10 min at 3000 rpm. The samples were analysed for F^-, pH, Temperature and EC using a Thermo Scientific Orion Versa Star Advanced Electrochemistry meter.

3.6.2.2 Adsorption of fluoride as a function of adsorbent dosage

To evaluate the effect of adsorbent dosage on the fluoride removal capacity of iron(III) oxide coated bentonite clay, 24 samples of 100 mL solutions of 5, 10 and 20 mg/L F- solution were pipetted into 24, 250 mL bottles and 0.1 g, 0.5 g, 0.8 g, 1 g, 2 g, 3 g, 4 g and 5 g of iron(III) oxide coated bentonite clay was added to each bottle. The mixtures were then agitated for 30

© University of Venda

min at 250 rpm using the Stuart reciprocating shaker. The experiments were carried out in triplicate at room temperature (25°C) and the mean values reported. After equilibration, the mixtures were centrifuged for 10 min at 3000 rpm. The samples were analysed for F-, pH, Temp and EC using a Thermo Scientific Orion Versa Star Advanced Electrochemistry meter.

3.6.2.3 Adsorption of fluoride as a function of adsorbate concentration

To evaluate the effect of initial fluoride concentration on the fluoride removal capacity of iron(III) oxide coated bentonite clay 12 samples of 100 mL with 5, 10, 20, 40, 60 and 80 mg/L F^- solution was pipetted into 12, 250 mL bottles and 2 g and 3 g of iron(III) oxide coated bentonite clay was added to each bottle separately. The mixtures were then agitated for 30 min at 250 rpm using the Stuart reciprocating shaker. The experiments were carried out in triplicate at room temperature (25°C) and the mean values reported. After equilibration, the mixtures were centrifuged for 10 min at 3000 rpm. The samples were analyzed for F-, pH, Temperature and EC using a Thermo Scientific Orion Versa Star Advanced Electrochemistry meter.

3.6.2.4 Adsorption of fluoride as a function of temperature

To evaluate the effect of temperature on the fluoride removal capacity of iron(III) oxide coated bentonite clay the procedure written in 3.6.2.3 was repeated at different temperatures of 298 K, 308 K and 318 K. The shaking process was done using a Daihan Labtech thermostatic water bath shaker.

3.6.2.5 Adsorption of fluoride as a function of competing ions

To evaluate the effect of competing ions on the fluoride removal capacity of iron(III) oxide coated bentonite clay, fluoride, sulphate, carbonate, nitrate and phosphate ions were used. To each 250 mL bottle, 10 mg/L of fluoride and 10 mg/L of each competing ion was added. To one 250 ml bottle, no competing ion was added (the control). 3 g of adsorbent dosage was added to each bottle. The mixtures were then agitated for 30 min at 250 rpm using the Stuart reciprocating shaker. The experiments were carried out in triplicate at room temperature (25°C) and the mean values reported. After equilibration, the mixtures were centrifuged for 10 min at 3000 rpm. The samples were analysed for F^-, pH, Temperature and EC using a Thermo Scientific Orion Versa Star Advanced Electrochemistry meter.

© University of Venda

3.6.2.6 Adsorption of fluoride as a function of pH

To evaluate the effect of pH on the fluoride removal capacity of iron(III) oxide coated bentonite clay, 100 mL with 5 mg/L of F^- solution was pipetted into 18, 250 mL bottles. The pH of the solution was adjusted to 2, 4, 6, 8, 10 and 12 using 0.1 M of HCl and 0.1 M NaOH. 3 g of adsorbent dosage was added to each bottle. The mixtures were then agitated for 30 min at 250 rpm using the Stuart reciprocating shaker. The experiments were carried out in triplicate at room temperature (25°C) and the mean values reported. After equilibration, the mixtures were centrifuged for 10 min at 3000 rpm. The samples were analysed for F^-, pH, Temperature and EC using a Thermo Scientific Orion Versa Star Advanced Electrochemistry meter.

3.6.2 Application of the optimised conditions for F^- adsorption using Siloam borehole water

The optimised conditions of 30 min of contact time, 3 g of adsorbent dosage, 298 K temperature and a pH of 2 established in the optimization stage were applied to defluoridation of Siloam borehole water.

3.7 Chemical stability testing

The chemical stability of the adsorbents was investigated by measuring the concentration of dissolved metals in the solution before and after fluoride adsorption experiments. The adsorbents (1.5 and 3 g) of silica rich reddish black Mukondeni clay soils and iron(III) oxide coated bentonite clay respectively was added to 100 mL fluoride solution (10 mg/L) samples over a pH range of 2 –12. The supernatant was separated through filtration using a 0.45 µm pore cellulose nitrate membranes after shaking for 60 min at 250 rpm using the Stuart reciprocating shaker. The concentration of dissolved metals was measured by inductively coupled plasma mass spectrometry (ICP-MS, DIONEX ICS-2100 from Thermo).

3.8 Regeneration studies

The regeneration potential of the iron(III) oxide coated bentonite clay was evaluated by using 0.01 M NaOH. A defluoridation experiment was done using 2 g iron(III) oxide coated

© University of Venda

bentonite clay in a 100 mL, 10 mg/L F^- solution. The amount of fluoride adsorbed was noted and the adsorbent was dried in the oven for 12 h at 105°C. Afterwards the adsorbent was soaked into 100 mL, 0.01 M NaOH solution and the mixture was centrifuged at 50 000 rpm for 15 min. The amount of fluoride desorbed into the solution was recorded. The adsorbent was again washed by 100 mL MilliQ water to wash off any fluoride on the adsorbent and the amount of fluoride in the wash was recorded again. The desorbed adsorbent was again dried in the oven for 12 h at 105°C. The dried adsorbent was again used for another defluoridation experiment as described above. The same procedure using the same adsorbent was repeated until the adsorbent's fluoride removal capacity was at its lowest.

3.10 Calculation of % F^- removal and Adsorption Capacity

The % fluoride removal by the adsorbents was calculated by the following equation:

$$\%\ Removal = \left(\frac{Co-Ce}{Co}\right) \times 100 \quad \ldots\ldots\ldots\

University of Venda
Creating Future Leaders

parameters and the underlying assumptions of these equilibrium models are capable of predicting ion adsorption and vital information on the mechanism of sorption. The Langmuir, Freundlich and Dubinin- Radushkevich isotherms were tested in this study.

3.11.1 The Langmuir Isotherm

The Langmuir isotherm equation (3.4) assumes that adsorption cannot proceed beyond the monolayer and the ability of a molecule to be adsorbed at a given site is independent of the occupation of neighbouring sites (Zawani, et al., 2009)

UNIVERSITY OF VENDA
LIBRARY

Expressed mathematically,

$$\frac{Ce}{Qe} = \frac{1}{Qmb} \quad \ldots\ldots\ldots\

University of Venda
Creating Future Leaders

3.11.3 The Dubinin–Radushkevich isotherm

This isotherm was applied to the experimental data, in order to investigate the mean free energy of adsorption. The linearized Dubinin-Radushkevich isotherm is expressed in equation (3.6)

$$lnQ_e = lnQ_D\ 2B_D\ RT \ln\left(1+\frac{1}{C_e}\right) \ldots\ldots\ldots\

$$K = \left(\frac{C_i - C_e}{C_e}\right) M \ldots\ldots\ldots\

$$\log(q_e - q_t) = \log q_e - (\frac{K}{2.303})t \quad \ldots\ldots\ldots\

Where *kid* is intraparticle diffusion rate constant (mg/g/min) and *qt* is the amount of fluoride adsorbed at any time *t* (mg/g) and *C* is the intercept.

3.14.2 External diffusion

The likelihood of external diffusion being the rate controlling step was also tested using the model by Lee, et al. (1999). The diffusion model is given as:

$$ln\frac{C_t}{C_o} = -k_f \frac{A}{V} t \quad \ldots\ldots\ldots\

University of Venda
Creating Future Leaders

3.16 References

Azizian, S., 2004. Kinetic models of sorption: a theoretical analysis. *J. Colloid Interface Sci*, 27, pp. 47–52.

Chapman, H.D. 1962. Cation Exchange Capacity. In: C. A. Black (ed.) Methods of soil analysis - Chemical and microbiological properties. *Agronomy,* 9, pp. 891-901.

Ho, Y.S., 2006. Review of second-order models for adsorption systems, *J.Hazard Mater*, 136, pp. 681–689.

Ho, Y.S., 2004. Citation review of Lagergren kinetic rate equation on adsorption reactions, *Scientometrics,* 59, pp. 171–177.

Krishnaiah, A. and Vijaya, Y. Sorptive response profile of chitosan coated silica in the defluoridation of aqueous solution. *E-Journal of Chemistry,* 6 (3), pp. 713–724.

Lee, C.K., Low, K.S. and Chew, S.L., 1999. Removal of anion dyes by water hyacinth roots. *Adv. Environ. Re,*. 3 (3), pp. 343-351.

Mahramanlioglu M., Kizilcikli I. and Bicer I. O., 2002. Sorption of fluoride from aqueous solution by acid treated spent bleaching earth. *Journal of Fluorine Chemistry.* 115, pp. 41-47.

Zawani, Z., Luqman, C.A. and Thomas, S.Y.C., 2009. Equilibrium, kinetics and thermodynamic studies: Adsorption of remazol black 5 on the palm kernel shell activated carbon (PKS-AC). *European Journal of Science Research*, 37 (1), pp. 67–76.

© University of Venda

University of Venda
Creating Future Leaders

CHAPTER FOUR

DEFLUORIDATION OF GROUNDWATER USING SILICA RICH REDDISH BLACK MUKONDENI CLAY SOILS

ABSTRACT

The potential of silica rich reddish black Mukondeni clay soils as an adsorbent for the removal of fluoride from aqueous solution was investigated. The purpose of this study was to evaluate the possible application of silica rich reddish black Mukondeni clay soils as a convenient and cheap technology for the removal of excess fluoride from ground water. Characterisation was done by XRF, XRD, SEM, BET and FTIR. CEC and PZC were determined using standard methods. Parameters optimized included: contact time, adsorbent dosage, initial concentration, competing ions, pH and temperature. Optimisation experiments were done in batch procedures. The results showed that the optimum conditions for the defluoridation of water using silica rich reddish black Mukondeni clay soils are 60 min, 1.5 g, 9 mg/L, 1.5/100 S/L ratios a pH of 2 and a temperature of 25°C. The equilibrium isotherm regression parameter (R^2) showed that the Freundlich isotherm (0.95) gave a better fit than the Langmuir isotherm (0.52), and the Dubinin-Radushkevich isotherm (0.78) which indicates multilayer adsorption. The value of the activation energy (58.8554 kJ/mol) obtained from the Arrhenius equation indicates chemisorption. Kinetic studies revealed that the adsorption followed pseudo second order kinetics. This study established that silica rich reddish black Mukondeni clay soils are fairly good in the defluoridation of groundwater but modification through blending with metal oxide modified bentonite can enhance their adsorption.

Key words: fluoride, adsorption, silica rich reddish black Mukondeni clay soils, groundwater and adsorption models.

© University of Venda

University of Venda
Creating Future Leaders

4.0 Introduction

Mukondeni clay soils are used for pottery making and ceramic water filters and are recently getting more attention in water treatment applications (Abebe, et al., 2014; Denga, 2013 Hackett, et al., 2013; Tyeryar, 2012). However, there seems to be very few scientific studies done to investigate their physicochemical characteristics and the link to water treatment. Many studies have shown that clay soils are good adsorbents for fluoride removal (Thakre, et al., 2010; Karthkeyan, et al. 2005; Srimurali, et al., 2005) Thus, it becomes significant that the basic characteristics of Mukondeni clay soils are evaluated and their scientific application in the treatment of water be assessed. Moreover these clay soils are locally and readily available, hence a breakthrough in their ability to remove contaminants from drinking water will come as an advantage to the local communities, most of whom are poor and cannot afford expensive water treatment methods.

This chapter therefore seeks to present results on:

(i) physicochemical and mineralogical characterisation of the silica rich reddish black Mukondeni clay soils

(ii) optimisation of the fluoride adsorption conditions

(iii) adsorption capacity, isotherms, kinetics and mechanisms of fluoride adsorption using silica rich reddish black Mukondeni clay soils.

4.1. Materials and methods

All chemicals used in the present study were of analytical reagent grade. Silica rich reddish black Mukondeni clay soils were collected from Mukondeni Village in Limpopo province. Fluoride rich water was collected from a borehole in Siloam village in Limpopo province. Sodium fluoride and (TISAB-III) were obtained from Rochelle Chemicals and Lab Equipment CC, South Africa Ltd. The detailed experimental procedure has been presented in Chapter 3, section 3, page 46 – 63.

© University of Venda

University of Venda
Creating Future Leaders

4.2 Results and discussions

4.2.1 Physicochemical and mineralogical characterisation of silica rich reddish black Mukondeni clay soils.

4.2.1.1 Cation Exchange Capacity (CEC)

Table 4.1 shows the concentration of exchangeable cations in silica rich reddish black Mukondeni clay soils.

Table 4.1: Cation Exchange Capacity of silica rich reddish black Mukondeni clay soils at pH 5.4 and 7.4

	Exchangeable cations				CEC (meq/100 g)
pH	Na^+	K^+	Ca^{2+}	Mg^{2+}	Total
5.4	44.79	1.4	0.40	24.00	70.59
7.4	111.30	2.00	0.40	24.00	137.70

The exchangeable cations identified were Na^+, Ca^{2+} Mg^{2+} and K^+. The concentrations of the exchangeable cations were determined in mg/L and then converted to milliequivalent per 100 g (meq/100 g) as shown in Table 4.1. The CEC results showed a high concentration of exchangeable Na^+ at both pHs and Ca^{2+} had the least concentration. Since CEC is an intrinsic property of soil defining the concentration of negatively charged sites on soil colloids that can adsorb exchangeable cations, the identified exchangeable cations in silica rich Mukondeni clay soils shows that it can be a good material for use in the adsorption process. This clay typically contains SiO_2, Al_2O_3 and oxides of Mg, Ca and K which might contribute towards the fluoride adsorption (Thakre, et al., 2011). It is well documented that that fluoride has a strong affinity for electropositive species and therefore these cations can enhance the fluoride adsorption (Karthkeyan, et al. 2005; Srimurali, et al., 2005).

4.2.1.2 Point of zero charge (PZC) of silica rich reddish black Mukondeni clay soils.

Figure 4.1 shows the point of zero charge of silica rich reddish black Mukondeni clay soils.

© University of Venda

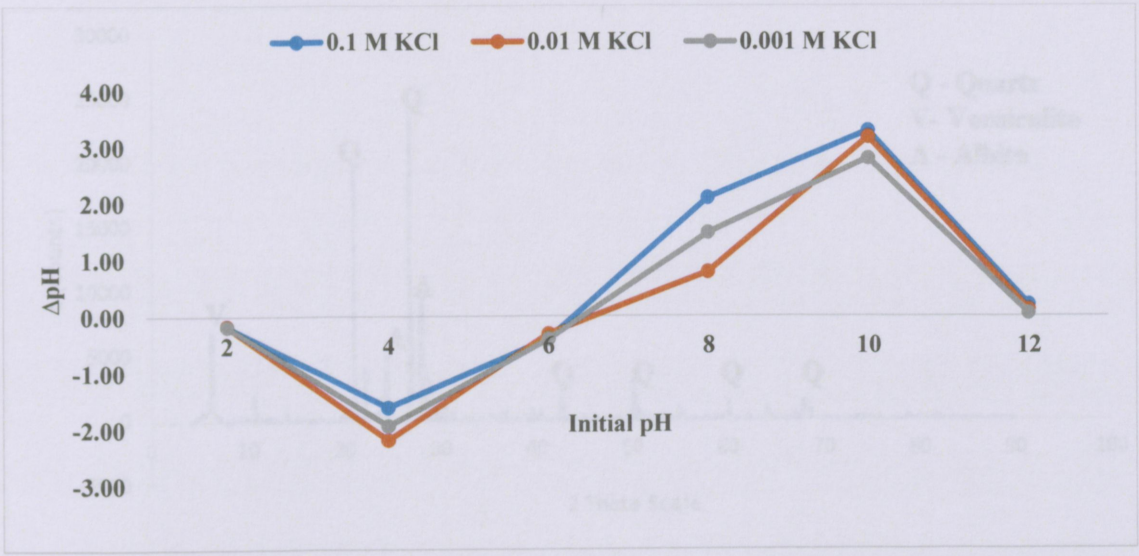


Figure 4.1: Point of zero charge of silica rich reddish black Mukondeni clay soils

The pH where the net total particle charge is zero is called the point of zero charge (PZC), which is one of the most important parameters used to describe variable-charge surfaces (Morais, et al., 1976). If the pH of a soil is above its PZC the soil surface will have a net negative charge and predominantly exhibit an ability to exchange cations (CEC - exchange of one positive ion by another), while the soil will mainly retain anions (electrostatically) if its pH is below its PZC (AEC - exchange of one negative ion for another) (Appela, et al., 2003). Figure 4.1 shows that silica rich reddish black Mukondeni clay soils have a PZC at pH 6.5 which is slightly acidic. This means that adsorption of F^- using silica rich reddish black Mukondeni clay soils will be effective only in acidic conditions below pH 6.5 because the surfaces will be positively charged enhancing the uptake of anions.

4.2.1.3 X - Ray Diffraction (XRD) analysis

Figure 4.2 shows the XRD spectrum of silica rich reddish black Mukondeni clay soils

© University of Venda

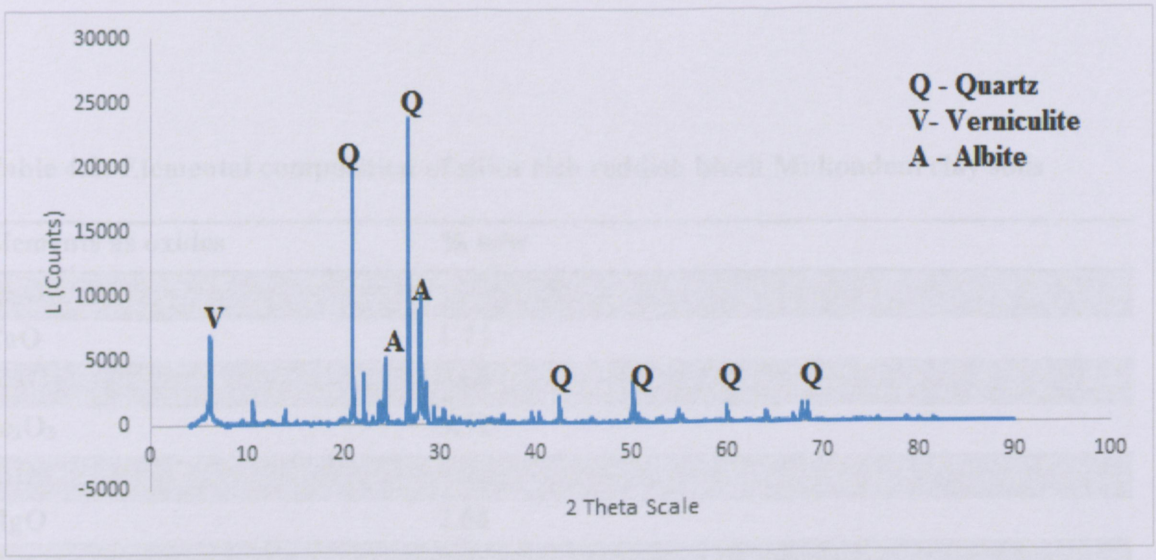


Figure 4.2: XRD diffractogram of silica rich reddish black Mukondeni clay soils.

Figure 4.2 shows a sample diffractogram data analyzed with reference to International Center for Diffraction Data ICDD Standard; Card number 36- 0426. The diffractogram shows that quartz makes the greatest part of the clay soils as can be seen in the spectrum that many peaks and the highest counts are observed with quartz. Quartz is made up of a continuous framework of SiO_4 silicon – oxygen tetrahedral, with each oxygen being shared between two tetrahedral, giving an overall formula SiO_2. In light of that, these clay soils can be said to be silicate materials. The spectrum also show the presence of vermiculite and albite which are $Mg_3Si_4O_{10}(OH)_2$ and $Na,Ca,Al(Si,Al)_3O_8$ respectively. Quantitative XRD further confirmed that it contains pargasite - $NaCa_2Mg_4Al_3Si_6O_{22}(OH)_2$ (3.12 %) as the other major mineral phases with minor quantities of anthophyllite ($Mg_5Fe_2Si_8O_{22}(OH)_2$) (1.82 %)

4.2.1.4 X – Ray Fluorescence (XRF) Analysis

The percentages of major elements presented as oxides in silica rich reddish black Mukondeni clay soils are shown in Table 4.2.

UNIVERSITY OF VENDA
LIBRARY

© University of Venda

Table 4.2: Elemental composition of silica rich reddish black Mukondeni clay soils

Elements as oxides	% w/w
Al_2O_3	14.36
CaO	1.75
Cr_2O_3	0.04
Fe_2O_3	5.52
K_2O	0.9
MgO	2.68
MnO	0.08
Na_2O	2.53
P_2O_5	0.04
SiO_2	61.76
TiO_2	0.57
L.O.I.	9.3
Total	99.53

Table 4.2 presents the major chemical constituents of silica rich reddish black Mukondeni clay soils. The high concentrations of SiO_2 and Al_2O_3 confirmed that this clay is an alumino-silicate. There are however other metal oxides like Fe_2O_3, MgO and Na_2O. As it was mentioned earlier in 4.2.1.1, these metal oxides might contribute towards the fluoride adsorption and hence their presence in these clay soils plays a significant role in the adsorption process. The Loss on Ignition value was quite high compared to other values meaning that a significant amount of moisture and impurities was lost when the sample was ignited.

4.2.1.5 Scanning Electron Microscopy (SEM) analysis

The morphology of silica rich reddish black Mukondeni clay before and after defluoridation is shown in Figure 4.3.

© University of Venda

University of Venda
Creating Future Leaders

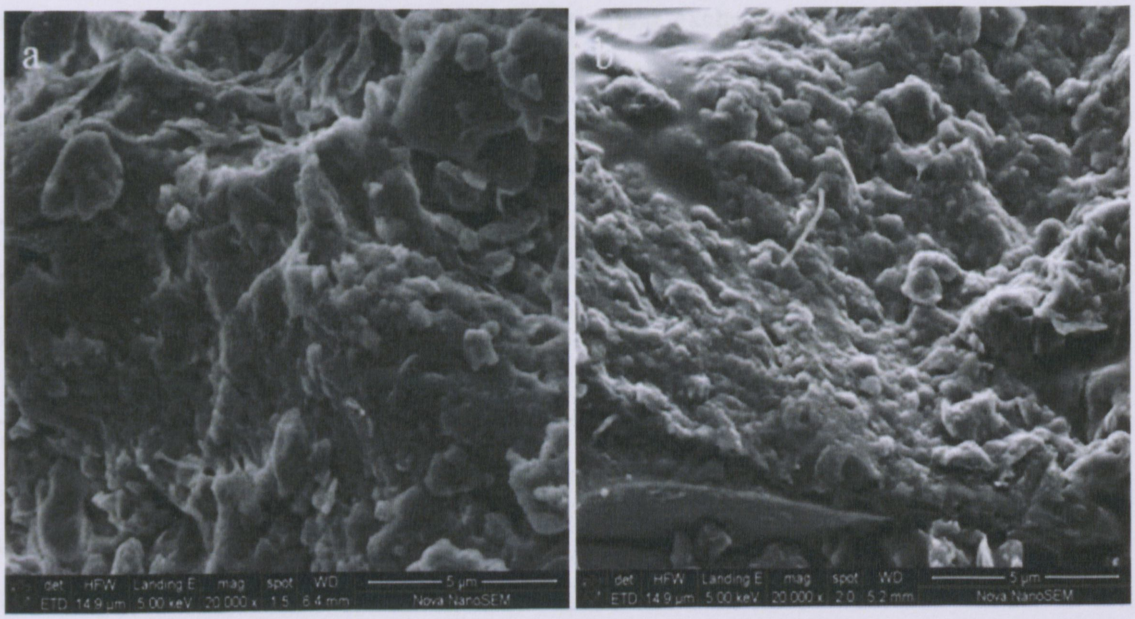


Figure 4.3: SEM images of silica rich reddish black Mukondeni clay soils before (a) and after (b) defluoridation

SEM images of silica rich reddish black Mukondeni clay soils before and after defluoridation are presented by Figure 4.3 (a) and (b) respectively. Careful examination of both the SEM images shows clay particles of varying sizes that do not conform to any pattern of arrangement. Some individual well crystalline pseudohexagonal edges of clay particles as well as some roll, rough and sharp edged particles are also observed. Figure 4.3 (a) reveals a rough texture with an irregular structure and shapes in the surface morphology. However after defluoridation as shown in Figure 4.3 (b), the clay soils appear to have small particle sizes with undefined shapes. The adsorption of fluoride seemed to have made the clay soils to shows agglomerates of very fine particles clustered together with some appearing threadlike and some having very flat surfaces.

4.2.1.6 Brunauer–Emmett–Teller (BET) analysis

Surface area is a surface phenomenon and it is dependent upon soil particle size, the smaller the soil particle size the higher the surface area and the bigger the soil particle size the smaller the surface area. In contrast to sand, clay minerals have the smallest particle size which ultimately leads to large surface area. The large specific surface area of clay soils provides sites in which molecules from soil solution can bind through weak van der Waal forces. Clay soils are charged colloid fractions which contain electrostatic surface charge, a

© University of Venda

property which accounts for adsorption, binding, and exchange of ions and molecules on particle surface (WHO, 2005). Table 4.3 gives the surface area, pore volume and pore size of silica rich reddish black Mukondeni clay soils.

Table 4.3: Surface area, pore volume and pore size of silica rich reddish black Mukondeni clay soils

Parameter	Silica rich reddish black Mukondeni clay soils
Surface area (m^2/g)	
Single point surface area	35.4612
BET Surface Area	43.2077
BJH Adsorption cumulative surface area of pores	30.9090
BJH Desorption cumulative surface area of pores	28.7297
Pore Volume (cm^3/g)	
Single point adsorption total pore volume of pores	0.037698
BJH Adsorption cumulative volume of pores	0.035524
BJH Desorption cumulative volume of pores	0.034952
Pore Size (Å)	
Adsorption average pore width (4V/A by BET)	41.8647
BJH Adsorption average pore diameter (4V/A)	45.9720
BJH Desorption average pore diameter (4V/A)	48.6640

UNIVERSITY OF VENDA
LIBRARY

© University of Venda

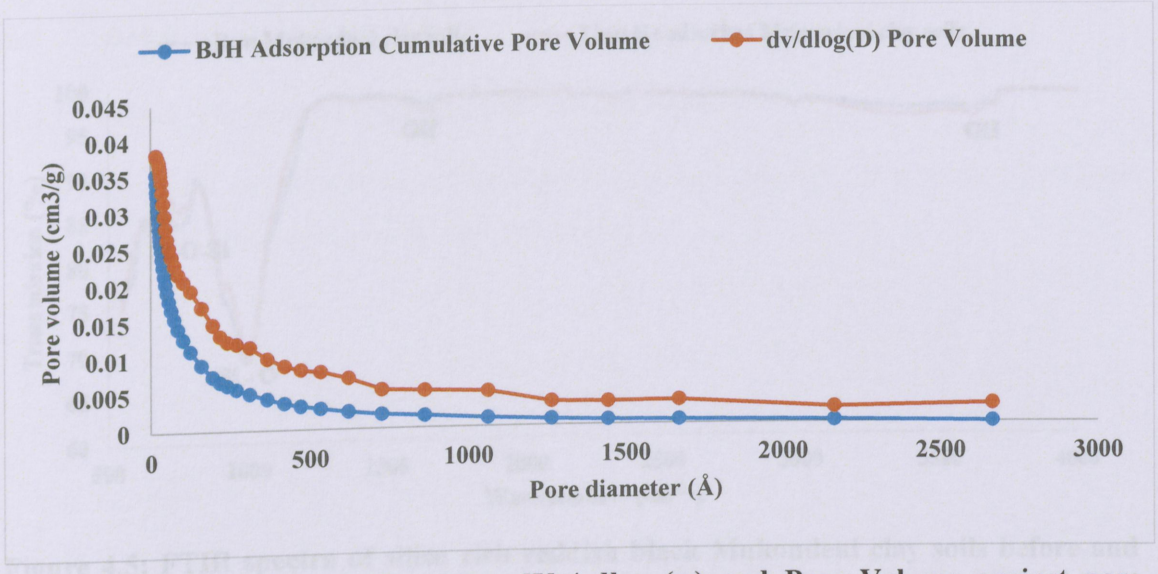


Figure 4.4: Plot of BJH Adsorption dV / dlog (w) and Pore Volume against pore diameter for silica rich reddish black Mukondeni clay soils

The BET-N_2 surface area represents the total surface area (external surface area + micro pore area). Results in Table 4.3 show that silica rich reddish black Mukondeni clay soils has a BET surface area of 35.4613 m^2/g. The surface area is high compared to typical soils but lower than pure phase goethite and illite, which range from 45 to 169 and 65 to 100 m^2/g, respectively (Langmuir, 1997). Compared to other adsorbents used in defluoridation, it has a moderate surface area. A study by Gitari, et al. (2013) showed that raw bentonite clay has a surface area of 16,015 m^2/g while Goswami and Purkait (2013) used schwertmannite with a surface area of 314.55 m^2/g. Figure 4.4 shows the pore diameters of silica rich reddish black Mukondeni clay soils which helps us to differentiate between the materials in terms of their pores. From what is shown in Figure 4, most of the particles have pore sizes which fall between 2 and 500 Å, basically meaning that silica rich reddish black Mukondeni clay soils are mesoporous.

4.2.1.7 Fourier Transform Infrared (FTIR) analysis

The FTIR spectra of silica rich reddish black Mukondeni clay soils is shown in Figure 4.5.

© University of Venda

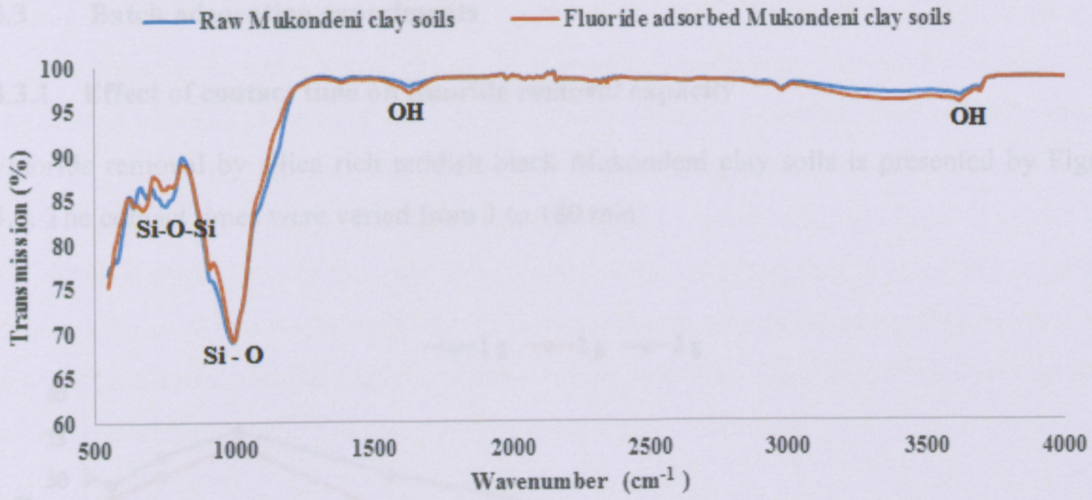


Figure 4.5: FTIR spectra of silica rich reddish black Mukondeni clay soils before and after defluoridation

FTIR spectroscopy was utilized to indicate the functional groups present on the surface of the adsorbent. As shown in Figure 4.5 the pattern of vibration obtained indicates that there are a number of functional groups in the clay sample. The FTIR spectra of the samples show a number of sharp and small bands. The presence of absorption bands at 457, 529 and 670 cm^{-1} on the spectrum corresponds to the Si-O-Si bending hence showing that that the material understudy is a silicate (Madejova and Komadel, 2001). Silica rich reddish black Mukondeni clay soils showed a very high absorbance at wavelength number 910 and 995 cm^{-1} which corresponds to OH deformations linked to Al^{3+} (Madejova and Komadel, 2001) hence showing that aluminium is a building block of the clay minerals in the soils. The spectrum also shows peaks at 1635 cm^{-1} and this shows the presence of H-O-H bonding of water molecules (Yuan-hu, et al., 2006). A wide but small absorption band is observed between 3690 and 3370 cm^{-1} and this band basically corresponds to a variety of OH bonds like OH stretching and crystalline hydroxyl, H-O-H stretching and absorbed water. The results corroborates the XRD and XRF results confirming that the material understudy is an alumino silicate. There is no major difference between the raw clay soils and the fluoride adsorbed clay soils. However on the fluoride adsorbed clay soils, the transmittance is quite high at about a 1000 cm^{-1}. That wavenumber corresponds variety forms of OH groups and that high transmittance is probable because the OH ions were exchanged for the fluoride ions during the adsorption process hence the reduction in the amount of OH ions leading to a higher transmittance.

© University of Venda

4.3 Batch adsorption experiments

4.3.1 Effect of contact time on fluoride removal capacity

Fluoride removal by silica rich reddish black Mukondeni clay soils is presented by Figure 4.6. The contact times were varied from 1 to 180 min.

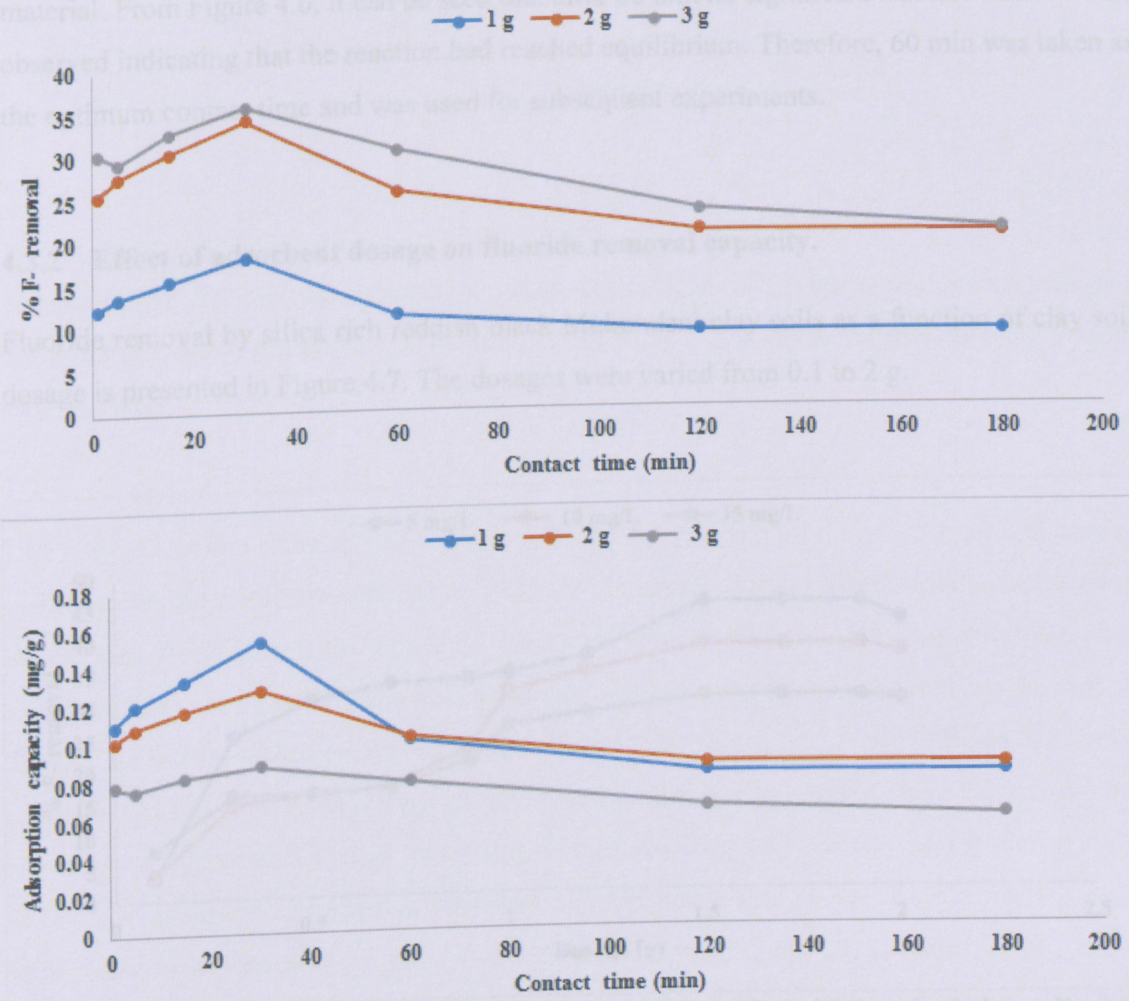


Figure 4.6: Percentage removal and adsorption capacity of silica rich reddish black Mukondeni clay soils as a function of contact time (1, 2 and 3 g, 10 mg/L F^-, 25°C room temperature, 100 mL, 250 rpm, pH*i* = 6.423)

In order to establish the equilibrium time of adsorption of fluoride onto silica rich reddish black Mukondeni clay soils, the effect of contact time was evaluated (1 min to 180 min) at an initial fluoride concentration of 10 mg/L. Figure 4.6 shows that there was a rapid rise in

© University of Venda

fluoride removal from the first minute of contact up to 30 min followed by a gradual decrease at all adsorbent dosages. The same trend is also observed with adsorption capacity. The increase in percentage removal of fluoride with an increase in contact time could be due to the fact that as time increased the fluoride ions were finding the unoccupied adsorption sites and getting adsorbed. Further increase in contact time did not increase the fluoride uptake due to sufficient deposition of fluoride ions on the available adsorption sites of the adsorbent material. From Figure 4.6, it can be seen that after 60 min no significant fluoride removal was observed indicating that the reaction had reached equilibrium. Therefore, 60 min was taken as the optimum contact time and was used for subsequent experiments.

4.3.2 Effect of adsorbent dosage on fluoride removal capacity.

Fluoride removal by silica rich reddish black Mukondeni clay soils as a function of clay soil dosage is presented in Figure 4.7. The dosages were varied from 0.1 to 2 g.

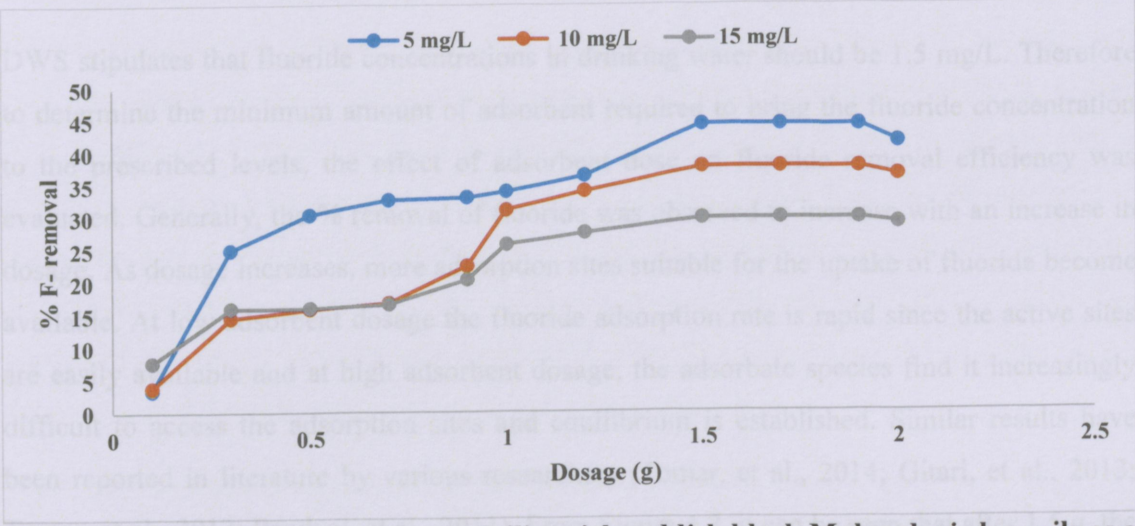


Figure 4.7(a): Percentage removal of silica rich reddish black Mukondeni clay soils as a function of dosage (60 min contact time, 10 mg/L F^-, 25°C room temperature, 250 rpm, pH*i* = 5.937)

© University of Venda

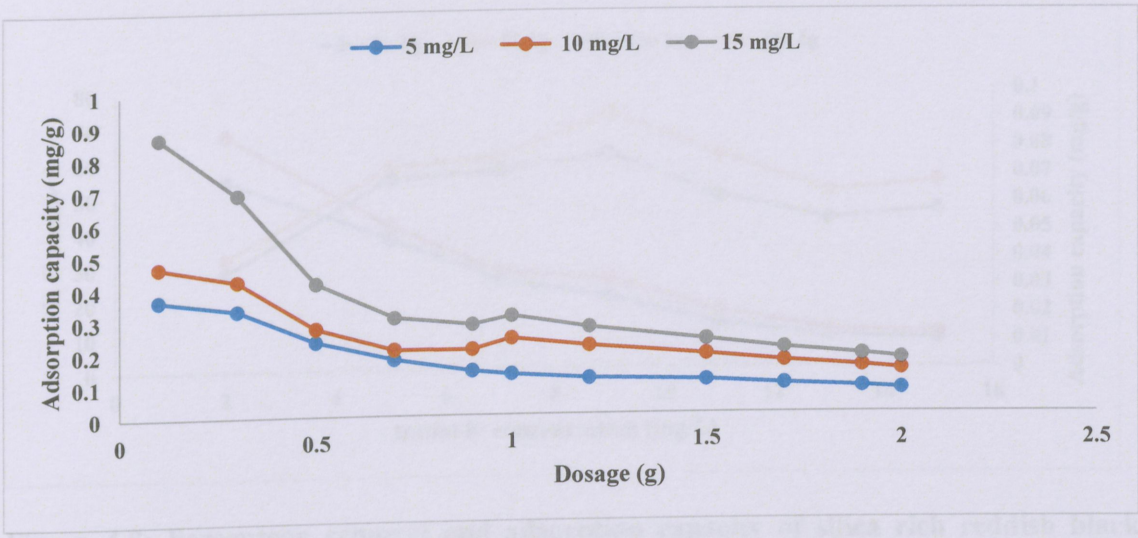


Figure 4.7(b): Adsorption capacity of silica rich reddish black Mukondeni clay soils as a function of dosage (60 min contact time, 10 mg/L F^-, 25°C room temperature, 250 rpm, pH*i* = 5.937)

DWS stipulates that fluoride concentrations in drinking water should be 1.5 mg/L. Therefore to determine the minimum amount of adsorbent required to bring the fluoride concentration to the prescribed levels, the effect of adsorbent dose on fluoride removal efficiency was evaluated. Generally, the % removal of fluoride was observed to increase with an increase in dosage. As dosage increases, more adsorption sites suitable for the uptake of fluoride become available. At low adsorbent dosage the fluoride adsorption rate is rapid since the active sites are easily available and at high adsorbent dosage, the adsorbate species find it increasingly difficult to access the adsorption sites and equilibrium is established. Similar results have been reported in literature by various researchers (Tomar, et al., 2014; Gitari, et al., 2013; Tomar, et al., 2013; Paudyal, et al., 2011). From Figure 4.7, it can be seen that after 1.5 g, the percentage removal remained fairly constant indicating that the reaction had reached equilibrium. Thus based on the present study 1.5 g of the adsorbent was selected for further experiments as the optimum dosage.

4.3.3 Effect of fluoride ion concentration on fluoride removal capacity

Fluoride removal by silica rich reddish black Mukondeni clay soils as function of initial F^- concentration is presented in Figure 4.8.

© University of Venda

University of Venda
Creating Future Leaders

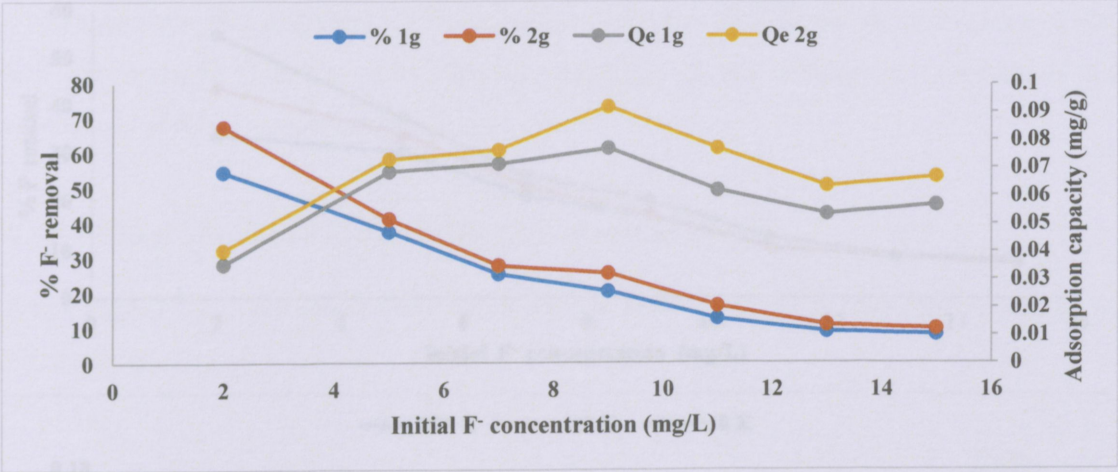


Figure 4.8: Percentage removal and adsorption capacity of silica rich reddish black Mukondeni clay soils as a function of initial fluoride concentration (60 min contact time, 1.5 g dosage, 25°C room temperature, 100 mL, 250 rpm, pH*i* = 6.111).

The effect of initial concentration of fluoride on the adsorption and uptake of fluoride from solution by the silica rich reddish black Mukondeni clay soils was evaluated by varying the fluoride concentration solutions from 1 to 15 mg/L. The adsorption capacity of the adsorbent rose with increasing initial fluoride concentration until 9 mg/L then dropped gradually at high F^- concentration. An opposite trend was shown with percentage fluoride removal, which is shown to decrease with increase in initial fluoride concentration. This may be attributed to the presence of more fluoride ions being greater than the adsorption capacity of the adsorbent and similar results have been reported by Ghandi, et al. (2012) and Chen, et al. (2010). The maximum adsorption capacity was observed at 9 mg/L and therefore it was taken as the optimum initial fluoride concentration for subsequent experiments.

4. 3.4 Effect of temperature on fluoride removal capacity

Percentage fluoride removal by silica rich reddish black Mukondeni clay soils is presented in Figure 4.9. The temperatures were varied from 298 to 308 K.

© University of Venda

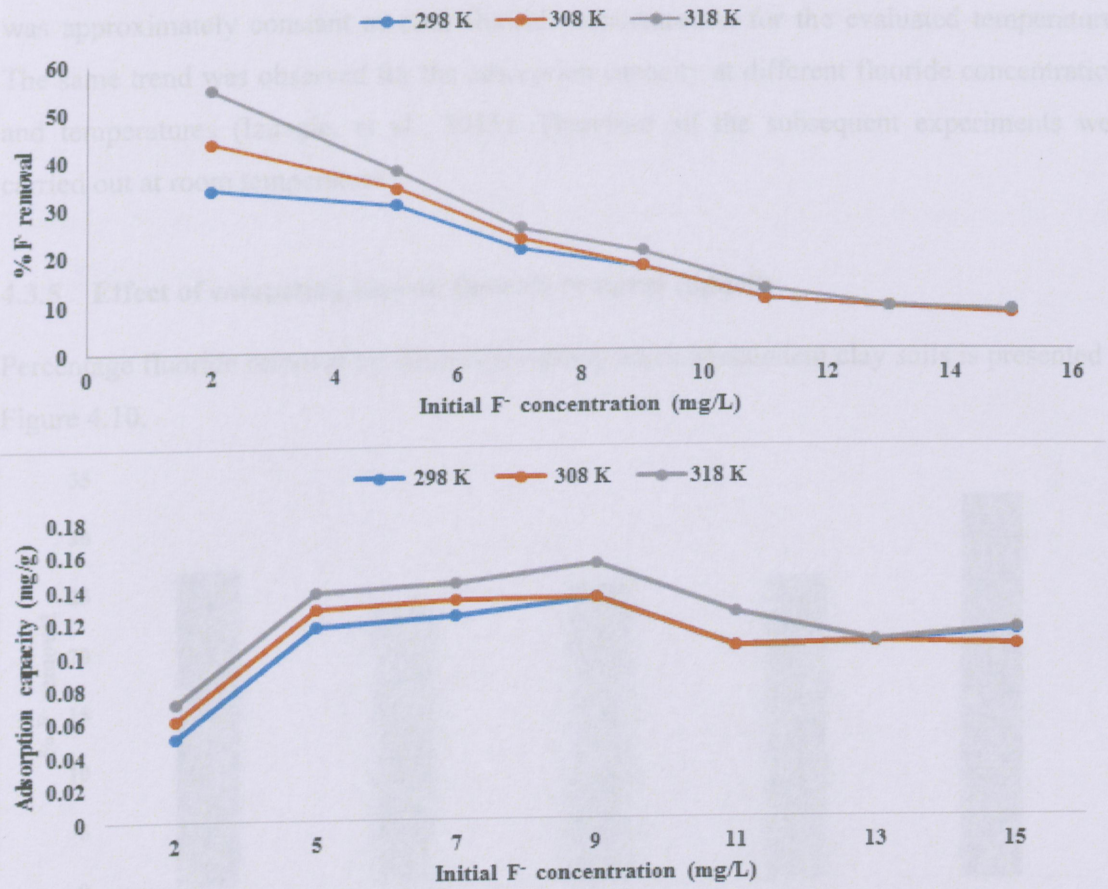


Figure 4.9: Percentage removal and adsorption capacity of silica rich reddish black Mukondeni clay soils as a function of temperature (60 min contact time, 1.5 g dosage, 100 mL, 250 rpm, pH*i* = 6.111).

Temperature usually has a notable effect on reaction rate. If temperature increases, the rate of chemical reaction also increases. As the temperature was increased, fluoride removal was also observed to increase at lower fluoride concentrations (Ce < 7 mg/L) but at higher initial fluoride concentrations (Ce > 9 mg/L) the temperature difference had little or no effect at all on fluoride removal. From Figure 4.9 it can be seen that at (Ce = 13 and 15 mg/L), the percentage removal was the same. The highest adsorption capacity was observed at 9 mg/L across the 3 different temperatures and the difference in adsorption capacities between 318 K and 298 K is only 0.02 mg/g. Based on this observation, variation of temperature at the optimum initial fluoride concentration had little effect on fluoride removal hence there seemed to be no need to adjust the temperatures in the defluoridation experiments. The effect of temperature on fluoride sorption onto Mg/Ce/Mn oxide-modified Diatomaceous Earth was evaluated at 297 K, 310 K and 326 K (Izuagie, et al., 2015). The percent fluoride removal

© University of Venda

was approximately constant at each fluoride concentration for the evaluated temperatures. The same trend was observed for the adsorption capacity at different fluoride concentrations and temperatures (Izuagie, et al., 2015). Therefore all the subsequent experiments were carried out at room temperature.

4.3.5 Effect of competing ions on fluoride removal capacity

Percentage fluoride removal by silica rich reddish black Mukondeni clay soils is presented in Figure 4.10.

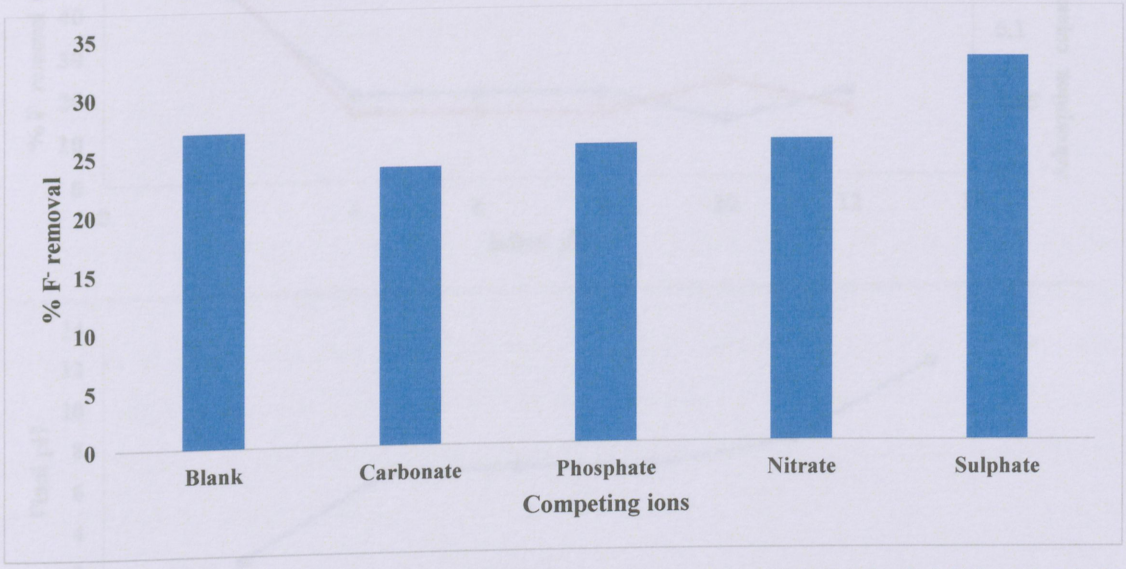


Figure 4.10: Percentage removal of fluoride by silica rich reddish black Mukondeni clay soils as a function of competing ions (60 min contact time, 9 mg/L, 1.5 g dosage, 25°C room temperature, 100 mL, 250 rpm, pH*i* = 6.587).

Taking the complexity of groundwater into account, more than one anion might be present such as sulphate, phosphate, carbonate and nitrate. Considering the competition for the binding sites between fluoride ions and these anions, they might interfere with the removal efficiency of fluoride. So, the effect of various co-existing ions upon adsorption of fluoride was investigated. From the results obtained it can be seen that none of the tested competing had a negative effect on the removal of fluoride. It is rather shown that the presence of sulphate even enhances the fluoride removal from aqueous solution by 5.91% and the other anions do not affect the fluoride removal. Karthikeyan et al. (2010) also found similar results were they reported that addition of co-ions, in the concentration ranges investigated, had no

© University of Venda

appreciable effect on the amount of fluoride ions removed by the adsorbents (Karthikeyan et al., 2010).

4.3.6 Effect of pH on fluoride removal capacity

Fluoride removal by silica rich reddish black Mukondeni clay soils is presented in Figure 4.11. The pH was varied from 2 to 12.

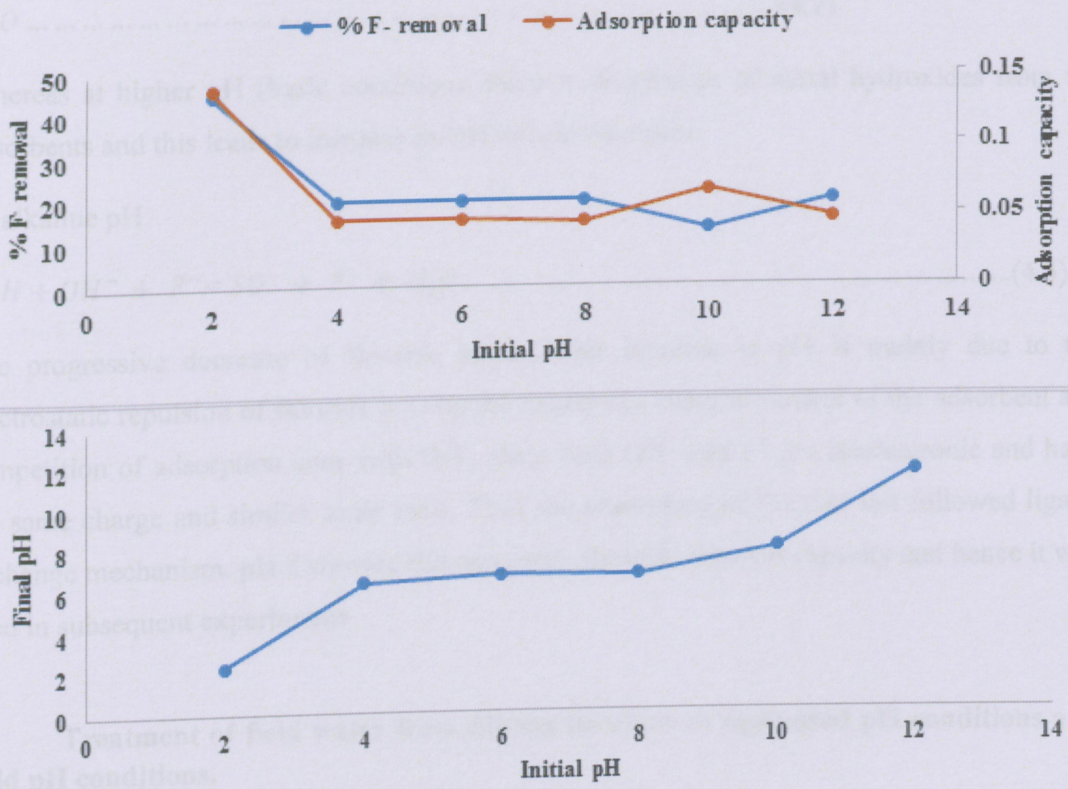


Figure 4.11: Percentage removal of fluoride by silica rich reddish black Mukondeni clay soils as a function of pH (60 min contact time, 1.5 g dosage, 9 mg/L F^- , 25°C room temperature, 100 mL , 250 rpm)

The pH of a medium is one of the most important parameters that can influence fluoride removal a lot (Tomar, et al., 2014; Gitari, et al., 2013; Ramdani, et al., 2010). It also helps in understanding the fluoride uptake mechanism of the adsorbent. As shown in Figure 4.11, the adsorption decreases with increase in pH. At low pH the surface of the adsorbent will be positively charged enhancing F^- adsorption. An interaction between the metal hydroxides (Si-OH, Al-OH and Fe-OH) at the surface of the clay adsorbent and fluoride ions is shown by equation (4.1) and (4.2). The specific adsorption of fluoride on the clay surface (S) follows the outline:

© University of Venda

University of Venda
Creating Future Leaders

At acidic pH.

$SOH + H^+ = SOH_2^+$ ..... (4.1)

$SOH_2^+ + F^- = SF + H_2O$ ..... (4.2)

Whereas at higher pH (basic condition), there is dissolution of metal hydroxides from the adsorbents and this leads to increase in OH ions in the water.

At alkaline pH

$SOH + OH^- + F^- = SO^- + F^- + H_20$ ..... (4.3)

The progressive decrease of fluoride uptake with increase in pH is mainly due to the electrostatic repulsion of fluoride ions by the negatively charged surface of the adsorbent and competition of adsorption sites with OH^-, since both OH^- and F^- are isoelectronic and have the same charge and similar ionic radii. Thus the adsorption of fluoride ion followed ligand exchange mechanism. pH 2 showed the maximum fluoride removal capacity and hence it was used in subsequent experiments

4.4 Treatment of field water from Siloam borehole at optimized pH conditions and field pH conditions.

Table 4.4 shows the adsorption of fluoride from Siloam borehole water by silica rich reddish black Mukondeni clay soils at optimized pH and field pH conditions. Tables 4.4 and 4.5 displays the physicochemical characteristics of the underground water sample, demonstrating the complexity of substances in the water and high fluoride concentration exceeding the limit of safe drinking. The optimum conditions for removal of fluoride from borehole were 60 min of contact time, 1.5 g of adsorbent dosage, pH of 2.12 and room temperature.

© University of Venda

University of Venda
Creating Future Leaders

Table 4.4: Adsorption of fluoride onto silica rich reddish black Mukondeni clay soils under field pH and optimized pH conditions.

Parameter	Siloam borehole water	Field pH (pH = 7.81)	Optimized pH (pH = 2.12)	DWS guidelines
pH	7.037	7.091	6.424	6 – 9
EC (µS/cm)	25.74	25.22	25.20	0 – 150
F^- (mg/L)	5.53	4.233	3.95	1 – 1.5
Cl^-(mg/L)	31.6	38.1	67.1	0 – 250
SO_4^-(mg/L)	11.9	10.5	9.6	0 – 250
Br^-(mg/L)	2.08	N.D	N.D	0 – 6
NO_3^-(mg/L)	1.13	N.D	N.D	0 – 6
PO_4^{3-}(mg/L)	ND	N.D	N.D	0 - 5

© University of Venda

Table 4.5: Concentration of metals before and after defluoridation with silica rich reddish black Mukondeni clay soils

Metals (µg/L)	Field water (pH = 7.11)	Treated water (pH = 7.82)	Metals (mg/L)	Field water (pH = 7.11)	Treated water (pH = 7.82)
Li	8.824888	5.856447	Al	0.04392	1.985
Be	<0.005	0.094879	Ca	3.163	3.783
B	22.61723	20.00836	Fe	0.163251	2.175
V	0.084965	11.35984	K	2.544	3.746
Cr	0.227367	26.72726	Mg	0.0396	3.195
Mn	17.46683	134.6121	Na	67.58	69.69
Co	0.028445	3.562425	P	< 0.01	0.0126
Ni	0.741724	23.37819	Si	45.51	43.98
Cu	10.74428	9.60313	Sr	0.0234	0.016
Zn	11.47378	24.45615			
As	<0.03	0.22741			
Se	< 0.54	0.896867			
Mo	1.352091	1.571776			
Cd	< 0.04	0.010104			
Sb	< 0.01	0.062888			
Ba	40.61815	28.57132			
Hg	< 0.01	<0.004			
Pb	0.592015	1.113431			

From Table 4.4, the fluoride removal efficiency on borehole water at field pH conditions was found to be slightly lower than that at optimized pH conditions. A possible explanation to this could be that, the borehole water had a circumneutral pH and according to Figure 4.11 which shows the effect of pH on fluoride removal, at that pH percentage fluoride removal is very low. However, at both field and optimized pH conditions fluoride levels were above permissible limits of 1.5 mg/L. This may be due to the fact that that the fluoride removal capacity of silica rich reddish black Mukondeni clay soils is fairly low. The other parameters are however within the permitted ranges of the DWA water quality guidelines. From Table 4.5, it is only Al and Fe which are slightly above the permissible limits of the DWA water

© University of Venda

University of Venda
Creating Future Leaders

quality guidelines. The Fe levels have no health effects but rather adverse aesthetic effects whereas the Al levels shown in Table 4.5 do not have acute health effects.

4.5 Chemical stability of the adsorbent

The changes in water quality were measured after treatment with adsorbent using synthetic fluoride water.

Table 4.6: Leaching of metals into solution after defluoridation at pH 2, 6 and 12

Metals (µg/L)	2	6	12	Metals (mg/L)	2	6	12
Li	3.54	4.33	6.31	Ca	22.95	1.431	6.231
Be	2.93	0.27	1.60	K	2.465	0.9728	2.236
B	4.46	2.61	<0.000	Mg	20.33	1.314	9.39
Al	5681.6	3851.3	17337.4	Na	12.99	9.353	272.7
V	15.83	4.70	66.38	P	0.0394	0.0166	0.068
Cr	14.05	23.94	171.75	Si	5.49	8.216	40.62
Mn	1405.1	44.11	396.36				
Fe	112.866	2486.13	16615.10				
Co	43.15	1.70	18.45				
Ni	220.08	19.59	166.86				
Cu	24.88	2.86	54.54				
Zn	25.55	5.41	40.26				
As	0.11	0.08	0.39				
Se	0.73	0.45	2.76				
Sr	169.07	6.99	35.88				
Mo	0.07	0.25	0.14				
Cd	0.23	0.01	0.05				
Sb	0.01	0.01	0.02				
Ba	424.07	7.26	124.48				
Hg	< 0.01	0.01	0.01				
Pb	1.62	0.42	5.94				

© University of Venda

University of Venda
Creating Future Leaders

From Table 4.6, it can be observed that higher leaching of metals occurred at pH 12. However with Al, Mn and Fe leaching occurred at all the tested pHs. When compared to the DWS water quality guidelines, the metal Al exceeds the recommended limits at those different pHs but since at pH 6 the leaching of metals is quite low and those Fe levels have no acute health effects, hence defluoridation can be done at this pH which does not need pH adjustment. Contrary to other metals, Na shows a quite different trend. According to DWS water quality guidelines, Na should range between 0 – 100 mg/L and in Table 4.6, the Na concentration at pH 12 is 272.7 mg/L which is above the recommended water quality guidelines. The high Na concentration could be coming from the NaOH which was used to adjust the pH to 12. However, since pH is extremely alkaline, it will not be used for defluoridation for future drinking purposes.

UNIVERSITY OF VENDA
LIBRARY

4.6 Adsorption Isotherms

4.6.1 Langmuir Isotherm

Figure 4.12 shows the Langmuir adsorption isotherm for fluoride adsorption onto silica rich reddish black Mukondeni clay soils and Table 4.7 shows the adsorption isotherm parameters.

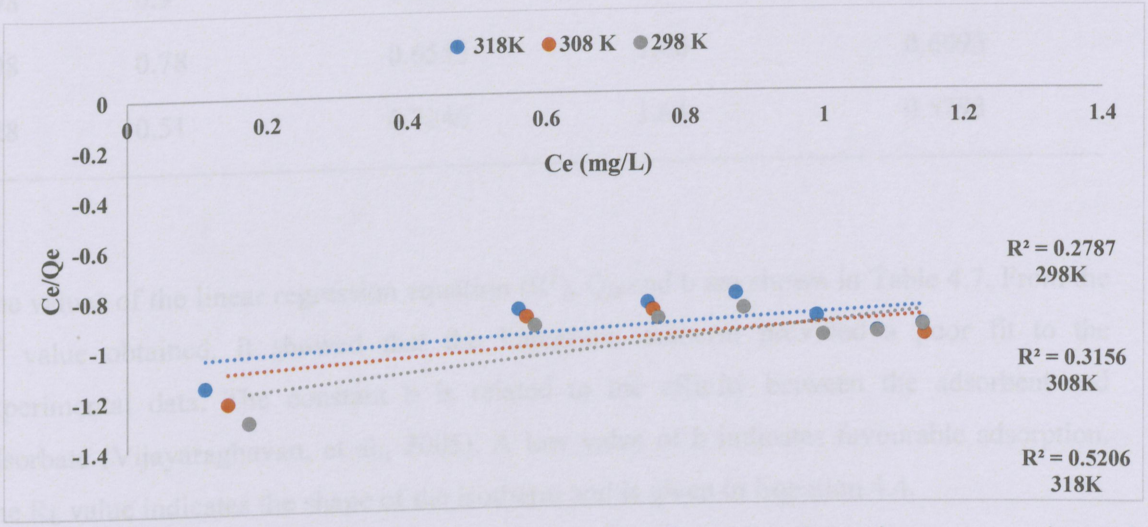


Figure 4.12: Langmuir adsorption isotherm for fluoride adsorption onto variegated silica rich reddish black Mukondeni clay soils (1.5 g adsorbent dosage, 60 min of equilibration time, concentration was varied from 1 – 15 mg/L, pH*i* = 6,111)

© University of Venda

University of Venda
Creating Future Leaders

Table 4.7: Adsorption isotherm parameters

Adsorption isotherms and parameters				
Langmuir Isotherm				
Temp (K)	Qm (mg/g)	b(L/mg)	R_L	R^2
298	0.18	1.74	0.06	0.5203
308	0.11	3.25	0.03	0.3107
328	0.11	1.9	0.06	0.2893
Freundlich Isotherm				
Temp (K)	K_F	1/n	n	R^2
298	0.06	3.33	0.2997	0.9529
308	0.07	5.23	0.191	0.9687
328	0.09	6.03	0.1658	0.9558
Dubinin- Radushkevich Isotherm				
Temp (K)	Q_D	B_D	E(J/mol)	R^2
298	0.9	0.518	1.03	0.7793
308	0.78	0.6553	1.40	0.6093
328	0.51	0.7246	1.64	0.5793

The values of the linear regression equation (R^2), Q_m and b are shown in Table 4.7. From the R^2 value obtained, it showed that the Langmuir isotherm provided a poor fit to the experimental data. The constant b is related to the affinity between the adsorbent and adsorbate (Vijayaraghavan, et al., 2005). A low value of b indicates favourable adsorption. The R_L value indicates the shape of the isotherm and is given in Equation 4.4.

$$R_L = \frac{1}{(1 + bCo)} \quad \text{.....(4.4)}$$

© University of Venda

R_L values between 0 and 1 indicate favourable adsorption, 0 indicates irreversible adsorption, 1 means linear adsorption while a value greater than 1 indicates an unfavorable adsorption. The value of R_L obtained at different temperatures is shown in Table 4.7. The values lie between 0 and 1 which shows that the adsorption of F^- on silica rich reddish black Mukondeni clay soils is a favourable adsorption process. The calculated adsorption capacities (Qm) shown in Table 4.7 are very high compared to the experimental adsorption capacity (0.08mg/g). This is also another indication that the Langmuir isotherm did not describe the adsorption process that took place.

4.6.2 Freundlich Isotherm

The Freundlich isotherm was applied to deduce the adsorption intensity of the adsorbent towards the adsorbate. Unlike the Langmuir isotherm the Freundlich isotherm assumes that the removal of ions occurs on a heterogeneous surface, involving a multilayer adsorption of ions.

Figure 4.13 shows the Freundlich adsorption isotherm for fluoride adsorption onto silica rich reddish black Mukondeni clay soils

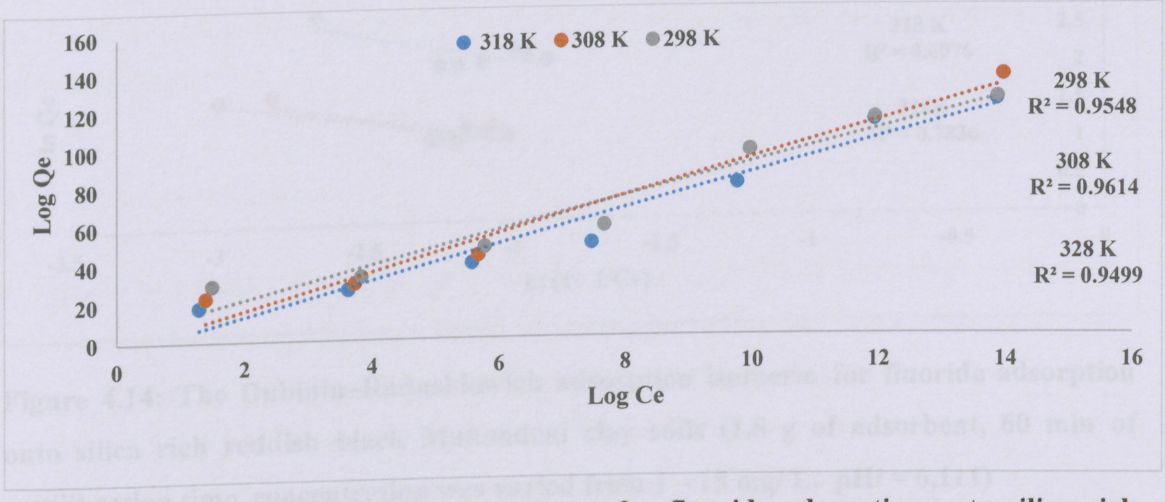


Figure 4.13. Freundlich adsorption isotherm for fluoride adsorption onto silica rich reddish black Mukondeni clay soils (1.5 g adsorbent, 60 min of equilibration time, concentration was varied from 1 – 15 mg/ L, pH*i* = 6,111)

The plot of log Qe against log Ce is shown in Figure 4.13. The constants n and K_F were obtained from the slope and the intercept respectively. Table 4.7 shows the Freundlich

© University of Venda

isotherm parameters. The high R^2 values obtained clearly suggest that the applicability of the Freundlich adsorption isotherm is feasible and that the adsorption process occurred on a heterogeneous surface. Furthermore the calculated adsorption capacities (0.06, 0.07 and 0.09 mg/g) are very close and comparable to the experimental adsorption capacity (0.08 mg/g) substantiating that the Freundlich adsorption isotherm best describes the adsorption of fluoride onto silica rich reddish black Mukondeni clay soils.

4.6.3 Dubinin–Radushkevich isotherm model

The Dubinin–Radushkevich is generally applied to express the adsorption mechanism with a Gaussian energy distribution onto a heterogeneous surface (Dabrowski, 2001 and Dubinin, 1960). This isotherm is more general than Langmuir isotherm because it does not assume a homogenous surface or a constant adsorption potential (Vermeulan, et al., 1996).

Figure 4.14 shows the Dubinin – Radushkevich adsorption isotherm for fluoride adsorption onto silica rich reddish black Mukondeni clay soils.

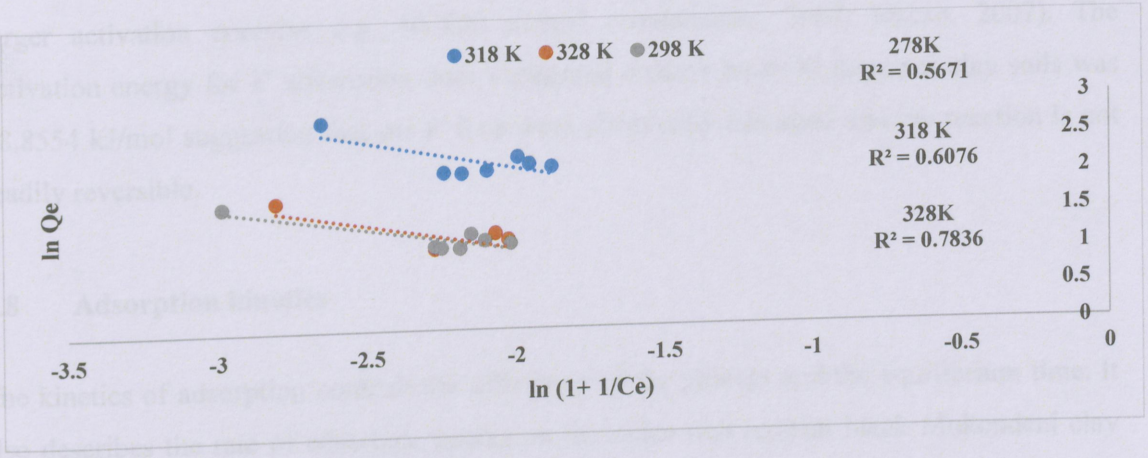


Figure 4.14: The Dubinin–Radushkevich adsorption isotherm for fluoride adsorption onto silica rich reddish black Mukondeni clay soils (1.5 g of adsorbent, 60 min of equilibration time, concentration was varied from 1 – 15 mg/ L, pH*i* = 6,111)

Table 4.7 shows the Dubinin-Radushkevich isotherm parameters. The value of the regression (R^2) obtained (0.78) showed that this model provided a fairly good fit to the experimental data compared to the Langmuir isotherm. The free energy *E* for the transfer of 1 mol of solute from infinity to the surface of the adsorbent was computed and found to be 1.03 kJ/mol.

© University of Venda

University of Venda
Creating Future Leaders

4.7 Thermodynamic parameters

In order to evaluate the feasibility of the adsorption process, thermodynamic parameters were evaluated by conducting the adsorption experiments at different temperatures. Table 4.8 shows the activation energy for the removal of fluoride from solution by reddish silica rich black Mukondeni clay soils

Table 4.8: Activation energy values of removal of fluoride by silica rich Mukondeni clay soils

Chemical element	K_1	K_2	Ea (kJ/mol)
Fluoride	0.79	0.8	58.8554

The magnitude of the activation energy is commonly used as the basis for differentiating between physical and chemical adsorption. Physical adsorption reactions are readily reversible, equilibrium attained rapidly and thus energy requirements are small, ranging from 5 to 40 kJ/mol. Chemical adsorption is specific, involves stronger forces and thus requires larger activation energies e.g. 40–800 kJ/mol (Unuabonah, 2007; Ozcan, 2007). The activation energy for F^- adsorption onto variegated reddish black Mukondeni clay soils was 58.8554 kJ/mol suggesting that the F^- ions were chemically adsorbed and the reaction is not readily reversible.

4.8 Adsorption kinetics

The kinetics of adsorption controls the efficiency of the process and the equilibrium time. It also describes the rate of adsorbate uptake on the silica rich reddish black Mukondeni clay soils. To identify the potential rate controlling steps involved in the process of adsorption, two kinetic models were studied and utilized to fit the experimental data from the adsorption process. These models are the pseudo-first-order and the pseudo-second-order models.

4.8.1 The pseudo first-order and pseudo second order models

To evaluate the kinetics of the adsorption process, the pseudo first-order and pseudo second order models were tested to interpret the experimental data. Figure 4.15(a) and (b) shows the

© University of Venda

adsorption kinetics for fluoride sorption onto silica rich reddish black Mukondeni clay soils and Table 4.9 shows the pseudo-second-order kinetic parameters for different adsorbent dosages for fluoride removal silica rich reddish black Mukondeni clay soils.

Table 4.9: Pseudo-second-order kinetic parameters for different adsorbent dosages for fluoride removal by silica rich reddish black Mukondeni clay soils.

Dosage (g)	qe exp (mg/g)	K_2(gmh)	qe cal (mg/g)	R^2
1	0.15	2.02.	0.078	0.9933
2	0.12	2.52	0.083	0.9959
3	0.08	32.91	0.057	0.9915

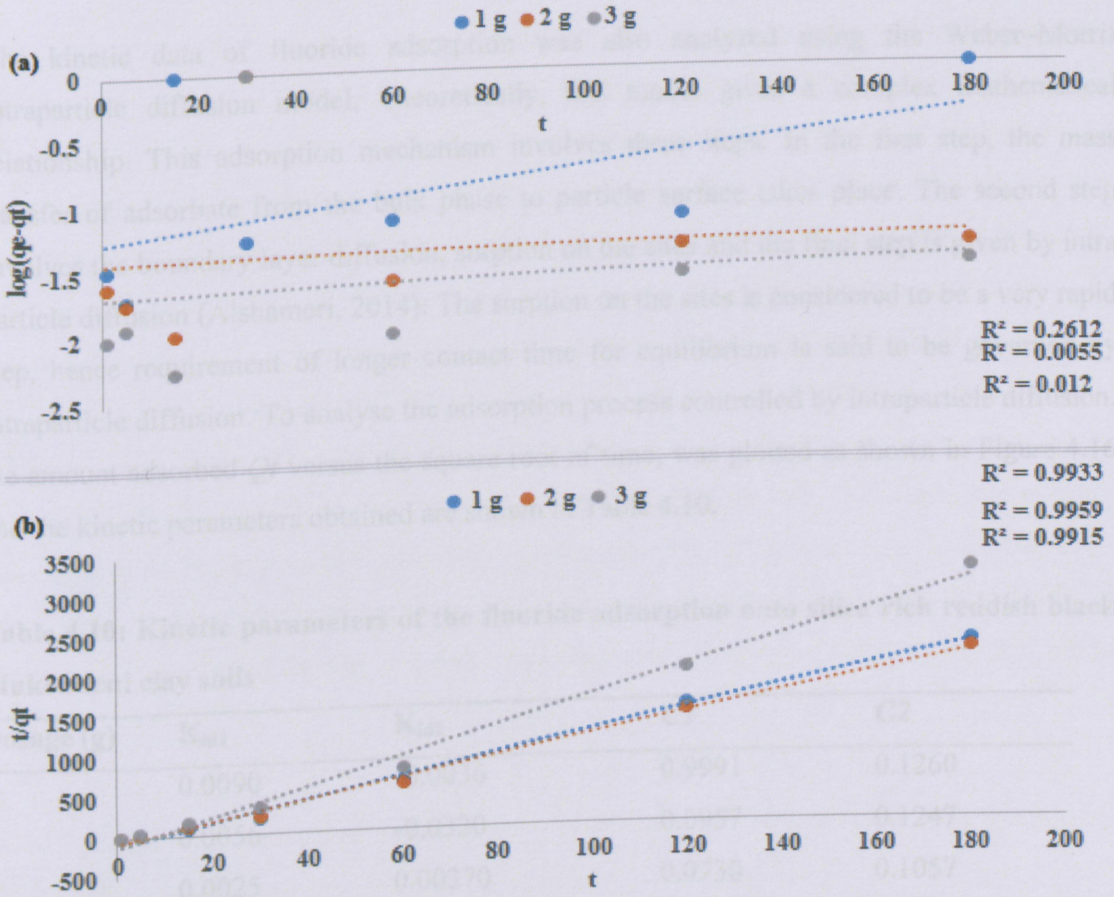


Figure 4.15 (a) and (b): Adsorption kinetics for fluoride sorption onto silica rich reddish black Mukondeni clay soils (1 g dosage, 10 mg/L adsorbate concentration, 25°C room temperature, and 250 rpm, pH*i* = 6.423).

© University of Venda

The pseudo-first-order kinetics best fit line at room temperature yielded relatively low R^2 value as observed in Figure 4.15(a). This suggests that the application of the pseudo first-order is inappropriate hence indicating that the adsorption of fluoride onto silica rich reddish black Mukondeni clay soils did not follow pseudo first-order kinetics. On the other hand, the correlation coefficient (R^2) for the pseudo second-order kinetic model fit is ≈1, much higher than the correlation coefficient derived from pseudo first-order model. Given the good agreement between model fit and experimentally observed equilibrium adsorption capacity in addition to the large correlation coefficients, it can be suggested that fluoride adsorption followed pseudo second-order kinetics and F^- ions were adsorbed onto the silica rich reddish black Mukondeni clay soils surface via a chemical interaction.

4.9. Diffusion based models

The kinetic data of fluoride adsorption was also analyzed using the Weber–Morris intraparticle diffusion model. Theoretically, this model gives a complex mathematical relationship. This adsorption mechanism involves three steps. In the first step, the mass transfer of adsorbate from the bulk phase to particle surface takes place. The second step involves the boundary layer diffusion, sorption on the sites and the final step is given by intra particle diffusion (Alshameri, 2014). The sorption on the sites is considered to be a very rapid step, hence requirement of longer contact time for equilibrium is said to be governed by intraparticle diffusion. To analyse the adsorption process controlled by intraparticle diffusion, the amount adsorbed *Qt* versus the square root of time, was plotted as shown in Figure 4.16 and the kinetic parameters obtained are shown in Table 4.10.

Table 4.10: Kinetic parameters of the fluoride adsorption onto silica rich reddish black Mukondeni clay soils

Dosage (g)	K_{id1}	K_{id2}	*C1*	*C2*
1	0.0090	-0.0036	0.9991	0.1260
2	0.0056	-0.0320	0.0957	0.1247
3	0.0025	0.00370	0.0730	0.1057

© University of Venda

University of Venda
Creating Future Leaders

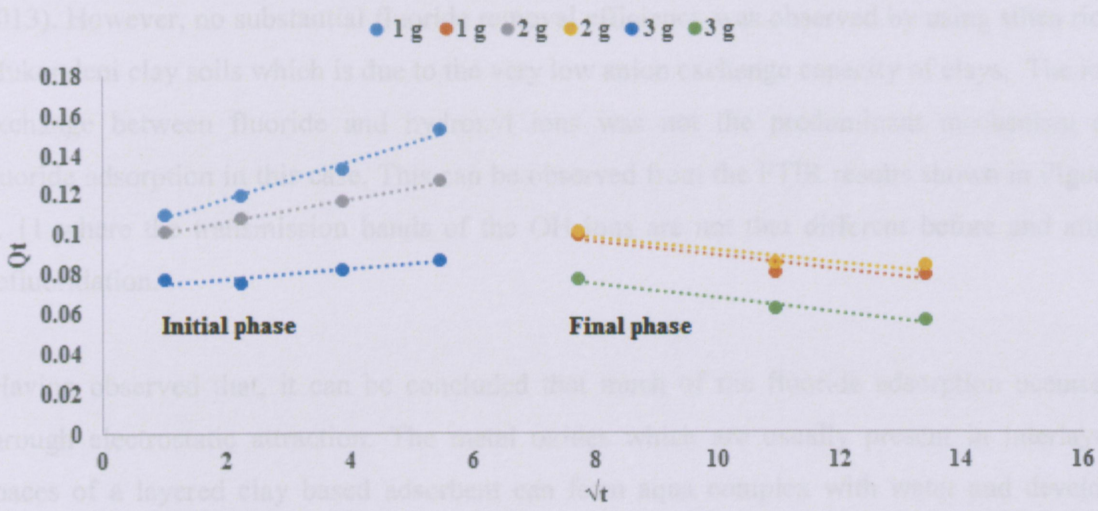


Figure 4.16: Data fit onto the Weber Morris intraparticle diffusion model (1 g dosage, 10 mg/L adsorbate concentration, 25°C room temperature, and 250 rpm, pH= 6.423).

The plots show two stages of adsorption indicating the occurrence of surface diffusion and internal diffuson i.e initial and final phase respectively. The slowest of the steps controls the overall rate of the process. Generally, pore diffusion and intra-particle diffusion are often rate-limiting in a batch reactor, which for continuous flow system film diffusion is more likely the rate limiting step (Kalavathy, et al., 2005). As shown in the diagram, the surface diffusion was rapid in the first 30 min and thereafter intraparticle diffusion became slow. The intraparticle diffusion constant, K_{id} values are obtained from the slope of the linear portion of the curve as shown in Table 4.10. From the results obtained, it is clear that the intraparticle diffusion was slow and the rate limiting step because the K_{id2} values are smaller than the K_{id1} values for all adsorbent dosages. The deviation of straight lines from the origin, was observed which may be because of the difference between the rate of mass transfer in the initial and final steps of adsorption. Further, such deviation of the straight line from the origin indicates that the intraparticle diffusion is not the sole rate controlling step (Thilagavathy and Santhi, 2014).

4.10 Proposed adsorption mechanism of fluoride onto using silica rich Mukondeni clay soils

The two most proposed mechanisms of fluoride sorption onto several adsorbents including clays are ion exchange between fluoride and hydroxyl groups present on adsorbent surface and electrostatic attraction between the metals on the surfaces of the clay (Guo and Guo,

© University of Venda

UNIVERSITY OF VENDA
LIBRARY

2013). However, no substantial fluoride removal efficiency was observed by using silica rich Mukondeni clay soils which is due to the very low anion exchange capacity of clays. The ion exchange between fluoride and hydroxyl ions was not the predominant mechanism of fluoride adsorption in this case. This can be observed from the FTIR results shown in Figure 4. 11 where the transmission bands of the OH ions are not that different before and after defluoridation.

Having observed that, it can be concluded that much of the fluoride adsorption occurred through electrostatic attraction. The metal oxides which are usually present in interlayer spaces of a layered clay based adsorbent can form aqua complex with water and develop charged surface through amphoteric dissociation (Kim, et al., 2013). At acidic pH, more positively charged surface sites are developed which attract the negatively charged fluoride ions by electrostatic attraction, resulting in enhanced fluoride removal at acidic pH (corroborated by results shown in Figure 4.13 which shows high fluoride removal at pH 2, as expressed in Equations. (4.5) – (4.7).

$$MOH + H^+ \leftrightarrow MOH^{2+} \quad \ldots (4.5)$$

$$MOH^{2+} + F^- \leftrightarrow MF + H_2O \quad \ldots (4.6)$$

Total reaction can be written as follows:

$$MOH + H^+ + F^- \leftrightarrow MF + H_2O \quad \ldots (4.7)$$

where M represents metal ion in this case which can be Mg, Ca, Na and K as shown by the cation exchange results

4.11 Performance comparison of silica rich reddish black Mukondeni clay soils with other clay adsorbents

A substantial amount of literature is available on fluoride sorption by a wide variety of low cost adsorbents as shown in Table 4.10.

Table 4.10: Comparison of different adsorption capacities of different clay adsorbents for fluoride

© University of Venda

University of Venda
Creating Future Leaders

Adsorbent	Adsorption capacity	Experimental conditions	References
Silica rich reddish black Mukondeni clay soils	0.08 mg/g	pH 2, 9 mg/L	Present study
Kaolinite	0.7 mg/g	pH 6-7, 5 mg/L	Srimurali, et al. (1998)
Mg^{2+} bentonite	2.3 mg/g	pH 3-10, 5 mg/L	Thakre, et al. (2010)
Montmorillonite clay	1.5 mg/g	Neutral	Karthkeyan, et al. (2005)
Bentonite	1.2 mg/g	pH 2.8, 5 mg /L	Srimurali, et al. (1998)

A summary of adsorption capacities of various adsorbents for fluoride removal from water under various experimental conditions has been presented in Table 4.10. A perusal of Table 4.10 revealed that mineral-based sorbents have been found to be promising for fluoride removal. As can be seen from the Table 4.10, silica rich reddish black Mukondeni clay soils have the lowest adsorption capacity when compared to other materials that have been previously used for adsorption but the highest adsorption capacities are observed with modified clays.

4.12 Concluding remarks and future perspectives

The following conclusions were arrived at from this study:

- silica rich reddish black clay Mukondeni clay soils were found to be fairly good and cheap adsorbent for the removal of fluoride ions from aqueous solution but could be further modified to increase their adsorption capacity,
- the Freundlich isotherm gave a much better fit than Langmuir isotherm and the Dubinin-Radushkevich isotherm indicating that the adsorption occurred on a heterogeneous surface,
- the value of the Activation energy, E, of adsorption obtained from the thermodynamic studies indicated a chemical adsorption process,

© University of Venda

University of Venda
Creating Future Leaders

- fluoride adsorption followed pseudo second-order kinetics and fluoride ions were adsorbed onto the silica rich reddish black Mukondeni clay soils surface through a chemical interaction,
- silica rich reddish black Mukondeni clay soils have shown fairly good fluoride uptake capacity in the laboratory.
- It is recommended that a clay composite be made between the locally available silica rich reddish black Mukondeni clay soils and iron(III) oxide modified bentonite clay for defluoridation purposes.

UNIVERSITY OF VENDA
LIBRARY

© University of Venda

University of Venda
Creating Future Leaders

4.13 References

Abebe, L.S., Smith, J.A., Narkiewicz, S., Oyanedel-Craver, V., Conaway, M., Singo, A., Samie, A., Mojapelo, P., Brant, J. and Dillingham, R., 2014. Ceramic water filters impregnated with silver nanoparticles as a point-of-use water-treatment intervention for HIV-positive individuals in Limpopo Province, South Africa: A pilot study of technological performance and human health benefits. *Journal of Water and Health,* 12(2), pp. 288-300.

Alshameri, A., Yan, C., Al-Ani, Y., Dawood, A.S., Ibrahim, A., Zhou, C. and Wang, H., 2014. An investigation into the adsorption removal of ammonium by salt activated Chinese (Hulaodu) natural zeolite: Kinetics, isotherms, and thermodynamics. *Journal of the Taiwan Institute of Chemical Engineers*, 45, pp.554–564.

Appela, C., Lena Q., Ma, R. and Kennelley, D.R.E., 2003. Point of zero charge determination in soils and minerals via traditional methods and detection of electroacoustic mobility. *Geoderma,* 113, pp. 77– 93.

Chen, N., Zhang, Z.C., Feng, C., Li, M., Zhu, D., Chen, R and Sugiura, N., 2010. An excellent fluoride sorption behavior of ceramic adsorbent, *J. Hazard. Mater*. 183, pp. 460–465.

Dabrowski, A., 2001. Adsorption—from theory to practice, *Adv. Colloid Interface Sci.* 93, pp. 135–224.

Denga, M.E., 2013. Evaluation of the fluoride adsorption capacity of locally available clay in Vhembe district. A thesis submitted to the department of Ecology and Resource Management, School of Environmental Sciences. University of Venda.

Dubinin, M.M., 1960. The potential theory of adsorption of gases and vapours for adsorbents with energetically non-uniform surface, *Chem. Rev*. 60, pp. 235–266.

Gandhi, N., Sirisha, D., Asthana, S. and Manjusha, A., 2012. Adsorption studies of fluoride on multani matti and red soil, *Res. J. Chem. Sci*. 2, pp. 32–37.

© University of Venda

University of Venda
Creating Future Leaders

Gitari, W.M., Ngulube, T., Masindi, V. and Gumbo, J.R., 2013. Defluoridation of groundwater using Fe^{3+} - modified bentonite clay: optimization of adsorption conditions. *Desalin. Water Treat*. 53, pp. 1578–1590.

Goswami, A. and Purkait, M.K., 2013. Defluoridation of Water by Schwertmannite. World Academy of Science, Engineering and Technology. 73.

Hackett, C., Hackett, T., Harsh, D. and Schrider, S., 2013. Assessing the establishment of a ceramic water filter factory in Limpopo Province, South Africa. Public: 9-12.

Izuagie, A.A., Gitari, W.M. and Gumbo, J.R., 2015. Defluoridation of groundwater using diatomaceous earth: optimization of adsorption conditions, kinetics and leached metals risk assessment. Desalination and Water Treatment. Pp. 1- 13

Kalavathy, M.H., Karthikeyan, T., Rajgopal, S. and Miranda, L.R., 2005. Kinetic and isothermstudies of Cu(II) adsorption onto H3PO4 activated rubber wood sawdust. *J. Colloid Interface Sci*, 292, pp. 354–362.

Karthikeyan, G., Pius, A., and Alagumuthu, G., 2005. Fluoride adsorption studies of montmorillonite clay. *Indian Journal of Chemical Technology*, 12, pp. 263-272.

Langmuir, D., 1997. *Aqueous environmental geochemistry*. Prentice-Hall, Inc. Upper Saddle River: New Jersey.

Madejova, J. and Komadel, P. 2001. Baseline studies of the clay minerals society source clays: infrared methods. *Clays and Clay Minerals*, 49(5), pp. 410 – 432.

Morais, F.I., Page, A.L. and Lund, L.J., 1976. The effect of pH, salt concentration, and nature of electrolytes on the charge characteristics of Brazilian tropical soils. *Soil Sci. Soc. Am. J.* 40, pp. 521–527.

Ozcan, A., Ozcan, A.S. and Gok, O., 2007. Adsorption kinetics and isotherms of anionic dye of reactive blue19 from aqueous solutions onto DTMA-sepiolite, in: A.A.Lewinsky (Ed.), Hazardous Materials and Wastewater-Treatment, Removal and Analysis, Nova Science Publishers, NewYork.

Paudyal, H., PangenI, B., Inoue, K., Kawakita, H., Ohto, K., Harada, H. and Alam, S., 2011. Adsorptive removal of fluoride from aqueous solution using orange waste loaded with multi-valent metal ions. *J. Hazard. Mater,* 192, pp. 676–682.

© University of Venda

University of Venda
Creating Future Leaders

Srimurali, M., Pragathi, A. and Karthikeyan, J., 1998. "A study on removal of fluorides from drinking water by adsorption onto low-cost materials." *Environ. Pollut*, 99(2), pp. 285–289.

Thakre, D., Rayalua, S., Kawadea, R., Meshramb, S., Subrtc, J. and Labhsetwara, N., 2010. Magnesium incorporated bentonite clay for defluoridation of drinking water. *Journal of Hazardous Materials*, 180, pp. 122 –130.

Thilagavathy, P. and Santhi, T., 2014. Kinetics, Isotherms and Equilibrium Study of Co(II) Adsorption from Single and Binary Aqueous Solutions by Acacia nilotica Leaf Carbon Chinese. *Journal of Chemical Engineering*, 22, pp. 1193–1198.

Tomar, V., Prasad, S. and Kumar, D., 2013. Adsorptive removal of fluoride from water samples using Zr–Mn composite material. *Microchem. J.* 111, pp. 116–124.

Tomar, V., Prasad, S., Kumar, D., 2014. Adsorptive removal of fluoride from aqueous media using citrus limonum (lemon) leaf. *Microchem. J.* 112, pp. 97–103.

Tyeryar, M., C. Hackett, D. Harsh and T. Hackett (2012). Establishing a ceramic water filter factory in Limpopo Province, South Africa. Public: 104-110.

Vermeulan, T.H., Vermeulan, K.R., and Hall, L.C., 1966. Fundamental. *Ind. Eng. Chem.* 5, pp. 212–223.

Unuabonah, E.I., Adebowale, K.O and Olu-Owolabi, B.I., 2007. Kinetic and thermodynamic studies of the adsorption of lead(II) ions onto phosphate-modified kaolinite clay, *J.Hazard.Mater,* 144, pp. 386–395.

Vijayarahgavan, K., Jegan, J.R., Palanivelu, K. and Velan, M., 2005. Nickel Recovery from Aqueous Solution using Crab Shell Particles. *Adsorption Science Technology*. 23, pp. 303-311.

World Health Organisation. 2005. Bentonite, kaolinite, and selected clay minerals. Environmental health criteria 231.ISBN 92 4 157231 0.

Zhang, Y., Cheng, Y., Bao, F. and Wang, Y., 2006. Synthesis and magnetic properties of Fe_3O_4 nanoparticles. *Material Research bulletin*. 41, pp. 525-529.

© University of Venda

University of Venda
Creating Future Leaders

CHAPTER FIVE

SYTHESIS OF IRON(III) OXIDE COATED BENTONITE CLAY AND ITS PERFORMANCE IN THE DEFLUORIDATION OF GROUNDWATER

ABSTRACT

Locally available bentonite clay was converted into a promising adsorbent for fluoride as a result of chemical loading with iron(III) oxides. This study investigated the removal of fluoride from aqueous solutions by newly synthesised iron(III) oxide coated bentonite clay. The bentonite clay was first activated by NaOH to remove geological fluoride from it and thereafter coated with iron(III) oxides. Physicochemical and mineralogical characterisation was done by XRF, XRD, SEM – EDS, FTIR and BET. CEC and PZC were determined using standard methods. Results showed that iron(III) oxide coated bentonite clay is an alumino silicate material, has a surface area of 132.3018 m^2/g and quartz is the major mineral phase on the clay. A batch fluoride sorption system was applied and the system variables investigated included, initial concentration of the sorbate, agitation time, adsorbent dose, co-existing ions, pH and temperature. The iron(III) oxide coated bentonite clay reduced the fluoride concentration to 0.789 from 5 mg/L. This was below the level recommended by WHO. It was also observed that the iron(III) oxide coated bentonite clay worked effectively over a wide range of pH (2 – 12) but the maximum fluoride removal was at pH 2. A maximum fluoride removal capacity of 1.596 mg/g was observed at an initial fluoride concentration of 80 mg/ L, which was higher compared to the unmodified bentonite. Between the pH range of 6 and 9 the removal capacity was above 70% and the material exhibited minimal metal leaching. The regeneration studies demonstrated a decrease in the adsorption of fluoride from 76.67% to 35.86% after four consecutive cycles. The experimental data fitted well to the Freundlich isotherm compared to the Langmuir isotherm but the best fit was given by the Dubinin Radushkevich isotherm which showed that adsorption took place on a multilayer surface. The adsorption kinetics fitted the pseudo second order model indicating chemisorption. Thermodynamic parameters such as ΔH and ΔS were calculated and observed to be 58.74 kJ/mol and 5.891 kJ/mol/K, respectively. The

© University of Venda

University of Venda
Creating Future Leaders

positive value of enthalpy change suggested that the fluoride adsorption process was endothermic in nature. The high adsorption capacity of iron(III) oxide coated bentonite clay indicated the potential use of this adsorbent for fluoride removal from aqueous medium.

Keywords: Adsorption isotherms, fluoride, kinetics, thermodynamics, bentonite clay, iron oxide, pH.

© University of Venda

5.0 Introduction

Bentonite clay can sorb fluoride in acid conditions and has a high pH dependency (Tor, 2006 and Kau 1998). Although bentonite clay can adsorb many pollutants, its use as an adsorbent in a filtration mode is limited in practice because on contact with water, bentonite clay swells and forms a highly stable colloidal suspension, making its separation from water following adsorption very difficult (Kapoor, 1998). Modification of bentonite is vital to increase its applicability potential for the adsorption of fluoride in a continuous flow regime.

The existence of various functional groups like OH, H-O-H and absorbed water were confirmed on the surfaces of bentonite clay by FTIR in the present study and these functional groups have been considered to effectively form some physicochemical interactions, e.g. inner-sphere complex formation or ion exchange with ion charge balancing alkaline/alkaline earth metal ions such as Na^{+}, Mg^{2+} and Ca^{2+} in the clay interlayers. Easily exchangeable OH groups are those found in metal hydroxides or hydrated metal oxides such as aluminium or iron oxides. An ion exchange mechanism whereby F^{-} is exchanged with OH groups in the mineral structure is generally assumed to be the rate determining step in the adsorption process (Hauge, et al., 1994). Modifying bentonite clay with iron oxides introduces OH groups that increases the capacity of the modified material to adsorb fluoride from solution. This is because the modification process increases the surface area of the bentonite clay and it also makes the surfaces of the bentonite clay to be more positive therefore enhancing the uptake of the negatively charged fluoride ions.

The objectives of the work presented here are therefore:
(i) to activate bentonite clay with NaOH,
(ii) to coat bentonite clay's surfaces with iron(III) oxides and characterise the solid product,
(iii) to evaluate the solid product for its water defluoridation potential.

5.1 Materials and methods

All chemicals used in this study were of analytical grade and all stock solutions were prepared with MilliQ water ($18\Omega cm^{-1}$). NaOH solutions ranging in concentrations from (0.01 – 0.5 M) were prepared from analytical grade NaOH pellets in MilliQ water. Fe^{3+} solutions of concentrations ranging from (0.1 - 0.5 M) were prepared from analytical grade anhydrous

© University of Venda

$FeCl_3$ (molysite) (Rochelle Chemicals) salt dissolved in MilliQ water. The detailed experimental procedure has been presented in Chapter 3, section 3, page 46 – 63.

5.2 Results and discussions

5.2.1 Activating bentonite clay with NaOH: Optimisation of reaction conditions

Clays invariably contain exchangeable cations and anions held to the surface. The prominent cations and anions found on clay surfaces are Ca^{2+}, Mg^{2+}, H^+, K^+, Na^+, SO_4^{2-}, Cl^-, PO_4^{3-} and NO_3^-. Most clays also contain fluoride. Concentrations of 2 to 4g/F/kg have been reported (Day, 1963). These ions can be exchanged with other ions relatively easily without affecting the clay mineral structure (Tohidi and Ramez, 1997).

A study done by Gitari, et al. (2013) showed that raw bentonite leached some fluoride into water when used as an adsorbent for defluoridation. This shows that bentonite contained geological fluoride in its structure hence the need to be activated to remove the fluoride ions. Alkaline treatment will lead to a fluoride free bentonite.

Results of batch experiments of activating bentonite clay with NaOH are presented in Figure 5.1.1, 5.1.2 and 5.1.3.

5.2.1.1 Release of fluoride from bentonite clay as a function of contact time

Figure 5.1 shows the release of fluoride from raw bentonite clay as a function of contact time

© University of Venda

University of Venda
Creating Future Leaders

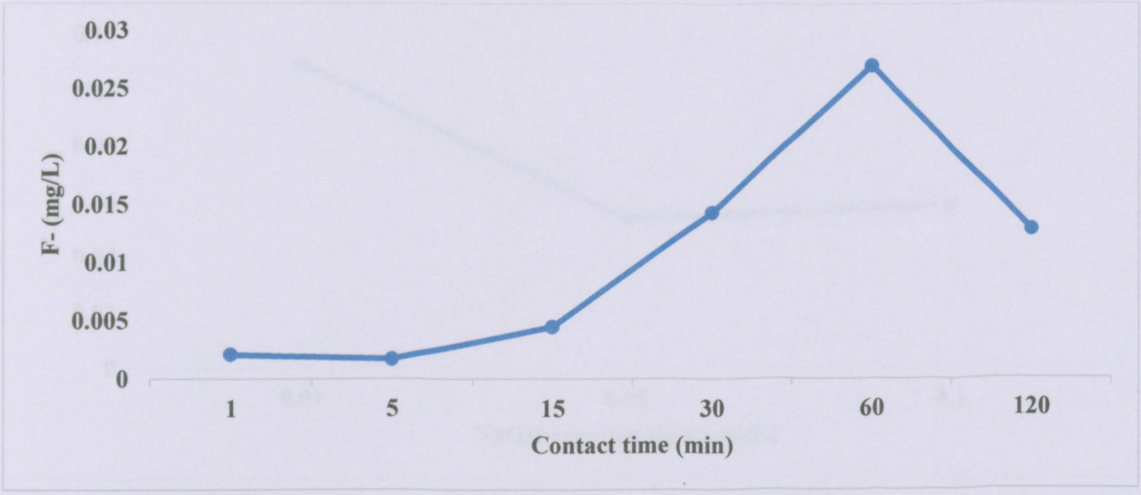


Figure 5.1: Release of fluoride from raw bentonite clay with time (0.1 M NaOH, 1 g/50 mL S/L ratio, 250 rpm, room temperature)

Figure 5.1 shows that as contact time increased the concentration of fluoride released into solution also increased until it reached a peak at 60 min after which the concentration decreased. As time increased the OH^- from the NaOH solution replaced the F^- in the interlayers of the clay until a time when all the F^- was released after 60 min. Therefore 60 min optimum time was adopted for subsequent experiments

5.2.1.2 Release of fluoride as a function of NaOH concentration

Figure 5.2 shows the release of fluoride from bentonite clay as a function of NaOH concentration.

© University of Venda

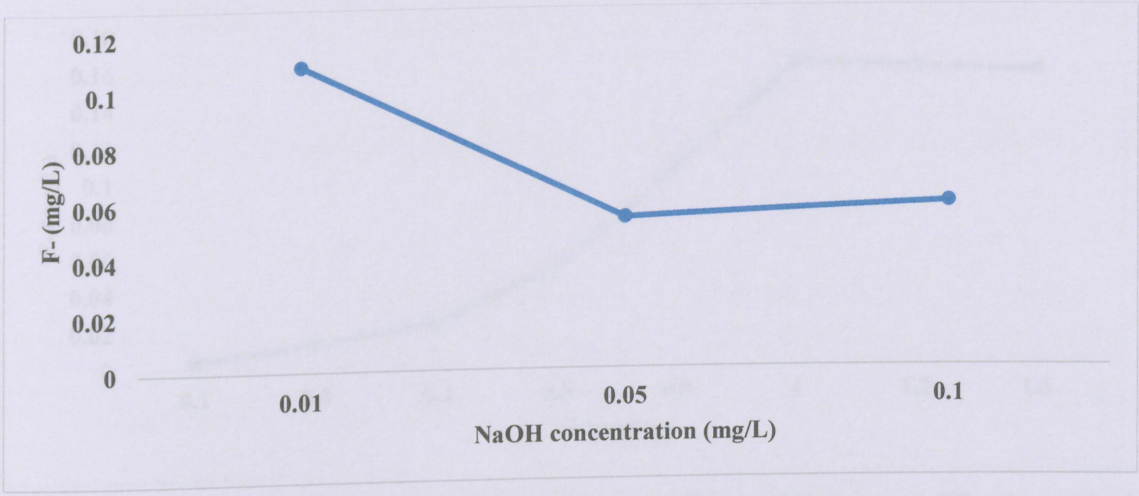


Figure 5.2: Release of fluoride from raw bentonite clay with varied NaOH concentrations (60 min contact time, 1 g/50 mL S/L ratio, 250 rpm, room temperature)

As shown in Figure 5.2 there was a decrease in fluoride concentration with increase NaOH concentration. Maximum removal is shown with 0.01 M. Poor removal is shown when NaOH concentrations are increased. The possible explanation is the destruction on the crystalline nature of the bentonite clay by NaOH. XRD quantitative results between raw and NaOH activated bentonite clay showed a notable decrease of the two major minerals, making up bentonite clay i.e. quartz and montmorillonite. The minerals compositions were reduced from 95.83 – 32% and 14.58 – 5.97% respectively. The significant loss of the major minerals could be the possible explanation for less fluoride released from the clay interlayers with increase in NaOH concentrations because very high concentrations of the NaOH destroyed the bentonite structure.

5.2.1.3 Release of fluoride as a function of dosage

Figure 5.3 shows the release of fluoride from bentonite clay as a function of dosage

© University of Venda

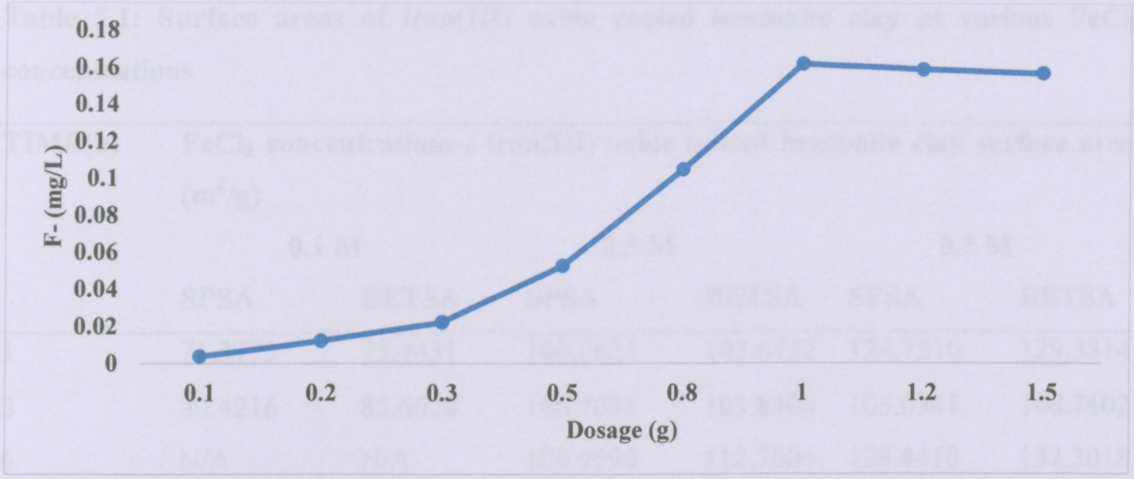


Figure 5.3: Release of fluoride from bentonite clay with varied dosages (60 min contact time, 0.01 M NaOH, 1 g/50 mL S/L ratio, 250 rpm, room temperature)

Figure 5.3 shows a direct proportion between F^- and dosage i.e. as dosage increases more F^- is also released. This can be explained in terms of more available F^- that is released as the dosage increases. However, after 1 g, the amount of fluoride released into the solution seems to be constant when the dosage is increased. In that regard 1 g/50 mL S/L ratio was taken as the optimum dosage to be used in subsequent experiments.

Optimisation of conditions of activating bentonite with NaOH was performed using batch experiments and the following conditions were established: 60 min contact time, 1 g dosage, 0.01 M NaOH concentration and 25°C room temperature

5.3 Coating NaOH-activated bentonite clay with iron(III) oxides: Optimisation of reaction conditions.

Table 5.1 shows the results of each stage of optimisation at different agitation times and molar concentrations.

© University of Venda

University of Venda
Creating Future Leaders

Table 5.1: Surface areas of iron(III) oxide coated bentonite clay at various $FeCl_3$ concentrations

TIME(h)	$FeCl_3$ concentrations / iron(III) oxide coated bentonite clay surface area (m^2/g)					
	0.1 M		0.3 M		0.5 M	
	SPSA	BETSA	SPSA	BETSA	SPSA	BETSA
1	71.3773	75.4431	100.0624	103.6732	124.7210	129.3314
3	80.4216	85.6620	100.7035	103.8400	105.0341	108.7602
6	N/A	N/A	109.9590	112.7004	128.4410	132.3018

Note: Single Point Surface Area (SPSA) Brunnet Emmett Teller Surface Area (BETSA)

On the basis of the results shown in Table 5.1, it was concluded that 0.5 M $FeCl_3$ and 6 h of agitation time were the optimum conditions of coating the NaOH activated bentonite clay with iron oxides since these conditions gave the highest surface areas of the clay. The NaOH activated bentonite had a BET Surface Area of 60.2992 m^2/g. Upon modification with $FeCl_3$ the surface area increased by approximately 41%. These optimised conditions were then applied in modification of the bentonite clay used in subsequent defluoridation experiments.

5.4 Characterisation of the adsorbents

5.4.1 Cation Exchange Capacity (CEC)

The cation exchange capacity (CEC) of a soil is a measure of the quantity of negatively charged sites on soil surfaces that can retain positively charged ions (cations) such as calcium (Ca^{2+}), magnesium (Mg^{2+}) and potassium (K^+) by electrostatic forces. Cations retained electrostatically are easily exchangeable with cations in the soil solution. So a soil with a higher CEC has a greater capacity to maintain adequate quantities of Ca^{2+}, Mg^{2+} and K^+ than a soil with a low CEC (Ross and Ketterings, 2011). Table 5.2 shows the concentration of exchangeable cations identified in raw and iron(III) oxide coated bentonite clay.

© University of Venda

University of Venda
Creating Future Leaders

Table 5.2: Cation Exchange Capacity of raw bentonite and iron(III) oxide coated bentonite clay

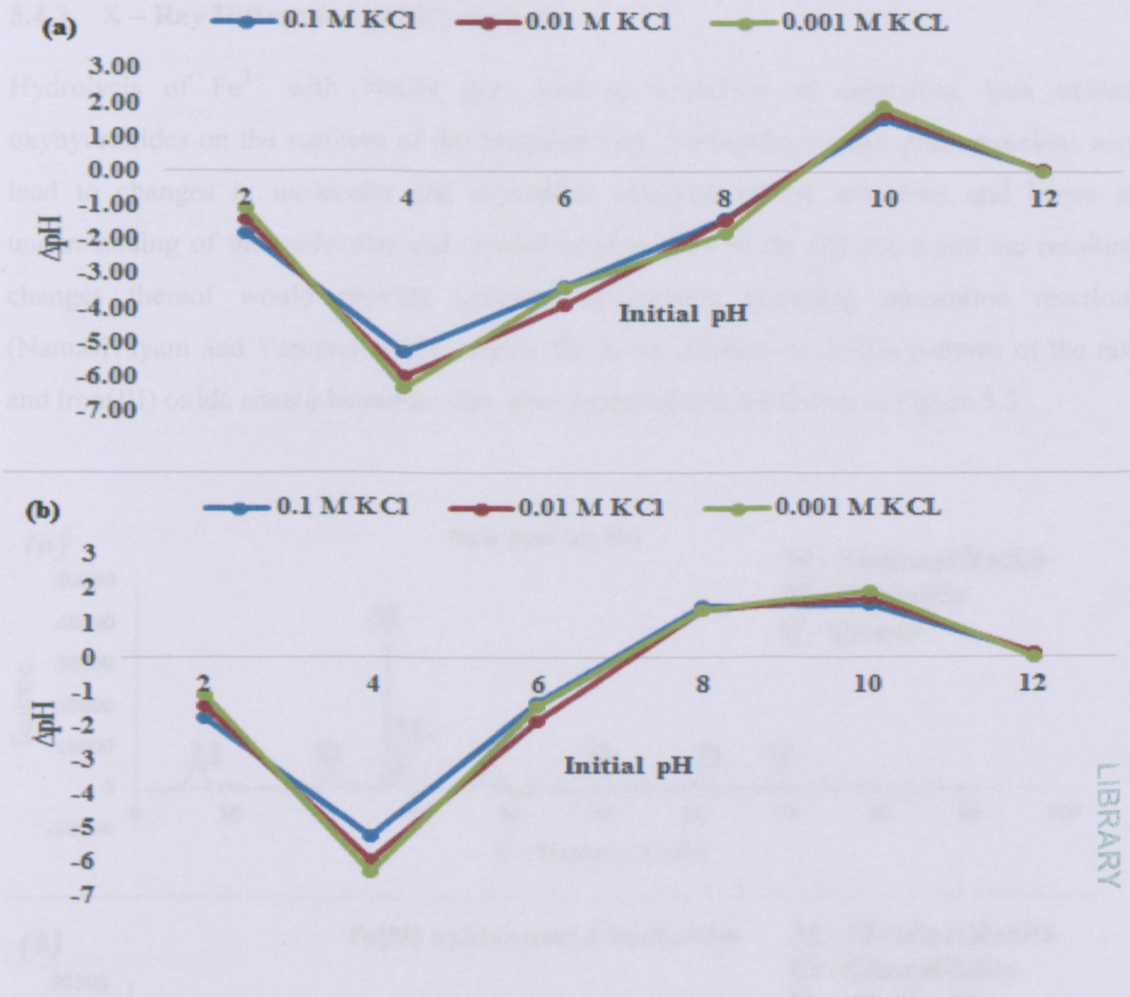
	Na^+	K^+	Ca^{2+}	Mg^{2+}	CEC(meq/100 g)
Raw bentonite					
pH 5.4	75.54	7.00	1.08	127.54	127.54
pH 7.4	111.34	6.9	1.90	142.04	142.04
Iron(III) oxide coated bentonite					
pH 5.4	49.2	6.8	1.0	45.7	97.5
pH 7.4	47.6	6.6	1.8	22.9	88.9

Table 5.2 shows the cation exchange capacity of raw and iron(III) oxide coated bentonite clay. As can be seen from the Table, the main exchangeable cations found in bentonite clay are Na^+, K^+, Ca^{2+} and Mg^{2+}. From all these cations Mg^{2+} had the highest concentration with Ca^{2+} having the lowest concentration. Comparing the CEC of the iron(III) oxide coated and raw bentonite clay it can be seen that after modification the CEC was greatly reduced at all pHs. A significant reduction was noted on the concentration of Na^+ and Mg^{2+}. This could be as result of exchange of these with trivalent Fe^{3+} during modification with $FeCl_3$.

5.4.2 Point of Zero Charge (PZC) analysis

The point (pH) where the electrical charge density is zero, is called the point of zero charge (PZC) and is a fundamental phenomenon in the process of adsorption. If the pH of a soil is above its PZC the soil surface will have a net negative charge and predominantly exhibits an ability to exchange cations, while the soil will mainly retain anions if its pH is below its PZC (Appela, et al., 2003). Figure 5.4 shows the point of zero charge of raw bentonite clay and iron(III) oxide modified bentonite clay respectively.

© University of Venda



UNIVERSITY OF VENDA
LIBRARY

Figure 5.4: pHpzc of raw bentonite clay (a) and iron(III) oxide coated bentonite clay (b)

From Figure 5.4, the raw bentonite has a PZC at pH 8.8. Spark (1997) reported that aluminium and iron oxides have high PZC values that can go up to 8. Hence, the high PZC of bentonite clay could be due to the presence of aluminium and iron oxide or hydroxides in the clay. On the contrary, the iron(III) oxide coated bentonite has a PZC at pH 7.5 which is slightly lower than that of the raw bentonite. Similar observations were made by Schwertmann and Fechter (1982) on natural and synthetic ferrihydrated clays. They pointed out that, the point of zero charge of synthetic Fe-oxides is well documented and usually ranged between pH 7 and 9 (Parks, 1965; Schwertmann and Taylor, 1977). A PZC at 7.5 means that adsorption of fluoride using iron(III) oxide coated bentonite clay is effective in acidic conditions since the surfaces of the clay will be positively charged at that pH range.

© University of Venda

University of Venda
Creating Future Leaders

5.4.3 X – Ray Diffraction (XRD) analysis

Hydrolysis of Fe^{3+} with NaOH may lead to formation of crystalline iron oxides-oxyhydroxides on the surfaces of the bentonite clay. Furthermore, adsorption reactions may lead to changes in molecular and crystalline structure of the adsorbent and hence an understanding of the molecular and crystalline structures of the adsorbent and the resulting changes thereof would provide valuable information regarding adsorption reactions (Namasivayam and Yamuna 1995). Hence, the X-ray diffraction (XRD) patterns of the raw and iron(III) oxide coated bentonite clay were recorded and are shown in Figure 5.5

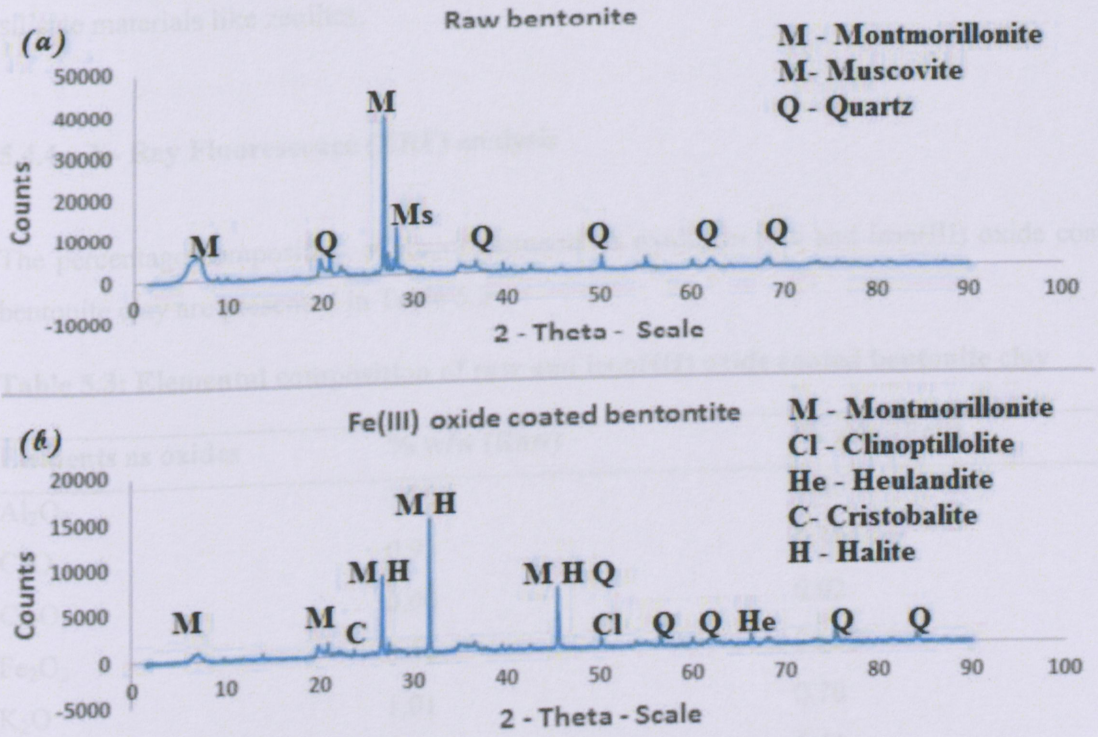


Figure 5.5: XRD diffractogram of raw bentonite and iron(III) oxide coated bentonite clay

Figure 5.5 shows a sample diffractogram data analyzed with reference to International Center for Diffraction Data ICDD Standard; Card number 36- 0426. The XRD pattern of both raw bentonite (a) and iron(III) oxide coated bentonite (b) clay suggests that the clays are highly crystalline and have quartz and montmorillonite as the major mineral components. Intense peaks for montmorillonite on raw bentonite clay at 27 degrees (2-theta) and the wide

© University of Venda

distribution of quartz from 20-85 degrees (2-theta) are evidence of this fact. The XRD spectra presented in Figure 5.5 shows that some crystalline minerals are significantly added during the modification process. However, the disappearance of certain peaks and appearance of new peaks is relative to the crystalline impurities. At 27 degrees (2-Theta) the montmorillonite peak decreased by a factor of 3 and there is a development of a halite peak on the iron(III) oxide coated bentonite clay. Halite which is basically NaCl has a wide distribution from 27 – 85 degrees (2-Theta) range. The mineral cristobalite is seen throughout the whole diffractrogram of iron(III) oxide coated bentonite clay. Cristobalite is basically a polymorph of silica, meaning that it has the same chemical formula as quartz, SiO_2, but a distinct crystal structure. This means that modifying the clay produced different forms of silicate materials like zeolites.

5.4.4 X- Ray Fluorescence (XRF) analysis

The percentage composition of major elements as oxides in raw and iron(III) oxide coated bentonite clay are presented in Table 5.3

Table 5.3: Elemental composition of raw and iron(III) oxide coated bentonite clay

Elements as oxides	% w/w (Raw)	% w/w (FeB)
Al_2O_3	14.04	8.80
CaO	0.93	0.37
Cr_2O_3	0.00	0.02
Fe_2O_3	3.31	28.35
K_2O	1.01	0.70
MgO	2.68	1.64
MnO	0.05	0.09
Na_2O	2.69	8.99
P_2O_5	0.06	0.05
SiO_2	58.84	37.33
TiO_2	0.47	0.18
L.O.I	14.79	14.44
TOTAL	**98.87**	**100.96**

© University of Venda

XRF analysis (Table 5.3) recorded an appreciable amount of SiO_2 and Al_2O_3 for both raw bentonite and iron(III) oxide coated bentonite clay suggesting that this clay is an aluminosilicate. However upon modification the amount of Al_2O_3 was reduced. Most of the Al dissolved during the activation of bentonite with NaOH hence the decrease of Al_2O_3. A notable increase is shown in Fe_2O_3 percentage. This is to be expected because the clay was modified by coating it with iron oxides. This confirms the introduction of Fe on the bentonite clay surface. A significant increase is also shown with Na_2O before and after modification. Activating with NaOH increased the Na content in the modified bentonite.

5.4.5 Scanning Electron Microscopy analysis

The morphology and SEM-EDS of raw bentonite and iron(III) oxide coated bentonite clay is shown in Figure 5.6 and 5.7 respectively.

© University of Venda

University of Venda
Creating Future Leaders

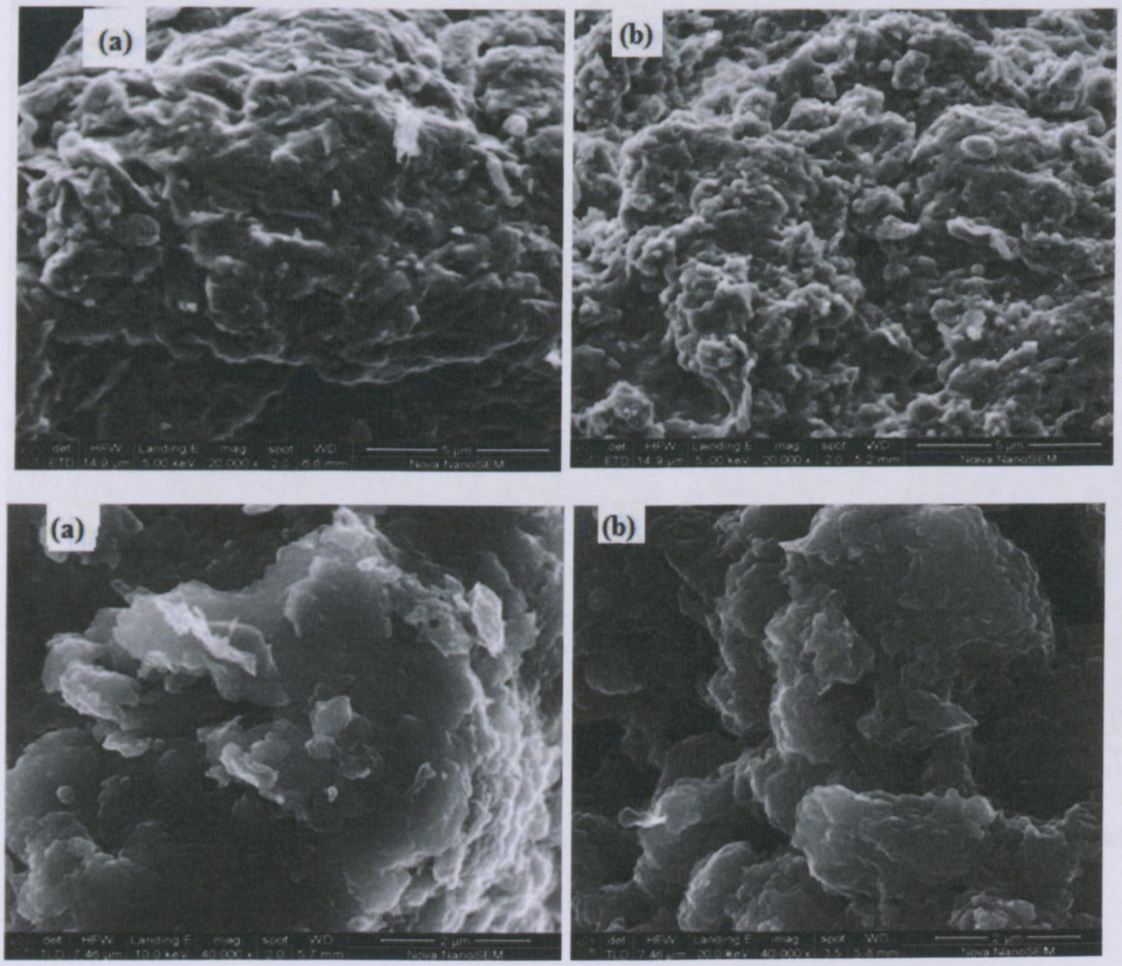


Figure 5.6: Morphology of raw bentonite (a) and iron(III) oxide coated bentonite clay (b) at different magnifications

UNIVERSITY OF VENDA
LIBRARY

© University of Venda

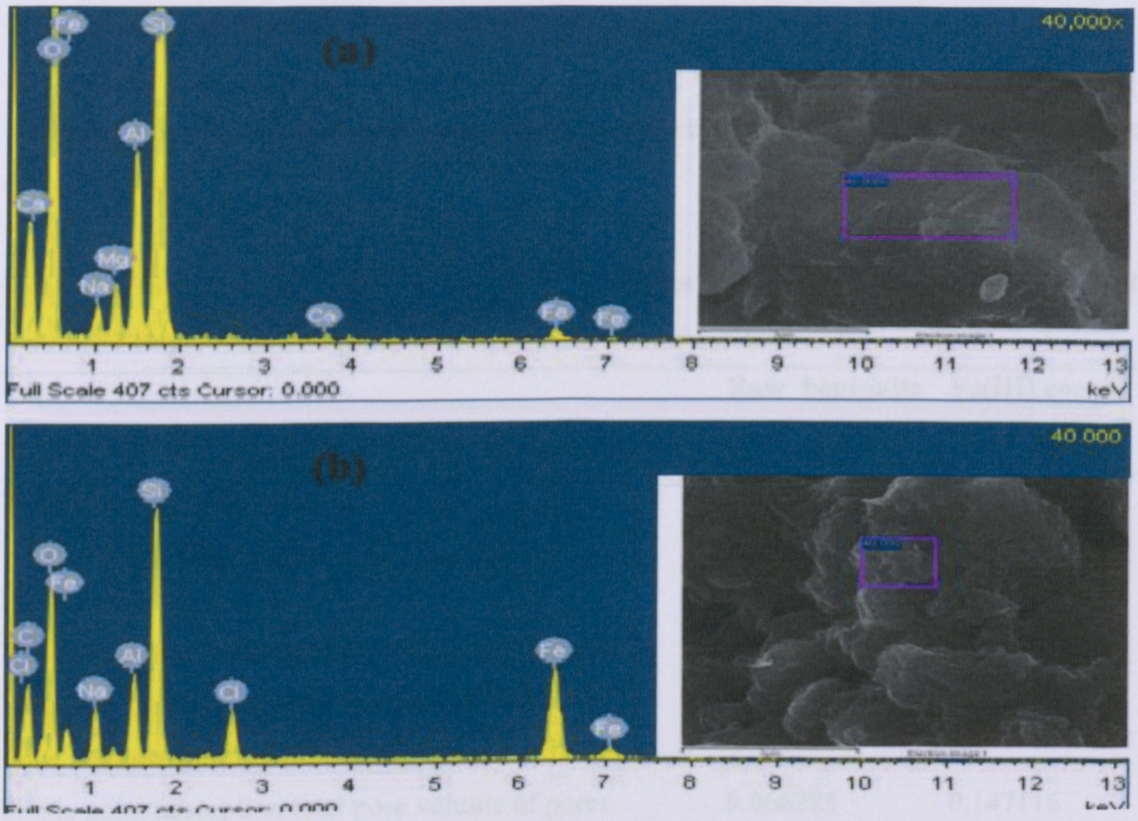


Figure 5.7: EDS analysis of the adsorbents: Raw bentonite (a) and iron(III) oxide coated bentonite clay (b).

The images of raw and iron(III) oxide coated bentonite are shown in Figure 5.6. The images show that the morphology of bentonite clay changed after modification (Figure 5.6 (a) and (b) respectively). The images reveal clay particles with different shapes and sizes. However 5.6(a) shows an irregular structure in the surface morphology of the raw bentonite clay compared to (b) which appears to be smoother. The porous nature of the raw bentonite seemed to have reduced after modification. This may be because the voids that were available in the raw bentonite were filled by the iron oxides hence the image 5.6 (b) shows smoothened surfaces as compared to the raw bentonite which mainly consists of agglomerated granule like structures which also exposes the porous opening in the material. These openings are not seen in the iron oxide coated bentonite, they are smothered out. The SEM-EDS analysis of the adsorbents is presented in Figure 5.7. As it can be seen from the figure that there is a notable difference between the two materials. Additional elements and increase in amount of others can be seen after modification. These include Na, Fe and Cl. Some elements were eradicated and these include O, Mg, and Ca. The increase by percentage weight of Fe confirms the successful coating of the bentonite clay by ferrous oxides.

© University of Venda

University of Venda
Creating Future Leaders

5.4.6 Brunauer–Emmett–Teller (BET) analysis

Table 5.4 gives the surface area, pore volume and pore size of the raw and iron(III) oxide coated bentonite clay.

Table 5.4: Surface area, pore volume and pore sizes of raw and iron(III) oxide coated bentonite clay

	Raw bentonite clay	Fe(III) coated bentonite clay
Surface area (m^2/g)		
Single point surface area	42.9136	128,4410
BET Surface Area	43.2077	132,3018
BJH Adsorption cumulative surface area of pores	27.816	129.660
BJH Desorption cumulative surface area of pores	33.8529	125.3499
Pore Volume (cm^3/g)		
Single point adsorption total pore volume of pores	0.066285	0.147116
BJH Adsorption cumulative volume of pores	0.059269	0.150779
BJH Desorption cumulative volume of pores	0.064930	0.155407
Pore Size (Å)		
Adsorption average pore width (4V/A by BET)	61.3637	14.4863
BJH Adsorption average pore diameter (4V/A)	85.231	17.106
BJH Desorption average pore diameter (4V/A)	76.720	18.596

© University of Venda

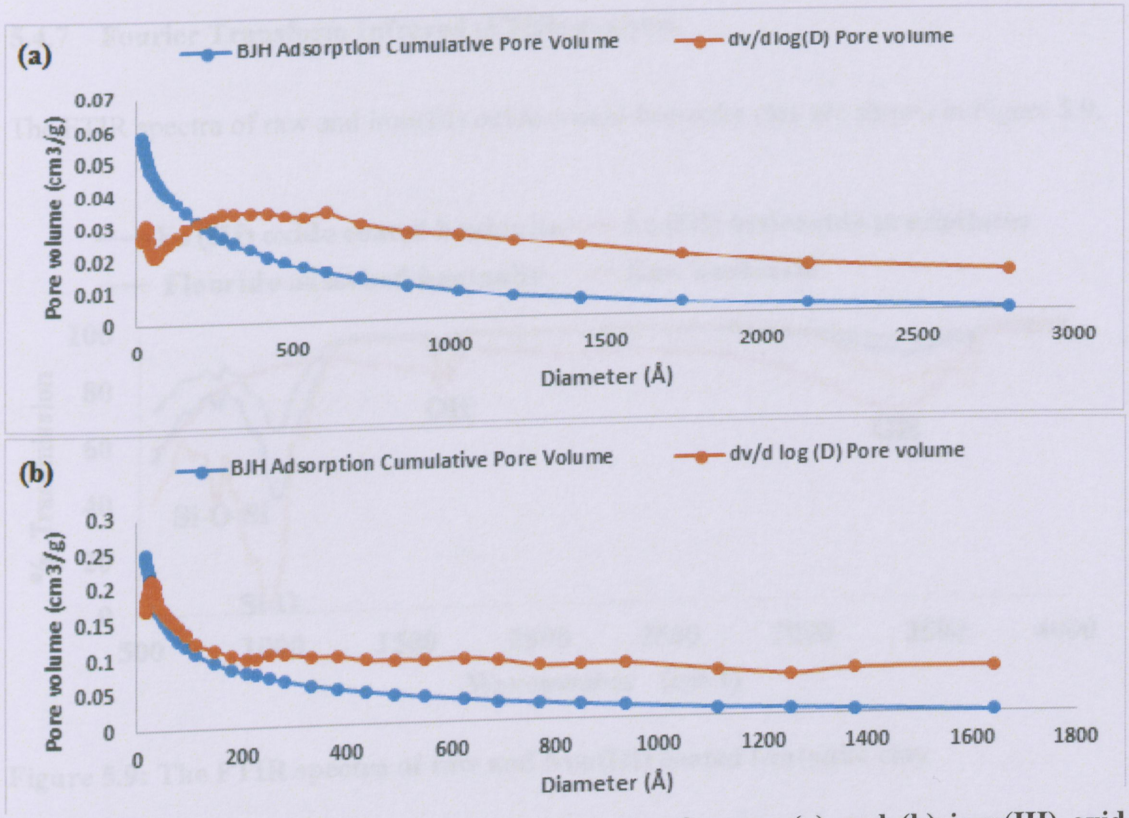


Figure 5.8: Plot of pore volume against diameter for raw (a) and (b) iron(III) oxide coated bentonite clay

The BET surface area of the raw bentonite and iron(III) oxide coated bentonite was observed to be 43.2077 and 132.3018 m^2/g respectively. As shown in Table 5.4, the coatings of iron oxide substantially changed the surface area of the raw bentonite clay. The BET surface area of the iron(III) oxide coated bentonite was more than that of the raw bentonite and it increased by a factor of ≈ 3 which may be due to the upsurge of the clay interlayers by the iron oxides/hydroxides precipitates formed during modification this resulting in the expansion of pore interlayer spaces of bentonite clay eventually leading to the increased surface area. The same observation is also shown with the pore volume. The pore volume increases after modification of the clay. Figure 5.8 shows the pore diameters of the raw and iron(III) oxide coated bentonite clay which helps us to differentiate between the materials in terms of their pores. From what is shown in Figure 5.8 most of the particles have pore sizes which fall between 2 and 50 nm basically meaning that bentonite clay is a mesoporous material.

© University of Venda

5.4.7 Fourier Transform Infrared (FTIR) analysis.

The FTIR spectra of raw and iron(III) oxide coated bentonite clay are shown in Figure 5.9.

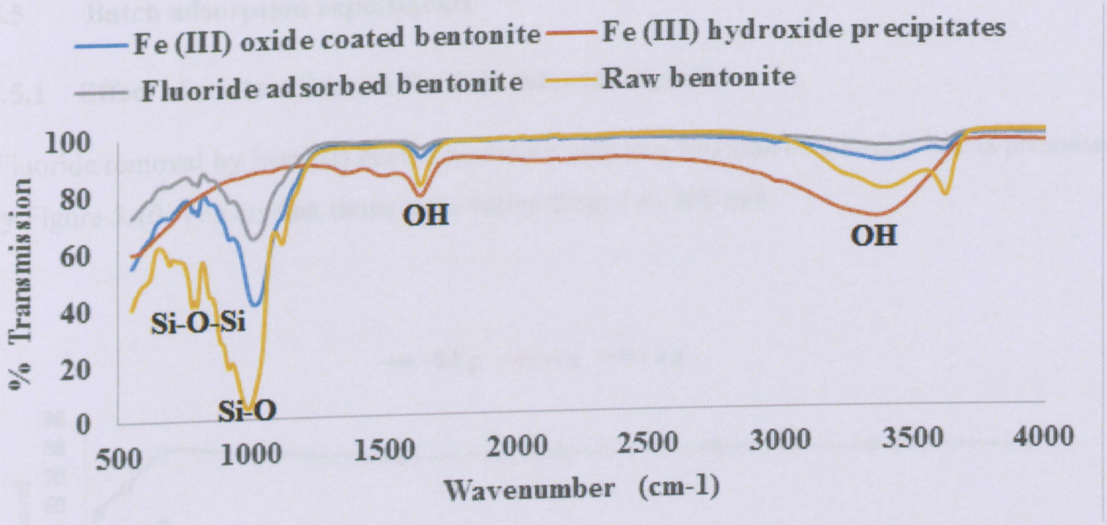


Figure 5.9: The FTIR spectra of raw and iron(III) coated bentonite clay

Figure 5.9 shows the spectrums of the raw bentonite clay and the iron(III) coated bentonite clay. The peak between 3700cm^{-1} and 3200cm^{-1} on both spectrums is indicative of free OH bending and OH band stretching for Al and Si and absorbed water. Comparing the peaks, it shows that transmission was higher on the modified clay than the raw clay. This could also be due to hydrated Fe^{3+} /Fe(OH)x species in the interlayer and on the clay surface on hydrolysis of Fe^{3+} by NaOH. Further comparison between the fluoride adsorbed bentonite peak and the iron(III) coated bentonite clay shows that % transmission slightly increased on the fluoride adsorbed bentonite. The reduction in the intensity of the OH functional groups for fluoride adsorbed bentonite is indicative of the main mechanism of fluoride removal being the interaction of fluoride with surface OH groups. The peaks at 1500cm^{-1} are probably due to OH ions of absorbed water (Zhang, et al., 2006). The peaks at 1000cm^{-1} are assigned to characteristic bands of silicates which are mostly closely related to stretching vibrations of X-O (where X = Si, Al). A substantial difference is noted between the 1000cm^{-1} peak between the raw and iron (III) coated bentonite clay. The huge absorbance on the modified clay is indicative of a different silicate material than that of the raw bentonite. This is validated by the results shown on the XRD diffractograms where a different silicate material (zeolites) appeared after modification of the clay. The presence of absorption bands at 529 and 670 cm^{1}

© University of Venda

on the spectrum corresponds to the Si-O-Si bending and Si-O bending respectively confirming that bentonite clay is a silicate material (Madejova and Komadel, 2001).

5.5 Batch adsorption experiments

5.5.1 Effect of contact time on fluoride removal capacity

Fluoride removal by iron(III) coated bentonite clay as a function of contact time is presented by Figure 5.10. The contact times were varied from 1 to 360 min.

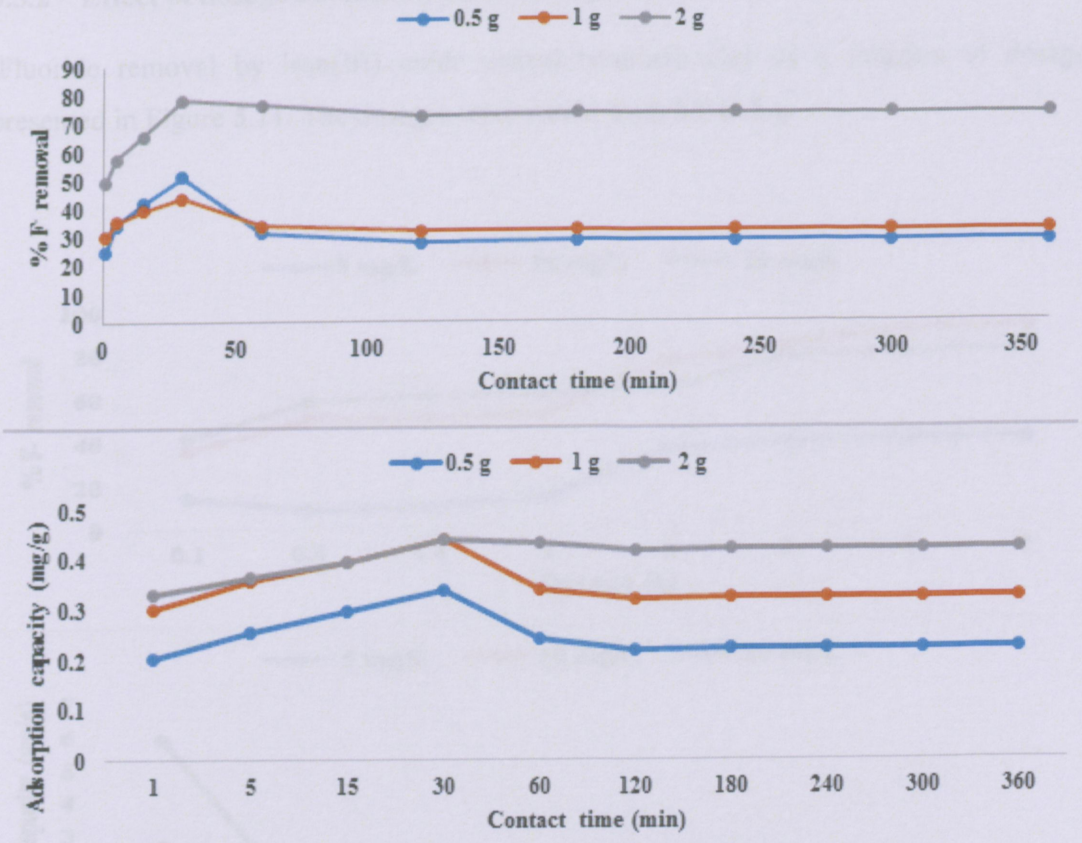


Figure 5.10: Removal of fluoride by iron(III) oxide coated bentonite clay as a function of contact time (0.5, 1 and 2 g , 10 mg/L F^- , 25°C room temperature, 100 mL solution, 250 rpm, pH*i* = 6.653)

The removal of fluoride as a function of contact time is shown in Figure 5.10. It was observed that the adsorption capacity of iron(III) oxide coated bentonite clay increases

© University of Venda

slightly by increasing contact time from 1 min to 30 min. The maximum adsorption capacity was observed to be 0.44 mg/g at adsorbent dosages of 1 and 2 g at 30 min. After that, the adsorption capacity dropped by 0.11 mg/g no further change was observed till 360 min. The theoretical explanation to this trend can be ascribed to the number of active site on the adsorbents. The fast adsorption rate at the initial stage is likely due to the availability of a large number of active sites on the adsorbent surface. Similar phenomena were also observed on Fe(III) modified zeolite and other metal-loaded adsorbents reported for fluoride adsorption (Sun, et al., 2011; Liu, et al., 2014). Based on equilibration time, 30 min was selected as optimum contact time and was applied in subsequent experiments.

5.5.2 Effect of dosage on fluoride removal capacity

Fluoride removal by iron(III) oxide coated bentonite clay as a function of dosage is presented in Figure 5.11. The dosages were varied from 0.1 to 5 g.

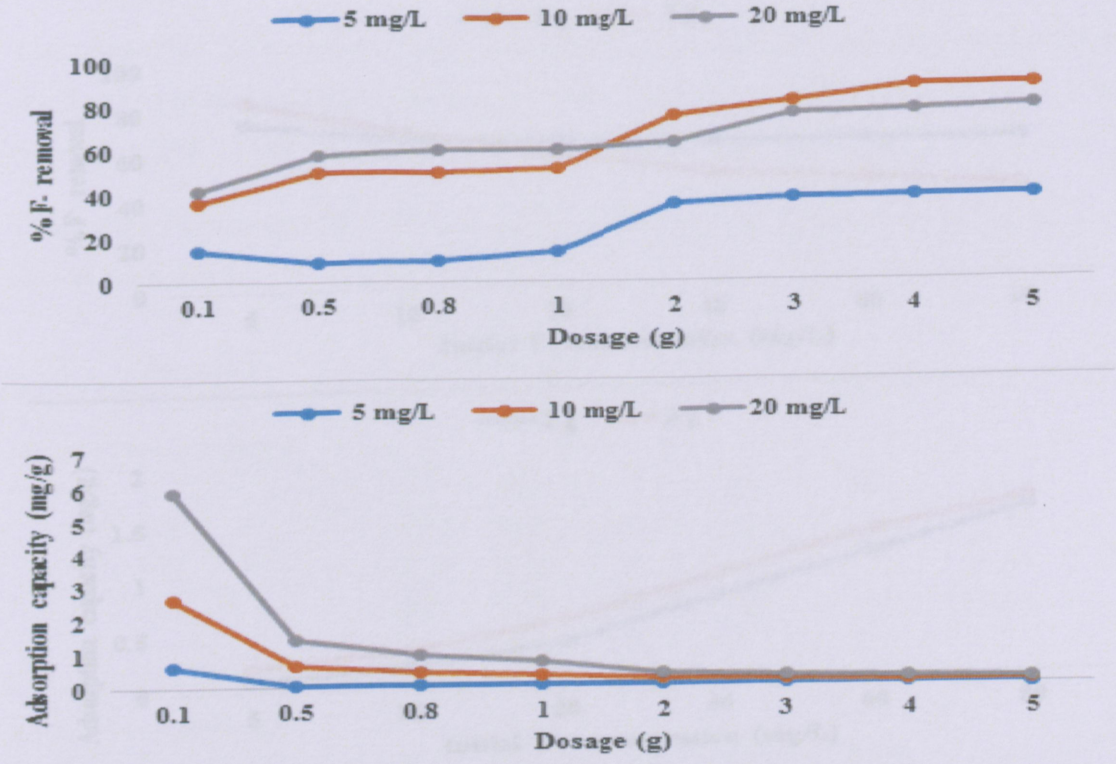


Figure 5.11: Removal of fluoride by iron(III) oxide coated bentonite clay as a function of dosage (30 min contact time, 5, 10, 20 mg/L F^-, 25°C room temperature, 250 rpm pH*i* = 7.434)

© University of Venda

The effect of adsorbent dose on F^- adsorption was evaluated at room temperature (25°C) using 3 different initial F^- concentrations of 5, 10 and 20 mg/L and a contact time of 30 min. It was observed that the amount (mg/g) of F^- adsorbed decreased with increase in adsorbent dosage. The maximum adsorption capacity was found to be 5.92 mg/g at a dose of 0.1 g/100 mL (20 mg/L). The increase in the fluoride removal with dosage of the adsorbent is likely driven by the enhanced availability of active sites (Sundaram, et al. 2009). The maximum F^- removal was observed with 3 g adsorbent dose at all initial fluoride concentrations. It was noted that a further increase in the absorbent dosage did not considerably change the removal capacity. Hence, the dose of 3 g was fixed as optimum dosage for subsequent experiments.

5.5.3 Effect of concentration on fluoride removal capacity

Fluoride removal by iron(III) oxide coated bentonite clay as a function of initial fluoride concentration is presented by Figure 5.12. The concentrations were varied from 5 to 80 mg/L.

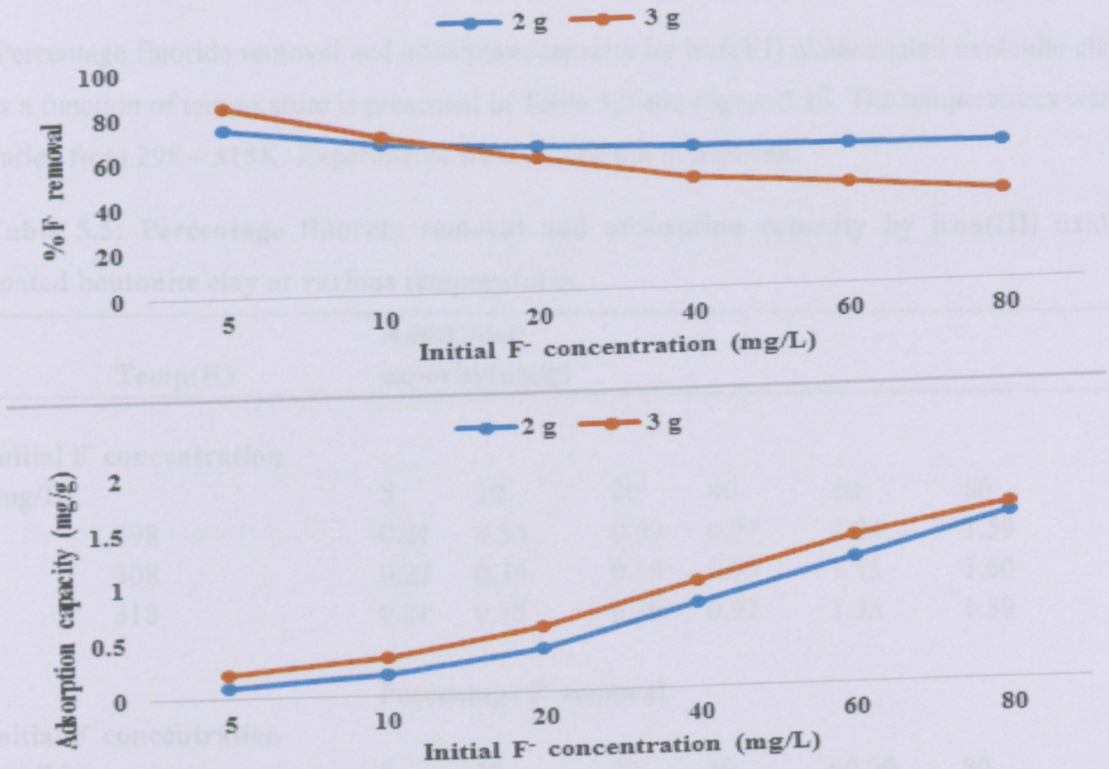


Figure 5.12: Removal of fluoride by iron(III) oxide coated bentonite clay as a function of concentration (30 min contact time, 2 and 3 g, 25°C room temperature, 100 mL solution, 250 rpm pH*i* = 6.263)

© University of Venda

University of Venda
Creating Future Leaders

The effect of initial concentration on fluoride removal is shown in Figure 5.12. It is observed that the percent of the adsorbed fluoride ions decreases with increase in the fluoride concentration which indicates that adsorption depends upon the availability of binding sites for fluoride ions. At low adsorbate concentration, the ratio of surface active sites to total fluoride is high, hence the fluoride ions could interact with the sorbent to occupy the active sites on the adsorbent surface sufficiently and be removed from the solution. But with the increase in adsorbate concentration, the number of active adsorption sites is not enough to accommodate fluoride ions hence the decrease in percentage removal. However an opposite trend is shown with adsorption capacity. The adsorption capacity increases with increasing initial fluoride concentration. When the initial fluoride concentration is 5 mg/L, with 3 g adsorbent dose, the equilibrium concentration of fluoride is reduced down to below the level of 1.5 mg/L under the current experimental conditions, which approaches the DWS drinking water standards of fluoride concentration.

5.5.4 Effect of temperature on fluoride removal.

Percentage fluoride removal and adsorption capacity by iron(III) oxide coated bentonite clay as a function of temperature is presented in Table 5.5 and Figure 5.13. The temperatures were varied from 298 – 318K. Experiments were carried out in triplicate.

Table 5.5: Percentage fluoride removal and adsorption capacity by iron(III) oxide coated bentonite clay at various temperatures

Temp(K)	Adsorption capacity(mg/g)					
Initial F^- concentration (mg/L)	5	10	20	40	60	80
298	0.21	0.35	0.59	0.97	1.34	1.59
308	0.22	0.36	0.59	0.97	1.35	1.60
318	0.21	0.35	0.59	0.97	1.35	1.59
	Percentage F^- removal					
Initial F^- concentration (mg/L)	5	10	20	40	60.00	80
298	84.22	70.07	59.1	48.50	44.83	39.75
308	88.22	72.07	59.6	48.75	45.16	40.00
318	86.22	71.07	59.6	48.75	45.00	39.87

© University of Venda

University of Venda
Creating Future Leaders

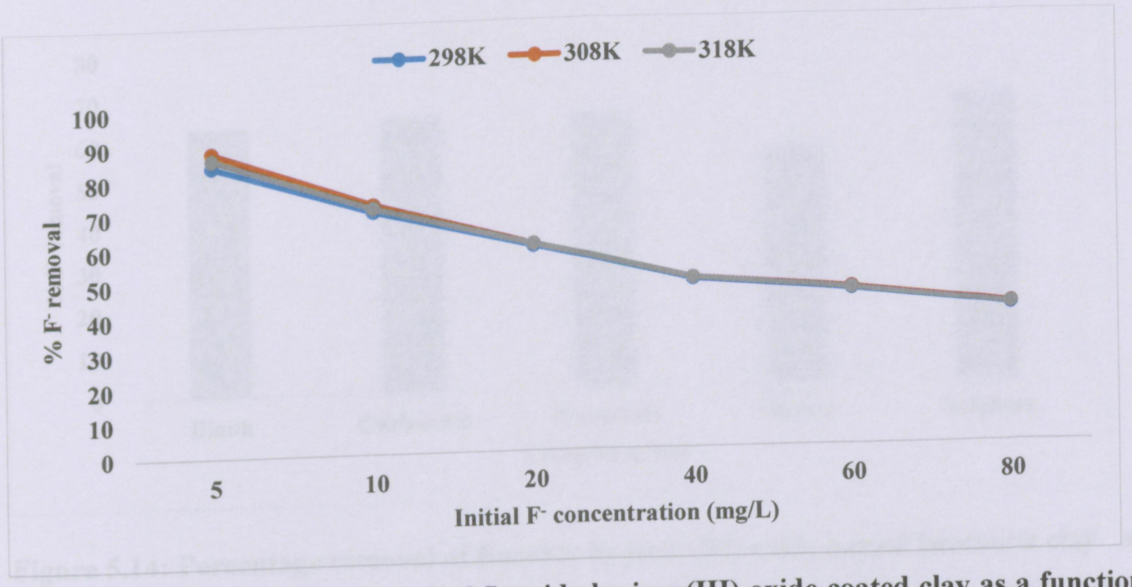


Figure 5.13: Percentage removal of fluoride by iron(III) oxide coated clay as a function of temperature. (30 min contact time, 25°C room temperature, 3 g/100 mL S/L ratio, 250 rpm).

Fluoride ion uptake capacity was determined as a function of temperature to determine an optimum temperature for the adsorption of fluoride onto iron(III) oxide coated bentonite clay. It was observed that the differences in temperature had a negligible influence on the adsorption capacity of the adsorbent. On the basis of that, it was concluded that there was no need to adjust the temperatures for defluoridation experiments hence 298 K (room temperature) was fixed as the optimum temperature to be used in subsequent experiments.

5.5.5 Effect of competing ions on fluoride removal capacity

Percentage fluoride removal by iron(III) oxide coated bentonite clay as a function of co-existing ions is presented in Figure 5.14

UNIVERSITY OF VENDA
LIBRARY

© University of Venda

University of Venda
Creating Future Leaders

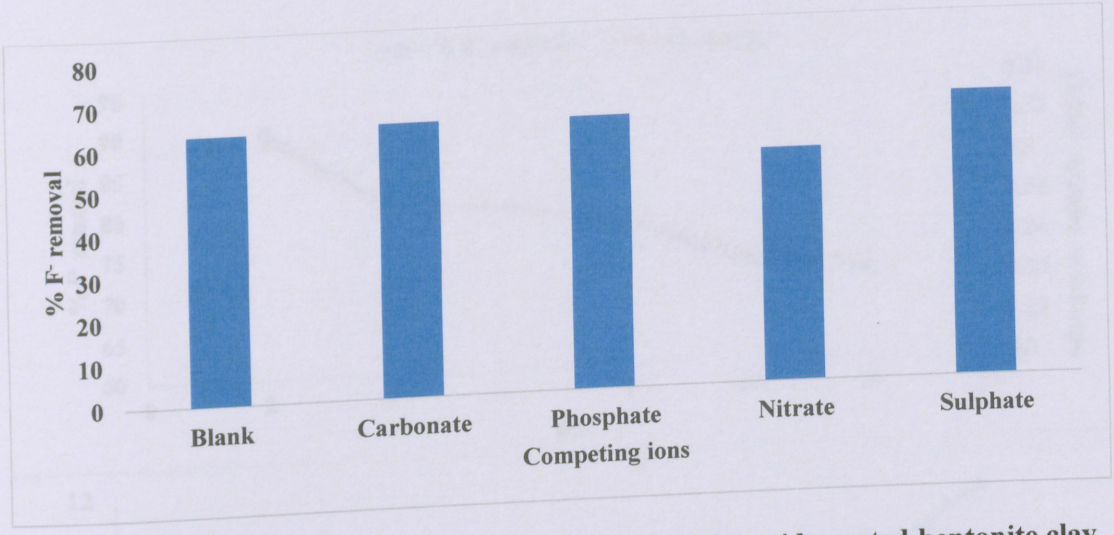


Figure 5.14: Percentage removal of fluoride by iron (III) oxide coated bentonite clay as a function of co-existing ions (30 min contact time, 10 mg/L F^-, 25°C room temperature, 3 g/100 mL S/L ratio, 250 rpm pHi = 6.474)

The influence of competing ions, carbonate, phosphate, nitrate and sulphate on fluoride adsorption was studied. Tests were conducted in the presence of 10 mg/L of fluoride and 10 mg/L each of ion. It was observed that the adsorption capacity for fluoride decreased from 63 to 55% in the presence of nitrate. It is expected that the presence of anions in solution would enhance coulombic repulsion forces between the anions and fluoride or would compete with fluoride for the active sites. However, the other ions did not negatively affect the percentage fluoride removal. In the presence of sulphate, the fluoride removal efficiency was even higher compared to the blank sample.

5.5.6 Effect of pH on fluoride removal capacity

Percentage fluoride removal by iron(III) oxide coated bentonite clay as a function of pH is presented in Figure 5.15. The pH was varied from 2 to 12.

© University of Venda

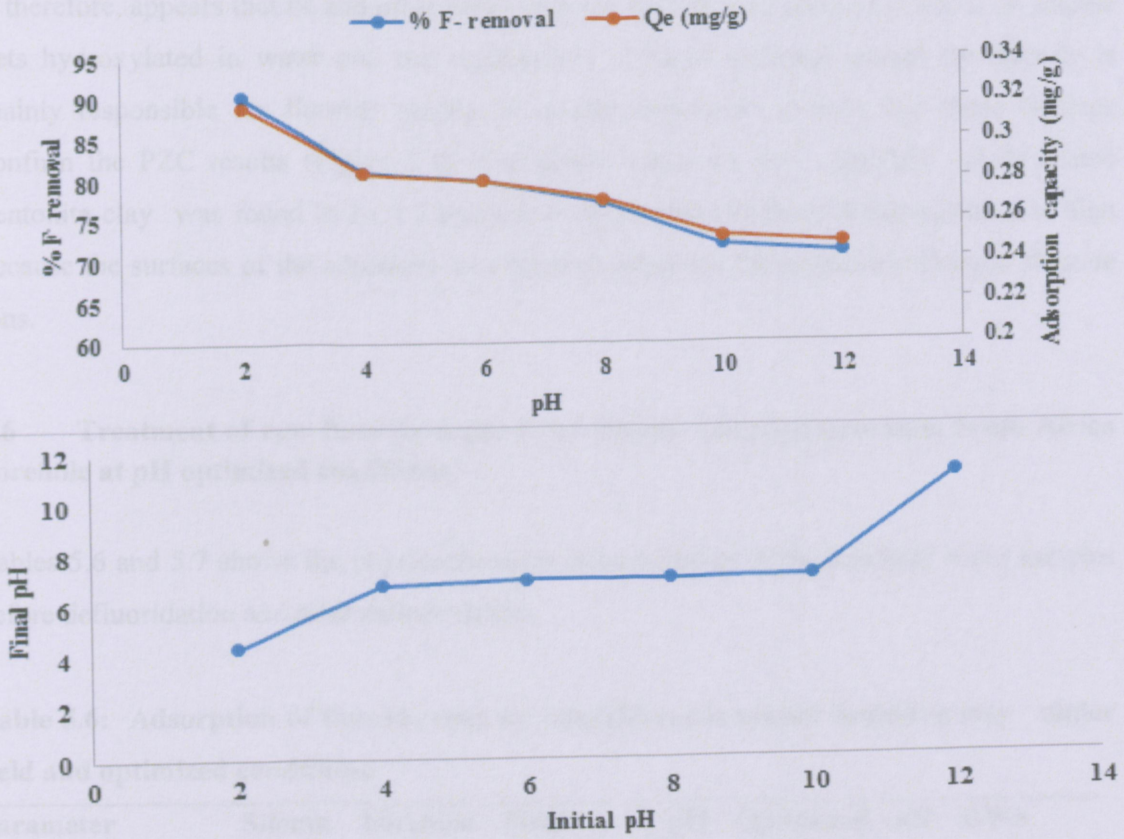


Figure 5.15: Percentage removal of fluoride by iron (III) oxide coated bentonite clay as a function of pH (30 min contact time, 5 mg/L F^-, 25°C room temperature, 3 g/100 mL S/L ratio, 250 rpm)

Figure 5.15 shows that there was high F^- adsorption observed at pH 2 which gradually decreased with an increase in the initial pH of the solution. Several dominating factors might be responsible such a trend. One factor is related to the production of the fluoride complex at acidic or basic media. The second factor responsible for fluoride removal might be through ligand exchange type interactions between the hydroxyl groups and fluoride.

The iron oxide coated on to the surface of bentonite can form $Fe(OH)_3$ in aqueous solution, which further reacts with fluoride ion to form FeF_3 by replacing hydroxide ions. This exchange of fluoride and hydroxide ions is due to their similar size/comparable ionic radius, while both are also iso-electronic in nature. This exchange mechanism between fluoride and hydroxide ion was further confirmed from the results that the equilibrium pH of the solution after treatment with iron(III) oxide coated bentonite clay slightly increases to alkaline range.

$$Fe(OH)_3 + 3F^- \leftrightarrow FeF_3 + 3OH^- \quad \ldots\ldots\ldots\

It therefore, appears that Fe and other metals present in interlayer spaces as well as on surface gets hydroxylated in water and the replacement of these hydroxyl groups by fluoride is mainly responsible for fluoride uptake. It is also imperative to note that these findings confirm the PZC results (Figure 5.4). The pHzpc value for the iron(III) oxide coated bentonite clay was found to be 7.5 and hence below that pH fluoride adsorption was high because the surfaces of the adsorbent was positive attracting the negatively charged fluoride ions.

5.6 Treatment of raw fluoride water from Siloam, Limpopo province, South Africa borehole at pH optimized conditions

Tables 5.6 and 5.7 shows the physicochemical characteristics of the borehole water samples before defluoridation and after defluoridation.

Table 5.6: Adsorption of fluoride onto by iron(III) oxide coated bentonite clay under field and optimized conditions.

Parameter	Siloam borehole water	Field pH (pH = 7.81)	Optimized pH (pH = 2. 12)	DWS guidelines
pH	7.81	7.624	7.11	6 – 9
EC (µS/cm)	25.74	25.12	25.10	0 – 150
F^- (mg/L)	5.53	4.233	3.23	1 – 1.5
Cl^- (mg/L)	31.6	180.1	189.1	0 – 250
SO_4^- (mg/L)	11.9	N.D	N.D	0 – 250
Br^- (mg/L)	2.08	N.D	N.D	0 – 6
NO_3^- (mg/L)	1.13	N.D	N.D	0 – 6
PO_4^{3-} (mg/L)	ND	N.D	N.D	0 - 5

© University of Venda

University of Venda
Creating Future Leaders

Table 5.7: Concentration of metals before and after defluoridation using iron(III) oxide coated bentonite clay

Metals (µg/L)	Field water (pH = 7.81)	Treated water (pH = 7.11)	Metals (mg/L)	Field water (pH = 7.81)	Treated water (pH = 7.11)
Li	8.824888	9.071993	Al	0.04392	0.8336
Be	< 0.005	0.039969	Ca	3.163	10.56
B	22.61723	12.401841	Fe	0.163251	10.25
V	0.084905	0.373527	K	2.544	4.916
Cr	0.227367	4.165272	Mg	0.0396	8.992
Mn	17.46683	39.14397	Na	67.58	1423
Co	0.028445	0.549693	P	< 0.01	0.0043
Ni	0.741724	2.789933	Si	45.51	13.38
Cu	10.74428	7.319199	Sr	0.0234	0.1277
Zn	11.47378	8.552546			
As	< 0.03	0.124786			
Se	< 0.54	0.721939			
Mo	1.352091	0.508769			
Cd	< 0.04	0.007985			
Sb	< 0.01	0.053063			
Ba	40.61815	104.776			
Hg	< 0.01	<0.004			
Pb	0.592015	0.789663			

As shown in Table 5.6, all the measured parameters besides fluoride were within the DWS water quality guidelines when the defluoridation was performed at both field pH and optimised pH conditions. However the fluoride removal efficiency was higher at optimised conditions. The percentage fluoride removal at field conditions is 31% whereas at optimised conditions the fluoride removal is 71%. The lower % F^- removal for field water at field conditions could be due to the effect of co-existing ions which competed for adsorption sites with F^-. It is expected that the presence of anions in solution would enhance coulombic repulsion forces between the anions and fluoride or would compete with fluoride for the active sites (Onyango, et al., 2004). In the present study, nitrates were shown to have an effect on the removal of fluoride. In the presence of nitrates, the removal of fluoride was

© University of Venda

slightly reduced. It is also shown that after the defluoridation experiments all the nitrates that were in solution were taken up meaning that nitrates could have filled up adsorption sites before fluoride could be adsorbed. The negative effect of competing ions were also reported in other studies. Daifulla et al. (2007) observed that the adsorption capacity for fluoride decreased from 100 to 91% in the presence of sulphate and to 94% in the presence of bromide but chloride does not affect fluoride adsorption. Another study by Thakre et al, (2010) showed a significant drop in the fluoride removal efficiency in the presence of bicarbonate ion. From Table 5.7, all the metals were within permissible limits besides Al, Na and Fe in treated water. However at these levels Al and Fe have no health effects but rather aesthetic effects. At 1423 mg/L Na will cause a highly salty taste and there is a likelihood of nausea and vomiting. At those levels the Na may be highly undesirable for infants or persons on a sodium restricted diet (DWAF, 1996).

5.7 Chemical stability of the adsorbent

The chemical stability of the adsorbent under various pH values was assayed by measuring the concentration of dissolved metals in the solution after adsorption. The concentration of metals leached at various initial pHs are presented in Table 5.8.

© University of Venda

University of Venda
Creating Future Leaders

Table 5.8: Concentration of metals in solution after defluoridation at pH 2, 6 and 12

Metals(µg/L)	pH 2	pH 6	pH 12	Metals(mg/L)	pH 2	pH 6	pH 12
Li	20.20	15.87	7.08	**Ca**	37.15	18.67	1.42
Be	2.82	<0.000	0.74	**K**	6.06	7.40	5.18
B	32.37	15.06	30.21	**Mg**	27.61	14.54	1.10
Al	3202.86	17.10	6397.2	**Na**	2200.0	2142.0	2236.0
V	<0.000	<0.000	1.88	**P**	0.01	0.01	0.06
Cr	<0.000	0.56	8.21	**Si**	8.47	0.94	13.84
Mn	1180.86	6.79	27.48				
Fe	30.549	15.774	5668.28				
Co	25.96	0.08	0.51				
Ni	91.02	0.67	2.58				
Cu	14.20	0.20	4.48				
Zn	30.95	2.00	7.38				
As	<0.1	<0.1	0.54				
Se	2.12	2.56	3.99				
Sr	895.00	267.53	4.96				
Mo	0.27	0.31	10.97				
Cd	0.41	0.05	0.05				
Sb	0.08	0.11	0.16				
Ba	1059.14	110.00	11.66				
Hg	0.01	<0.05	0.04				
Pb	<0.05	<0.05	1.08				

pH had a major influence on the chemical stability of iron(III) oxide coated bentonite clay. From Table 5.8 it can be observed that high leaching of metals occurred at pH 2 and 12. However at pH 6 which is near neutral, the leaching of metal species was minimal. When compared to the DWS water quality guidelines, the concentration of metals Al, Mn and Fe exceeds the recommended limits at pH 2 and 12. This indicates that defluoridation at pH 2 using the iron oxide coated bentonite would be unsuitable for defluoridation of groundwater for drinking purposes. However it can be seen that it is only Na that considerably leached into solution at all the tested pHs. According to DWS water quality guidelines, Na should

© University of Venda

range between 0 – 100 mg/L and the Na concentration ranged between 2142.0 and 2236.0 mg/L which is above the recommended water quality guidelines and is highly undesirable for infants or persons on a sodium restricted diet. The high Na concentration could be coming from the NaOH used during the bentonite activation process.

5.8 Comparison of the percentage removal capacities of the raw bentonite clay and iron (III) oxide coated bentonite clay.

Defluoridation experiments were performed using the optimised pH conditions using raw bentonite clay and iron(III) oxide coated bentonite clay. The results are presented in Table 5.9

Table 5.9: Comparison of the percentage removal capacities of the raw bentonite clay and iron(III) oxide coated bentonite clay.

Optimised parameters	% removal by raw bentonite	% removal by iron(III) oxide coated bentonite clay.
Contact time (60 min)	1.00%	44.00%
Dosage (1 g)	-2.50%	13.63%
Concentration (9 mg/L (F^-))	-20.00%	67.00%
Temperature (298K)	2.00%	70.00%
pH 2	85.00%	90.00%

From Table 5.9 it can be shown that modifying bentonite clay by coating its surfaces with iron(III) clearly improved its adsorption capacity. The results show an increase in the fluoride percentage removal across all parameters. However the percentage removal obtained with iron(III) oxide coated bentonite clay is high enough for efficient defluoridation. It can also be observed that the raw bentonite showed desorption characteristics but after modification no desorption was observed. On the basis of the above results, it can be said that modifying the raw bentonite clay greatly increased its adsorption capacity.

5.9 Adsorption Isotherms

The concentration of an adsorbate (F^-) in a bulk solution is in dynamic balance with that of the adsorbent interface. The analysis of equilibrium data helps to develop mathematical

© University of Venda

models that could be used for the quantitative description of the results. The equation parameters and the underlying assumptions of these equilibrium models are capable of predicting ion adsorption and vital information on the mechanism of sorption.

The Langmuir, Freundlich and Dubinin- Radushkevich isotherms were tested in this study and their parameters are given in Table 5.10.

5.9.1 Langmuir Isotherm

Figure 5.16 shows the Langmuir adsorption isotherm for fluoride adsorption onto iron(III) oxide coated bentonite clay at various temperatures

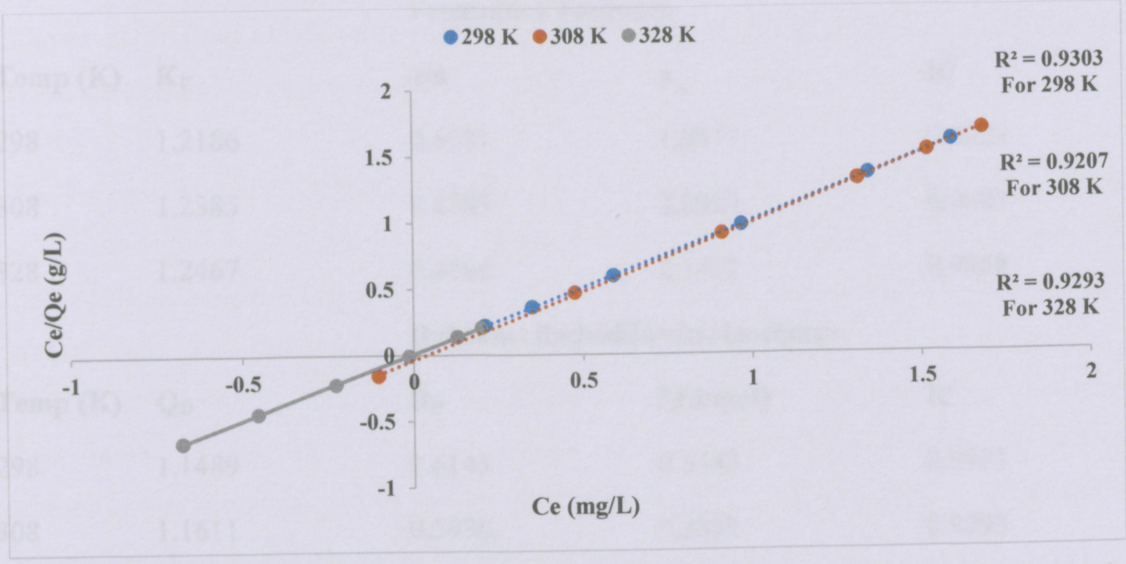


Figure 5.16: Langmuir adsorption isotherm (3 g adsorbent, 30 min of equilibration time, concentration was varied from 5 – 80 mg/ L pH*i* = 6.263)

R_L value indicates the adsorption nature to be either unfavourable if $R_L > 1$, linear if $R_L = 1$, favourable if $0 < R_L < 1$ and irreversible if $R_L = 0$. From the data in Table 5.10 the R_L values (the separation factors) are 0.148, 0.133 and 0.139. They are all greater than 0 but less than 1 indicating that Langmuir isotherm is favourable. The maximum Langmuir monolayer coverage capacity (Q_m) at all temperatures was determined to be 1.93, 1.88 and 1.9 mg/g. When compared to the experimental adsorption capacity 1.52 mg/L, the Langmuir monolayer coverage capacity is slightly higher. The R^2 values all between 0.92 and 0.94 proving that the sorption data fitted well to Langmuir Isotherm.

UNIVERSITY OF VENDA
LIBRARY

© University of Venda

University of Venda
Creating Future Leaders

Table 5.10: Langmuir, Freundlich and Dubinin-Radushkevich isotherm parameters for the sorption of fluoride onto iron(III) oxide coated bentonite clay.

		Adsorption isotherms and parameters		
		Langmuir Isotherm		
Temp (K)	**qm (mg/g)**	**b (L/mg)**	**R_L**	**R^2**
298	1.93	0.072	0.148	0.9303
308	1.88	0.0816	0.133	0.9207
328	1.9	0.077	0.139	0.9293
		Freundlich Isotherm		
Temp (K)	**K_F**	**1/n**	**n**	**R^2**
298	1.2186	0.5031	1.9877	0.9929
308	1.2385	0.4783	2.0907	0.9887
328	1.2467	0.4666	2.1432	0.9858
		Dubinin- Radushkevich Isotherm		
Temp (K)	**Q_D**	**B_D**	**E(J/mol)**	**R^2**
298	1.1489	0.6145	0.5543	0.9993
308	1.1611	0.5936	0.3852	0.9993
328	1.1628	0.5899	0.3840	0.9993

5.9.2 Freundlich Isotherm

The Freundlich isotherm is mainly used to describe the adsorption characteristics for heterogeneous surfaces (Krishnaiah and Vijaya, 2009). The plot of Log Qe against Log Ce is shown in Figure 5.17.

© University of Venda

University of Venda
Creating Future Leaders

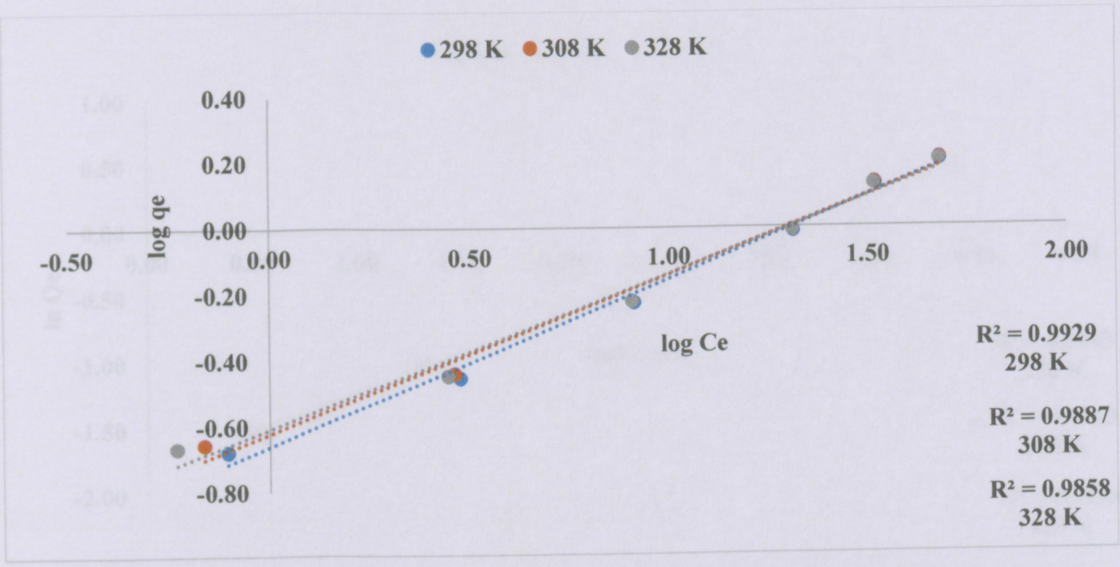


Figure 5.17. Freundlich adsorption isotherm (3 g adsorbent, 30 min of equilibration time, concentration was varied from 5 – 80 mg/L pH*i* = 6.263)

The constant K_F is an approximate indicator of adsorption capacity, while 1/n is a function of the strength of adsorption in the adsorption process (Voudrias, et al. 2002). If n lies between one and ten, this indicates a favourable sorption process (Goldberg, 2005). From the data in Table 5.10, the values of n are between 1 and 3 which indicates that the sorption of fluoride onto iron(III) oxide coated bentonite clay is favourable and the R^2 values are above 0.98 showing a good fit to the Freundlich adsorption isotherm compared to the Langmuir isotherm. The experimental adsorption capacity (1.52 mg/g) was also close to the calculated adsorption capacity (K_F) shown in Table 5.10.

5.9.3 Dubinin–Radushkevich isotherm model

This isotherm was applied to the experimental data, in order to investigate the mean free energy of adsorption. Figure 5.18 shows the Dubinin–Radushkevich adsorption isotherm for fluoride adsorption onto iron(III) oxide coated bentonite clay

© University of Venda

University of Venda
Creating Future Leaders

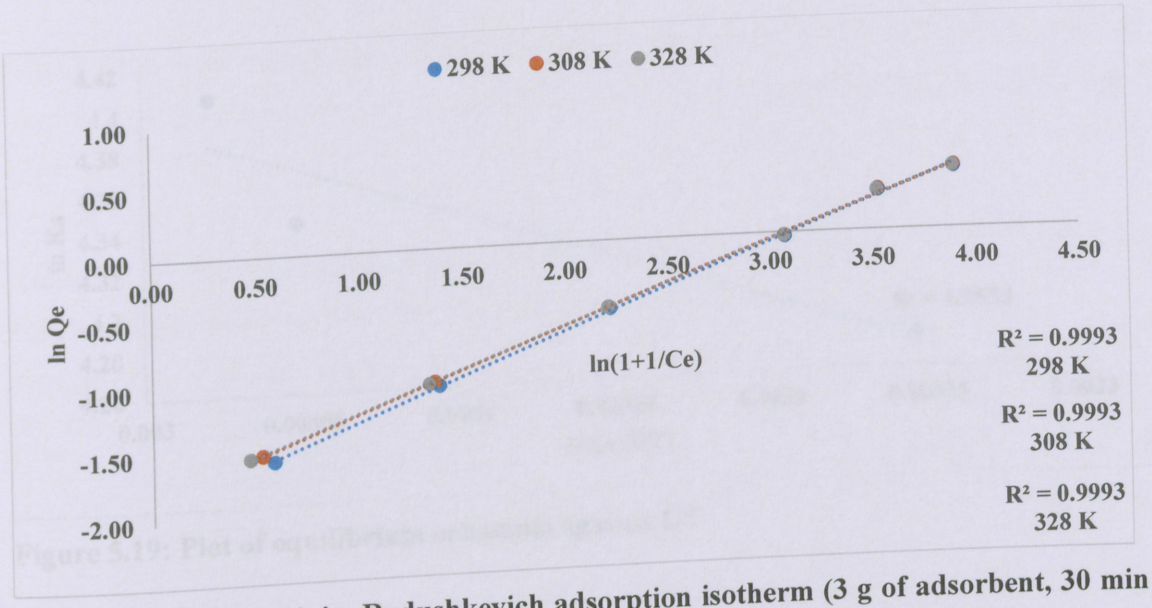


Figure 5.18. The Dubinin–Radushkevich adsorption isotherm (3 g of adsorbent, 30 min of equilibration time, concentration was varied from 5 – 80 mg/ L pH*i* = 6.263)

The Dubinin-Radushkevich isotherm parameters are shown in Table 5.10. The value of the regression (R^2) obtained showed that this model provided a fairly good fit to the experimental data compared to the Langmuir and Freundlich isotherm. The Dubinin-Radushkevich also describes a multilayer surface and the high values of R^2 show that adsorption onto the iron(III) oxide coated bentonite clay occurred on a heterogeneous surface. This is also corroborated by the good fit shown by the Freundlich isotherm. The magnitude of the mean free energy of adsorption (E) calculated from Dubinin-Radushkevich equation is useful for estimating the type of adsorption. If (E) is less than 16 kJ/mol, the adsorption type can be explained by ion exchange (Qadeer, et al., 1995). Fluoride ions in the solution were exchanged with the OH group on the iron(III) oxide coated bentonite clay as explained in section 5.4.6.

5.10 Thermodynamics

In order to evaluate the feasibility of the adsorption process, thermodynamic parameters were evaluated.

Figure shows 5.19 the Van Hoff's plot of ln(Ko) vs 1/T

© University of Venda

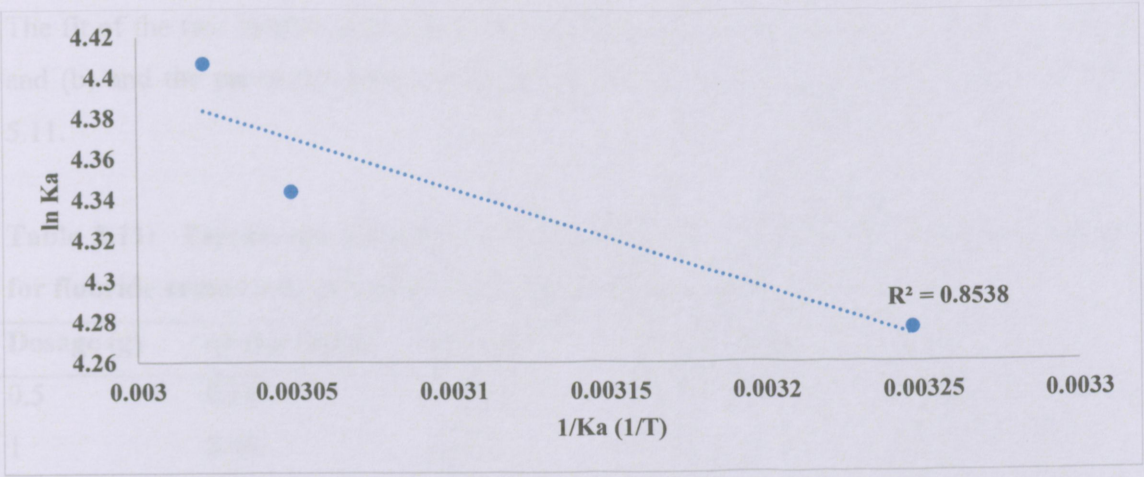


Figure 5.19: Plot of equilibrium constants against 1/T

Table 5.11: Thermodynamic parameters

Parameter	ΔG kJ/mol	ΔH (kJ/mol)	ΔS (kJ/mol/K)	Ka (L/g)
Value	-10604.0082	58.74	5.891	72

The values of ΔH and ΔScan be obtained from the slope and intercept of the Van Hoff's plot of ln (Ko) vs 1/T as shown in Figure 5.19. These are observed to be 58.74 kJ/mol and 5.891 kJ/mol/K, respectively. The positive value of enthalpy change suggests that the fluoride adsorption process is endothermic in nature and corroborates with the findings reported in literature (Sundaram et al. 2009). The negative value of free energy change at all temperatures evaluated and positive value of entropy change suggests that fluoride adsorption process is favourable and spontaneous.

5.11 Adsorption kinetics

Adsorption is a time-dependent process and it is very important to know the rate of the adsorption process for design purposes. The kinetics data of the fluoride adsorption onto the iron(III) oxide coated bentonite clay were tested by fitting the data onto two adsorption kinetic models i.e. the pseudo first-order (Lagergren model) and the pseudo second-order kinetic models.

© University of Venda

The fit of the two models to the fluoride adsorption kinetic data is shown in Figure 5.20 (a) and (b) and the parameter values obtained by curve-fitting kinetic data are listed in Table 5.11.

Table 5.11: Pseudo-second-order kinetic parameters for different adsorbent dosages for fluoride removal by iron(III) oxide coated bentonite clay

Dosage (g)	qe exp (mg/g)	K_2(gmh)	qe cal (mg/g)	R^2
0.5	0.34	1.4082	0.2205	0.9994
1	0.44	1.2554	0.3203	0.9997
2	0.44	3.9003	0.4232	1

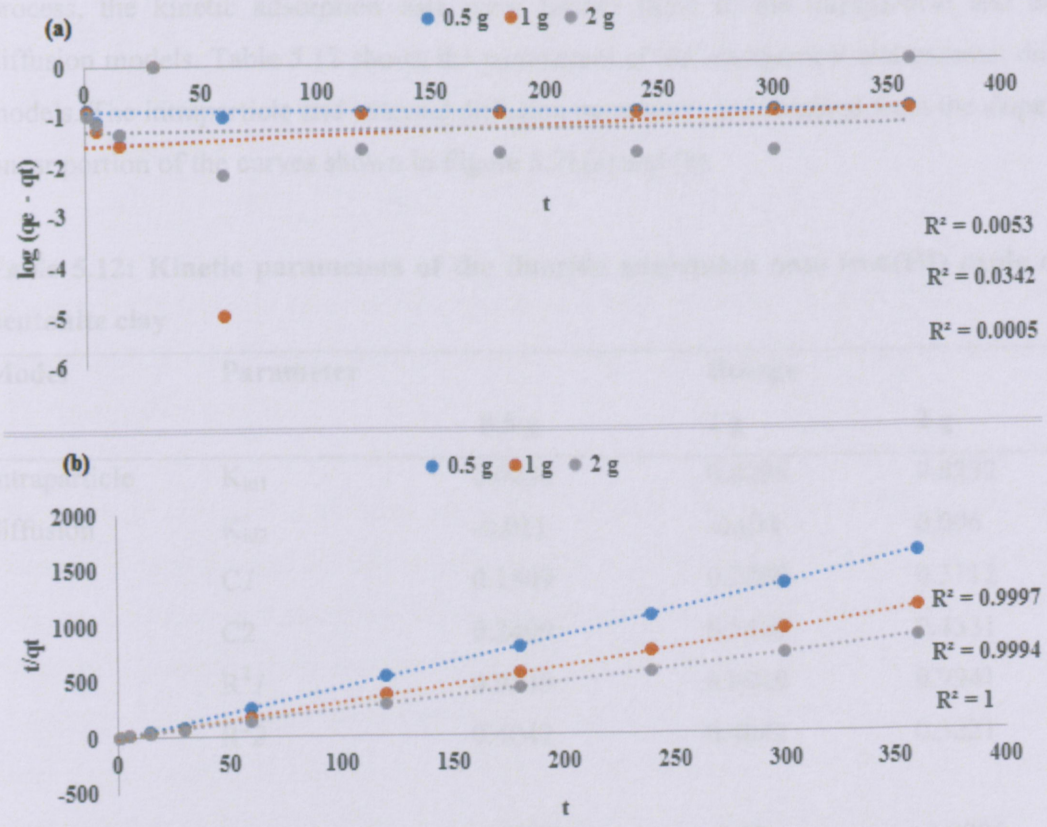


Figure 5.20 (a) and (b): Adsorption kinetics for fluoride sorption onto iron (III) oxide coated bentonite clay as a function of contact time (0.5, 1 and 2 g , 10 mg/L F- , 25°C room temperature, 100 mL fluoride solution, 250 rpm pH*i* = 6.653)

UNIVERSITY OF VENDA
LIBRARY

© University of Venda

The pseudo-second-order kinetic model proved to be more suitable in describing the adsorption kinetics of fluoride based on the correlation coefficient ($R^2 > 0.99$) as shown in Table 5.12, suggesting that a chemisorption step might be rate determining in the fluoride adsorption process (Ho, et al., 1995). Furthermore, it could be seen that the theoretical adsorption capacities, q_e, were all very close to the experimental capacity. Similar results were observed for the adsorption of fluoride by various adsorbents (Caia, 2015; Tchomgui-Kamga, et al., 2010)

There are three steps involved in pseudo second order kinetic model: (i) the fluoride ions diffuse from liquid phase to liquid–solid interface; (ii) the fluoride ions move from liquid–solid interface to solid surfaces; and (iii) the fluoride ions diffuse into the particle pores (Liao, 2012). To reveal the relative contribution of surface and intraparticle diffusion to the kinetic process, the kinetic adsorption data were further fitted to the intraparticle and external diffusion models. Table 5.12 shows the parameters of the intraparticle and external diffusion models. The intraparticle and external diffusion parameters are obtained from the slope of the linear portion of the curves shown in Figure 5.21(a) and (b)

Table 5.12: Kinetic parameters of the fluoride adsorption onto iron(III) oxide coated bentonite clay

Model	Parameter	Dosage		
		0.5 g	1 g	2 g
Intraparticle diffusion	K_{id1}	0.0296	0.0296	0.0232
	K_{id2}	-0.011	-0.011	0.006
	C*1*	0.1809	0.2809	0.3112
	C2	0.2409	0.3409	0.4331
	R^2*1*	0.9849	0.9849	0.9941
	R^2*2*	0.4042	0.4042	0.3221
External diffusion	kf*1*	-0.0026	-0.03	-0.0025
	kf*2*	-0.5	-0.5	-0.5
	R^2*1*	0.9294	0.9298	0.9718
	R^2*2*	0.2336	0.3104	0.2402

© University of Venda

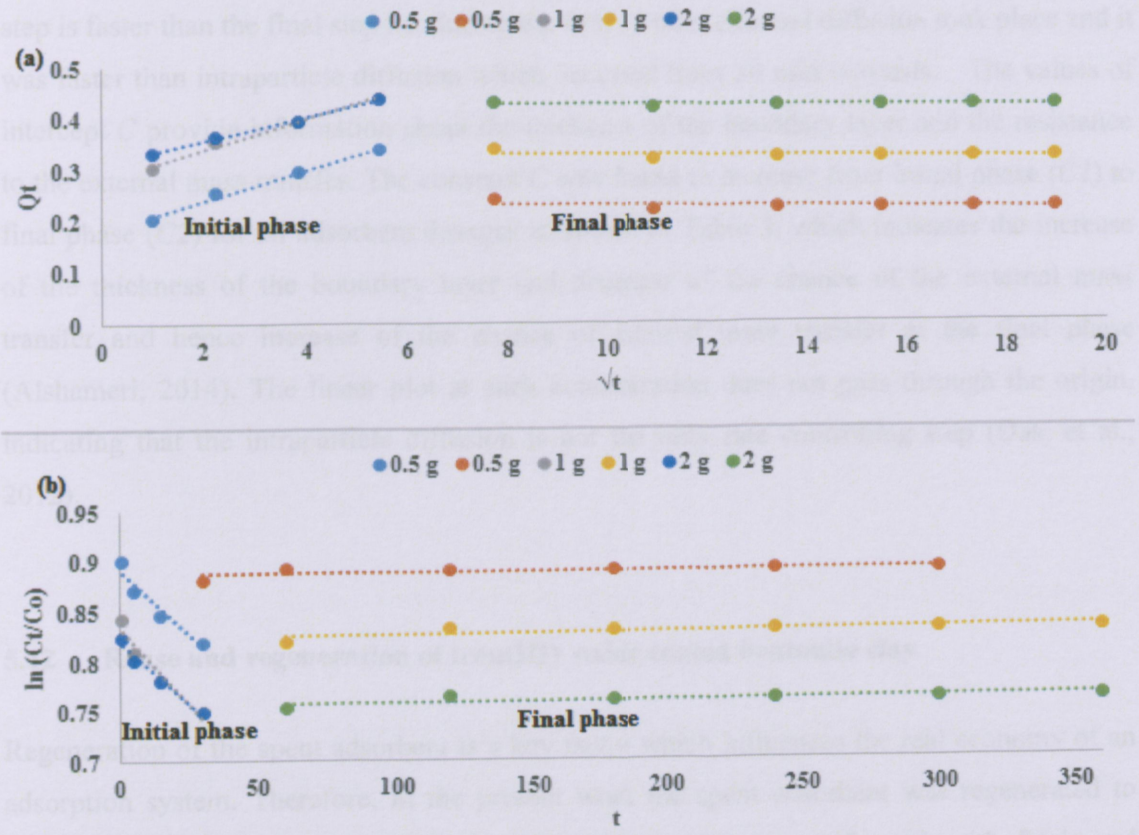


Figure 5.21: Data fit into (a) Intraparticle diffusion model and (b) External diffusion model (0.5, 1 and 2 g , 10 mg/L F^- , 25°C room temperature, 100 mL fluoride solution, 250 rpm pH*i* = 6.653)

Intraparticle diffusion is assumed to be the sole rate-controlling step if the regression of Qt versus $t^{1/2}$ is linear and the plot passes through the origin (Arami, 2008). The fitting results (Figure 5.21a) show that the regression was linear, but the plot did not pass through the origin (C≠ 0). Therefore, the adsorption kinetics of fluoride ions onto iron(III) oxide coated bentonite clay was regulated by both external and intraparticle diffusion processes. As can be seen from Figure 5.21 (a) and (b), fluoride exchange by iron(III) oxide coated bentonite clay involves two stages. These two stages suggest that the ion exchange process proceeds by surface sorption and intraparticle diffusion. The first sharp linear region is a diffusion adsorption stage, attributing to the diffusion of fluoride molecules through the solution to the external surface of adsorbent (film diffusion). The second linear region is a gradual adsorption stage, where the intraparticle diffusion is rate-controlled (intraparticle diffusion) (Yao, et al., 2010). The intra-particle rate constants Ki_{d1} and K_{id2} obtained from the show that

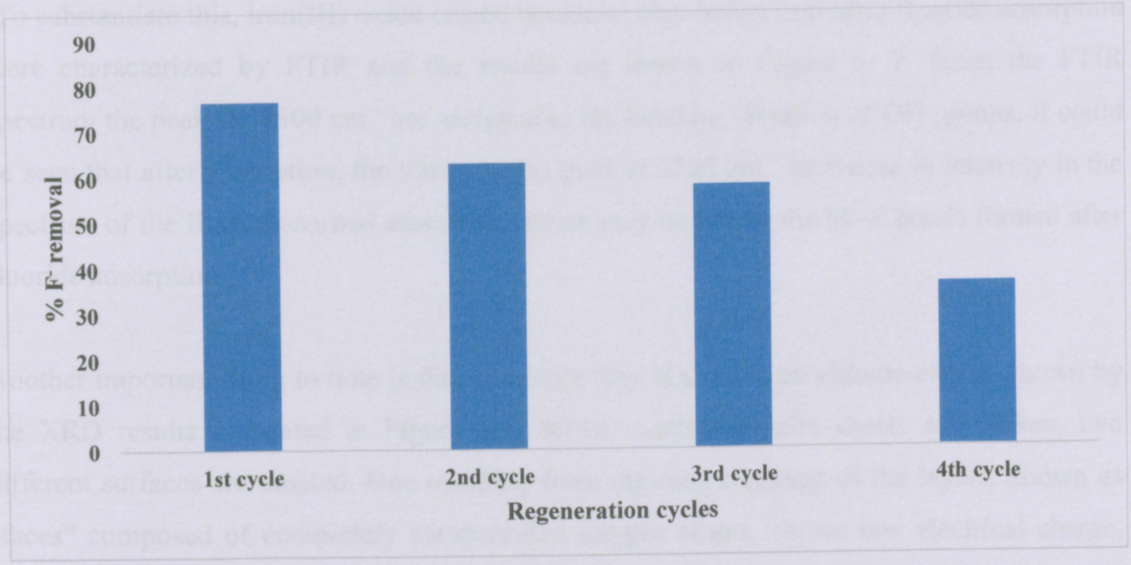
© University of Venda

University of Venda
Creating Future Leaders

at all adsorbent dosages, the K_{id1} value is greater than the K_{id2} value, indicating that the initial step is faster than the final step i.e. during the first 30 min, external diffusion took place and it was faster than intraparticle diffusion which occurred from 30 min onwards, The values of intercept C provide information about the thickness of the boundary layer and the resistance to the external mass transfer. The constant C was found to increase from initial phase ($C1$) to final phase ($C2$) for all adsorbent dosages as shown in Table 3, which indicates the increase of the thickness of the boundary layer and decrease of the chance of the external mass transfer and hence increase of the chance of internal mass transfer at the final phase (Alshameri, 2014). The linear plot at each concentration does not pass through the origin, indicating that the intraparticle diffusion is not the only rate controlling step (Das, et al., 2012).

5.12 Reuse and regeneration of iron(III) oxide coated bentonite clay

Regeneration of the spent adsorbent is a key factor which influences the real economy of an adsorption system. Therefore, in the present work the spent adsorbent was regenerated to assess its reusability. A fluoride adsorption experiment was performed with fresh and regenerated iron(III) oxide coated bentonite clay to determine the effectiveness of the regeneration process and adsorption capacity of regenerated adsorbent. The results are presented in Figure 5.22.



© University of Venda

University of Venda
Creating Future Leaders

Figure 5.22: Regeneration studies using 0.01 M NaOH (10 mg/L F^- , 100 mL solution, 2 g adsorbent dosage)

As can be seen from Figure 5.22, the regenerated adsorbent has less adsorption capacity as compared to fresh iron(III) oxide coated bentonite clay. The adsorption capacity decreases more as the adsorbent is regenerated again and again. However for the first 2 regeneration cycles the adsorbent has a fairly good fluoride removal capacity. This indicates that used adsorbent can be regenerated by the alkali treatment. This further substantiates the mechanism of fluoride uptake through the replacement of hydroxyl group/anions from the metal oxide sites of bentonite clay as the material is being regenerated by NaOH providing OH ions.

5.13 Proposed mechanism of fluoride adsorption onto iron(III) oxide coated bentonite clay

Revealing the adsorption mechanism plays an important role in understanding the material characteristics and designing the application purpose of the new adsorbent. It has been reported that the hydrolysis reaction occurring between the metal oxide and water results in the formation of surface hydroxyl groups. The surface hydroxyl groups on metal oxides are considered as the most abundant and active adsorption sites for adsorption of anions from water (Tamura, 2001 and Wang, 2013).

To substantiate this, iron(III) oxide coated bentonite clay before and after fluoride adsorption were characterized by FTIR and the results are shown in Figure 5. 7. From the FTIR spectrum the peaks at 3500 cm^{-1} are assigned to the bending vibration of OH groups. It could be seen that after adsorption, the transmission peak at 3500 cm^{-1} increased in intensity in the spectrum of the fluoride-sorbed adsorbent, which may be due to the M–F bonds formed after fluoride adsorption.

Another important thing to note is that bentonite clay is a montomorillonte clay as shown by the XRD results presented in Figure 5.5. When montmorillonite sheets are broken, two different surfaces are created. One resulting from the easy cleavage of the layers, known as "faces" composed of completely compensated oxygen atoms, shows low electrical charge, and have nonpolar properties in water and hydrophobic. The other arising from the break of

© University of Venda

University of Venda
Creating Future Leaders

the ionic bonds within the layers, named "edges" made up of hydroxyl ions, siloxane groups (–Si–O–Si), O^{2-} , Mg^{2+}, Fe $^{3+}$ and Ca^{2+} that simply undergoes hydrolysis, provide a comparatively high level electrical charges in water. The faces and the edges of the clay particles can adsorb polar pollutants, some anions and cations, from water. One main reaction mechanisms have been reported for the adsorption of fluoride ions process on montmorillonite. Ion exchange, which is mainly of electrostatic nature on the permanent positively charged sites by forming outer-sphere complex and other one is complexation on the edge sites by forming inner-sphere complex which is mainly of chemical nature.

5.14 Comparing the adsorption capacity of iron(III) oxide coated bentonite clay with other clay adsorbents

To assess how the fluoride adsorption capacity of iron(III) oxide coated bentonite clay compares with other bentonite clays, a number of studies were consulted and the results are listed in Table 5.13

Table 5.13: Comparison of different adsorption capacities of different clay adsorbents for fluoride

Adsorbent	Adsorption capacity	Experimental conditions	References
Fe(III) oxide bentonite	1.59 mg/g	pH 2, 80mg/L	Present study
Al^{3+} bentonite	5.7 mg/g	pH 2-12, 60 mg/L	Vhahangwele, et al. (2014)
Fe^{3+} bentonite	2.91 mg/g	pH 2, 60 mg/L	Gitari, et al. (2013)
Mg^{2+} bentonite	2.3 mg/g	pH 3-10, 5 mg/L	Thakre, et al. (2010)
La modified bentonite	1.5 mg/g	Neutral	Maiti, et al. (2011)
Bentonite	1.2 mg/g	pH 2.8, 5 mg /L	Srimurali et al. (1998)

UNIVERSITY OF VENDA
LIBRARY

© University of Venda

A comparison on fluoride sorption capacities as presented in Table 5.13 shows that modified bentonite clays present better fluoride removal capacities than raw bentonite clay. These clay minerals are very abundant in nature, and inexpensive when compared to other adsorbents. Clay minerals are physically or chemically modified with other materials to attain high fluoride adsorption capacities. When the fluoride adsorption capacities for clay minerals and the low cost adsorbents are compared, the clay minerals have been found to be better materials to use for adsorption purposes especially for rural people who cannot afford expensive water treatment technologies. There are however other various adsorbent other than clays that have very good adsorption capacities but because of the nature of their synthesis, there are quite expensive compared to locally available clays. For example, the highest adsorption capacity of modified double layered hydroxides of Mg–Al–CO_3 was recorded to be 303.54 mg/g (Batistella et al., 2011) and that of aluminum hydroxide impregnated with lime stone was recorded to be 84.03 mg/g (Jain and Jayaram, 2009) and these adsorption capacities are way above that of most clays. Chemical modifications of different materials have often been correlated with increase in the adsorption capacities, but the technological cost must be taken into consideration while checking in to a real low-cost adsorbent.

5.15 Conclusions and Recommendations

Based on the experimental data, the following conclusions can be drawn:

- The equilibrium adsorption is practically achieved in 30 min.
- Solution pH played a major role in fluoride removal by iron (III) oxide coated bentonite clay with an optimum pH being pH 2. High adsorption >70% was observed over the pH range 2-12 which is significant for application in defluoridation of groundwater whose pH is circumneutral Furthermore, the residual concentrations of metals in drinking water treated with iron(III) oxide coated bentonite clay at pH values, ranging from 6 to 9, were below the WHO standards.
- The sorption data fitted into Langmuir, Freundlich and Dubunin – Radushkevich isotherms but Dubunin – Radushkevich model had the best fit, implying that the adsorption process took place on a heterogeneous surface of the adsorbent.

© University of Venda

- The pseudo-second-order kinetic model could be used to describe the fluoride adsorption behaviours and both intra and external diffusion regulated the adsorption process.
- From the results, we can conclude that iron(III) oxide coated bentonite clay is a promising sorbent for defluoridation of water and further studies including its composites with locally available Mukondeni clays need to be evaluated.

It is also recommended that its performance be tested on a column study since it showed high removal capacity on batch studies.

© University of Venda

University of Venda
Creating Future Leaders

5.16 References

Alshameri, A., Yan, C., Al-Ani, Y., Dawood, A.S., Ibrahim, A., Zhou, C. and Wang, H., 2014. An investigation into the adsorption removal of ammonium by salt activated Chinese (Hulaodu) natural zeolite: Kinetics, isotherms, and thermodynamics. *Journal of the Taiwan Institute of Chemical Engineers*, 45, pp.554–564.

Appela, C., Lena Q., Ma, R. and Kennelley, D.R.E., 2003. Point of zero charge determination in soils and minerals via traditional methods and detection of electroacoustic mobility. *Geoderma*, 113, pp. 77– 93.

Arami, M., Limaee, N.Y. and Mahmoodi, N.M. 2008. Evaluation of the adsorption kinetics and equilibrium for the potential removal of acid dyes using a biosorbent. *Chem Eng J*, 139, pp. 2–10.

Batistella, L., Venquiaruto, L.D., Di Luccio, M., Oliveira, J.V., Pergher, S.B.C., Mazutti, M.A., de Oliveira, D., Mossi, A.J., Treichel, H. and Dallago, R., 2011. Evaluation of acid activation under the adsorption capacity of double layered hydroxides of Mg–Al–CO_3 type for fluoride removal from aqueous medium. *Ind. Eng. Chem. Res.* 50, pp. 6871–6876.

Cai, H., Chen, G., Peng, C., Zhang, Z., Dong, Y., Shang, G., Zhu, X., Gao H. and Wan. X., 2015. Removal of fluoride from drinking water using tea waste loaded withAl/Fe oxides: A novel, safe and efficient bio sorbent. *Applied Surface Science*, 328, pp. 34–44

Daifullah, A.A.M., Yakout, S.M. and Elreefy, S.A., 2007. Adsorption of fluoride in aqueous solutions using KMnO4-modified activated carbon derived from steam pyrolysis of rice straw. *Journal of Hazardous Materials*, 147, pp. 633–643.

Dai, J.C. and Huang, J.T., 1991. Surface modification of clays and clay rubber composite. *App.Clay Sci,* 15, pp. 51 – 65.

Day, F.H., 1963. *The chemical elements in nature*. Harrap p. 306. London, England.

Goldberg. S., 2005. Equations and Models Describing Adsorption Processes in Soils‘‘. Soil Science Society of America, 677 S. Segoe Road, Madison, WI 53711, USA. Chemical Processes in Soils. SSSA Book Series, no. 8.

Hauge, S., Österberg, R., Bjorvatn, K. and Selvig K., 1994.Defluoridation of drinking water with pottery: effect of firing temperature. *Scand. J. Dent. Res,* 102, pp. 329 – 333.

Ho, Y. S., Wase, D. A. J. and Forster, C. F., 1995. Batch Nickel removal from aqueous solution by Sphagnum moss peat. *Water Research*, 29 (5), pp. 1327–1332.

© University of Venda

University of Venda
Creating Future Leaders

Jain, S. and Jayaram, R.V., 2009. Removal of fluoride from contaminated drinking water using
unmodified and aluminium hydroxide impregnated blue lime stone waste. *Sep. Sci. Technol.* 44, pp. 1436–1451.

Kapoor, A and Viraraghavan,T., 1998. Use of immobilized bentonite in removal of heavy metals from wastewater, *J. Environ. Eng. ASCE,* 124, pp. 1020–1024.

Kau, P.M.H., Smith, D.W., and Binning, P., 1997. Fluoride detention by kaolin clay. *J. Contamin. Hydrol*, 28, pp. 267–288.

Liao, P., Ismael, Z.M., Zhang, W., Yuan, S., Tong, M and Wang, K., 2012 Adsorption of dyes from aqueous solutions by microwave modified bamboo charcoal. *Chem Eng J*, 195 pp. 339–346.

Liu, J., Li, W.Y., Liu, Y.G., Zeng, Q.H. and Hong, S. 2014. Titanium (IV) hydrate based on chitosan template for defluoridation from aqueous solution, *Appl. Surf. Sci.* 293, pp. 46–54.

Parks, G.A., 1965. The isoelectric points of solid oxides, solid hydroxides and aqueous hydroxy complex systems. *Chem. Rev*. 65, pp. 177-198.

Madejova, J. and Komadel, P., 2001. Baseline studies of the clay minerals society source clays: infrared methods. *Clays and Clay Minerals,* 49(5), pp. 410 – 432.

Maiti, A., Basu, J.K., De, S., 2011. Chemical treated laterite as promising fluoride adsorbent for aqueous system and kinetic modelling. *Desalination* 265, pp. 28–36.

Namasivayam, C; Yamuna, R T (1995). Adsorption of direct red 12B, biogas residual slurry: equilibrium and rate processes. *Environ Poll,* 89, pp. 1-7.

Onyango, M.S., Kojima, Y., Aoyi, O., Bernardo, E.C. and Matsuda, H., 2004. Adsorption equilibrium modeling and solution chemistry dependence of fluoride removal from water by trivalent-cation-exchanged zeolite F-9, J. *Colloid Interface Sci*. 279, pp. 341–350.

Qadeer, R., Hanif, J., Khan, M.and Salem, M., 1995. Uptake of uranium ions by molecular sieve, *Radiochim. Acta,* 68, pp. 197–201.

Ross, D.S. and Ketterings, Q., 2011. Recommended Methods for Determining Soil Cation Exchange Capacity Chapter 9. Cooperative Bulletin No. 493 Recommended Soil Testing Procedures for the Northeastern United States: 75 – 86.

Schwertmann, U. and Fechter, C., 1982. The point of zero charge of natural and synthetic ferrihydrites and its relation to adsorbed silicate. *Clay Minerals,* 17, pp. 471-476.

© University of Venda

Schwertmann, U. and Taylor R.M., 1977. Iron oxides. In: Minerals in Soil Environments. (J.B. Dixon and S.B. Weed, editors). *Soil Sci. Soc. Amer*. pp. 145-180.

Srimurali, M., Pragathi, A and Karthikeyan, J., 1998. A study on removal of fluorides from drinking water by adsorption onto low-cost materials. *Environ Pollut,* 99(2), pp. 285–289.

Sun, Y.B., Fang, Q.H., Dong, J.P., Cheng, X.W. and Xu, J.Q., 2011. Removal of fluoride from drinking water by natural stilbite zeolite modified with Fe (III), *Desalination*, pp. 277, pp. 121–127.

Sundaram, C.S, Viswanathan, N.and Meenakshi, S, 2009. Defluoridation of water using magnesia/chitosan composite. *J Hazard Mater*, 163, pp. 618–624.

Tamura, H.A. Mita, K., Tanaka, A and Ito, M., 200. Mechanism of hydroxylation of metal oxide surfaces. *J. Colloid Interface Sci*, 243, pp. 202–207.

Tchomgui-Kamga, E., Alonzo, V., Nanseu-Njiki, C.P., Audebrand, N., Ngameni, E. and Darchen, A., 2010. Preparation and characterization of charcoals that contain dispersedaluminum oxide as adsorbents for removal of fluoride from drinking water, *Carbon,* 48, pp. 333–343.

Thakre, D., Rayalua, S., Kawadea, R., Meshramb, S., Subrtc, J. and Labhsetwara, N., 2010. Magnesium incorporated bentonite clay for defluoridation of drinking water. *Journal of Hazardous Materials*, 180, pp. 122–130.

Tohidi, N. and Ramez, V., 1997. Preparation of Iron and Steel Burden, Tehran University, 577.

Tor, A., 2006. Removal of fluoride from an aqueous solution by using montmorillonite. *Desalination*, 201, pp. 267 – 276.

Vhahangwele, M., Mugera, G.W. and Tholiso, N., 2014. Defluoridation of drinking water using Al^{3+}-modified bentonite clay: optimization of fluoride adsorption conditions. *Toxicol. Environ. Chem*. 96, pp.1–16.

Voudrias, E., Fytianos, F. and. Bozani, E., 2002. Sorption Description isotherms of Dyes from aqueous solutions and Waste Waters with Different Sorbent materials, *Global Nest, The Int.J.* 4(1), pp. 75-83.

Wang, J., Xu, W., Chen, L., Jia, Y., Wang, L., Huang, X and Liu, J., 2013. Excellent fluoride removal performance by CeO2–ZrO2 nanocages in water environment. *Chemical Engineering Journal,* 231, pp. 198–205.

© University of Venda

University of Venda
Creating Future Leaders

Yao, Z.Y., Qi, J.H and Wang, L.H., 2010. Equilibrium, kinetic and thermodynamic studies on the biosorption of Cu(II) onto chestnut shell, *J. Hazard. Mater,* 174 pp. 137– 143.

© University of Venda

University of Venda
Creating Future Leaders

CHAPTER 6

FABRICATION OF IRON(III) OXIDE COATED BENTONITE CLAY - SILICA RICH REDDISH BLACK MUKONDENI CLAY SOILS CERAMIC COMPOSITE PELLETS AND THEIR PERFORMANCE IN GROUNDWATER DEFLUORIDATION

ABSTRACT

A novel iron(III) oxide coated bentonite – silica rich reddish black Mukondeni clay soil composite ceramic pellet adsorbent was synthesized for efficient treatment of fluoride in aqueous solutions. X Ray Diffraction studies showed that the adsorbent was of a crystalline nature and Transmission Electron Microscopic studies showed that the composite is composed of aggregated small particles with different sizes. To establish parameters effective for the fabrication of ceramic pellets for fluoride adsorption, fabrication conditions were optimised. These included, particle size, furnace temperature, firing time and clay ratios. From the fluoride removal experiments, it was observed that the optimum conditions for fabricating the pellets for fluoride removal were 250 µm particle size, 600°C furnace temperature,1 h firing time and 5:1 (iron(III) oxide coated bentonite: silica rich reddish black Mukondeni clay soil) clay ratios. The results of the adsorption tests demonstrated that the defluoridation capacity of the adsorbent decreased with increasing sintering temperature. The optimum adsorption capacity was found to be 0.03 mg/g with 10 mg/L initial fluoride concentration and 2 g of the adsorbent at pH 6.8. The adsorption capacities of the ceramic pellets also increased with increasing iron(III) oxide coated bentonite clay volume fraction. The potential implications of the results are important in the development of future point-of-use water filtration devices for the removal of fluoride from water using these two clays.

Keywords: Composite, ceramic pellets, fabrication, iron(III) oxide coated bentonite, silica rich reddish black Mukondeni clay soils and defluoridation.

© University of Venda

University of Venda
Creating Future Leaders

6.0 Introduction

A simple method to fabricate a compatible ceramic composite from silica rich reddish black Mukondeni clay soils and iron(III) oxide coated bentonite clay was developed. Clay composites have been found to be good in fluoride removal and heating clays was also observed to increase the adsorption capacity of clays. Adsorbent composites usually have combined advantages of their components when used for water treatment (Tran, et al., 2013). Chapter 4 and 5 of this work showed the performance of silica rich reddish black Mukondeni clay soils and iron(III) oxide coated bentonite clay on fluoride removal independently. This chapter seeks to fabricate a composite adsorbent from the two clays, in a bid to increase the stability of the adsorbents by heating in the furnace to make ceramic pellets. Hence the main objectives of this chapter are to present results on

(i) optimisation of parameters for the production of ceramic composite pellets

(ii) fabrication of the ceramic composite pellets out of the optimised parameters

(iii) evaluation of the performance of these pellets in water defluoridation.

6.1 Materials and methods

Both silica rich reddish black Mukondeni clay soils and iron(III) oxide coated bentonite clay were prepared according to method given in previous Chapters 4 and 5 respectively. The two clays were mixed by MilliQ water (resistivity 18.2MΩcm at room temperature) to prepare the ceramic composite pellets based on simple manual moulding method. The detailed procedure of fabricating the ceramic composite pellets was given in Chapter 3, section 3, page 46 – 63.

6.2 Results and discussions

6.2.1 Optimisation of particle size

From the pellets fabricated out of 125, 250 and 500 µm particles of both silica rich reddish black Mukondeni clay soils – iron(III) oxide coated bentonite clay, the 250 µm particle sized pellets produced minimum cracks and therefore this particle size was selected as the best for further optimisation experiments.

6.2.2 Optimisation of furnace temperature

It has been well known for many years that the different types of clay minerals exhibit characteristic behaviour on heating. Earlier work consisted for the most part, of correlating

© University of Venda

the amounts of water lost on ignition with the temperature, of determining the thermal energy associated with the dehydration, and of identifying the products formed at high temperatures (Warsha, 1960). Firing clays causes the aggregates to have a rough and microscopic porous surface with an increased surface area. High temperatures can also change the lattice structure of various minerals in the clays. Since firing clays alters the clay materials physicochemically and minerologically, it becomes imperative that these characteristics be analysed to determine which ones can help improve the adsorption capacity of the clay materials. Thus at different optimisation stages in the preparation of the ceramic pellets, various analytical techniques were used to determine how firing influences the clay minerals with respect to adsorption.

6.2.2.1 X-ray Diffraction analysis

Figure 6.1 shows images of iron(III) oxide coated bentonite – silica rich reddish black Mukondeni clay soil composite pellets before and after calcination at (a)100, (b)600, (c)700 and (d)800^{o}C.

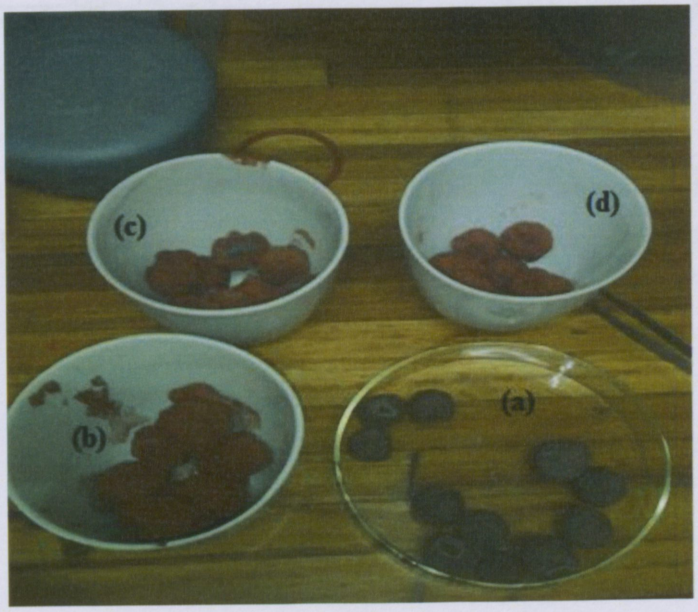


Figure 6.1: Iron oxide(III) coated bentonite – silica rich reddish black Mukondeni clay soil composite pellets before (a) and after calcination (b,c,d)

© University of Venda

The prepared iron(III) oxide coated –silica rich reddish black Mukondeni clay soil composite pellets are grayish in colour (a) before calcination but after calcination the ceramic adsorbents were reddish brown in colour (shown in Figure 6.1 (b,c,d)). The reddish brown-coloured particles is an indication of the presence of iron oxides.

Figure 6. 2 shows XRD diffractograms of iron(III) oxide coated bentonite – silica rich reddish black Mukondeni clay soil composite pellets at 100, 600, 700, 800 and 900°C

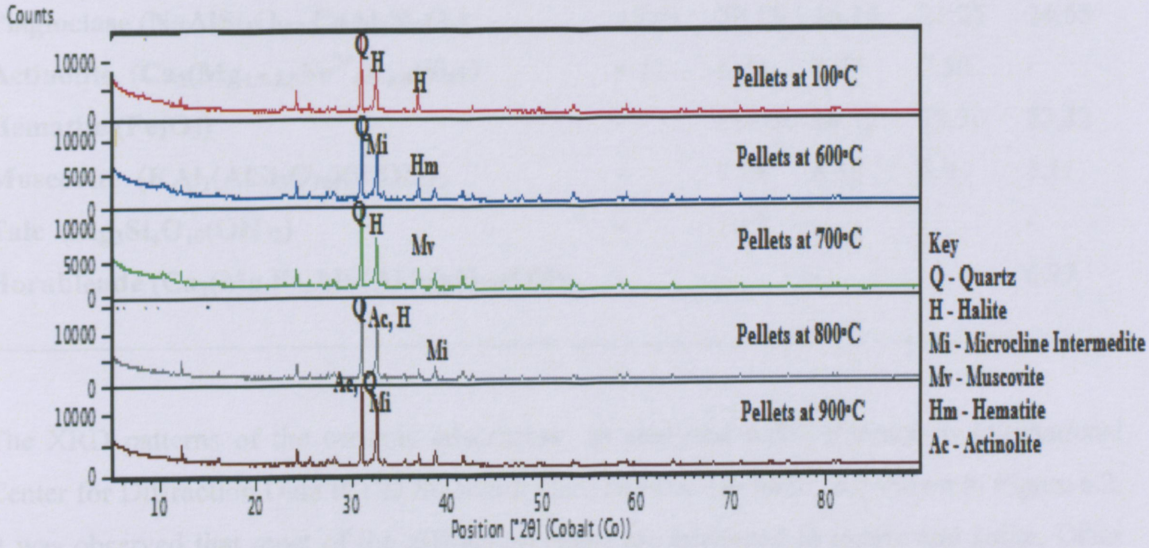


Figure 6.2: XRD diffractogram of iron(III) oxide coated bentonite – silica rich reddish black Mukondeni clay soil composite pellets at 100, 600, 700, 800 and 900°C

© University of Venda

University of Venda
Creating Future Leaders

Table 6.1: Percentage weight of minerals in iron(III) oxide coated bentonite –silica rich reddish black Mukondeni clay soil composite pellets at different calcination temperatures

Mineral (w/w %) / T°C	100	600	700	800	900
Quartz (SiO_2)	27.2	25.37	30.91	31.14	31.14
Halite (NaCl)	9.62	10.11	10.36	6.82	7.53
Microcline ($KAlSi_3O_8$)	3.82	3.32	5.31	8.1	4.95
Plagioclase ($NaAlSi_3O_8$– $CaAl_2Si_2O_8$)	15.01	20.55	16.15	21.25	24.55
Actinolite ($Ca_2(Mg_{4.5\text{-}2.5}Fe^{2+}_{0.5\text{-}2.5})Si_8O$	4.11	6.44	8.77	7.53	-
Hematite (Fe_2O_3)	-	16.63	20.15	19.36	23.32
Muscovite ($KAl_2(AlSi_3O_{10})(F,OH)_2$	-	7.48	8.35	5.9	3.11
Talc ($Mg_3Si_4O_{10}(OH)_2$)	-	10.1	-	-	-
Hornblende ($Ca_2(Mg,Fe,Al)_5(Al,Si)_8O_{22}(OH)_2$	-	-	-	-	6.37

The XRD patterns of the ceramic adsorbents as analyzed with reference to International Center for Diffraction Data ICDD Standard; Card number 36- 0426 are shown in Figure 6.2. It was observed that most of the diffraction peaks are attributed to quartz and halite. Other small peaks are attributed to crystalline iron oxide such as hematite and muscovite. These results are also corroborated by quantitative XRD results shown in Table 6.1 wherein a large percentage weight is attributed to quartz, plagioclase and hematite. The peaks of hematite are due to the ceramic pellets containing iron(III) oxide coated bentonite. Table 6.1 also shows that there was no substantial change in the mineralogical composition with increase in temperature though at 600°C there is a notable addition of microcline intermediate and hematite. Hematite is the mineral form of iron(III) oxide and microcline ($KAlSi_3O_8$) typically contains minor amounts of sodium.

UNIVERSITY OF VENDA
LIBRARY

© University of Venda

6.2.2.2 Scanning Electron Microscopy (SEM) – SEM coupled with Energy Dispersive Spectroscopy analysis

Morphological aspects of the iron(III) oxide coated bentonite – silica rich reddish black Mukondeni clay soil composite pellets are outlined in Figure 6.3 at different calcination temperatures (100, 600 and 800°C)

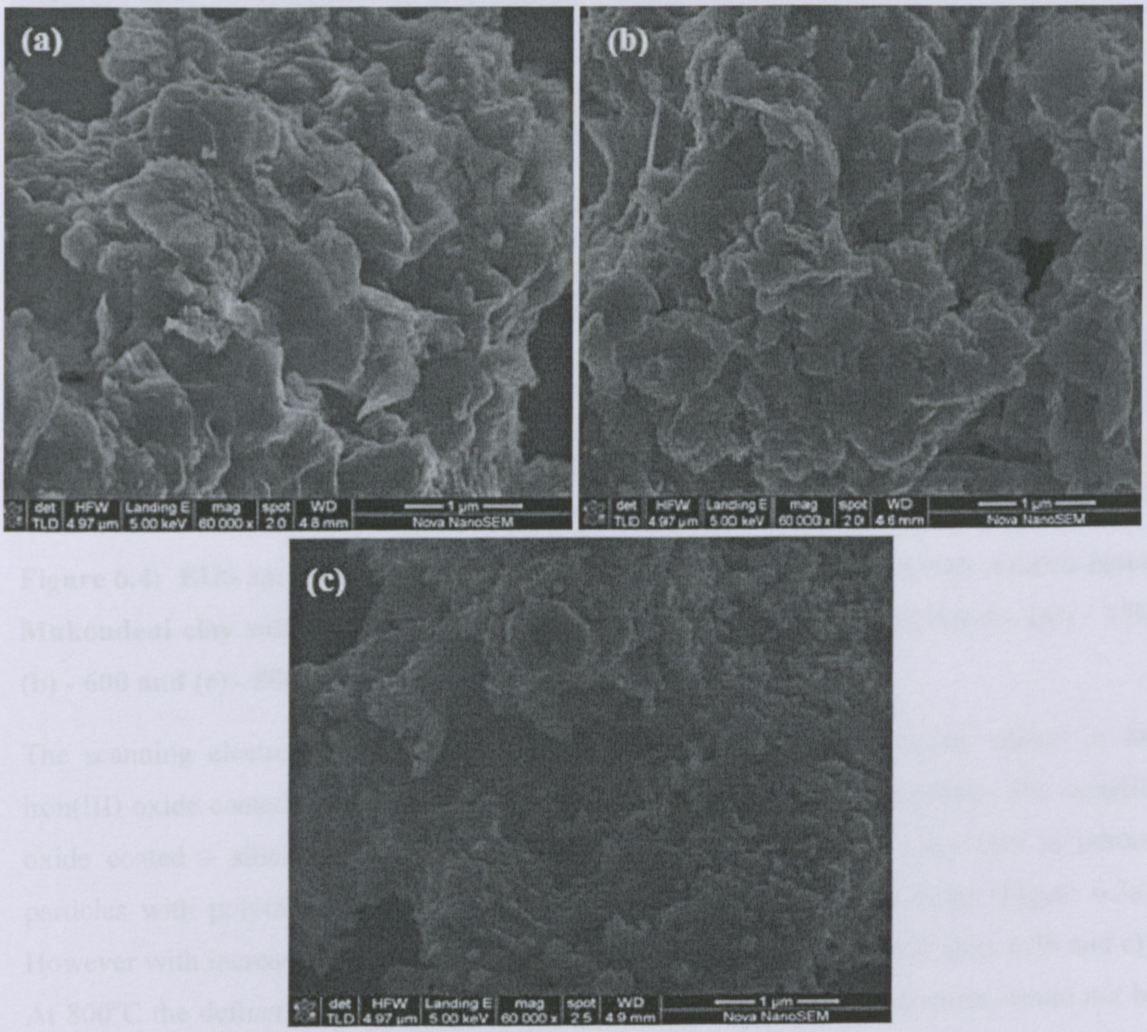


Figure 6.3: SEM micrographs of iron(III) oxide coated bentonite – silica rich reddish black Mukondeni clay soil composite pellets at different calcination temperatures ((a) - 100, (b) - 600 and (c) - 800°C)

© University of Venda

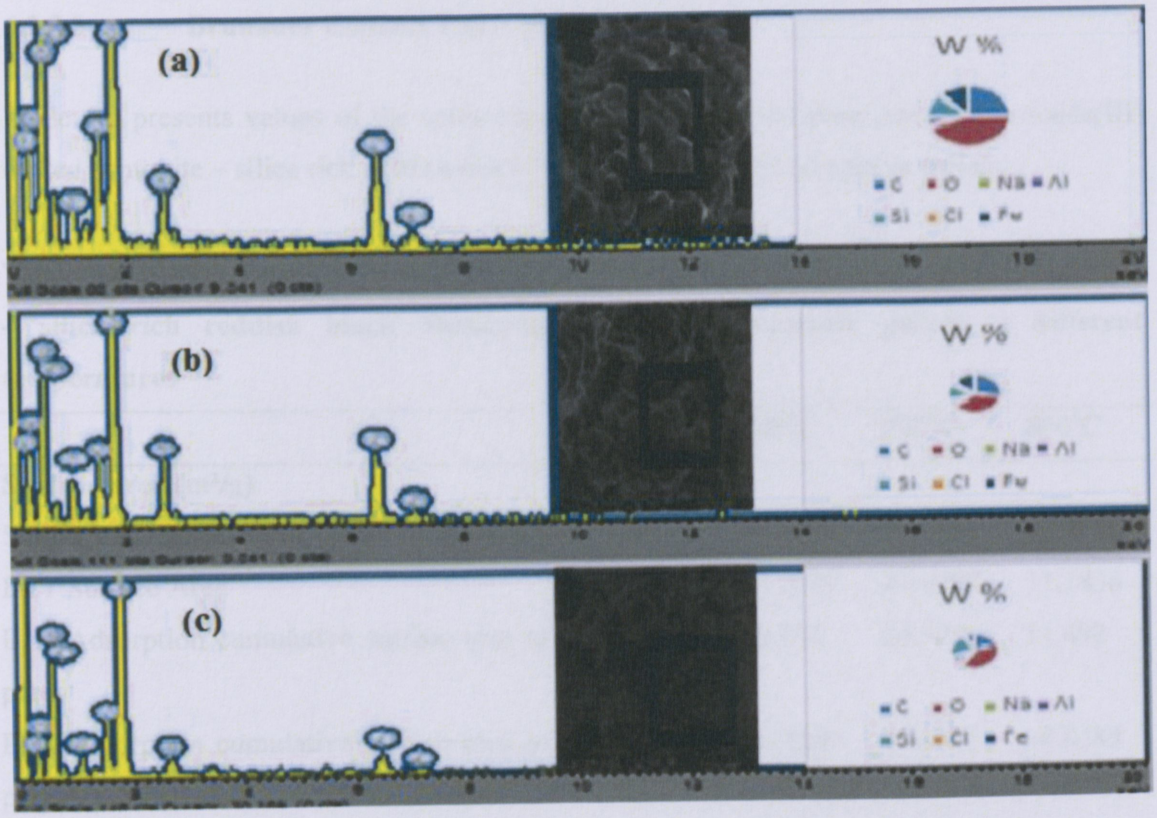


Figure 6.4: EDS spectrum of iron(III) oxide coated bentonite – silica rich reddish black Mukondeni clay soil composite pellets at different calcination temperatures ((a) - 100, (b) - 600 and (c) - 800°C)

The scanning electron micrographs on Figure 6.3 show typical irregular shapes of the iron(III) oxide coated – silica rich reddish black Mukondeni clay soil particles. The iron(III) oxide coated – silica rich reddish black Mukondeni clay soil pellets are rich in porous particles with polytonous morphology and also of angular-shaped particles (Figure 6.3a). However with increase in temperature that morphology is gradually lost (Figure 6.3b and c)). At 800°C the defined shapes are totally lost and therefore higher temperatures would not be suitable for calcination temperatures because the porous nature of the adsorbent material is lost and this means the adsorption capacity of the material would be reduced.

The SEM-EDS analysis for iron(III) oxide coated bentonite – silica rich black reddish Mukondeni clay soil composite pellets sample was determined and is presented in Figure 6.4. Figure 6.4 indicated the presence of C, O, Fe, Al, Si, and Na in the surface of adsorbent. The significant peaks due to Fe can be attributed to the impregnation process with $FeCl_3$ salt solutions during bentonite modification.

© University of Venda

University of Venda
Creating Future Leaders

6.2.2.3 Brunauer Emmett Teller (BET) analysis

Table 6.2 presents values of the surface area, pore volume and pore size of iron oxide(III) coated bentonite – silica rich reddish black Mukondeni clay soil composite pellets.

Table 6.2: Surface area, pore volume and pore sizes for iron(III) oxide coated bentonite – silica rich reddish black Mukondeni clay soil composite pellets at different temperatures

	100°C	600°C	700°C	800°C
Surface area (m^2/g)				
Single point surface area	174.8883	67.4040	20.9545	10.7040
BET Surface Area	181.4154	70.0027	21.6908	11.1836
BJH Adsorption cumulative surface area of pores	0.250779	79.964	24.321	11.492
BJH Desorption cumulative surface area of pores	0.255407	95.7350	28.6141	10.6389
Pore Volume (cm^3/g)				
Single point adsorption total pore volume of pores	0.247116	0.254653	0.102287	0.037817
BJH Adsorption cumulative volume of pores	0.250779	0.263065	0.104873	0.036650
BJH Desorption cumulative volume of pores	0.255407	0.294424	0.120568	0.039979
Pore Size (Å)				
Adsorption average pore width (4V/A by BET)	54.4863	145.5103	188.6275	135.2590
BJH Adsorption average pore diameter (4V/A)	57.106	131.592	172.484	127.569
BJH Desorption average pore diameter (4V/A)	58.596	123.016	168.543	150.313

The BET surface area of the iron(III) oxide coated bentonite – silica rich reddish black Mukondeni clay soil composite pellets was observed to be 174.8883 m^2/g when the pellets where dried in the oven at 100°C. As shown in Table 6.2, increasing temperatures by firing in

© University of Venda

the furnace substantially changed the surface area. The BET surface area of the iron(III) oxide coated –silica rich reddish black Mukondeni clay soil composite pellets at 800°C was less than that at 100°C and it decreased by a factor of ≈ 16. The reduction trend with temperature is also shown with pore volume. The BJH Adsorption cumulative volume of pores decreased from 0.250779 to 0.036650 (cm^3/g). However a different trend is shown by pore size. As the firing temperatures are increased, the pore sizes of the pellets are increased although very high temperatures of 800°C decreases the pore size. Since calcination at higher temperatures reduces the surface area and adsorption mainly depends on surface area i.e. the higher the surface area, the higher the adsorption rate, 600°C was then adopted as the optimum temperature for fabricating the pellets.

6.2.2.4 Fluoride adsorption experiments

Table 6.3 shows the performance of the ceramic composite when used for fluoride removal on synthetic fluoride water.

Table 6.3: Adsorption performance of iron(III) oxide coated bentonite – silica rich reddish black Mukondeni clay soil composite pellets at different temperatures.

Parameter	Initial	(600°C)	(700°C)	(800°C	(900°C)	DWA guidelines
pH	6.02	6.44	6.79	6.68	6.64	6 – 9
TDS (mg/L)	18.6	121.53	114.22	113.74	112.34	0 – 500
EC (µS/cm)	12.42	111.27	111.36	110.43	111.87	0 – 150
F^- (mg/L)	10	7.12	7.34	8.26	8.34	1 – 1.5
% F removal	-	40.45	36.24	21.06	19.91	-

From Table 6.3, it can be observed that as the firing temperature is increased from 600 to 900°C, the percentage fluoride removal capacity decreases by a factor of 2.03. This decrease in the adsorption capacity can be due to the decrease in surface area of the adsorbent as shown in Table 6.2 that higher temperatures substantially decreases the surface area and since

© University of Venda

surface area plays a critical role in the adsorption process, a lower surface area will lead to poor adsorption. From the results, 600°C showed higher percentage fluoride capacity and hence it was taken as the optimum firing temperature. These results confirm that higher temperatures reduce clay's adsorption capacity by reducing its surface area for adsorption. Heating above 600°C appears to result in a progressive loss of sorption capacity. Besides surface area reduction, perhaps the low sorption capacity is also due to dehydration of some of the hydrous Fe(III) oxide phases that may be responsible for the clay 's F^- removal properties.

6.2.3 Optimization of firing time

Section 6.2 consisted of work correlating the effect of furnace temperatures with the change in physicochemical characteristics of the clay soils, to check how different temperatures will affect the adsorption capacity of the clay. The duration in which the clays stay in the furnace is also critical in fabricating ceramic pellets for adsorption processes. The effective time period in the furnace varies between types of clay. Thus, tests should be conducted to find the effective time period for each clay to be used in manufacturing.

6.2.3.1 SEM – EDS analysis

The morphology and SEM-EDS of the iron(III) oxide coated bentonite – silica rich reddish black Mukondeni clay soil composite pellets at different firing times is shown in Figure 6.5 and 6.6 respectively.

© University of Venda

University of Venda
Creating Future Leaders

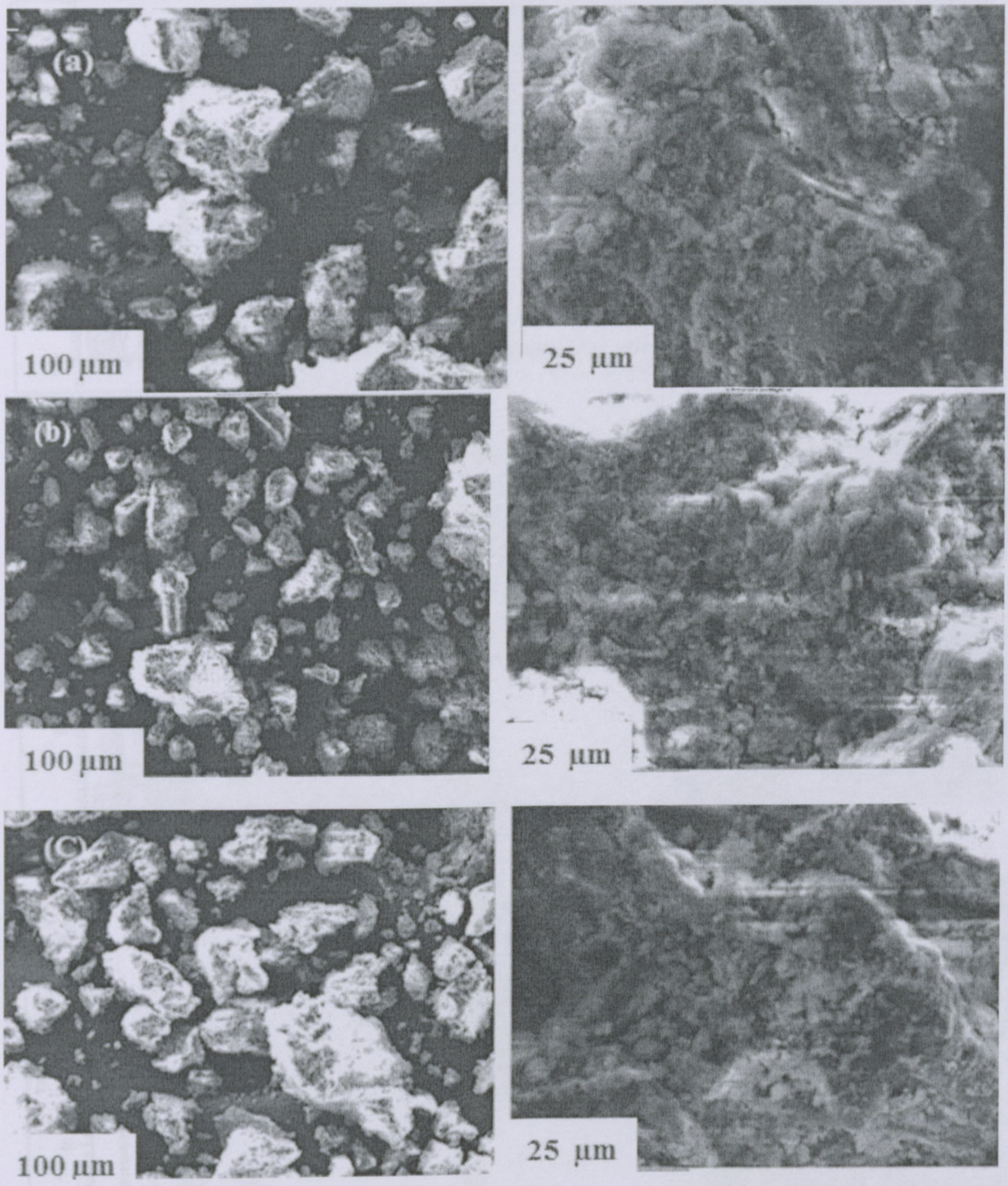


Figure 6.5: Morphology of iron(III) oxide coated bentonite – silica rich reddish black Mukondeni clay soil composite pellets at two magnifications and different firing times ((a) – 1 h, (b) – 2 h and (b) - 3 h)

© University of Venda

University of Venda
Creating Future Leaders

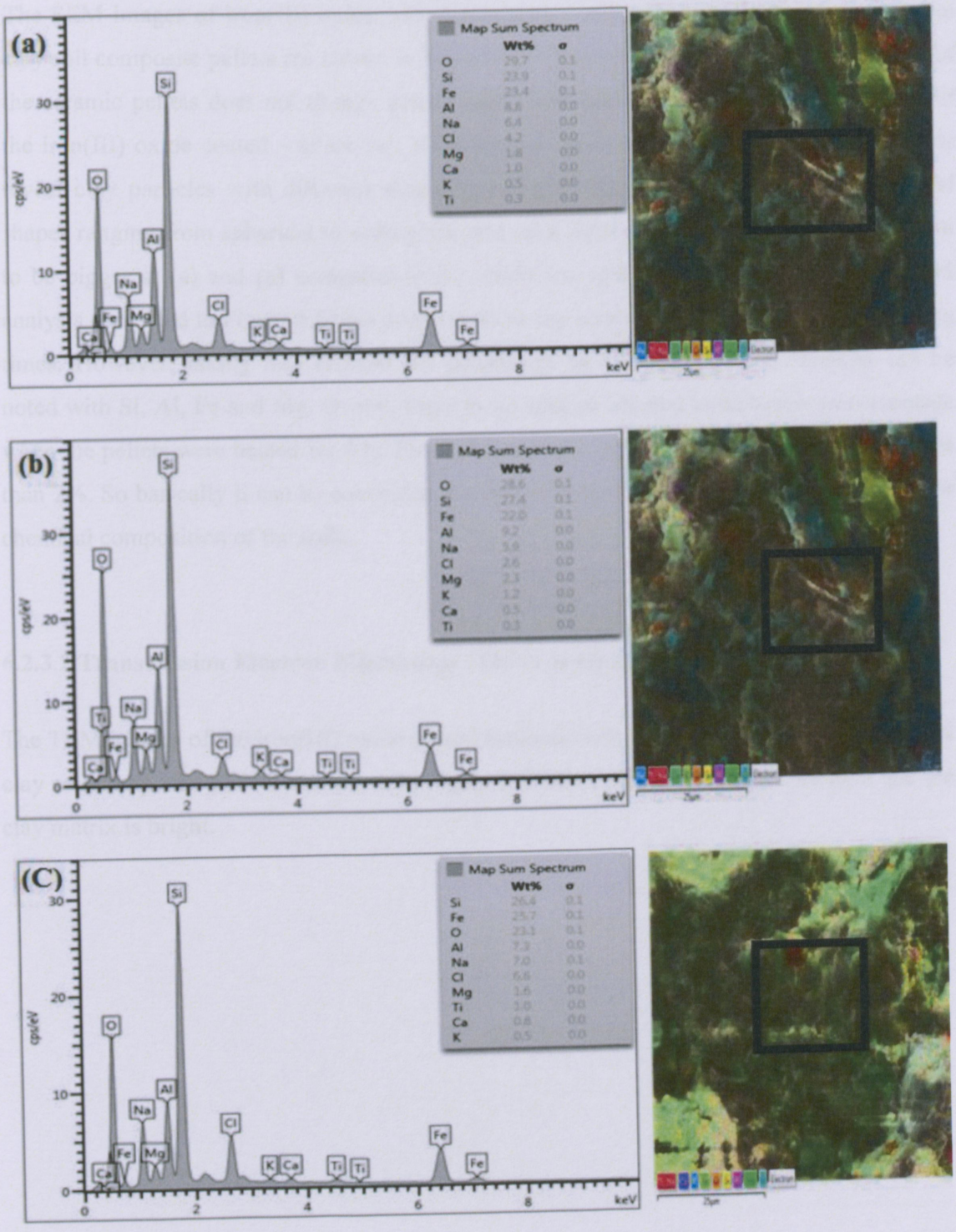


Figure 6.6: SEM - EDS of iron(III) oxide coated bentonite – silica rich reddish black Mukondeni clay soil composite pellets at different firing times ((a) – 1 h, (b) – 2 h and (b) - 3 h)

UNIVERSITY OF VENDA
LIBRARY

© University of Venda

University of Venda
Creating Future Leaders

The SEM images of iron(III) oxide coated bentonite – silica rich reddish black Mukondeni clay soil composite pellets are shown in Figure 6.5. The images show that the morphology of the ceramic pellets does not change considerably with different firing times. The images of the iron(III) oxide coated – silica rich reddish black Mukondeni clay soil composite pellets reveal clay particles with different shapes and sizes. The pellets have defined polygonal shapes ranging from spherical to pentagonal and octahedral shapes. The sizes however seem to be bigger at (a) and (c) compared to (b) which has smaller particles. The SEM – EDS analysis presented in Figure 6.6 also does not show any notable variation between the 3 firing times. However, taking into account the percentage by weight, minor differences can be noted with Si, Al, Fe and Mg. Overal, these metal species seemed to be higher in percentage when the pellets were heated for 2 h. The differences are very minor because they are all less than 2%. So basically it can be concluded that the 3 firing times did not alter the structure or chemical composition of the soils.

6.2.3.2 Transmission Electron Microscopy (TEM) analysis

The TEM images of the iron(III) oxide coated bentonite silica rich reddish black Mukondeni clay soil composite pellets are shown in Figure 6.7 where the clay particles are dark and the clay matrix is bright.

© University of Venda

University of Venda
Creating Future Leaders

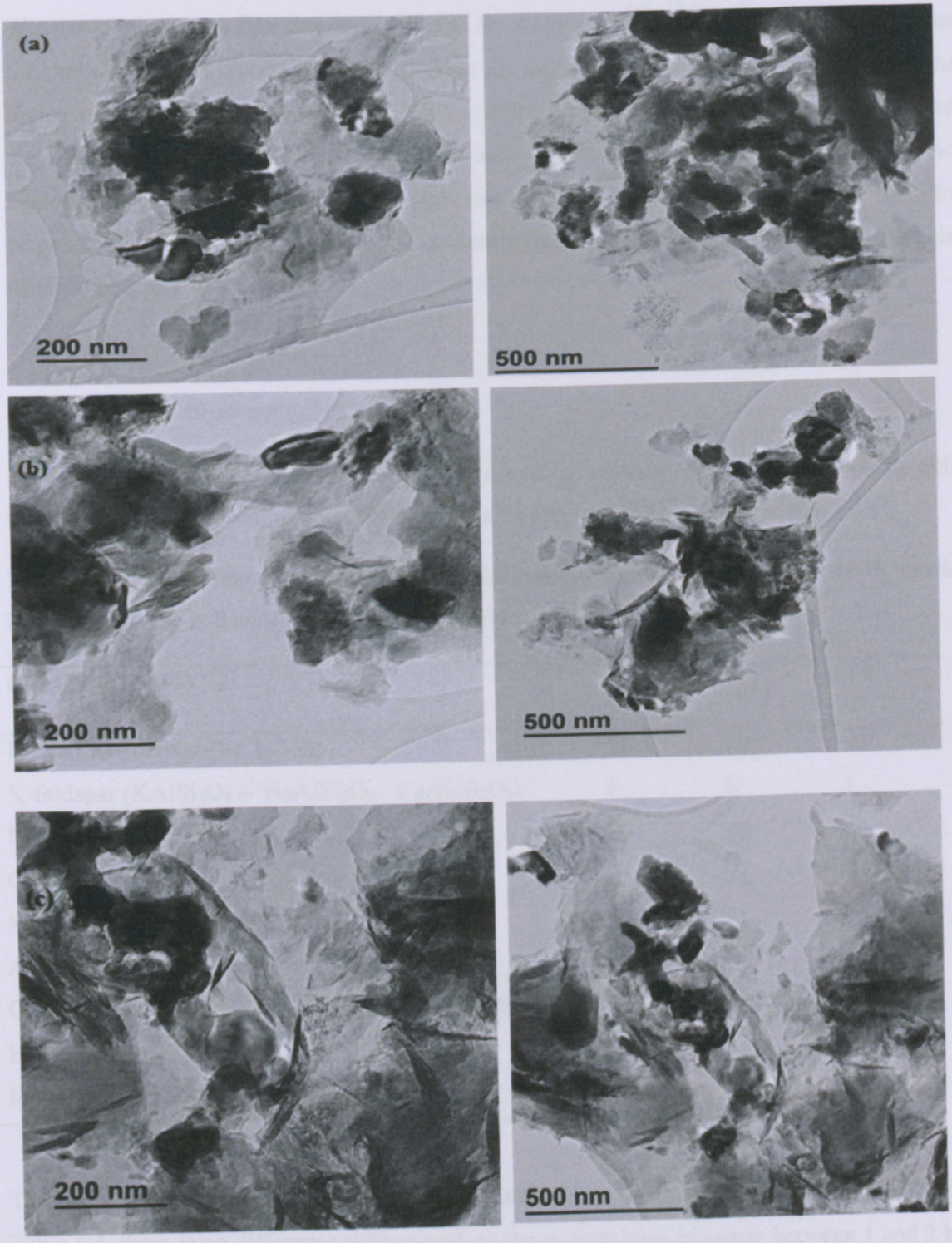


Figure. 6.7: TEM image of iron(III) oxide coated bentonite – silica rich reddish black Mukondeni clay soil composite pellets at two magnifications and different firing times ((a) – 1 h, (b) – 2 h and (b) - 3 h)

© University of Venda

The particles are very fine and were found to be < 100 nm. It is evident from the images that the particles are highly crystalline and some are agglomerated at lower magnifications. At higher magnification, Figure 6.7 (a) shows a TEM micrograph of stacked clay layers. The clay particles are rather well dispersed and distributed. Individual clay layers and agglomerates consisting of three or more stacked layers are observed in Figure 6.7 (b) whereas in Figure 6.7 (c), the layers are uniformly spaced with an observed average interlayer distance of 2 nm.

6.2.3.3 X Ray Diffraction (XRD) analysis

The percentage composition of minerals in the iron(III) oxide coated bentonite – silica rich reddish black Mukondeni clay soil composite pellets in is presented in Table 6.4

Table 6.4: Mineralogical composition iron(III) oxide coated silica rich reddish black Mukondeni clay soil composite pellets at different times

SAMPLE (W %)	1 h	2 h	3 h
Hematite/ Goethite (FeO(OH))	18	20	18
K-feldspar ($KAlSi_3O_8$ – $NaAlSi_3O_8$ - $CaAl_2Si_2O_8$)	1	6	1
Plagioclase ($NaAlSi_3O_8$– $CaAl_2Si_2O_8$)	23	20	24
Quartz (SiO_2)	29	29	34
Mica AB – 2-3 (X, Si)4O10(O, F, OH)2	6	6	6
Amphibole (SiO_4)	9	3	4
Clinoptilolite (Na,K,Ca)2-3Al_3(Al,Si)2Si_{13}O. 12H2O	3	7	5
Halite (NaCl)	7	6	6
I/S Interstratification	4	5	4

The major mineral found in the two clay soils forming the ceramic composite is quartz. From Table 6.4, there is no difference with regards to the composition of quartz between 1 and 2 h but its composition increased slightly by 0.14% at 3 h. Other minerals of the silicate family like quartz identified were feldspar (group of minerals distinguished by the presence of alumina and silica (SiO_2) in their chemistry), plagioclase (silicate framework), mica (phyllosilicate), amphibole (dark-colored, inosilicate) and clinoptilolite (natural zeolite). The

© University of Venda

presence of these minerals shows that the clay composite is highly crystalline because silicate minerals are generally crystalline and some of them like mica have a tendency towards pseudohexagonal crystals. Besides these silicate minerals, there is also goethite (FeO(OH)), an iron bearing hydroxide mineral which can highly enhance the fluoride removal capacity of the clay pellets. Again the composition did not vary considerably with different firing temperatures. Halite the mineral form of NaCl was also detected and it also has a tendency to form isometric crystals. Statistical analysis by One-way Analysis of Variance (ANOVA) showed that variation among column averages is significantly greater than expected by chance. Further analysis by Bartlett's test suggests that the differences among the standard deviations are not significant. On that basis the firing times did not have a notable impact on the clay soils and thus 1 h can be used as the optimum firing time.

6.2.3.4 X-ray Fluorescence (XRF) analysis

The percentage composition of major elements given as metal oxides in iron(III) oxide coated bentonite – silica rich reddish black Mukondeni clay soil composite pellets is presented in Table 6.5.

© University of Venda

Table 6.5: Elemental composition of iron(III) oxide coated – silica rich reddish black Mukondeni clay soil composite pellets at different firing times

Sample	1 h	2 h	3 h
SiO_2	54.72	54.78	54.76
TiO_2	0.49	0.49	0.49
Al_2O_3	12.87	12.96	12.91
Fe_2O_3	16.45	16.66	16.67
MnO	0.081	0.082	0.082
MgO	2.64	2.59	2.65
CaO	1.64	1.64	1.64
Na_2O	5.65	5.67	5.66
K_2O	1.07	1.12	1.14
P_2O_5	0.030	0.028	0.029
Cr_2O_3	0.058	0.058	0.060
LOI	3.36	2.99	3.03
Total	99.05	99.07	99.10

As can be seen from Table 6.5 the difference in elemental composition was not major enough to be considered as a notable variation. All the metal oxides did not increase or decrease by over 1% at all firing times hence 1 h of firing time can still be used as the optimum firing time.

6.2.3.5 Branuer Emmett Teller (BET) analysis

Table 6.6 gives the surface area, pore volume and pore size for iron(III) oxide coated bentonite – silica rich reddish black Mukondeni clay soil composite pellets.

© University of Venda

University of Venda
Creating Future Leaders

Table 6.6: Surface area, pore volume and pore sizes for iron(III) oxide coated bentonite – silica rich reddish black Mukondeni clay soil composite pellets at different temperatures

	1 h	2 h	3 h
Surface area (m^2/g)			
Single point surface area	16.4828	15.1817	16.2468
BET Surface Area	16.8741	15.5784	16.6521
BJH Adsorption cumulative surface area of pores	15.655	15.257	16.245
BJH Desorption cumulative surface area of pores	23.7305	21.9098	24.0498
Pore Volume (cm^3/g)			
Single point adsorption total pore volume of pores	0.063804	0.061239	0.072138
BJH Adsorption cumulative volume of pores	0.073067	0.070720	0.081151
BJH Desorption cumulative volume of pores	0.079739	0.076082	0.086606
Pore Size (nm)			
Adsorption average pore width (4V/A by BET)	15.12479	15.72402	17.32834
BJH Adsorption average pore diameter (4V/A)	16.6691	18.5411	19.9822
BJH Desorption average pore diameter (4V/A)	13.4407	13.8901	14.4044

Table 6.6 shows that the surface area and pore volume of the iron(III) oxide coated – silica rich reddish black Mukondeni clay soil composite pellets decreased slightly when the clay pellets where heated for 2 h when compared to 1 h and 3 h. Firing for 3 h however gave the widest pore diameter when compared to the others. Again, varying firing temperatures did not considerably affect the surface areas.

6.2.3.6 FTIR analysis

The FTIR spectra of for iron(III) oxide coated – silica rich reddish black Mukondeni clay soil composite pellets is shown in Figure 6.8.

© University of Venda

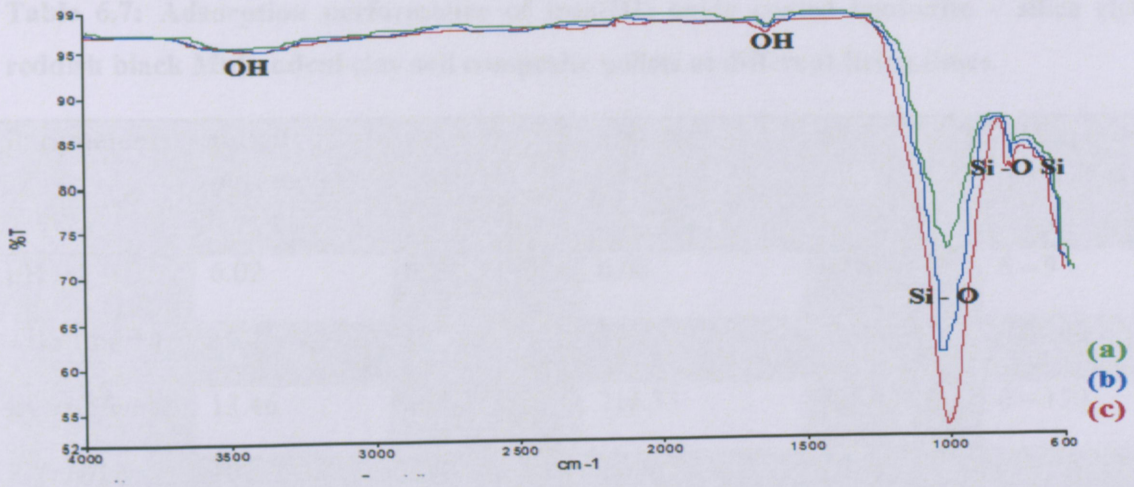


Figure 6.8: The FTIR spectra of iron(III) oxide coated – silica rich reddish black Mukondeni clay soil composite pellets at different firing times ((a) – 1 h, (b) – 2 h and (b) - 3 h)

The FTIR spectrum shows absorption bands at 3500. 1550, 1000 and 700 cm^{-1}. With all other absorption bands besides 1000 cm^{-1}, there is no major variation. At 1000 cm^{-1} though, the peaks vary by a difference of 10 % each. It can be noted that % transmission decreased from 70 to 60 to 52 as the temperature increased from 1 h to 3 h meaning that , the more time the clay material was being heated in the furnace, the more the Si-O compounds were lost by evaporation. Hence, a longer period of time in the oven evaporated some functional groups of the clay materials and therefore cannot be used for firing leaving 1 h being the best firing time.

6.2.3.7 Fluoride adsorption experiments

Table 6.7 shows the performance of the ceramic pellets when used for fluoride removal on synthetic fluoride water.

© University of Venda

Table 6.7: Adsorption performance of iron(III) oxide coated bentonite – silica rich reddish black Mukondeni clay soil composite pellets at different firing times.

Parameter	Initial parameters	1 h	2 h	3 h	DWA guidelines
pH	6.02	6.34	6.66	6.86	6 – 9
TDS (mg/L)	16.4	138.53	273	294.34	0 – 500
EC (µS/cm)	13.46	109.27	216.33	225.87	0 – 150
F^- (mg/L)	10	7.20	7.18	7.14	1 – 1.5
% F removal	-	38.89	39.28	40.06	-

From Table 6.7 the percentage fluoride removal capacity increase by a factor of 0.01 from 1 h to 2 h and by a factor of 0.03 from 1 h to 3 h firing time. The degree of variation of the fluoride removal capacities is generally low across the 3 firing times. However 3 h of firing time showed the highest fluoride capacity compared to the other firing times. Table 6.6 shows that at 3 h, the ceramic pellets had an adsorption average pore width of 17.32834 nm which is slightly higher compared to the other 2 firing times. This might be the possible explanation of the increased fluoride removal capacity observed at 3 h nonetheless statistical analysis by ANOVA showed that the significant variation is by chance hence 1 h was adopted as the optimum firing time to fabricate the iron(III) oxide coated bentonite – silica rich black reddish Mukondeni clay soil ceramic pellets.

6.2.4 Optimization of clay ratios

The performance of the iron(III) oxide coated bentonite – silica rich reddish black Mukondeni clay soil composite pellets was tested on fluoride synthetic water using different clay ratios to make the ceramic pellets. The results are presented in Table 6.8.

© University of Venda

University of Venda
Creating Future Leaders

Table 6.8: Adsorption performance of iron(III) oxide coated bentonite silica rich reddish black Mukondeni clay soil composite pellets at different clay ratios.

Parameter	Initial	1:1	1:2	2:1	3:1	4:1	5:1	6:1	DWS guidelines
pH	6.02	6.34	6.66	6.86	6.47	6.49	6.61	6.78	6 – 9
TDS (mg/L)	16.4	138.5	273.0	294.3	301.2	332.6	345.3	348	0 – 500
EC (µS/cm)	13.4	109.2	216.3	225.8	264	278	294	306	0 – 150
F^- (mg/L)	10	7. 15	7.23	7.03	6.87	6.45	6.41	6.38	1 – 1.5
% F removal	-	39.86	38.31	42.23	45.5	55.0	56.0	56.7	-

As can be seen from Table 6.8 the fluoride removal efficiency of the clay pellets was poor. The mean percentage removal across all clay ratios was 41.64%. It is also observed that, as the iron(III) oxide coated bentonite clay is increased the equilibrium fluoride concentration is reduced, though the difference between the 5:1 and 6:1 ratio is very small. This means that, increasing the amount of iron(III) oxide coated bentonite clay enhances the fluoride removal ability of the ceramic pellets. Statistical analysis by ANOVA showed that there is a significant difference across all clay ratios, though the variation among means is significantly greater than expected by chance. Further analysis of the variation between one clay ratio and the next by Tukey-Kramer Multiple Comparisons Test showed that there is a significant variation between all the ratios but 5:1 and 6:1. Since the difference between the last 2 ratios is negligible, it would be more cost effective to use the 5:1 ratio than the 6:1 ratio and on that basis 5:1 clay ratio was taken as the optimum ratio for preparing the ceramic composite pellets.



© University of Venda

University of Venda
Creating Future Leaders

6.3 Conclusions

In the process of synthesising the composite ceramic pellets, 4 parameters were optimised for efficient fluoride removal from water and these were: clay particle size, furnace temperature, firing time and clay ratios. On the basis of different analytical techniques and the fluoride removal capacities, it was concluded that the optimum conditions for fabricating the composite ceramic pellets were 250 µm particle size, 600°C furnace temperature, 1 h firing time and 5:1 (iron oxide(III) coated bentonite clay: silica rich reddish black Mukondeni clay soils). However, the fluoride removal of the clay pellets was found to be low compared to that of the clay soils used independently. For that reason, the ceramic pellets could not be tested for dynamic flow column adsorption experiments.

© University of Venda

University of Venda
Creating Future Leaders

6.4 References

Tran, C.D., Duri, S., Delneri, A. and Franko, M., 2013. Chitosan – cellulose compsie materials: preparation, charactrerisationand application for removal of microcystin. *J Hazard Material*, 10. pp. 252 – 366.

Warshaw, C. M., Rosenberg, P.E. and Roy. R., 1960. Changes effected in layer silicates by heating below 550°C. *Clay minerals bulletin*, (4) 23, pp. 113 -125.

© University of Venda

University of Venda
Creating Future Leaders

CHAPTER SEVEN

CONCLUSIONS AND RECOMMENDATIONS

This study arrived at the following conclusions

- The optimum conditions for the defluoridation of water using silica rich reddish black Mukondeni clay soils and iron(III) oxide coated bentonite clay are 60 and 30 min, 1.5 and 3 g, 9 and 5 mg/L respectively, a pH of 2 and a temperature of 25°C for both clays.
- The optimum conditions for fabricating the composite ceramic pellets were 250 µm particle size, 600°C furnace temperature, 1 h firing time and 5:1 (iron oxide(III) coated bentonite clay: silica rich reddish black Mukondeni clay soils).
- Solution pH played a major role in fluoride removal by both clays with the optimum pH of 2 recorded for highest fluoride removal. For iron(III) oxide coated bentonite clay high adsorption (>70%) was observed over the pH range 2-12 which is significant for application in defluoridation of groundwater whose pH is circumneutral. Furthermore, the residual concentrations of metals in drinking water treated with iron(III) oxide coated bentonite clay at pH values, ranging from 6 to 9, were below the WHO standards. On the other hand, silica rich reddish black Mukondeni clay soils only showed a high percentage removal only at pH 2 but exhibited minimal metal leaching across a wide range of pH 4 – 10.
- The sorption data for both clays was fitted into the Langmuir, Freundlich and Dubunin – Radushkevich isotherms but Dubunin – Radushkevich model had the best fit for iron(III) oxide coated bentonite clay and the Freundlich model gave the best fit for the silica rich reddish black Mukondeni clay soils, implying that the adsorption processes took place on a heterogeneous surface of both the adsorbents.
- The pseudo-second-order kinetic model could be used to describe the fluoride adsorption behaviours on both clays and the adsorption kinetics of fluoride ions onto iron(III) oxide coated bentonite clay and silica rich reddish black Mukondeni clay soils was regulated by both external and intraparticle diffusion processes.
- The adsorption mechanism of adsorbents for fluoride could involve anion exchange and electrostatic interaction based on PZC and FTIR results.

© University of Venda

- From the results, we can conclude that iron(III) oxide coated bentonite clay is good sorbent for defluoridation of water and it can be used for small scale defluoridation purposes. Silica rich reddish black Mukondeni clay soils have shown fairly good fluoride uptake capacity in the laboratory further studies including its modification with metal oxides need to be evaluated.
- The overall adsorption performance of iron(III) oxide coated bentonite - silica rich reddish black Mukondeni clay soil composite pellets showed a very poor fluoride removal. It is recommended that the pellets be modified further by making them porous by adding saw dust or starch during the fabrication process.

© University of Venda

University of Venda
Creating Future Leaders

APPENDICES

APPENDIX A: Evaluation of fluoride removal using silica rich reddish black Mukondeni clay soils.

A1: Effect of contact time; equilibrium fluoride concentration, % fluoride removal and adsorption capacity of silica rich reddish black Mukondeni clay soils

Time(g)	Ce 1 g	Ce 2 g	Ce 3 g	%R 1 g	%R 2 g	%R 3 g	Qe 1 g	Qe 2 g	Qe 3 g
1	8.900	7.967	7.667	12.360	25.523	30.435	0.110	0.102	0.078
5	8.800	7.833	7.733	13.636	27.660	29.310	0.120	0.108	0.076
15	8.667	7.667	7.533	15.385	30.435	32.743	0.133	0.117	0.082
30	8.467	7.457	7.367	18.110	34.108	35.740	0.153	0.127	0.088
60	9.000	7.967	7.667	11.111	25.523	30.435	0.100	0.102	0.078
120	9.193	8.300	8.133	8.782	20.482	22.951	0.081	0.085	0.062
180	9.200	8.320	8.293	8.696	20.192	20.579	0.080	0.084	0.057

A2: Effect of adsorbent dosage; equilibrium fluoride concentration, % fluoride removal and adsorption capacity of silica rich reddish black Mukondeni clay soils

Dosage (g)	Ce 5 mg/L	Ce 10 mg/L	Ce 15 mg/L	%R 5 mg/L	%R 10 mg/L	%R 15 mg/L	Qe 5 mg/L	Qe 10 mg/L	Qe 15 mg/L
0.1	4.83333	9.63333	13.9333	3.44828	3.80623	7.6555	0.16667	0.36667	1.06667
0.3	3.99933	8.73333	12.9333	25.0208	14.5038	15.9794	0.33356	0.42222	0.68889
0.5	3.83333	8.63333	12.9333	30.4348	15.8301	15.9794	0.23333	0.27333	0.41333
0.7	3.76667	8.56667	12.8667	32.7434	16.7315	16.5803	0.17619	0.20476	0.30476
0.9	3.75667	8.16667	12.4667	33.0967	22.449	20.3209	0.13815	0.2037	0.28148
1	3.73333	7.63333	11.9333	33.9286	31.0044	25.6983	0.12667	0.23667	0.30667
1.2	3.66667	7.46667	11.7667	36.3636	33.9286	27.4788	0.11111	0.21111	0.26944
1.5	3.46667	7.26667	11.5667	44.2308	37.6147	29.683	0.10222	0.18222	0.22889
1.7	3.4677	7.2677	11.5677	44.1878	37.5951	29.6714	0.09014	0.16072	0.2019
1.9	3.47	7.27	11.57	44.0922	37.5516	29.6456	0.08053	0.14368	0.18053
2	3.533	7.333	11.633	41.5228	36.3698	28.9435	0.07335	0.13335	0.16835

© University of Venda

University of Venda
Creating Future Leaders

A3: Effect of initial fluoride concentration; equilibrium fluoride concentration, % fluoride removal and adsorption capacity of silica rich reddish black Mukondeni clay soils

Conc (mg/L)	Ce 1 g	Ce 2 g	%R 1 g	%R 2 g	Qe 1 g	Qe 2 g
2	1.2933	1.1943	54.6396	67.4579	0.0353	0.0403
5	3.6333	3.5433	37.6148	41.1114	0.0683	0.0728
7	5.5778	5.4778	25.4982	27.7892	0.0711	0.0761
9	7.4678	7.1678	20.5178	25.5619	0.0766	0.0916
11	9.7678	9.4678	12.6152	16.1836	0.0616	0.0766
13	11.9337	11.7337	8.9352	10.7920	0.0533	0.0633
15	13.8667	13.6667	8.1731	9.7561	0.0567	0.0667

A4: Effect of temperature; equilibrium fluoride concentration, % fluoride removal and adsorption capacity of silica rich reddish black Mukondeni clay soils

Conc (mg/L)	Ce 318 K	Ce 308 K	Ce 298 K	%R 318 K	%R 308 K	%R 298 K	Qe 318 K	Qe 308 K	Qe 298 K
2	1.2933	1.3933	1.4933	54.6396	43.5410	33.9289	0.0707	0.0607	0.0507
5	3.6333	3.7333	3.8333	37.6148	33.9287	30.4349	0.1367	0.1267	0.1167
7	5.5778	5.6778	5.7778	25.4982	23.2878	21.1540	0.1422	0.1322	0.1222
9	7.4678	7.6678	7.6678	20.5178	17.3743	17.3743	0.1532	0.1332	0.1332
11	9.7678	9.9678	9.9678	12.6152	10.3556	10.3556	0.1232	0.1032	0.1032
13	11.9337	11.9437	11.9437	8.9352	8.8440	8.8440	0.1066	0.1056	0.1056
15	13.8667	13.9667	13.8767	8.1731	7.3986	8.0951	0.1133	0.1033	0.1123

© University of Venda

A5: Effect of pH; equilibrium fluoride concentration, % fluoride removal and adsorption capacity of silica rich reddish black Mukondeni clay soils

Initial pH	Final pH	Ce	%R	Qe
2	2.33	8.05	0.45	0.14
4	6.40	12.67	0.20	0.05
6	6.71	12.67	0.20	0.05
8	6.66	12.76	0.20	0.04
10	7.98	11.67	0.13	0.07
12	11.71	12.67	0.20	0.05

APPENDIX B: Evaluation of fluoride removal using iron(III) oxide coated bentonite clay

B1: Effect of contact time; equilibrium fluoride concentration, % fluoride removal and adsorption capacity of iron(III) oxide coated bentonite clay

Time (min)	Ce 0.5 g	Ce 1 g	Ce 2 g	%R 0.5 g	%R 1 g	%R 2 g	Qe 0.5 g	Qe 1 g	Qe 2 g
1	7.9657	6.9667	6.6667	25.5230	30.3333	50.0000	0.20333	0.30333	0.33333
5	7.4343	6.4333	6.3333	34.5291	35.6667	57.8947	0.25667	0.35667	0.36667
15	7.0322	6.0333	6.0333	42.1801	39.6667	65.7459	0.29667	0.39667	0.39667
30	6.6000	5.6000	5.6000	51.5152	44.0000	78.5714	0.34000	0.44000	0.44000
60	7.6002	6.6000	5.6667	31.5789	34.0000	76.4706	0.24000	0.34000	0.43333
120	7.8000	6.8000	5.8000	28.2051	32.0000	72.4138	0.22000	0.32000	0.42000
180	7.7667	6.7667	5.7667	28.7554	32.3333	73.4104	0.22333	0.32333	0.42333
240	7.7668	6.7667	5.7667	28.7548	32.3330	73.4094	0.22333	0.32333	0.42333
300	7.7670	6.7670	5.7670	28.7498	32.3300	73.4004	0.22330	0.32330	0.42330
360	7.7700	6.7700	5.7700	28.7001	32.3000	73.3102	0.22300	0.32300	0.42300

© University of Venda

B2: Effect of adsorbent dosage; equilibrium fluoride concentration, % fluoride removal and adsorption capacity of iron(III) oxide coated bentonite clay

Dosage (g)	Ce 5 mg/L	Ce 10 mg/L	Ce 20 mg/L	%R 5 mg/L	%R 10 mg/L	%R 20 mg/L	Qe 5 mg/L	Qe 10 mg/L	Qe 20 mg/L
0.1	4.3700	7.3600	14.0800	14.4165	35.8696	42.0455	0.6300	2.6400	5.9200
0.5	4.6000	6.6778	12.7000	8.6957	49.7508	57.4803	0.0800	0.6644	1.4600
0.8	4.5667	6.6667	12.5000	9.4890	49.9999	60.0000	0.0542	0.4167	0.9375
1	4.4000	6.6000	12.4860	13.6364	51.5152	60.1794	0.0600	0.3400	0.7514
2	3.6893	5.7000	12.2460	35.5258	75.4386	63.3186	0.0655	0.2150	0.3877
3	3.6300	5.5000	11.3600	37.7410	81.8182	76.0563	0.0457	0.1500	0.2880
4	3.6050	5.3000	11.2600	38.6963	88.6792	77.6199	0.0349	0.1175	0.2185
5	3.6080	5.2960	11.1600	38.5823	88.8218	79.2115	0.0278	0.0941	0.1768

B3: Effect of initial fluoride concentration; equilibrium fluoride concentration, % fluoride removal and adsorption capacity of iron(III) oxide coated bentonite clay

Conc (mg/L)	Ce 298 K	Ce 308 K	Ce 318 K	Qe 298 K	Qe 308 K	Ce 318 K	%R 298 K	%R 308 K	%R 318 K
5	0.7890	0.6890	0.5890	0.2106	0.2206	0.2156	84.2200	88.2200	86.2200
10	2.9930	2.8930	2.7930	0.3504	0.3604	0.3554	70.0700	72.0700	71.0700
20	8.1800	8.0800	8.0800	0.5910	0.5960	0.5960	59.1000	59.6000	59.6000
40	20.6000	20.5000	20.5000	0.9700	0.9750	0.9750	48.5000	48.7500	48.7500
60	33.1000	33.0000	32.9000	1.3450	1.3550	1.3500	44.8333	45.1667	45.0000
80	48.2000	48.1000	48.0000	1.5900	1.6000	1.5950	39.7500	40.0000	39.8750

© University of Venda

University of Venda
Creating Future Leaders

B4: Effect of temperature; equilibrium fluoride concentration, % fluoride removal and adsorption capacity of iron(III) oxide coated bentonite clay

Conc (mg/L)	Ce 298 K	Ce 308 K	Ce 318 K	Qe 298 K	Qe 308 K	Ce 318 K	%R 298 K	%R 308 K	%R 318 K
5	0.789	0.689	0.589	0.210	0.220	0.215	84.22	88.22	86.22
10	2.993	2.893	2.793	0.350	0.360	0.355	70.07	72.07	71.07
20	8.180	8.080	8.080	0.591	0.596	0.596	59.10	59.60	59.60
40	20.60	20.50	20.50	0.970	0.975	0.975	48.50	48.75	48.75
60	33.10	33.00	32.90	1.345	1.355	1.350	44.83	45.16	45.00
80	48.20	48.10	48.00	1.590	1.600	1.595	39.75	40.00	39.87

B5: Effect of pH; equilibrium fluoride concentration, % fluoride removal and adsorption capacity of iron(III) oxide coated bentonite clay

Initial pH	Final pH	Ce	%R	Qe
2	4.3950	0.67333	90.38095	0.31633
4	6.8310	1.33333	80.95238	0.28333
6	7.0200	1.40000	80.00000	0.28000
8	7.0600	1.60000	77.14286	0.27000
10	7.1230	1.96667	71.90476	0.25167
12	11.1550	2.03333	70.95238	0.24833

© University of Venda